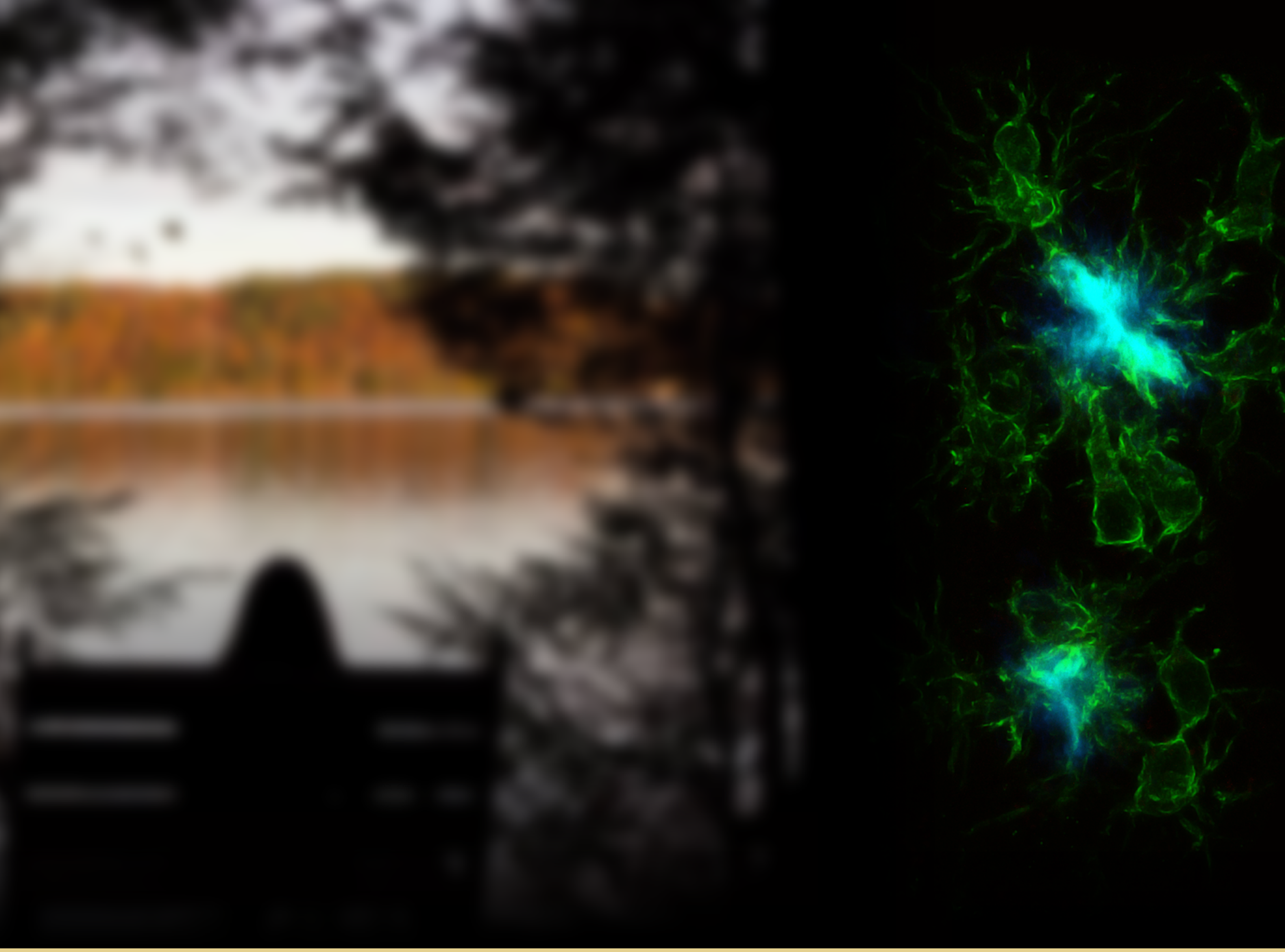

Joana Ribeiro Guedes

INFLAMMATION IN ALZHEIMER'S DISEASE: DEREGULATION AND MODULATION OF miRNA EXPRESSION IN THE MONONUCLEAR PHAGOCYTE SYSTEM

Tese de Doutoramento em Biologia Experimental e Biomedicina, ramo de Neurociências e Doença, orientada pelas Doutora Ana Luísa Colaço Cardoso e Professora Doutora Maria da Conceição Pedroso de Lima e apresentada ao Instituto de Investigação Interdisciplinar da Universidade de Coimbra.

Setembro de 2015

· U C ·

UNIVERSIDADE DE COIMBRA

Joana Ribeiro Guedes

Inflammation in Alzheimer's disease: deregulation and modulation of miRNA expression in the mononuclear phagocyte system

2015

Thesis submitted to the Institute for Interdisciplinary Research of the University of Coimbra to apply for the degree of Doctor in Philosophy in the area of Experimental Biology and Biomedicine, specialization in Neurosciences and Disease.

· U C ·

This work was conducted at the Center for Neuroscience and Cell Biology (CNC) of University of Coimbra, under the scientific supervision of Doctor Ana Luísa Cardoso and Professor Maria da Conceição Pedroso de Lima. Part of this work was also performed at the Center for Immunology and Inflammatory Diseases of Massachusetts General Hospital under supervision of Doctor Joseph El Khoury.

Joana Ribeiro Guedes was a student of the Doctoral Programme in Experimental Biology and Biomedicine coordinated by the Center for Neuroscience and Cell Biology (CNC) of the University of Coimbra and a recipient of the fellowship SFRH/BD/51667/2011 from the Portuguese Foundation for Science and Technology (FCT). The execution of this work was supported by FCT and FEDER/COMPETE (PTDC/BIM-MEC/0651/2012, PEst-C/SAU/LA0001/2013-2014 and UID/NEU/04539/2013) and the National Institute of Aging-NIH 1R01 AG032349-05.

CNC
CENTER FOR NEUROSCIENCE AND CELL BIOLOGY
UNIVERSITY OF COIMBRA, PORTUGAL

· U C ·
UNIVERSIDADE DE COIMBRA

CHUC
CENTRO HOSPITALAR E UNIVERSITÁRIO DE COIMBRA

BEB PhD Programme
Biologia Experimental e Biomedicina

· U C ·
IIIUC INSTITUTO DE INVESTIGAÇÃO INTERDISCIPLINAR
UNIVERSIDADE DE COIMBRA

MGH 1811
MASSACHUSETTS GENERAL HOSPITAL

VE RI TAS
THE HARVARD MEDICAL SCHOOL

FCT
Fundação para a Ciência e a Tecnologia
MINISTÉRIO DA EDUCAÇÃO E CIÊNCIA

COMPETE
PROGRAMA OPERACIONAL FACTORES DE COMPETITIVIDADE

QREN
QUADRO DE REFERÊNCIA ESTRATÉGICO NACIONAL
PORTUGAL 2007.2013

UNIÃO EUROPEIA
Fundo Europeu de Desenvolvimento Regional

NIH National Institutes of Health

“Todos os instantes, ao longo do nosso corpo, os fluxos elétricos bailam
em cada órgão ao ritmo de sinfonias silenciosas, cujo compasso é
coordenado por milhares de células invisíveis.”

José Rodrigues dos Santos
In A Fórmula de Deus

To my parents and grandparents

To Nuno

ACKNOWLEDGMENTS

At the end of this journey it is paramount to acknowledge all the people that made this work possible and contributed to shape the person I am today. Along four years full of work, passion and friendship, it is inevitable to recognize the value that my friends and coworkers have in my life.

First of all, I would like to thank to the supervisor of my Thesis Dr. Ana Luísa Cardoso. Anything that I could write in these acknowledgments is never going to be enough to express my gratitude. For the friendship, guidance, mentorship, incentive and, above all, for believing in me and teach me, from the very beginning, the meaning of doing science. Your passion about our work made me remember, every day, why I embraced this path.

Second, I would like to express my sincere gratefulness to the supervisor of my Thesis, Prof. Maria Conceição Pedroso de Lima, who I greatly respect and admire, for allowing me to be part of the Vectors and Gene Therapy Group from the Center for Neuroscience and Cell Biology (CNC) of the University of Coimbra, and who, since my BSc in Biochemistry, always supported and encouraged me.

Third, I would like to thank Dr. Joshep El Khoury, Principal Investigator of the Laboratory of Neuroimmunology and Innate Immunity of the Center for Immunology and Inflammatory Diseases of Massachusetts General Hospital, for receiving me in Boston, providing me all the necessary means to perform the *in vivo* part of this work and for always pushing me forward.

To Prof. Amílcar Falcão, Director of the Institute for Interdisciplinary Research of the University of Coimbra and to Prof. Catarina Resende de Oliveira, former President of CNC, for welcoming me in the respective institutions and offering me the conditions to perform this work.

To Prof. João Ramalho-Santos, current President of CNC and coordinator of the Doctoral Programme in Experimental Biology and Biomedicine (PDBEB), as well as to all the scientific committee who evaluated the students of the PDBEB 10th Edition, my deepest gratitude for choosing me to be part of this course.

My thankfulness to Dr. Isabel Santana and her team from the Memory Clinic, Neurology Department of the Coimbra Hospital and Universitary Centre for their indispensable and invaluable contribution to this work and for teaching me the importance of caring for the dementia patients who participated in this study, as well as their families.

To all the people who contributed with small reagents or expertise to the experiments presented in this Thesis, Prof. João Nuno Moreira, Prof. Ana Cristina Rego, Prof. Luís Pereira de Almeida, Dr. John Jones, Gladys Caldeira, Filipa Simões, to the heads of the CNC cores and also to Edward Seung, Zaida Ramirez-Ortiz, Ravi Mylvagana and Christina Luo from the Massachusetts General Hospital, which help was always important to overcome experimental difficulties.

My deepest thankfulness to my Boston family from the Laboratory of Neuroimmunology and Innate Immunity, Suzanne Hickman, Pritha Sen and Maike Gold for making me feel like I was home during my year in the USA. Also, for the invaluable scientific insight which allowed me to be a better as a scientist.

To my friends from the PDBEB 10th Edition which were more than my family during my first year of my PhD and who, despite the distance after that, were continuously by my side. Thank you guys!

To my colleagues from the Vectors and Gene Therapy Group for the companionship and who were, day after day, with me and endured all my foolishness in the diversion moments and lunch times. Thank you Sara, Ângela, Ana Gregório, Mariana, Dina and Rui for the healthy and joyful environment. It was awesome to be part of this family and an honor to become your friend.

To my "tuga" friends in Boston, Catarina, Ana Tellechea, Ana Metelo, João Ribas, João Neto, Teresa and Daniel, who allowed me to feel home even at 5200 km distant from Portugal. You made my last year much more interesting and funny!

To my work family/group, Ana Maria, Ana Teresa, Lara, Catarina, Pedro, Raquel, Rita and Prof. Amália Jurado for being incredible coworkers and for always respecting my scientific opinion.

To my true and old friends, back in Lamego, for all these years being supportive and making sure I was always in the right path. Thank you Denise, Flor, Susana and Tânia. Also, to the friends that always stayed tuned after our academic journey at the Biochemistry course at University of Coimbra: Mónica, Cláudia, Liliana and Miguel.

To all my family, aunts, uncles and cousins for never letting me forget the concept of "blood family". But a special acknowledgment to my new family (as they like to entitle themselves), Lúcia, Laurindo and Ana, for having me welcomed in their house and accepted me as their daughter and sister. It means the world to me to be cherished by you.

However, my deepest and greatest acknowledgment goes to my parents, Fátima and Zé and my grandparents Maria and Francisco, who raised me, taught me all the values I have today and supported my ride since my very first day at the University of Coimbra. Without you, all of this would have been impossible.

And finally, my most important “Thank you” is to my Love, Nuno. Wondrously and unexpectedly, you saw me become the scientist and the person I am today. And I think you have no idea the influence you had on me. Thank you for your expertise in the most various work-related subjects, for the intense and brainstorming scientific discussions but, above all, for being my best friend, my companion, my partner, my passion and my “Peaceful harbor”. Words will never be enough to describe the importance you have in my life, but I hope my actions, day by day, will give you an idea ;)

TABLE OF CONTENTS

Abstract I
Resumo III
Abbreaviations list VII
Preface XIII

Chapter 1

General Introduction 1
- ***1.1. The mononuclear phagocyte system*** 3
  - *1.1.1. Monocytes and macrophages* 3
    - *1.1.1.1. Monocyte development* 3
    - *1.1.1.2. Monocyte subsets and tissue infiltration* 4
  - *1.1.2. Microglia as the hematopoietic cells of the central nervous system* 6
    - *1.1.2.1. The origin of microglia* 6
    - *1.1.2.2. Microglia roles in brain homeostasis and injury* 7
  - *1.1.3. Distinguishing mononuclear phagocyte system cells: how to study the mononuclear phagocyte system?* 10
- ***1.2. Alzheimer's disease: a heavy burden for the future*** 13
  - *1.2.1. Pathophysiology of Alzheimer's disease* 16
  - *1.2.2. Inflammation in Alzheimer's disease* 19
    - *1.2.2.1. Novel inflammation-associated Alzheimer's disease risk genes* 20
    - *1.2.2.2. Unveiling the role of microglia in Alzheimer's disease inflammation and Aβ deposition* 20
    - *1.2.2.3. Implication of peripheral mononuclear cells in Alzheimer's disease*.26
- ***1.3. MicroRNAs: powerful regulatory small RNAs*** 29
  - *1.3.1. Immune-related miRNAs* 31
    - *1.3.1.1. Role of miRNAs in mononuclear phagocyte development* 31
    - *1.3.1.2. MiRNA regulation of inflammation* 33
    - *1.3.1.3. MiRNAs in Alzheimer's disease-related neuroinflammation* 34
  - *1.3.2. MiRNA-based therapeutic applications in neuroimmune and neurodegenerative diseases* 37

Chapter 2

Objectives 39

Chapter 3

Early miR-155 upregulation contributes to neuroinflammation in Alzheimer's disease triple transgenic mouse model 43
- **Abstract** 45
- ***3.1. Introduction*** 46
- ***3.2. Materials and Methods*** 48
  - *3.2.1. Materials* 48

3.2.2. Animals 48
3.2.3. Immunohistochemistry 49
3.2.4. Microglia and astrocyte cell culture 49
3.2.5. Preparation of amyloid-β (Aβ) oligomers and fibrils for microglia and astrocytes treatment 50
3.2.6. Transfection experiments 51
3.2.7. Quantitative real-time PCR 52
3.2.8. In situ *hybridization* 53
3.2.9. Western blot 54
3.2.10. Statistical analysis 54
3.3. Results 55
3.3.1. Inflammation precedes senile plaque deposition in the 3xTg AD model 55
3.3.2. MiR-155 is upregulated in the brain of the 3xTg AD model 59
3.3.3. SOCS-1 is downregulated in the brain of the 3xTg AD model 64
3.3.4. C-Jun is responsible for miR-155 upregulation in the presence of the Aβ peptide 65
3.4. Discussion 67
3.5. Supplementary Material 71

Chapter 4

MiRNA deregulation and chemotaxis and phagocytosis impairment in Alzheimer's disease 77
Abstract 79
4.1. Introduction 80
4.2. Methods 81
4.2.1. Patient selection 81
4.2.2. Isolation of BDMs 82
4.2.3. Flow cytometry analysis 82
4.2.4. Chemotaxis assay 82
4.2.5. Preparation of $A\beta_{1\text{-}42}$ fibrils and $A\beta_{1\text{-}42}$-FAM fibrils 83
4.2.6. Primary cultures of MDMs and phagocytosis assay 83
4.2.7. RNA extraction and qRT-PCR 83
4.2.8. ELISA for sTREM2 84
4.2.9. Statistical analysis 84
4.3. Results 85
4.3.1. The presence of chemokine receptors is reduced at the cell surface of BDMs from AD and MCI patients 85
4.3.2. CCL2-driven chemotaxis is impaired in BDM of AD and MCI patients 86
4.3.3. Phagocytosis of Aβ fibrils by MDMs is compromised in both AD and MCI patients 88

4.3.4. TREM2 expression is increased in MCI patients 88
4.3.5. Immune-related miRNAs are differentially expressed in AD and MCI patients 89
4.4. Discussion 91
4.5. Supplementary Material 95

Chapter 5

Ex vivo *modulation of miR-23a in bone-marrow-derived monocytes injected in 5XFAD mice decreases vascular amyloid beta* 97

Abstract 99
5.1. Introduction 100
5.2. Methods 101
5.2.1. Animals 101
5.2.2. Isolation and adoptive transfer of BM-derived monocytes 102
5.2.3. Flow cytometry analysis of BM-derived monocyte-injected 5XFAD brain cells 103
5.2.4. Intravital microscopy 103
5.2.5. Transfection of BM-derived monocytes 104
5.2.6. Immunohistochemistry 105
5.2.7. Stereology 106
5.2.8. $A\beta_{1\text{-}42}$ *ELISA* 106
5.2.9. RNA extraction and qRT-PCR 107
5.2.10. Statistical analysis 108
5.3. Results 108
5.3.1. BM-derived monocytes infiltrate into the brain of 5XFAD mice 108
5.3.2. Inhibition of miRNA-23a increases CCR2 expression in BM-derived monocytes 111
5.3.3. Injection of BM-derived monocytes into 5XFAD decreases cerebral vascular Aβ 113
5.3.4. BM-derived monocytes cluster around Aβ plaques in injected 5XFAD mice 115
5.4. Discussion 118
5.5. Supplementary Material 122

Chapter 6

General conclusions and future perspectives 125

References

List of bibliographic references (ordered alphabetically) 131

DRAWINGS

List of figures

Figure 1.1 | Mononuclear phagocyte system (MPS): cell progenitors, localization and functions. 4

Figure 1.2 | Amyloid precursor protein (APP) processing at the cell membrane and intracellular vesicle membrane. 17

Figure 1.3 | Role of mononuclear phagocytes in Alzheimer's disease. 27

Figure 1.4 | Canonical and non-canonical pathways of miRNA biogenesis. 30

Figure 1.5 | MiR-155 and miR-146a neuroinflammatory mechanisms in AD. 37

Figure 3.1 | Microgliosis and astrogliosis in 3xTg AD animals. 56

Figure 3.2 | Intraneuronal and extracellular Aβ accumulation in 3xTg AD mice. 57

Figure 3.3 | Cytokine production in 3xTg AD animals. 58

Figure 3.4 | MiR-155-5p levels in 3xTg AD mice. 60

Figure 3.5 | MiR-155-5p expression in Aβ-activated microglia and astrocyte cultures. 61

Figure 3.6 | IL-6 and IFN-β expression in Aβ-activated microglia and astrocyte cultures. 63

Figure 3.7 | SOCS-1 mRNA and protein levels in 12-month 3xTg AD mice. 64

Figure 3.8 | C-Jun expression in 3xTg AD mice. 66

Figure 3.9 | MiR-155-5p expression in microglia and astrocytes following c-Jun silencing and Aβ exposure. 66

Figure S3.1 | IBA-1, GFAP and $A\beta_{1-42}$ *staining in 3 months old 3xTg AD animals.* 71

Figure S3.2 | MiR-125b-5p expression in 3xTg AD mice. 71

Figure S3.3 | Time-course study on cytokine expression in N9 microglia cells activated with Aβ oligomers or Aβ fibrils. 72

Figure S3.4 | Quantification of cytokine and chemokine secretion in Aβ-activated N9 microglia cells. 73

Figure S3.5 | IL-1β and TNF-α expression in astrocytes exposed to Aβ. 74

Figure S3.6 | SOCS-1 mRNA expression in astrocytes following miR-155-5p modulation. 74

Figure S3.7 | NF-κB expression in 3xTg AD mice. 75

Figure S3.8 | Representative gel illustrating the different Aβ aggregated forms present in Aβ preparations. 75

Figure 4.1 | Presence of surface chemokine receptors CCR2 and CXCR4 is reduced in BDM of AD and MCI patients. 86

Figure 4.2 | CCL2-driven chemotaxis is impaired in AD and MCI BDMs. 87

Figure 4.3 | Internalization of Aβ fibrils is compromised in AD MDMs, while MCI MDMs present increased Aβ fibril uptake. 88

Figure 4.4 | Deregulation of TREM2 mRNA and sTREM2 levels in AD and MCI patients. 89

Figure 4.5 | Immune-related miRNAs are differentially expressed in AD and MCI patients. 90

Figure S4.1 | IL-6 and TNF-α mRNA levels in BDMs of AD and MCI patients. 96

Figure 5.1 | Quantification of GFP and RFP expression in bone-marrow (BM) cells before and after magnetic-activated cell sorting (MACS). 109

Figure 5.2 | Chemotaxis of monocytes into the brain of 3-months old 5XFAD mice. 110

Figure 5.3 | Delivery of anti-miR-23a-3p (anti-23a-3p) mediated by the Delivery Liposome System (DLS) to BM-derived monocytes increases CCR2 mRNA levels. 112

Figure 5.4 | 5XFAD mice injected with BM-derived monocytes, previously transfected with anti-23a-3p, present reduced vascular Aβ. 114

Figure 5.5. | BM-derived monocytes cluster around Aβ plaques and suppress inflammation in 5XFAD mice. 116

Figure S5.1 | Characterization of tissue-recovered monocytes following isolation. 122

Figure S5.2 | Stereologic analysis to quantify dense, diffuse and vascular Aβ deposits. 122

Figure S5.3 | Representative images of the hippocampus and subiculum of BM-monocyte-injected 5XFAD mice. 123

Figure S5.4 | BM-derived monocytes contribute to maintain an immunosuppressive environment in the brain of 5XFAD mice. 123

List of tables

Table 1.1 | Involvement of miRNAs in disease-related neuroinflammation. 36

Table S3.1 | Percentages of the Aβ assembly forms in the different Aβ preparations...............75

Table 4.1 | Characteristics of patient and control study populations. 85

Table S4.1 | MiRNAs quantified by PCR arrays using Pick-&-Mix microRNA PCR Panels. ..95

Table S4.2 | AD risk genes predicted to be regulated by immune-related miRNAs differentially expressed in AD patients. 96

ABSTRACT |

The discovery of small RNAs, which play a crucial role in the regulation of gene expression, has led to a significant revolution in the molecular biology dogma. The most extensively studied class of these molecules includes microRNAs (miRNAs), small 22 nucleotide RNAs that bind to mature mRNAs, repressing their translation. The lack of total complementarity between the miRNA and its targets accounts for a broad effect, where one miRNA can impact the translation of multiple proteins. When the expression of one or a set of miRNAs is disrupted, several cellular outputs can be compromised, disturbing the cellular homeostatic balance and triggering pathological states.

The mononuclear phagocyte system (MPS) comprises several cell types that, although with different tissue localizations, share cellular functions and phenotypes. Microglia and monocytes are MPS cells from the brain and blood vessels, respectively. During an inflammatory stimulus, blood-derived monocytes (BDM) infiltrate tissues and differentiate into monocyte-derived macrophages (MDM), which control the inflammatory environment and carry out cleaning functions. Primary inflammatory processes undertaken by these cells need to be tightly controlled to avoid chronic inflammation and, in this context, miRNAs have emerged as indispensable regulators of MPS function.

Microglia and other MPS cells have been largely implicated in neurodegenerative processes which are accompanied by uncontrolled neuroinflammation. One of the most prevalent and devastating of these disorders is Alzheimer's disease (AD), in which the accumulation of amyloid β (Aβ) peptides in the brain causes neuronal death. The most consensual theory for excessive Aβ deposition advocates that microglia loses the ability to phagocyte this peptide, due to the acquisition of a strongly pro-inflammatory phenotype (M1). BDMs have been proposed to infiltrate the brain parenchyma in AD and carry out immune functions which, in a non-pathological situation, would be performed by microglia.

The work developed in the context of this Thesis aimed at understanding how the above-mentioned processes and players are interconnected and contribute to AD progression. In this regard, an effort was made to clarify how inflammatory miRNAs control the function of MPS cells in AD. MiR-155-5p expression was found to be upregulated in 3xTg AD mice, before the appearance of extracellular Aβ aggregates, and in microglia following Aβ activation. Since the increase of miR-155-5p expression has been correlated with the establishment of the M1 activation phenotype in macrophages, this increment hinted on the presence of a pro-inflammatory environment in the brain of the 3xTg AD mice. This was further confirmed by the observed increase in IL-6 and IFN-β levels in these animals, as well as in Aβ-activated microglia. Moreover, miR-155 upregulation in 3xTg AD mice was suggested to play a role in the downregulation of the suppressor of cytokine signaling 1 (SOCS-1), a protein essential

during the resolution stage of inflammation. Importantly, the transcription factor c-Jun was found to be upregulated in 3xTg AD mice and its silencing led to a significant decrease in miR-155-5p expression in Aβ-activated microglia cells.

Given the contribution of BDMs to Aβ clearance in AD mouse models, it was essential to understand if, in humans, these cells are compromised in the context of disease, regarding cellular functions such as chemotaxis and phagocytosis. These cellular outputs are essential for brain infiltration and Aβ clearance and can be influenced by the expression of miRNAs. Importantly, miR-155-5p, -154-5p, -200c-3p, -27b-3p and -128-3p were found to be differentially expressed in BDMs from AD patients, with respect to age-matched controls and mild cognitive impairment (MCI) patients, indicating their potential role as disease biomarkers. Of special remark is the fact that some of these miRNAs are predicted to bind to chemokine receptors, such as CCR2, and phagocytosis proteins, as well as to several AD risk genes, including the triggering receptor expressed on myeloid cells 2 (TREM2). Interestingly, the CCL2/CCR2 axis was found to be impaired in BDMs from AD and MCI patients, causing a deficit in cell migration. Moreover, a decrease in MDM-mediated phagocytosis of Aβ fibrils was related with alterations in the expression and processing of TREM2.

Finally, in this Thesis, it was demonstrated that $CX3CR1^{+}CCR2^{+}$ bone-marrow (BM)-derived monocytes, when intravenously injected in 5XFAD AD mice, are able to reach the brain parenchyma in the absence of irradiation. The *ex vivo* delivery of miR-23a-3p anti-sense oligonucleotides using cationic liposomes (DLS) resulted in increased expression of CCR2 in BM-derived monocytes, while the intravenous injection of these cells in 5XFAD mice led to a significant decrease in the deposition of vascular Aβ. These results confirm that CCR2 is essential for vascular Aβ clearance in AD and place miR-23a-3p as an immune therapeutic target to be modulated in peripheral myeloid cells, in an AD context.

Altogether, this work affirms miRNAs as master regulators of MPS cell function in AD and demonstrates that, while these molecules contribute to the initiation of inflammation in this disease, they can also be useful to stage dementia and to generate new and effective therapeutic strategies towards AD.

RESUMO |

A descoberta de pequenos RNAs não codificantes, que desempenham um papel crucial na regulação da expressão genética, despoletou uma revolução no dogma da biologia molecular. Os microRNAs (miRNAs) constituem a classe mais estudada destas moléculas e compreendem pequenos RNAs com 22 nucleótidos que ligam ao RNA mensageiro maduro, inibindo a sua tradução. O facto destes miRNAs e os seus RNAs mensageiros alvo não serem totalmente complementares permite um efeito amplo no que diz respeito ao impacto que um simples miRNA pode ter na tradução de várias proteínas. A expressão anómala de um miRNA ou de um conjunto de miRNAs afeta vários processos celulares, causando um distúrbio na homeostasia celular que pode conduzir a estados patológicos.

O conjunto dos fagócitos mononucleares integra vários tipos celulares que, apesar de se encontrarem em diferentes tecidos, partilham funções e fenótipos. A microglia e os monócitos são células deste conjunto que se encontram no cérebro e nos vasos sanguíneos, respetivamente. Na presença de um estímulo inflamatório, monócitos provenientes do sangue infiltram-se nos tecidos onde se diferenciam em macrófagos (derivados de monócitos), os quais controlam o ambiente inflamatório no tecido e realizam funções de "limpeza". Os processos inflamatórios levados a cabo por estas células têm de ser estritamente controlados, no sentido de evitar situações de inflamação crónica. Neste contexto, os miRNAs têm emergido como reguladores indispensáveis na função dos fagócitos mononucleares.

A microglia e outros fagócitos mononucleares têm sido largamente implicados em processos neurodegenerativos que são, normalmente, acompanhados por neuroinflamação descontrolada. Uma das doenças neurodegenerativas mais prevalentes e devastadoras é a doença de Alzheimer (DA), caracterizada pela acumulação de peptídeos β amilóide (Aβ) no cérebro, conduzindo à morte neuronal. A teoria mais consensual que justifica a excessiva deposição de Aβ no parênquima cerebral defende que a microglia perde a capacidade de fagocitar este peptídeo devido à aquisição de um forte fenótipo pró-inflamatório M1. Tem vindo a ser proposto que, no contexto da DA, os monócitos circulantes possuem a capacidade de infiltrar o parênquima cerebral, desempenhando funções imunitárias que, numa situação não patológica, seriam realizadas pela microglia.

O trabalho desenvolvido no âmbito desta Tese teve como objetivo compreender o modo como os processos e intervenientes acima descritos estão interligados e contribuem para a progressão da DA. Neste contexto, procurou-se clarificar os mecanismos pelo quais os miRNAs inflamatórios controlam a função dos fagócitos mononucleares nesta doença. Verificou-se que a expressão do miR-155-5p se encontra aumentada no modelo triplo transgénico de Alzheimer (3xTg DA), antes do aparecimento de agregados extracelulares de Aβ, e também em microglia ativada com Aβ. Já que o aumento da expressão do miR-155-5p tem vindo a ser relacionado com o

fenótipo de ativação M1 em macrófagos, este resultado sugeriu que o cérebro dos ratinhos 3xTg DA poderia apresentar um ambiente pró-inflamatório. A favor desta proposta foi observado que os níveis de IL-6 e IFN-β estão aumentados no cérebro destes animais, bem como em microglia ativada com Aβ. Para além disso, a potenciação da expressão do mR-155-5p nos ratinhos 3xTg AD foi correlacionada com a diminuição dos níveis da proteína SOCS-1, essencial para o passo de resolução da inflamação. Verificou-se ainda que o fator de transcrição c-Jun se encontra aumentado nos ratinhos 3xTg DA e que o seu silenciamento contribui para uma diminuição significativa da expressão do miR-155-5p em células da microglia, após ativação com Aβ.

Dada a contribuição dos fagócitos mononucleares para a remoção de depósitos de Aβ em modelos animais da DA, era essencial perceber se no ser humano a função destas células está de alguma forma comprometida, num contexto clínico, especialmente no que diz respeito a funções celulares como a quimiotaxia e a fagocitose. Estas funções são essenciais para a infiltração destas células no cérebro, bem como para a remoção de Aβ, e podem ser influenciadas pela expressão de miRNAs. Verificou-se que os miRNAs miR-155-5p, -154-5p, -200c-3p, -27b-3p e -128-3p se encontram diferencialmente expressos em monócitos circulantes de doentes diagnosticados com a DA, em comparação com controlos com a mesma idade e com doentes com défice cognitivo ligeiro (DCL), o que evidencia o seu potencial como biomarcadores da doença. Alguns destes miRNAs estão previstos ligar a recetores de quemoquinas, como é o caso do CCR2, e a proteínas envolvidas no processo de fagocitose, bem como a vários genes de risco para esta doença, incluindo o TREM2. Assim, foi interessante observar que o eixo CCR2/CCL2 está comprometido nos monócitos de doentes com DA e com DCL, causando um défice na migração celular. Para além disso, verificou-se que a diminuição da fagocitose de fibrilhas de Aβ por parte dos macrófagos derivados destes monócitos está relacionada com alterações na expressão e processamento do TREM2.

Por último, foi demonstrado neste Trabalho que os monócitos derivados da medula óssea, que se apresentam positivos para os marcadores CX3CR1 e CCR2, quando injetados na corrente sanguínea de ratinhos do modelo de DA que possui 5 mutações (5XFAD), são capazes de migrar para o parênquima cerebral na ausência de irradiação. A entrega *ex vivo* de oligonucleótidos complementares ao miR-23a-3p, usando lipossomas catiónicos (DLS), resultou no aumento de expressão do recetor CCR2 nestes monócitos. Aquando da injeção destas células na corrente sanguínea de ratinhos 5XFAD verificou-se uma diminuição significativa da deposição de Aβ nos vasos sanguíneos cerebrais destes animais. Estes resultados confirmam que o CCR2 é essencial para a remoção de Aβ vascular no contexto da DA e sugerem o que o miR-23a-3p pode constituir um potencial alvo terapêutico a ser modulado em células mononucleares periféricas, no contexto da DA.

De um modo geral, os resultados apresentados nesta Tese vêm confirmar o papel dos miRNAs como reguladores importantes da função dos fagócitos mononucleares na DA, e demonstram que estas pequenas moléculas, para além de contribuirem para o despoletar dos processos inflamatórios nesta doença, podem ser úteis no seu diagnóstico e no desenvolvimento de terapias novas e mais eficazes.

ABBREAVIATIONS LIST

3’UTR	3’ untranslated region
3xTg	triple trangenic
ACH	amyloid cascade hypothesis
AD	Alzheimer’s disease
ADAS-cog	Alzheimer’s disease Assessment Scale-Cognitive
AGEs	advanced glycosylation end products
AGO	argonaute
AICD	amyloid intracellular domain
AP-1	activator protein-1
ApoE	apolipoprotein E
APP	amyloid precursor protein
Aβ	amyloid-beta peptide
BACE1	beta-secretase 1
BBB	blood-brain barrier
BDMs	blood-derived monocytes
BIN1	myc box-dependent-interacting protein 1
BM	bone-marrow
BSA	bovine serum albumine
C/EBPα	CCAAT-enhancer-binding protein alpha
C/EBPβ	CCAAT-enhancer-binding protein beta
CAA	cerabral amyloid angiopathy
CCL2	chemokine (C-C motif) ligand 2
CCL3	chemokine (C-C motif) ligand 3
CCL4	chemokine (C-C motif) ligand 4
CCL5	chemokine (C-C motif) ligand 5
CCR1	C-C chemokine receptor type 1
CCR2	C-C chemokine receptor type 2
CCR5	C-C chemokine receptor type 5
CCR8	C-C chemokine receptor type 8
CD115	cluster of differentiation 115
CD11b	cluster of differentiation molecule 11b
CD135	cluster of differentiation antigen 135
CD14	cluster of differentiation 14
CD16	cluster of differentiation 16
CD2AP	CD2-associated protein
CD33	cluster of differentiation 33
CD34	cluster of differentiation 34
CD36	cluster of differentiation 36
CD43	cluster of differentiation 43

CD45	cluster of differentiation 45
CD62	cluster of differentiation 62
CDK4	cyclin-dependent kinase 4
CDK5	cyclin-dependent kinase 5
CDK6	cyclin-dependent kinase 6
cDNA	complementary DNA
CDR	clinical dementia rating
CFH	glycoprotein immune repressor complement factor
CHF	complement factor H
CLU	clusterin
c-Maf	Transcription factor Maf
cMoPs	common monocyte progenitors
CMPs	common myeloid progenitors
CNS	central nervous system
CR	complement receptors
CR1	complement receptor 1
CR3	complement receptor 3
CSF	cerebral spinal fluid
Ct	treshold cycle
CT	Computarized tomography
CTFα	C-terminal fragment alpha (non-amyloidogenic pathway)
CTFβ	membrane-bound C-terminal fragment beta (amyloidogenic pathway)
CX3CL1	chemokine (C-X3-C motif) ligand 1 / fractalkine
CX3CR1	CX3C chemokine receptor 1
CXCL12	C-X-C chemokine ligand type 12
CXCR4	C-X-C chemokine receptor type 4
DAB	3,3'-diaminobenzidine tetrahydrochloride
DAP12	DNAX-activation protein 12
DCs	dendritic cells
DGCR8	DiGeorge syndrome chromosomal [or critical] region 8
DIG	digoxigenin
DLS	delivery liposome system
DMSO	dimethyl sulfoxide
DNA	deoxyribonucleic acid
DOGS	dioctadecylamidoglycylspermidine
DOPE	1,2-dioleoyl-sn-glycero-3-phosphoethanolamine
EAE	experimental autoimmune encephalomyelitis
ECF	enhanced chemifluorescence substrate
EDTA	Ethylenediaminetetraacetic acid
EGR2	early growth response protein 2
EMP	erythromyeloid precursor

EOAD	early-onset Alzheimer's disease
eQTL	specific quantitative trait locus
EWAS	epigenome-wide association studies
FAD	Familial Alzheimer's disease
FBS	fetal bovine serum
FcRs	Fc receptors
FDA	Food and Drug Administration
FITC	fluorescein isothiocyanate
G-CSF	granulocyte-colony stimulating factor
GDS	geriatric depression scale
GFAP	glial fibrillary acidic protein
GFP	green fluorescence protein
GR1	granulocyte antigen 1
GSK3β	glycogen synthase kinase 3-beta
GWAS	genome-wide association study
H3	Histone 3
hAPP	human amyloid precursor protein
HBSS	Hanks buffered salt solution
HEPES	4-(2-hydroxyethyl)-1-piperazineethanesulfonic acid
HFIP	1,1,1,3,3,3-hexafluoro-2-propanol
HSVTK	herpes simplex virus thymidine kinase
i.p.	intraperitoneal
i.v.	intravenous
IBA-1	ionized calcium-binding adapter molecule 1
IFN-β	interferon beta
IFN-γ	interferon gamma
Ig	immunoglobulins
IL-1	interleukin-1
IL-10	interleukin-10
IL-12	interleukin-12
IL-13	interleukin-13
IL-17	interleukin-17
IL-18	interleukin-18
IL-1β	interleukin-1 beta
IL-2	interleukin-2
IL-4	interleukin-4
IL-5	interleukin-5
IL-6	interleukin-6
IL-8	interleukin-8
iNOS	nitric oxide synthase
IRAK1	IL-1 receptor associated kinase

IRF8	Interferon regulatory factor 8
IVM	intravital microscopy
JAK	Janus kinase
JNK	Jun N-terminal kinase
LD	linkage disequilibrium
LGMN	legumain
LNA	locked nucleic acid
LOAD	late-onset Alzheimer’s disease
LPS	lipopolysaccharide
LTP	long term potentiation
LXRs	liver X receptors
Ly6C	lymphocyte antigen 6C
MACS	magnetic-activated cell sorting
MAPT	microtubule-associated protein tau
MCI	mild cognitive impairment
M-CSF	macrophage-colony stimulating factor
MDMs	monocyte-derived macrophages
MDPs	macrophage and dentritic cell precursors
MHC	major histocompatibility complex
miRNAs	microRNAs
MMSE	Mini–mental State Examination
MoCA	Montreal Cognitive Assessment
MPS	mononuclear phagocyte system
MRI	magnetic resonance imaging
mRNA	messenger RNA
MS4A4E	putative membrane-spanning 4-domains subfamily A member 4E
MS4A6A	myeloid cell-expressed membrane-spanning 4-domains subfamily A member 6A
MX04	methoxy-X04
MyD88	myeloid differentiation primary response 88
NEP	neprilysin
NFI-A	nuclear factor I/A
NFTs	neurofibrillary tangles
NF-κB	nuclear factor kappa B
NG2	neural/glial antigen 2
NGS	normal goat serum
NK	natural killer
NLRP3	NACHT, LRR and PYD domains-containing protein 3
NMDA	N-methyl-D-aspartate receptor
NO	nitric oxide
o.n.	over night

P2RY12	purinergic receptor P2Y, G-protein coupled, 12
PAMPs	pathogen-associated molecular patterns
PBMCs	peripheral blood mononuclear cells
PBS	phosphate buffer saline
PCR	polymerase chain reaction
PD	Parkinson’s disease
PDCD4	programmed cell death protein 4
PET	positron emission tomography
PFA	paraformaldehyde
PICALM	Phosphatidylinositol-binding clathrin
PMSF	phenylmethanesulfonylfluoride
Pol II	RNA polymerase II
PP2A	protein phosphatase-2A
PPARs	peroxisome proliferator activated receptors
PRRs	pattern recognition receptors
PS1	presenilin-1
PS2	presenilin-2
p-tau	hyperphosphorylated microtubule-associated protein tau
PVDF	Polyvinylidene fluoride
qRT-PCR	quantitative real-time polymerase chain reaction
RA	retinoic acid
RAGE	receptors for advanced glycation end products
RFP	red fluorescent protein
RGS10	regulator of G-protein signaling 10
RISC	RNA-inducing silencing complex
RNA	ribonucleic acid
RNA-seq	RNA sequencing
ROI	regions of interest
ROS	reactive oxygen species
RXR	retinoic X nuclear receptor
s.c.	subcutanous
sAPPα	soluble N-terminal fragment of APP alpha (non-amyloidogenic pathway)
sAPPβ	soluble N-terminal fragment of APP beta (amyloidogenic pathway)
SCARA-1	class A scavenger receptor 1
SD	standard deviation
SDS	Sodium dodecyl sulfate
Ser	serine
SHIP1	inositol 5-phosphatase 1
siRNA	small interfering RNA
SNALPs	stable nucleic acid lipid particles
SNPs	single-nucleotide polymorphisms

SOCS-1	suppressor of cytokine signaling 1
SORL1	sortilin-related receptor L 1
SR	scavenger receptors
STAT	signal transducer and activator of transcription
TBS	Tris-buffered saline
TGF-β	transforming growth factor beta
Thr	threonine
TLRs	toll-like receptors
TNF-α	tumor necrosis factor alpha
TPPP	tubulin polymerization promoting protein
TRAF6	TNF receptor associated factor 6
TRBP	TAR RNA binding protein 2
TREM2	triggering receptor expressed on myeloid cells 2
TRIF	TIR domain-containing adapter inducing IFN-β
TYROBP	TYRO protein tyrosine kinase binding protein
WT	wild-type

PREFACE |

The present Thesis explores the role of inflammatory miRNAs in the regulation of mononuclear phagocyte function in Alzheimer's disease (AD) and is divided into six chapters.

The ***first chapter*** is a General Introduction summarizing the recent work on the origin and functions of the different types of cells comprised in the mononuclear phagocyte system, as well as their involvement in the pathophysiology of AD. This chapter also addresses the importance of miRNAs as modulators of immune cell function and their contribution to the inflammatory component of AD. These concepts are instrumental to understand the work described in this Thesis and to acknowledge the important contribution of neuroimmune miRNAs to AD pathophysiology, as well as the pivotal role played by these small molecules in a clinical context.

The ***second chapter*** is a brief description of the main goals of this Work, in the context of the state-of-the-art, regarding the experimental work presented in the subsequent chapters.

The ***third chapter*** describes the characteristics of the inflammatory status of the triple transgenic mouse model of AD at different ages and addresses studies on how miR-155-5p and its transcription factor c-Jun contribute to an age-dependent M1 inflammatory phenotype. Studies on Aβ fibril/oligomer-activated microglia and astrocytes allowed the discovery of inflammatory signaling pathways controlled by miR-155-5p, in which the suppressor of cytokine signaling 1limits the inflammatory response. The contribution of the deregulation of this protein (as a consequence of miR-155-5p upregulation) to a chronic inflammatory state that precedes other important AD hallmarks is also discussed in this chapter.

The ***fourth chapter*** reports on the function of blood-derived monocytes and monocyte-derived macrophages in AD and mild cognitive impairment patients with respect to chemotaxis and phagocytosis, two cellular functions essential to Aβ clearance mechanisms mediated by peripheral mononuclear phagocytes. Moreover, the expression of several inflammatory miRNAs is evaluated and an association of the differences found in some of those miRNAs with the phenotypes observed in blood-derived monocytes is established.

The ***fifth chapter*** describes the potential of bone-marrow-derived monocytes to infiltrate the brain of a transgenic mouse model with five AD mutations. The *ex vivo* modulation of miR-23a-3p in these cells and their subsequent intravenous injection are explored as a possible strategy to decrease the vascular Aβ burden in the brain of these mice. Moreover, the use of miRNAs as therapeutic molecules and targets in the context of AD is proposed and cationic liposomes are investigated as useful vectors to mediate miRNA modulation in bone-marrow-derived monocytes. A manuscript addressing these issues is in preparation.

The ***sixth chapter*** summarizes the relevant findings described in the preceding chapters and contextualizes them regarding future work.

| CHAPTER 1

General Introduction

Part of this chapter was published in:

Reviews:

Guedes, J., Cardoso, A.L., and Pedroso de Lima, M.C. (2013). Involvement of microRNA in microglia-mediated immune response. Clin Dev Immunol 2013, 186872.

Guedes, J., and El Khoury, J. (2015). Role of Chemokines and their receptors in regulating Alzheimer's disease-associated β amyloid and Tau pathologies. Frontiers in Neuroscience; section Neurodegeneration; Research topic: Glial cells and inflammation: the fine intersection to initiation and progression of neuronal damage (in revision)

Cardoso, A.L., Guedes, J., and Pedroso de Lima, M.C. (2016). Role of microRNAs in the regulation of innate immune cells under neuroinflammatory conditions. Current Opinion in Pharmacology (in press)

Book Chapter:

Guedes, J., Viegas, A.T., Pedroso de Lima, M.C., and Cardoso, A.L. (2015). Microglia: A Double-Edged Sword for Alzheimer's Disease, In: Microglia: Physiology, Regulation and Health Implications (E. R. Giffard Editor), Nova Science Publishers, Inc. New York, Chapter 1, 1-65

1.1. *The mononuclear phagocyte system*

The innate immune system constitutes our first line of defense against most impending threats and is an integral part of the overall immune organization, comprising cells and mechanisms which primarily protect the host against infections by external organisms. The most important cellular players of innate immunity are components of the mononuclear phagocyte system (MPS), a concept established by van Furth and Cohn in 1968. These authors suggested, for the first time, that blood monocytes did not originate from lymphocytes, but were derived from bone-marrow progenitors and were able to infiltrate tissues during inflammation, leading to different types of macrophages (van Furth and Cohn, 1968).

Currently, the classification of mononuclear phagocytes remains a challenge owing to the lack of specific and irrefutable protein membrane markers. In this context, the different cell types of this system are categorized on the basis of a group of characteristics, rather than a single cellular property, such as protein/enzymatic markers, localization, function and cell progenitors. In the present thesis, the classification used for mononuclear phagocytes was that established by Ransohoff and Cardona in 2010. According to these authors, monocytes are mononuclear phagocytes which circulate in the blood stream, while macrophages are mononuclear phagocytes that reside within tissues; dendritic cells (DCs) are mononuclear phagocytes able to present antigens and activate naïve T cells; microglia are mononuclear phagocytes resident in the central nervous system (CNS) (Ransohoff and Cardona, 2010).

1.1.1. *Monocytes and macrophages*

1.1.1.1. *Monocyte development*

Monocytes are conserved leukocytes, representing between 5 and 10% of all peripheral blood mononuclear cells (PBMCs) with minimal pools in the spleen and lungs and, as more recently discovered, in lymph nodes (Jakubzick et al., 2013). During development, monocytes derive from myeloid bone-marrow precursors, termed macrophage and DC precursors (MDPs) (Fig. 1.1), which can also originate DCs in lymphoid and non-lymphoid tissues. In the bone-marrow, MDPs give rise to common monocyte progenitors (cMoPs) (Fig. 1.1), which lack CD135 expression when compared to MDPs and do not generate DCs (reviewed in (Ginhoux and Jung, 2014)). In mice, monocyte development is strictly dependent on the macrophage-colony stimulating factor (M-CSF) and its receptor CD115 (Cecchini et al., 1994), expressed in both MDPs and cMoPs. Nevertheless, representations of hematopoietic development should be considered with caution, since the different precursors and cell populations have been historically defined on the basis of a restrict panel of markers, often incomplete. Most of the identified distinct progenitors can be part of heterogeneous populations and the expression of specific surface markers can occur as a continuum that can only be fully understood taking into consideration the transcriptional kinetics of these proteins during differentiation. Moreover, distinction of bone-marrow monocyte precursors in humans is still an unexplored subject, although a very recent study identified two bone-marrow monocyte precursor intermediates using an *in vitro* culture system (Lee et al., 2015).

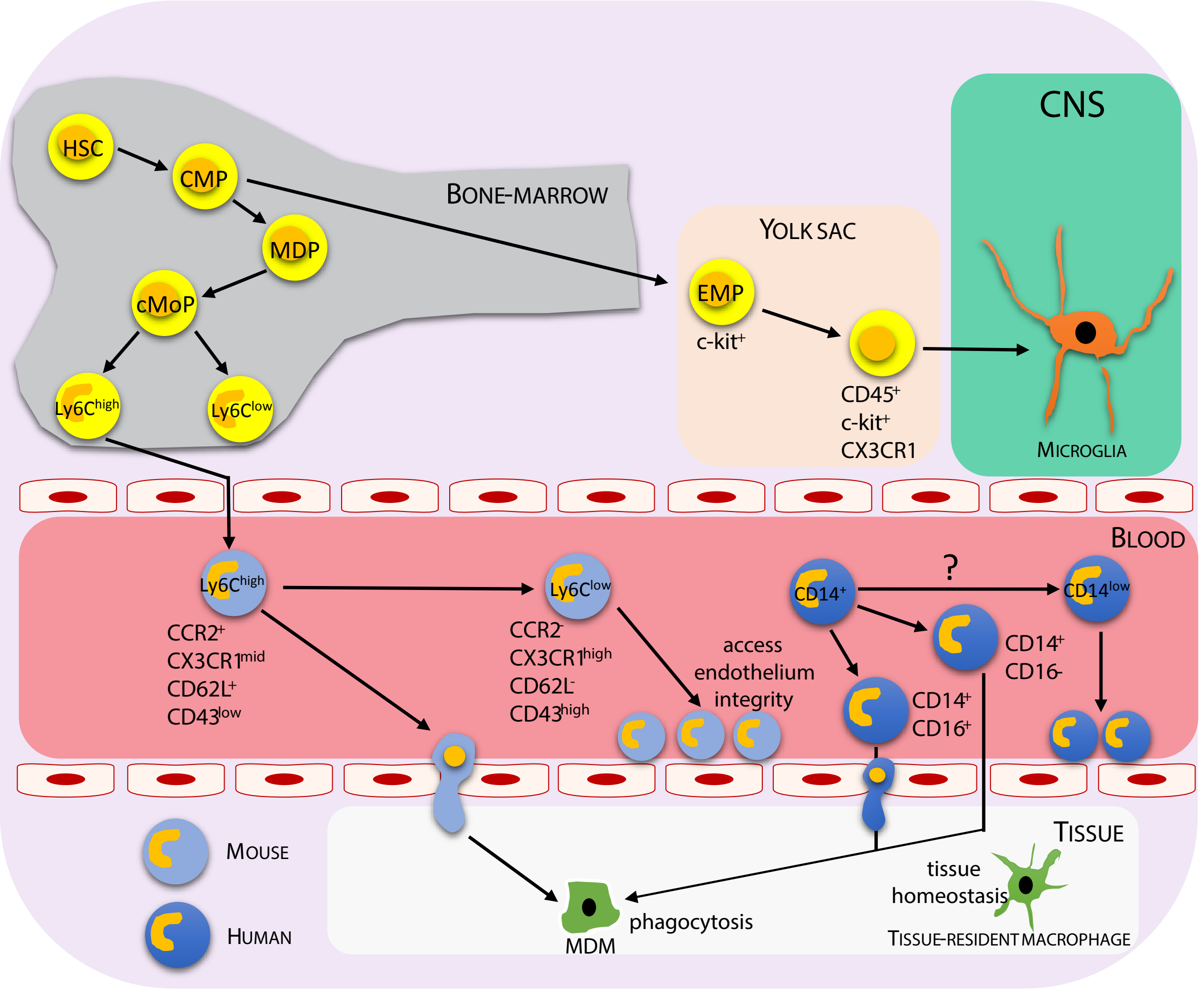
HSC
CMP
BONE-MARROW
MDP
cMoP
Ly6Chigh
Ly6Clow
YOLK SAC
EMP
c-kit+
CD45+
c-kit+
CX3CR1
CNS
MICROGLIA
BLOOD
Ly6Chigh
CCR2+
CX3CR1mid
CD62L+
CD43low
Ly6Clow
CCR2-
CX3CR1high
CD62L-
CD43high
access
endothelium
integrity
CD14+
?
CD14low
CD14+
CD16-
CD14+
CD16+
MOUSE
HUMAN
TISSUE
tissue
homeostasis
TISSUE-RESIDENT MACROPHAGE
phagocytosis
MDM

Figure 1.1 | Mononuclear phagocyte system (MPS): cell progenitors, localization and functions. Monocytes are generated in the bone-marrow from common myeloid progenitors (CMPs), macrophage and dendritic cell (DC) precursors (MDPs) and common monocyte progenitors (cMoP) intermediates (Ginhoux and Jung, 2014). In the blood, Ly6C^{high} monocytes in mice and their human counterparts, CD14^{+} monocytes, infiltrate tissues under certain inflammatory stimuli to give rise to monocyte-derived macrophages (MDM), while Ly6C^{low} and CD14^{low} monocytes patrol blood vessels and control endothelium integrity. During development, CMPs also generate erythromyeloid precursors (EPM) which, in turn, develop into CD45^{+}c-kit^{-}CX3CR1^{+} cells and proliferate, originating microglia in the central nervous system (CNS) (Kierdorf et al., 2013).

1.1.1.2. *Monocyte subsets and tissue infiltration*

In the blood, CD14 is accepted as the universal marker of human monocytes, although we can consider three distinct populations based on the differential expression of both CD14 and CD16: CD14^{+}CD16^{+}, CD14^{+}CD16^{-} and CD14^{low}CD16^{+} (Fig. 1.1). These monocyte populations have distinct capacities to secrete inflammatory cytokines, upon *in vitro* stimulation (Frankenberger et al., 1996). In mice, CD115$^+$ blood monocytes subsets comprise Ly6C^{high}CCR2$^+$CX3CR1^{mid}CD62L$^+$CD43^{low} and Ly6C^{low}CCR2$^-$CX3CR1^{high}CD62L$^-$CD43^{high} (Fig. 1.1) (Jakubzick et al., 2013). Mouse monocyte subsets have human counterparts (Fig. 1.1), yet they present important differences and their functions remain to be fully elucidated.

Even though, for many years, circulating monocytes were thought to infiltrate tissues and differentiate into macrophages, we now believe that monocytes do not substantially contribute to the subpopulations of macrophages within tissues (Hashimoto et al., 2013; Yona et al., 2013), unless under specific inflammatory conditions (Wynn et al., 2013). Instead, in order to originate tissue-resident macrophages, embryonic precursors travel to tissues during development and differentiate, *in situ*, under the influence of specific environmental cues, maintaining themselves through self-renewal during adult life. Despite the fact that all subtypes of monocytes and tissue-resident macrophages share similarities, in terms of their dependency on the transcription factor PU.1 and CD115 downstream signaling (Wynn et al., 2013), each population of tissue-resident macrophages has its own gene expression program (Gautier et al., 2012). PU.1 is absolutely essential for the hematopoietic system and its absence abolishes the development of macrophages (M. et al., 1996). PU.1 expression is directly controlled by C/EBPα, although its levels have to be relatively high when compared to C/EBPα, to avoid favoring the granulocyte lineage and promote monocyte development (Yeamans et al., 2007). In addition to PU.1 and C/EBPα, a very recent study showed the importance of another transcription factor, the interferon regulatory factor 8 (IRF8), for monocyte development. IRF8 physically interacts with C/EBPα and inhibits its binding to chromatin in MDPs and cMoPs, preventing neutrophil differentiation and promoting myeloid linages (Kurotaki et al., 2014).

In a steady state condition, monocyte subsets in the blood constitute a mere classification, since a cell Ly6C^{high} can rapidly change to Ly6C^{low} (Yona et al., 2013). Ly6C^{low} monocytes have as their main function to patrol blood vessels and access endothelium integrity, while LyC6^{high} cells, and their CD14$^+$ human counterparts, are considered the classic monocytes, with the capacity to infiltrate tissues upon inflammation (Fig. 1.1). Once in the tissues, these cells are the precursors of monocyte-derived macrophages (MDMs) (Fig. 1.1), which differ from tissue-resident macrophages. In terms of function, the differences between MDMs and tissue-resident macrophages are yet to be completely understood. Nevertheless, MDMs are believed to possess a high phagocytic ability and to contribute to the establishment and resolution of local inflammation, while tissue-resident macrophages are strictly important for tissue homeostasis purposes. Either way, it is reasonable to think that MDMs are more prone to manipulation in terms of inflammation-targeted therapies than tissue-resident macrophages, owing to the considerable accessibility to their blood monocyte precursors. However, it is imperative to discern the specific ontogenies of individual populations of monocytes and macrophages, in order to take full advantage of their therapeutic potential.

1.1.2. *Microglia as the hematopoietic cells of the central nervous system*

Microglia constitute a privileged type of tissue-resident macrophages that populate the unique environment of the nervous tissue. The absence of DCs, which are usually the innate immune cell type responsible for presenting antigens derived from external infection agents, makes the CNS a unique immune space, profoundly repressed (Galea et al., 2007). This status is essentially maintained by the interactions between microglia and neurons (Galea et al., 2007), which are responsible for shaping microglia phenotype through the activation of tissue-specific genomic super-enhancers near genes, such as *Cx3cr1* (Gosselin et al., 2014), which, in turn, are essential for brain function. Similarly to what occurs for other tissue macrophages, parabiosis studies have shown that blood monocytes and other bone-marrow progenitors do not contribute to the adult microglia population in the CNS (Hashimoto et al., 2013).

1.1.2.1. *The origin of microglia*

In the 1990s, Cuadros and colleagues suggested, for the first time, that microglia could derive from primitive myeloid cells originating from the embryonic yolk sac (Cuadros et al., 1993). This proposal was later supported by the work of Alliot and coworkers, who showed the presence of microglia precursors first in the yolk sac and later, at embryonic day 8, at the brain rudiment (Alliot et al., 1999). However, the first paper definitely establishing the hematopoietic origins of microglia dates from 1996, when PU.1 null mice were shown to lack tissue macrophages, including Kupffer cells and microglia (M. et al., 1996).

Nevertheless, it was only in 2010 that a fate mapping analysis revealed that adult microglia derive from primitive embryonic progenitors from the yolk sac, which arise before embryonic day 8 and maintain themselves by self-renewal, rather than from definitive circulating hematopoietic precursors (which include monocytes) (Ginhoux et al., 2010). This study also showed that microglia are dependent on the presence of CD115 but not M-CSF, and that the time-window in which microglia progenitors populate the CNS is very restrict (Ginhoux et al., 2010), suggesting that microglia development in CNS is a tightly controlled process, timely and spatially-regulated. Despite this instrumental achievement in the discovery of microglia origin, the true progenitor of the hematopoietic lineage remained unknown. Finally, in 2013, Kierdorf and coworkers discovered that microglia derive from c-kit$^+$ erythromyeloid precursors (EMP), which develop into CD45$^+$c-kit$^-$CX3CR1$^+$ cells and proliferate originating microglia, before their invasion of the developing brain (Fig. 1.1) (Kierdorf et al., 2013).

1.1.2.2. *Microglia roles in brain homeostasis and injury*

Although the multiple functions of microglia during brain injury are well established, the role of these cells under healthy conditions has been largely underestimated. Microglia cells found in the healthy mature CNS were considered to be mainly inactive and in a "resting state", characterized by the low or absent expression of activation-associated molecules and a "steady" ramified morphology (Kreutzberg, 1996). However, recent studies have revealed a set of new functions for these cells that are just beginning to be fully explored, suggesting that the term "resting state" is far from being realistic.

In 2005, the first *in vivo* imaging studies of microglia in the mouse cortex completely challenged the previous dogmas of microglia function. Indeed, based on real-time recordings, it was possible to observe the continuous cycles of extension and retraction of the finer microglial processes. These recordings proved that the smaller processes of branched microglia exhibited a highly motile behavior, while their cell bodies and main processes remained static (Davalos et al., 2005; Nimmerjahn et al., 2005), constituting the first real-time demonstrations of the tissue surveillance function of these cells in the unperturbed mammalian brain. Even when quiescent, microglia are extremely dynamic cells and their motile processes are constantly surveying the brain environment for signs of neural damage. Upon appearance of cues indicating a danger situation, these cells are ready to progress into "activated" states and respond quickly to any detected threat. Therefore, and based on these observations, we can consider a transition from a "surveying" to an "activated" phenotype, which represents a shift in the cell activity rather than "activation" *per se*, emphasizing that microglia is always functionally dynamic, without periods of inactivity (Kettenmann et al., 2011). The discoveries regarding microglia activity in the healthy brain have led to a series of recent studies that suggest potential roles for these cells during postnatal development and in the modulation of adult neuronal plasticity and circuit function (Tremblay et al., 2011), through the establishment of direct connections between microglia branches and presynaptic terminals, dendritic spines and perisynaptic astrocytic clefts (Tremblay et al., 2010).

Due to their potential to instigate good and bad outcomes, and in order to maintain normal tissue homeostasis, microglia activity must be closely regulated. Several mechanisms have been identified as being responsible for the shift between "surveying"/"activated" microglia. These mechanisms include the interaction of microglia with neurons and other glial cells, through secreted mediators, the activation or inhibition of transcription factors and, more importantly, the regulation of surface and nuclear receptors (Saijo et al., 2013). Astrocytes seem to play an important regulatory role during the processes of microglial differentiation and activation, given their capacity to act as antigen-presenting cells (Frohman et al., 1989). Although both astrocytes and microglia contribute to neuroinflammation, their response to similar stimuli is quite different, since astrocytes tend to produce neurotrophic support and tissue remodeling factors, even when microglia produce pro-inflammatory mediators. In what concerns neuron-microglia interactions, during embryonic development, microglia cells are responsible for early synaptic pruning and establishment of effective neuronal circuits. In the adult brain, microglia cells are capable of examining the brain microenvironment in order to identify and eliminate death or severely damaged neurons (Limatola and Ransohoff, 2014). The CX3CL1/CX3CR1 axis has been described as an important component in this interaction (Biber et al., 2007) and might have a role in the control of production and release of microglia cytokines (Zujovic et al., 2000; Mizuno et al., 2003).

The activation phenomenon in microglia is characterized by profound cytoskeletal rearrangements that allow extensive morphological changes, stereotypic transcriptional alterations and cell proliferation and migration to the threatened region, participating in phagocytosis and destruction of pathogens, as well as in the removal of cellular debris (Salter and Beggs, 2014). Furthermore, during this process, microglia can acquire the ability to act as antigen-presenting cells and upregulate the expression of a large number of molecules, such as adhesion molecules, transcription factors and surface receptors, including the major histocompatibility complex (MHC) and complement receptors (Lynch, 2009). Microglia response is defined by the exact nature of the perceived threat and can range from an overtly pro-inflammatory reaction (M1 classical activation phenotype), designed to destroy invading pathogens and characterized by a strong expression of pro-inflammatory mediators, including cytokines, chemokines, nitric oxide (NO), reactive oxygen species (ROS) and proteolytic enzymes, to a more restrained state, which promotes communication with other immune cell types, tissue remodeling, production of anti-inflammatory molecules, trophic support and phagocytosis (M2 alternative activation phenotypes) (Heneka et al., 2014).

Microglia ability to perceive its environment is possible due to the expression of several surface and nuclear receptors. The pattern recognition receptors (PRRs) are the most important membrane receptors studied in mononuclear phagocytes and constitute a broad family of proteins responsible for identification of exogenous pathogens, which then translates into the production of extracellular superoxide, the release of pro-inflammatory compounds and the removal and destruction of toxic molecules through phagocytosis. However, neurotoxicity can occur through PRR activation when pathogen-associated molecular patterns (PAMPs) trigger an excessive immune response, or when stimuli of endogenous origin (toxins, endogenous proteins and neuronal damage leftovers) are misinterpreted as pathogens.

PRRs comprise several receptor subfamilies, including Toll-like receptors (TLRs), whose members are able to recognize PAMPs of different origins and initiate a strong immune response. This family of membrane proteins comprises 12 members in mammals, some of which are expressed in a variety of cells, including microglia and astrocytes (Doens and Fernandez, 2014).

TLRs are activated by lipopolysaccharide (LPS), teichoic acids, peptidoglycans and diverse forms of nucleic acids, triggering innate inflammatory responses that are usually dominated by NF-κB-mediated production of cytokines, and chemokines. Thus, TLR-mediated response is known to progress as a pro-inflammatory host-defense response, helping removing invading pathogens (Walter et al., 2007). TLR expression is hardly detectable in "surveying" microglia, in the healthy CNS. Nevertheless, multiple TLRs rapidly appear at the cell surface and in the lysosomal membrane upon microglia activation. Although microglia cells have been reported to express TLRs 1-9 (Doens and Fernandez, 2014) at readily detectable levels (Bsibsi et al., 2002), TLRs 1-4 are the ones mainly expressed in these cells. TLR4 has been described as an LPS and INF-γ receptor, although it is capable of recognizing other endogenous and exogenous molecules. Therefore, LPS and INF-γ are TLR agonists that induce the classical M1 activation phenotype, which is relevant to respond to bacterial and viral infections (Saijo and Glass, 2011).

The members of the TLR family share structural properties in their extracellular leucin-rich repeat structures, designed to register the presence of multiple ligands, and also in their intracellular domains, which interact with intracellular adapter proteins that relay the agonist engagement signal. The MyD88 is the most notorious adapter of the TLR family. In fact, the signaling pathways activated by TLRs are broadly classified into MyD88-dependent and independent pathways. MyD88 relays the signal for most TLR family members to other adapter molecules and predominantly induces NF-κB-mediated activation of gene expression, leading to an increase in the levels of TNF-α, CCL5, IL-1β, and IL-8. When MyD88 and TIR domain-containing adapter inducing INF-β (TRIF) are recruited to the membrane domain of the TLR receptor, the signal cascades are initiated. MyD88 serves as a bridge between TLR and IL-1 receptor associated kinase (IRAK1) and the signaling complex TNF receptor associated factor 6 (TRAF6). Thus, all TLRs elicit conserved inflammatory pathways, culminating in the activation of the transcription factors NF-κB and AP-1. My-D88-independent activation of TLRs normally depends on JAK-STAT proteins, both being targets of the suppressor of cytokine signaling 1 (SOCS-1), which directly inhibits LPS signaling (Kimura et al., 2005).

Other membrane receptors are important for the regulation of microglia functions: the Fc receptors (FcRs), capable of binding to the constant domain (Fc) of immunoglobulins (Ig), thus triggering phagocytosis, degranulation and cytokine and chemokine secretion; scavenger receptors (SR), divided into two classes - class A SR (SR-A/SCARA-1) and class B SR type 2 (also known as CD36), which are important for lipid metabolism, and receptors for advanced glycation end products (RAGE), natural receptors for advanced glycosylation end products (AGEs), which are formed when a reduced sugar reacts with proteins and complement receptors (CR), promoting phagocytosis of pathogens.

Regarding nuclear receptors, one of the largest families identified in microglia cells are the peroxisome proliferator activated receptors (PPARs). These receptors are ligand-inducible transcription factors, belonging to the superfamily of nuclear hormone receptors bearing an E/F domain responsible for their dimerization with liver X receptors (LXRs) (Heneka and Landreth, 2007; Mandrekar-Colucci et al., 2012). PPARγ is the dominant form in microglia and an important regulator of the M2 alternative activation state. Finally, inflammasomes are intracellular multiprotein complexes involved in caspase-1 activation, mediating the cleavage of inactive IL-1β and IL-18 precursors and leading to the secretion of the mature forms of these cytokines. Altogether, all these receptor families coordinate the surveillance and detection response of microglia cells, contributing to their function as enforcers of brain homeostasis and to the triggering of the different activation phenotypes.

1.1.3. *Distinguishing mononuclear phagocyte system cells: how to study the mononuclear phagocyte system?*

In addition to having the same hematopoietic precursors and similar functions in different tissues, the various cell types of the MPS share transcriptional similarities based on the actions of important transcription factors, such as PU.1 and NF-κB (Heinz et al., 2013). These linage- and signal-determining transcription factors have collaborative and hierarchical relationships, which allow to establish the mononuclear phagocyte linage and, equally important, to transduce the effect of a particular microenvironment into specific behaviors of macrophages within different tissues, without loss of the overall macrophage identity (Heinz et al., 2013). Recently, high-throughput studies focusing on the transcriptome of different types of MPS allowed to better understand the diversity of gene expression observed among different macrophage populations, also revealing new cues on how to distinguish these cells from DCs (Gautier et al., 2012).

Importantly, and owing to the particular nature of the immune environment within the brain, a specific interest has grown within the scientific community in understanding the differences in the transcriptome and epigenome between microglia and other tissue-resident macrophages and feeding the necessity to perform more complex and detailed studies.

In 2014, Gosselin and coworkers studied the role of the tissue microenvironment in determining the function of transcription factors, which hierarchically bind to genomic super-enhancers near genes essential for mononuclear phagocyte function within a specific tissue (Gosselin et al., 2014). This study demonstrated that the tissue environment regulates collaborative and signal-dependent transcription factor expression and binding, and that peritoneal macrophages and microglia cultured with retinoic acid (RA) and transforming growth factor beta (TGF-β) disproportionately regulate genes that drive macrophage- and microglia-specific phenotypes, respectively (Gosselin et al., 2014). This study corroborates the old hypothesis that culturing these cells modifies their phenotype, highlighting some features and hiding others, a subject discussed below.

Regarding the distinction between microglia and other tissue-resident macrophages, in addition to their different ontology, these cells present obvious differences in morphology. Microglia small body and ramified shape greatly contrast with the typical amoeboid form of macrophages. Although in early development microglia progenitors lack ramified processes, the proliferation and differentiation program that is triggered upon arrival at the brain rudiment leads to the acquisition of a typical ramified architecture, which is found in adult microglia and is crucial to allow the continuous monitoring of the brain environment.

In addition to visible morphological differences, microglia and other tissue-resident macrophages present intrinsic molecular signatures, derived from the function of specific signal-dependent transcription factors. Recently, several studies have used high-throughput analysis to ascertain the major differences and similarities between microglia, macrophages and monocytes. Hickman and colleagues used a combination of direct RNA sequencing (RNA-seq), fluorescent dual *in situ* hybridization, quantitative PCR and proteomic analysis to study the transcriptome and proteome of mouse microglia and peritoneal macrophages under surveillant conditions (Hickman et al., 2013). Of the top 10% transcripts with higher expression in both cell types, the authors found that 70% of the transcripts were shared between microglia and macrophages, while 30% were expressed by only one of these cell types. This allowed them to identify a molecular signature that defines microglia cells and distinguishes them from other types of tissue-resident macrophages. Included in this signature are several genes related with tissue surveillance (sensome genes), such as *P2ry12, P2ry13, Tmem119, Gpr34, Siglech, Trem2* and *Cx3cr1*, as well as other unexpected genes, such as *HexB,* that encodes the hexosaminidase B, and *Camp* and *Ngp*, which encode antimicrobial peptides (Hickman et al., 2013). Interestingly, a large number of the sensome genes that were found to be exclusively expressed by microglia, recognize endogenous ligands rather than pathogens, which implies that microglia cells express a unique set of genes that better suits them to carry their monitoring role specifically in the brain environment.

Another study, performed by Butovsky and coworkers, employing gene profiling analysis (gene arrays and nanostring technology) and quantitative mass spectrometry analysis, compared gene expression in adult mouse microglia and Ly6C$^+$CD11b$^+$ monocytes, suggested to be recruited to the CNS following neuroinflammatory insults (Butovsky et al., 2014). The authors identified 1572 genes enriched in microglia, from which *Fcrls, P2ry12, Mertk* and *Pros1* were particularly expressed in these cells. Mass spectrometry analysis confirmed the differential expression of 455 proteins between microglia and monocytes, highlighting 5 proteins as important microglia markers: purinergic receptor P2Y, G-protein coupled, 12 (P2RY12), legumain (LGMN), tubulin polymerization promoting protein (TPPP), myc box-dependent-interacting protein 1 (BIN1) and regulator of G-protein signaling 10 (RGS10). Importantly, in this work, the authors answered a crucial but often neglected question in this field, regarding the translation of results obtained in mouse microglia to the context of human cells. By performing qRT-PCR to quantify signature genes in human fetal and adult brain-derived microglia and blood-derived $CD14^+CD16^-$ and $CD14^+CD16^+$ monocytes, they found that *P2ry12, Gpr34, Merkt, C1qa, Pros1* and *Gas6* were uniquely expressed or highly enriched in human microglia and not in mouse microglia (Butovsky et al., 2014). Finally, further comparison of the expression of the identified molecular signature genes with other CNS cell populations, including neurons, astrocytes and oligodendrocytes, revealed that *Fcrls, Olfm13, Tmem119, P2ry12, Hexb* and *Tgfbr1* were absent in all other brain cell types and could be considered unique microglial genes (Butovsky et al., 2014).

Although there is available information on different gene programs in different MPS cells, the underlying studies have been performed right after cell isolation. Often, we need to study basic functional features and, for that purpose, monocyte, macrophage and microglia primary cultures are obtained and employed as *in vitro* models. However, it is important to note that the extraction process, by itself, can modify the phenotypes of these cells and, as previously discussed, pups *vs* adult and mouse *vs* human microglia present significant differences in their transcriptome. Several technical complications are associated with *in vitro* cultures of primary microglia. First, the cell yield of microglia primary cultures from mouse brains is very low and the cells are difficult to maintain in culture in a "surveying" phenotype. Second, the mechanical isolation process contributes to microglia activation, making it very difficult to distinguish the changes in microglia phenotype associated with *in vitro* stimuli from changes due to the isolation procedure, *per se*. Third, the addition of non-physiological serum to the cell medium provides activating substances that mask the effects of the *in vitro* stimulus under study.

Although studies involving mononuclear phagocytes cultures have greatly contributed to our current knowledge about the important role of these cells, we lack powerful *in vivo* tools that allow the *in situ* visualization of these cells in their natural environment. Indeed, while *in vitro* studies have contributed to the discovery of activating molecules and important signaling pathways, *in vivo* systems enable us to understand the interactions between these molecules in space and time. Although there is still a long way to go, in recent years investigators have developed new techniques to visualize microglia *in vivo*, preserving normal cell composition, cellular interactions, morphology and dynamics. By creating transgenic mouse models that express fluorescent proteins under the control of specific promoters, originating microglia/monocyte markers, and by using real-time intra-vital microscopy, it is now possible to observe the behavior of these cells in their normal environment, both in health and disease. In this regard, Jung and coworkers developed an important mouse model in which the animals express the green fluorescence protein (GFP) under the control of the promoter of the *CX3CR1* gene ($Cx3cr1^{gfp/+}$ mice) (Jung et al., 2000), which encodes a chemokine receptor expressed in monocytes, subsets of natural killer (NK) cells and DCs. In the brain of these mice, microglia cells are the only cell type that expresses the CX3CR1 receptor, since GFP expression was shown to be undetectable in neurons, neural/glial antigen 2 (NG2) positive glia and glial fibrillary acidic protein (GFAP) positive astrocytes (Jung et al., 2000; Cardona et al., 2006). The development of this mouse model has allowed the use of two-photon *in vivo* imaging to clarify the surveying nature of microglia cells (Davalos et al., 2005; Nimmerjahn et al., 2005), to study morphological changes during LPS activation (Kozlowski and Weimer, 2012), to observe microglia turnover in the mouse retina after ionizing radiation and dexamethasone treatment (Alt et al., 2014), to investigate the efficacy of drugs and the differential role of microglia and blood-derived macrophages following spinal cord injury (Evans et al., 2014) and to understand the origin of microgliosis upon an ischaemic stroke (Li et al., 2013). Furthermore, in 2010, Saederup and coworkers created CCR2-red fluorescent protein knock-in mice ($Ccr2^{\mathrm{rfp}/+}$ mice) and crossed them with the $Cx3cr1^{\mathrm{gfp}/+}$ mice (Saederup et al., 2010). The resulting $Cx3cr1^{\mathrm{gfp}/+}Ccr2^{\mathrm{rfp}/+}$ mice have been used to disclose how myeloid lineages differentiate during development to generate microglial cells (Mizutani et al., 2012), and to study microglia behavior in an experimental autoimmune encephalomyelitis (EAE) model, as well as to distinguish microglia from infiltrating peripheral monocytes in this disease model (Yamasaki et al., 2014).

Studies performed in these mouse models have already changed our view on the nature of mononuclear phagocytes, by showing that these cells have different ontologies and roles in both tissue homeostasis and inflammation. At the moment, these mice constitute the most powerful tool to study the contribution of mononuclear phagocytes to CNS injury, but also in the healthy adult brain. Furthermore, these findings will undoubtedly have a major impact on the design of new cell-specific therapeutic strategies, aiming at promoting the modulation of neuroinflammatory events in the brain.

1.2. *Alzheimer's disease: a heavy burden for the future*

Dementia is a major global health concern, with an estimated worldwide prevalence in 2013 of 4.4 million people and a predicted increase of 75.6 million by 2030 and of 135.5 million by 2050 ("2014 Alzheimer's disease facts and figures," 2014). Alzheimer's disease (AD) is the most common form of elderly dementia worldwide and accounts for an estimated 60-80% of all dementia cases ("2014 Alzheimer's disease facts and figures," 2014).This disease was first reported in 1906 by the psychiatrist and neuropathologist Alois Alzheimer, and later named after him, who described it as a progressive neurodegenerative disease that could take from 5-20 years to run its course.

Early clinical symptoms, which can appear a decade before brain pathological markers, include difficulty in remembering recent conversations, names or events, apathy and depression. Later symptoms comprise memory, learning and communication impairment, disorientation and confusion, behavior changes, inability to execute motor activities, such as speaking, walking and swallowing, and general decline in cognitive skills that eventually lead to death ("2014 Alzheimer's disease facts and figures," 2014). AD is now considered one of the main economic burdens of the modern society, deeply affecting not only the patients but also their families. Since the burden imposed by this disease to the healthcare system is enormous and, with time, the costs to sustain and provide adequate care to patients will become unaffordable, it is absolutely essential to find proper diagnosis and treatment techniques which, at the moment, are almost inexistent.

The clinical diagnosis, although not definitive, is achieved with the use of cognitive tests, physical and neurologic examinations and other complementary tests, such as magnetic resonance imaging (MRI), employed to measure hippocampal volume, positron emission tomography (PET) scanning, which searches for brain changes, including metabolic alterations and neuroinflammation ("2014 Alzheimer's disease facts and figures," 2014), and biomarker analysis, which includes amyloid-β (Aβ) and hyperphosphorylated microtubule-associated protein tau (p-tau) quantification in the cerebral spinal fluid (CSF). However, the definitive diagnosis is only possible post-mortem through the detection of typical AD hallmarks in the brain tissue.

The clinical interest in establishing early diagnosis has led to the preposition of a transitional state between normal aging and dementia, classified as mild cognitive impairment (MCI) (Petersen et al., 1999). This state aims to identify and characterize individuals who present abnormal memory impairment considering their age, but continue to perform their daily-life activities and cannot be considered demented. The close observation of these individuals is essential to identify patients whose impairment will progress to AD, which occurs, every year, in 12% of the cases (Petersen, 2011). In the clinic, there are cognitive tests, such as the Mini–mental State Examination (MMSE), the Montreal Cognitive Assessment (MoCA) and the Alzheimer's disease Assessment Scale-Cognitive (ADAS-cog), which constitute valuable tools to allow the distinction between AD and MCI patients. Nevertheless, the experience of professional health workers, such as neurologists, phycologists and nurses, is absolutely essential to fully characterize these patients, allowing a proper clinical diagnosis and follow-up.

According to the current diagnosis criteria, AD can be divided into early-onset (EOAD) and late-onset Alzheimer's disease (LOAD). EOAD is a rare form of the disorder, affecting people before the age of 65 and accounting for 10% of AD cases. Familial Alzheimer's disease (FAD), which accounts for only 1% of all AD cases, can be included in EOAD and is characterized by a strong genetic predisposition, usually presenting an earlier onset during the fourth decade of life. The LOAD subgroup includes most cases of AD, comprising mostly people with more than 65 years of age. LOAD corresponds to 90% of all AD cases and its causes may or may not be hereditary.

The strongest and most well-known genetic risk factors for AD are mutations in *APP*, *PS1* and *PS2* genes. These genes encode the amyloid precursor protein (APP), presenilin-1 (PS1) and presenilin-2 (PS2), respectively. In addition to APP, which originates Aβ peptides, both PS1 and PS2 play essential roles during the production of Aβ, since they are important components of the γ-secretase complex, responsible for cleaving APP (reviewed in (Karch et al., 2014)). Mutations in these genes constitute the main evidence supporting the amyloid cascade hypothesis (ACH), which postulates that deposition of Aβ is the causative agent of AD and that all the following pathological hallmarks derive from this event (Hardy and Higgins, 1992). *APP* mutations correspond to approximately 14% of EOAD autosomal dominant cases, while *PS1* and *PS2* mutations constitute 85% of all early-onset FAD cases.

The most important LOAD risk factor to date is the apolipoprotein E (ApoE) genotype. ApoE is a protein expressed in the liver, brain and macrophages, being involved in cholesterol metabolism. There are five identified alleles of ApoE, three of them with high prevalence (*ApoEε2*, *ApoEε3* and *ApoEε4*). *ApoEε4* has been demonstrated to increase the risk of both familial and sporadic EOAD and LOAD. Heterozygous carriers have a 3-fold increased risk of developing AD, while homozygous carriers have a 8- to 10-fold risk increase (reviewed in (Karch et al., 2014)). Despite the strength of this risk factor, the mechanisms that explain the relationship between *ApoEε4* and AD remain somewhat unclear. Nevertheless, *ApoEε4* has been linked with an increase in Aβ production and oligomerization (Balin and Hudson, 2014; Karch et al., 2014).

Considering the important role of ACH in explaining the etiology and pathogenesis of AD, three mains therapeutic strategies have been acknowledged for this disease: 1) reducing Aβ production, 2) facilitating Aβ clearance and 3) preventing Aβ aggregation (Karran et al., 2011). However, at present, the only AD-targeted drugs approved by the USA Food and Drug Administration (FDA), consist in cholinesterase inhibitors or N-methyl-D-aspartate receptor (NMDA) antagonists, which try to restrict cognitive impairments and decrease excitotoxicity. These drugs act long after the appearance of pathological hallmarks, including neuron death and, therefore, constitute a poor attempt to prevent the progression of cognitive decline, only lessening disease symptoms. In the last decade, clinical trials with anti-inflammatory drugs have been performed, although with disappointing results (reviewed in (Heneka et al., 2015a)). This is not completely surprising if one considers that neuroinflammation is associated with normal ageing and is a stage-dependent event. Based on these observations, it is clear that, at present, therapeutic strategies targeting AD are scarce and, in general, unsuccessful.

In what concerns the approaches still under development, at a pre-clinical stage, most strategies aim to increase Aβ clearance or slowdown/prevent Aβ production through the inhibition of β-secretase (BACE1). This has been tried using microRNAs (miRNAs), targeting the 3' untranslated region (3'UTR) of BACE1 (clinicaltrials.gov identifier: NCT01819545), or through the use of γ-secretase inhibitors, such as the drug semagacestat (Doody et al., 2013).

More recently, immunotherapy strategies have gained some relevance in the context of AD treatment. Although many strategies involving active Aβ immunization have failed in the last years, there are ongoing clinical trials with anti-Aβ antibodies (clinicaltrials.gov identifier: NCT01900665) and one of the proposed mechanisms of action for the tested drugs is based on the modulation of microglia phagocytosis through FcRs and other receptors with similar function (Weiner and Frenkel, 2006). In fact, in non-genetic AD cases, the modulation of Aβ clearance by immune cells through phagocytosis is believed to be one of the most promising therapeutic strategies.

1.2.1. *Pathophysiology of Alzheimer's disease*

Pathologically, AD is characterized by progressive neuronal loss and neuroinflammation, particularly in the hippocampus and cerebral cortex. Two major hallmark lesions can be highlighted in this neurodegenerative disorder: extracellular senile plaques, composed of different aggregation forms of Aβ peptides, such as oligomers and fibrils, surrounded by astrocytes and microglia, and intraneuronal neurofibrillary tangles (NFTs), containing p-tau aggregates. These features are frequently accompanied by neuronal damage and death, since these protein aggregates present neurotoxic properties.

Aβ peptides, initially characterized by Glenner and Wong in 1984, are the main components of amyloid plaques and originate from the proteolytic processing of APP (Glenner and Wong, 1984). This protein is expressed in neuronal cells, as well as in other non-neuronal tissues and belongs to a large evolutionarily conserved family of type I transmembrane glycoproteins found in several organisms (Nalivaeva and Turner, 2013; Nicolas and Hassan, 2014). There are two different pathways for APP metabolism in the cell: the non-amyloidogenic pathway (90% of APP is metabolized through this pathway) and the amyloidogenic pathway (the minor pathway, corresponding to 10% of the APP metabolism) (Fig. 1.2). During the non-amyloidogenic pathway, APP is cleaved by α-secretase, leading to the formation of a soluble N-terminal fragment (sAPPα) and a C-terminal fragment (CTFα), which is retained in the membrane. This fragment is processed by presenilin-containing γ-secretase complex, originating a soluble extracellular N-terminal (p3) and a membrane-bound C-terminal fragment (amyloid intracellular domain – AICD) (Kim et al., 2011; Nalivaeva and Turner, 2013; Nicolas and Hassan, 2014) (Fig. 1.2). The amyloid pathway, or plaque-forming pathway, begins with the intervention of BACE1, instead of α-secretase, which generates several Aβ peptides of different lengths. BACE1 is a transmembrane aspartic protease that cleaves APP, yielding a soluble N-terminal fragment (sAPPβ) and a membrane-bound C-terminal fragment (CTFβ). This cleavage is performed closer to the N-terminal end of APP than the cut done by α-secretase, which allows CTFβ to be longer than CTFα. Subsequently, CTFβ is cleaved by the presenilin-containing γ-secretase complex originating a AICD and N-terminal fragments (Aβ peptides)

(Fig. 1.2), which are longer than p3 (Kim et al., 2011; Nalivaeva and Turner, 2013; Nicolas and Hassan, 2014). Although it has been suggested that Aβ peptides may be involved in neuronal function, when produced in high amounts, these peptides are known to aggregate, leading to the formation of suprastructures, such as Aβ oligomers and fibrils, which are neurotoxic and promote neuronal death.

Aβ peptides can differ in length from 38 to 42 amino acids, but $A\beta_{1\text{-}40}$ and $A\beta_{1\text{-}42}$ forms are the ones produced most abundantly in the brain and, while $A\beta_{1\text{-}40}$ is soluble, $A\beta_{1\text{-}42}$ is more hydrophobic and "sticky". $A\beta_{1\text{-}42}$ accumulates preferentially in neuritic plaques and is the most frequent form of Aβ to be deposited in the senile plaques (Kim et al., 2011). ACH defends that when the processing of APP through the amyloidogenic pathway increases, it leads to the excessive formation of Aβ peptides, potentiating their aggregation into oligomers, which cluster together to form fibrils bearing a β-sheet structure. These fibrils adhere to each other to form mats, which clump together to generate insoluble amyloid plaques. Although this hypothesis perfectly fits in the FAD cases, in the sporadic AD cases (non-genetic) there is no report on the increase in the amyloidogenic activity and, in this case, the accumulation of Aβ has been attributed to the lack of clearance mechanisms (Mawuenyega et al., 2010).

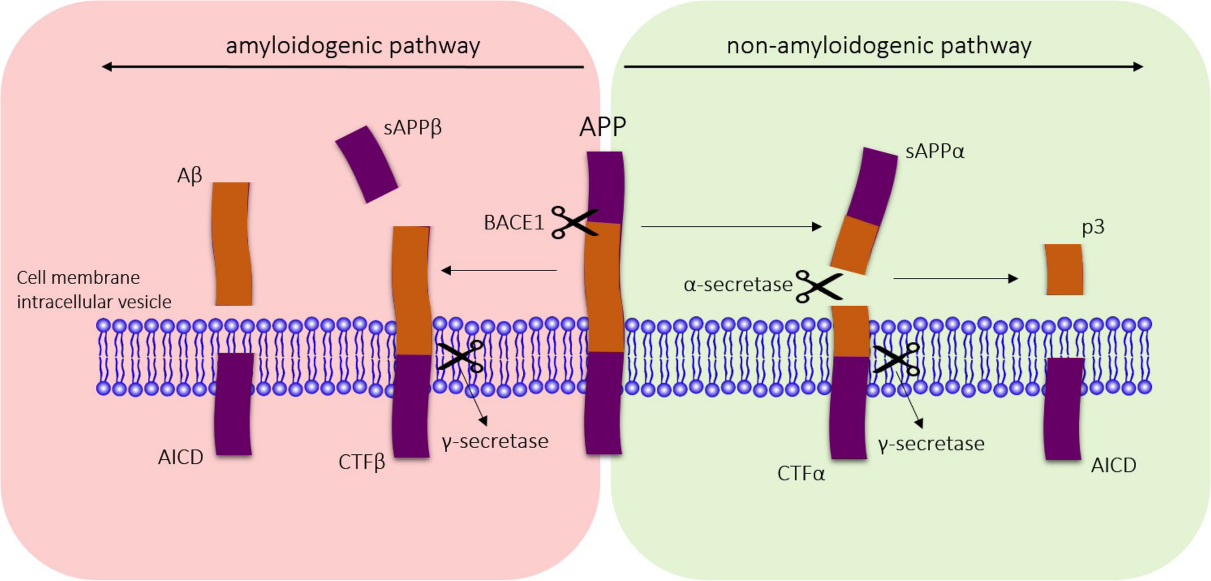

Figure 1.2 | Amyloid precursor protein (APP) processing at the cell membrane and intracellular vesicle membrane.
During the amyloidogenic pathway, the peptides derived from γ-secretase cleavage (Aβ) are longer than p3, originated during the non-amyloidogenic pathway. This difference renders Aβ peptides less soluble and with tendency to aggregate when released to the extracellular space or to the cytoplasm.

The tau protein is a highly soluble phosphoprotein essential for axonal microtubule stabilization and structural integrity, and is abundant in neurons, but not in astrocytes or oligodendrocytes (Kim et al., 2011). The six isoforms of tau phosphoproteins are produced by alternative splicing of a single gene that, in humans, is designated *Mapt* (microtubule-associated protein tau). There are about 80 potential serine (Ser) and threonine (Thr) phosphorylation sites in the longest isoform of tau but, in healthy conditions, phosphorylation seems to occur in only 30 sites. This phosphorylation process is regulated by several kinases, such as glycogen synthase kinase 3-β (GSK3β) and cyclin-dependent kinase 5 (CDK5), and phosphatases, like protein phosphatase-2A (PP2A), which is the major regulator of tau phosphorylation (Iqbal et al., 2014). A disruption of the regulatory mechanisms mediated by both kinases and phosphatases may lead to the hyperphosphorylation of the tau protein, which decreases its affinity towards microtubules, influencing their stabilization. Detached p-tau proteins bind to each other and originate fibrillar deposits that are insoluble and cytotoxic (Kim et al., 2011).

Published evidence suggests that tau pathology occurs subsequently to Aβ deposition (Fagan and Vos, 2013). In experimental animals, Aβ injection in the brain of P301L mice, a model for tau pathology, increases formation of NFTs (Gotz et al., 2001). Aβ accumulation appears to promote tau hyperphosphorylation via activation of GSK-3β (Tokutake et al., 2012). This was supported by recent work showing that breeding mice with 5 early onset FAD mutations (5XFAD) with mice expressing the TauP301S mutation (PS19) results in mice with a ~10 fold aggravated tauopathy (Stancu et al., 2014). The effects of Aβ deposition on tau pathology in mouse models may not necessarily be due to fibrillar Aβ deposits, such as senile plaques, since cognitive deficits start before formation of these plaques. It is possible that the accumulation of intraneuronal Aβ, soluble Aβ or Aβ oligomers are the main contributors to synaptic disruption and tau hyperphosphorylation. Regardless of the exact species of Aβ involved in this process, the co-localization of Aβ and p-tau in synaptic sites (Takahashi et al., 2010) suggest that the deposition of these protein aggregates and their contribution to neuronal loss is influenced by their interactions. In this regard, strategies for treatment of AD should consider both Aβ and p-tau aggregates and how they influence each other (Lanzillotta et al., 2011), as well as how neuroinflammation relates to them. Failure to take into account the link between these three AD hallmarks might explain the lack of success of past AD clinical trials employing anti-inflammatory strategies, since the onset of treatment was performed at a stage in which Aβ and inflammation-driven tau pathology and neuronal death had already occurred in a great extent (Heneka et al., 2015a).

In order to mimic the Aβ-tau axis, AD mouse models based on genetic mutations observed in AD patients have been developed. The most widely used models include transgenic animals bearing the human APP (hAPP) gene and producing Aβ, mice expressing mutant presenilin genes, mice modeling the role of hyperphosphorylated tau in AD and ApoE mouse models. Importantly, the biochemical composition of the protein deposits present in the brain of these animals was shown to be very similar to that found in humans. In addition, double or triple transgenic models have been generated to overlay pathologies (reviewed in (Duff and Suleman, 2004; Gotz and Ittner, 2008)). Although several mouse models of AD have been developed to showcase each of the disease-linked mutations and each model is currently being used for addressing specific questions, it is important to point out that there is currently no mouse model that exhibits all features of human AD (Puzzo et al., 2015). Therefore, care should be taken in the interpretation of the results derived from each specific AD model, which is additionally biased by the different mouse strains used to generate the models. The ideal model of AD should meet the full range of clinical and pathological features of the disease, including cognitive and behavioral deficits, amyloid plaques, neurofibrillary tangles, gliosis, synapse loss, neuron loss, neuroinflammation and neurodegeneration.

1.2.2. *Inflammation in Alzheimer's disease*

Although the use of anti-inflammatory drugs for the treatment of AD has, until now, failed, neuroinflammation is currently considered a very important hallmark of this disease. While inflammation is a broad concept, the term neuroinflammation is used to describe a specific set of features that occur in the CNS upon injury, infection or neurodegeneration, which are considered mostly deleterious to neurons. The particularity of these features is determined by the fact that the CNS, which is mechanically isolated from the rest of the organism by the skull and biochemically protected by the blood-brain barrier (BBB), presents limited regeneration properties, rendering any kind of impairment a possible threat to brain function. Following the first trigger of inflammation in the brain, this tightly regulated process is usually limited by immune suppressors, such as SOCS proteins (Baker et al., 2009). However, sustained or chronic brain inflammation, such as that found in AD, implies that the usual self-limiting resolution mechanisms are impaired, minimizing tissue repair and amplifying the production of neurotoxic factors that sustain disease states.

In AD, neuroinflammation is not a passive side event, but instead contributes directly to the disease pathogenesis, as much as senile plaques and NFTs (reviewed in (Heneka et al., 2015a)). The inflammatory component of AD relies on the activation of microglia cells (Glass et al., 2010; Perry et al., 2010; Heneka et al., 2014) in the brain. In addition to microglia, neutrophils, lymphocytes and monocytes can infiltrate the AD brain and, although their role in AD progression is unclear at this time, it has been proposed that they have both detrimental and beneficial effects depending on the stage of disease development (Hohsfield and Humpel, 2015). The most studied blood-derived cells in AD are monocytes and macrophages which share a common progenitor with microglia (Ginhoux et al., 2010) and, although they have been proposed to clear Aβ deposits, a possible contribution of monocytes to uncontrolled neuroinflammation and neurotoxicity cannot be excluded.

1.2.2.1. *Novel inflammation-associated Alzheimer's disease risk genes*

Very recently, genome-wide association study (GWAS) analyses provided evidence to strengthen the hypothesis that neuroinflammation is crucial to AD progression. Indeed, these analyses revealed that several new genes associated with inflammation have variants that may be involved in AD (reviewed in (Heneka et al., 2014)). This is the case of the genes that encode CR1 (Lambert et al., 2009a), myeloid cell-expressed membrane-spanning 4-domains subfamily A member 6A (MS4A6A), putative membrane-spanning 4-domains subfamily A member 4E (MS4A4E), CD33 (Hollingworth et al., 2011b) and the triggering receptor expressed on myeloid cells 2 (TREM2) (Guerreiro et al., 2013).

TREM2 is a receptor found in the membrane of cells of the innate immune system, such as myeloid cells. This protein forms a receptor-signaling complex with TYRO protein tyrosine kinase binding protein (TYROBP), also known as DAP12, which is involved in the activation of microglia in the presence of dying neurons, increasing the phagocytic ability of these cells, as well as the short term production of ROS. TREM2 has been suggested to serve as a marker of the M2 phenotype, attenuating macrophage pro-inflammatory activation (Ydens et al., 2012) in cooperation with its adapter DAP12 (Zhong et al., 2015). In 2013, two independent groups found a strong association between one rare variant of this protein, bearing the R47H mutation, and LOAD (Guerreiro et al., 2013; Jonsson et al., 2013). Although this variation occurs at a very low frequency, the strength of this association is similar to that of *ApoE*ε4 genotype. Furthermore, the authors also identified six other variants of this gene that are present in AD patients and not in controls: H157Y, R98W, D87N, T66M, Y38C, and Q33X (Guerreiro et al., 2013). Interestingly, TREM2 was the first protein of the immune system to be directly related with increased AD risk, confirming the importance of the immune response and neuroinflammation to disease progression. The exon 2 of *Trem2*, where most mutations are located, encodes the signal peptide of the protein, as well as part of the extracellular domain, suggesting that the identified mutations can influence the activation of the TREM2 receptor during the immune response, thus contributing to defective microglia activity. Interestingly, carriers of the LOAD R47H mutation present ionized calcium-binding adapter molecule 1 (IBA-1) microglia marker decreased compared to healthy controls (Korvatska et al., 2015). However, until now, the exact functional consequences associated with the R47H and the other identified mutations remain unclear (Jiang et al., 2013a; Kleinberger et al., 2014).

1.2.2.2. *Unveiling the role of microglia in Alzheimer's disease inflammation and Aβ deposition*

Both microglia and astrocytes have been reported to be crucial players in the molecular mechanisms underlying AD inflammation. The first evidence that microglia cells are in close contact with amyloid plaques came from early studies by del Rio Hortega and Penfield, who were the pioneers in describing these cells. However, it took fifty years to return the scientific spotlight to the role of microglia in AD, mainly thanks to the studies identifying microglia association with Aβ plaques in the brain of AD patients (Rozemuller et al., 1986; Dickson et al., 1988). Although our recent view of microglia phenotypes in AD has dramatically changed following the development of AD mouse models, these human neuropathological studies continue to be a crucial tool to determine the relevant players in AD development. R. E. Mrak suggested that microglia can actively influence the pattern of development of amyloid plaques, as well as neuronal tangle formation in AD brains (Griffin et al., 1995; Sheng et al., 1998), rather than merely associate with these lesions. This idea was later supported by Bolmont and colleagues (Bolmont et al., 2008). In their work, the authors used *in vivo* imaging to show that different stages of plaque formation are associated with different microglia morphologies (Bolmont et al., 2008), implying that these cells may play a dichotomous role in AD. Importantly, in 1989, Griffin and colleagues described, for the first time, the overproduction of IL-1 by microglia in AD brains (Griffin et al., 1989) and these findings, along with studies showing the involvement of IL-1 in the production of APP (Goldgaber et al., 1989), definitely placed microglia and the production of inflammatory mediators in the core of AD pathology. Notably, microglia activation has already been confirmed in AD and MCI patients by PET studies (Okello et al., 2009; Yokokura et al., 2011).

Although neuroinflammation is an unquestionable property of AD, the beneficial or deleterious nature of this process still constitutes a subject of intense debate. On one hand, microglia and astrocytes have the ability to phagocyte Aβ, helping to prevent Aβ deposition. On the other hand, the binding of Aβ to glial cells triggers the production of inflammatory mediators, leading to neuronal damage and thus contributing to disease progression. At present, it remains unclear whether the deregulation of microglia functions precedes the production and deposition of Aβ or whether the release of this peptide is a primary trigger of neuroinflammation, initiating a strong immune response that later converts into a chronic event due to the persistence of the insult.

The most important receptors' family for Aβ-related inflammation are TLRs and, as mentioned before, these receptors mediate the expression of various cytokines such as TNF-α, IL-1, IL-6 and IL-12. High levels of mRNA of TLR2, TLR4, TLR5, TLR7 and TLR9 have been detected in brain tissue of APP23 transgenic mice (Frank et al., 2009). TLR2 was recently identified as an important receptor in AD, since antisense knockdown of TLR2 suppressed Aβ-induced expression of pro-inflammatory molecules (Jana et al., 2008). In addition, TLR4, coupled with CD14, has been implicated in Aβ-dependent microglia activation (Walter et al., 2007) and the recognition of Aβ by CD36 was shown to trigger TLR4/TLR6 assembly, creating the first signaling complex for NLRP3 inflammasome activation (Stewart et al., 2010).

In general, the binding of Aβ to some of its receptors triggers normal inflammatory signaling pathways and several transcription factors have been found to be activated in this context. NF-κB, a major mediator of cytokine expression, was one of the first transcription factors associated with Aβ-derived inflammation (Bonaiuto et al., 1997). Following activation of the above-mentioned transcription factors, several inflammatory mediators are produced and released by Aβ-activated microglia cells. This subject has been largely explored in the literature, either by measuring cytokine and chemokine release by *in vitro* Aβ-activated microglia or by performing transcriptome studies in brains of AD patients and mouse models of AD. All these studies agree that microglia, in contact with Aβ, is able to produce IL-1, IL-6, IL-12, IL-1β, TNF-α, IFN-β, NO, and chemokines that induce cell migration, such as CCL2, CCL3, CCL4 and IL-8 (Fiala et al., 1998; Murphy et al., 1998; Yates et al., 2000; Lue et al., 2001; Walker et al., 2006). However, most of these studies present the problems associated with microglia cultures or are simple snapshots of cytokine expression at a certain point of disease progression. Although recent studies tried to give a clearer picture of the whole transcriptome of AD in post-mortem tissue (Twine et al., 2011), we still lack information about the inflammatory transcriptome of these brains and, more specifically, about microglia associated-genes, studied by the most powerful transcriptome sequencing tools available at present. Furthermore, even when this information is available, it will only reflect a post-mortem status, leaving an open question regarding how to study transcriptome changes, *in situ*, over time, beginning at pre-clinical stages of AD.

Another important issue to take into consideration when trying to correlate all data concerning Aβ-activated microglia is the use of different Aβ species. It is currently accepted that, while $A\beta_{1\text{-}40}$ is the most abundant form of Aβ, $A\beta_{1\text{-}42}$ is the most toxic and, therefore, it is also the most used in AD studies. Furthermore, when APP cleavage occurs and Aβ peptides are overproduced, these tend to aggregate inside neurons or outside the cells in the form of oligomers, which further aggregate in fibrils that ultimately join together to generate Aβ senile plaques. In addition to the issue regarding the different lengths of Aβ peptides, it is still not completely understood which Aβ form, the monomers, oligomers or fibrils, is the most toxic to neurons and has the potential to activate microglia (Jekabsone et al., 2006; Jana et al., 2008; Michelucci et al., 2009; Davenport et al., 2010), or if differentially activated microglia is associated with different Aβ oligomerization states. Moreover, although studies on microglia activation by different Aβ peptides and forms are easily performed *in vitro*, it is imperative to understand that, *in vivo*, microglia activation by different Aβ forms and Aβ aggregation itself are dynamic processes occurring simultaneously.

In contrast to our accumulated knowledge about microglia and Aβ, little is known regarding the relation between microglia and NFTs. Some anti-inflammatory drugs have been shown to reduce p-tau in P301S and in the triple transgenic (3xTg) mouse model of AD (Yoshiyama et al., 2007; Fonseca et al., 2009), but whether the mechanism behind this reduction is microglia-dependent remains to be determined. Published reports suggest that microglia activation induces tau phosphorylation and aggregation (Bhaskar et al., 2010) and that injured neurons, exhibiting tau hyperphosphorylation, can modulate microglia-mediated neuroinflammation (Lastres-Becker et al., 2014). While these studies are compelling, they do not provide clear evidence of direct activation of microglia by p-tau. However, they suggest that neuroinflammation is closely linked with tau pathologies.

Following this comprehensive review on the current knowledge regarding the role of Aβ in microglia-mediated inflammation, the influence of microglia on peptide clearance is an important issue that deserves to be explored. In AD, Aβ deposition is dependent on a balance between Aβ production and elimination, which means that the mechanisms involved in Aβ degradation should be taken into close consideration, especially when considering the high percentage of non-genetic AD cases where the production of Aβ is not caused by any known genetic mutations that interfere with APP processing. When we think of microglia as brain macrophages, it is easy to conclude that these cells are specialized in phagocytosis. Their homeostatic functions foresee the cleaning of neurotransmitters, synaptic debris, as well as apoptotic cells. In neurodegeneration, these cells have been proposed to phagocyte misfolded proteins which accumulate in the intercellular space. However, it is still a question of debate whether, at an advanced point of disease progression, microglia remains functional enough to clear Aβ, or whether it becomes a facilitator of cognitive decline. The most recent *in vitro* studies supporting a role for microglia in Aβ phagocytosis propose that this process can be regulated by several molecules, including cytokines and Aβ itself (Condic et al., 2014). Therefore, Aβ phagocytosis by microglia is an extremely regulated process and its modulation by other molecules may be of great importance for therapeutic purposes.

During the last twenty years, several potential phagocytosis-related Aβ receptors have been identified. The SR family, which includes SCARA-1, appears to be of great importance to AD since it was described to play a role in the clearance of Aβ. SCARA-1 has been shown to mediate human microglia binding, uptake and degradation of the Aβ peptide (Husemann and Silverstein, 2001). In addition, the CD36 and RAGE receptors have been described as important in the context of AD (reviewed in (Wilkinson and El Khoury, 2012)). CD36 and RAGE mediate microglia activation and the subsequent production of cytokines and chemokines, which can induce cell migration (Yan et al., 1996; Coraci et al., 2002). However, recent evidence, obtained in an AD mouse model deficient in RAGE, points towards a decrease in Aβ deposition, although with no improvement in cognitive function (Vodopivec et al., 2009). CRs have also been associated with senile plaques in the brains of AD patients (Afagh et al., 1996). CR1 and CR3 (CD11b), in particular, appear to be involved in the uptake and clearance of Aβ (Rogers et al., 2006; Fu et al., 2012). Moreover, microglia FcRs have been shown to mediate Aβ phagocytosis in the presence of antibodies. Active and passive Aβ immunization, in studies employing AD animal models, demonstrated an effect of anti-Aβ antibodies on Aβ clearance and resulted in a reduction of cognitive decline (Bard et al., 2000). However, other studies have shown that increased Aβ clearance *in vivo,* in the presence of anti-Aβ antibodies, is not dependent on FcR-mediated phagocytosis (Das et al., 2003).

Importantly, and as referred before, genetic variants of the genes encoding the membrane receptors CD33 and TREM2 have recently been considered new risk factors for LOAD. CD33$^{-/-}$ microglia showed an enhanced capacity to internalize Aβ, whereas the overexpression of CD33 impaired Aβ uptake (Griciuc et al., 2013). Indeed, AD mice deficient in CD33 exhibited a reduction in Aβ plaques, suggesting that CD33 favors Aβ accumulation (Griciuc et al., 2013). Regarding TREM2, this protein and its adapter protein TYROBP are highly expressed in amyloid plaque-associated microglia in APP23 transgenic mice (Frank et al., 2008). Although TREM2 is a phagocytosis receptor, the ligand of this receptor has not been well defined. It has been suggested that TREM2 can mediate Aβ phagocytosis by directly binding Aβ, although this hypothesis is far from being validated. Two very recent studies implicated TREM2 in the regulation of Aβ levels *in vivo*, although with contradictory results. On one hand, TREM2 deficiency increased Aβ accumulation in 5XFAD mice due to lack of microglia clustering around senile plaques (Wang et al., 2015). On the other hand, TREM2 was shown to be upregulated in Ly6C^{+}CD45^{high} cells located around plaques, which indicates that brain cells expressing TREM2 might be peripheral myeloid cells and not microglia and that its absence in both 5XFAD and APP/PS1 mice might contribute to ameliorate amyloid and tau pathologies (Jay et al., 2015). Although this last study contradicted the previously reported specific expression of TREM2 in microglia compared to other tissue-resident macrophages (Hickman et al., 2013), it is important to have in mind that more suitable markers, capable of differentiating myeloid subsets are needed before definitive conclusions can be drawn. Interestingly, the recent work of Wang and colleagues allowed the identification of lipids capable of associating with fibrillar Aβ in lipid membranes, which the authors suggest to be recognized by TREM2 (Wang et al., 2015). Since this function is likely to be impaired by the R47H mutation, this finding unveils a possible mechanism by which TREM2 regulates Aβ deposition.

Phagocytosis studies show that *in vivo* phagocytosis of fibrillar Aβ is usually less successful than *in vitro*, since large aggregates of fibrils are present not only as diffuse elements, but also in dense-core plaques. One can argue that the senile plaques composed of fibrillar Aβ surrounded by glia cells act as a protective mechanism for the surrounding tissue, preventing nearby neurons to be in close contact with neurotoxic Aβ forms. In this case, microglia associated with the dense-core plaques would not need to phagocyte large Aβ aggregates but, instead, should work to surround them without internalization. In fact, studies in AD mouse models have suggested that microglia cells do not influence Aβ deposition. In 2004, two studies from the same group suggested that although Aβ plaque growth is associated with a high number of surrounding microglia cells, they do not possess the ability to mediate Aβ internalization, contributing instead to their morphological and chemical evolution, by facilitating the conversion of local Aβ from the soluble and oligomeric forms into the fibrillar form (Nagele et al., 2004; Wegiel et al., 2004). Furthermore, by crossing two distinct APP transgenic mouse strains with CD11b-HSVTK mice (mice with the CD11b promoter controlling the expression of the herpes simplex virus thymidine kinase), in which ablation of microglia is achieved after ganciclovir treatment, Grathwhol and colleagues showed that neither amyloid plaque formation nor amyloid-associated neuritic dystrophy depended on the presence of microglia (Grathwohl et al., 2009). Another important study showed that, despite one of the features of microglia activation being cell proliferation, these cells lose the ability to divide and phagocyte Aβ over time, thus allowing the plaques to continue increasing in size and number (Bolmont et al., 2008). Importantly, *in vivo* two-photon microscopy showed that microglia motility and phagocytic activity were strongly impaired in AD mice (Krabbe et al., 2013), suggesting that, *in situ*, microglia do not contribute to Aβ clearance.

In this regard, if microglia cells are not crucial players in *in vivo* Aβ clearance, the question remains whether these cells can be manipulated to improve their ability to fight Aβ deposition. The use of bexarotene, an agonist of retinoic X nuclear receptors (RXRs), which exert their functions by forming dimers with PPARγ and LXRs and promoting *ApoE* transcription, was found to decrease Aβ levels and plaque burden in AD mice, also restoring cognitive function in these animals (Cramer et al., 2012). This report was one of the most promising studies of the last decade regarding new therapeutic strategies for AD. It is interesting to note that the mechanism of action of bexarotene is probably related with phagocytosis, suggesting that although microglia in the AD brain is not able to clear Aβ, due to aging, senescence or other yet undisclosed mechanisms, microglia function can still be stimulated and these cells can be used as a part of the solution to stop AD progression. Recently, RNA-seq (RNA sequencing) experiments showed that bexarotene-treated APP/PS1 mice present significantly upregulated TREM2 levels, when compared to untreated animals, implicating, once again, TREM2 in microglia-mediated Aβ clearance (Lefterov et al., 2015). Moreover, and since the role of microglia in AD inflammation and Aβ deposition is far from being clear, it is imperative to understand if the still ongoing controversy regarding microglia-related results in AD is due to technical issues or is, in fact, a matter of disease evolution. Nevertheless, the unquestionable relevance of these cells in the context of neurodegeneration renders them an important tool to consider when developing new diagnostic and therapeutic strategies.

1.2.2.3. Implication of peripheral mononuclear cells in Alzheimer's disease

Along with neuroinflammatory events, several studies have suggested that AD patients present a strong peripheral immune response, which implicates subsets of blood cells in this disease. Despite the fact that their contribution to disease progression is still not fully understood, it is now believed that AD behaves like a chronic systemic disease rather than a neurodegenerative disorder restricted to the CNS. The implication of the peripheral immune system in AD was described upon the discovery of deregulated levels of several inflammatory mediators in the blood of AD and MCI patients. These mediators included chemokines, such as CCL2 and CCL4 (Galimberti et al., 2006; Zhang et al., 2013), cytokines, such as IL-2, IL-4, IL-10, IL-5, IL-6, IL-8, IL-12, IL-13, IL-17, IFN-γ TNF-α and IL-1β and other secreted molecules and surface receptors (Laske et al., 2013; Leung et al., 2013). In this context, researchers have proposed to use these molecules as potential biomarkers for early disease diagnosis and to monitor disease progression. More recently, studies suggested that the deregulation of blood cytokine levels can be correlated with differences between the various subsets of blood cells in AD patients and in healthy subjects and that changes in the phenotypes of these cells can occur alongside brain alterations. Some authors reported important transcriptome changes in leukocytes (Maes et al., 2007; Lunnon et al., 2012), others observed changes in the percentages of T-cell subsets in the blood (Pellicano et al., 2012), while other studies focused on disclosing monocyte inflammatory profiles following *in vitro* cell activation with several molecules, including Aβ (Guerreiro et al., 2007; Pellicano et al., 2010; Saresella et al., 2014). Interestingly, a very recent study showed that there is an over-representation of T-cell specific quantitative trait locus (eQTL) among susceptibility alleles for autoimmune diseases, while AD variants present an increase in monocyte-specific eQTLs. This polarization implicates this particular cell type in AD and points to the need of determining the cell-autonomous effects of the identified disease susceptibility variants (Raj et al., 2014).

In light of these findings, researchers have been trying to study monocyte behavior *in vivo*, in AD animal models. In addition to neutrophils and lymphocytes, monocytes can enter the brain tissue during neuroinflammation. However, upon their entry in the brain environment, all mononuclear phagocytes are, at present, indistinguishable from resident immune cells, which constitutes a major drawback when trying to assess monocyte and MDMs contribution to disease progression. Nevertheless, the diverse ontologies of these cells suggest that they can exert different functions during physiological and pathological processes.

Although the BBB limits the entry of blood-derived cells that normally patrol blood vessels, several studies indicate that, in AD, peripheral mononuclear cells can accumulate in the brain and help in Aβ clearance, partly compensating for microglia loss of activity (Fig. 1.3).

Blood monocyte infiltration is mediated by chemokine receptors, such as CCR2, which bind the chemokine CCL2, released into the blood stream following production by Aβ-activated microglia and astrocytes. CCL2 is a chemokine (or a chemotactic cytokine) which mediates the migration of immune cells to the sites of inflammation (Fig. 1.3)

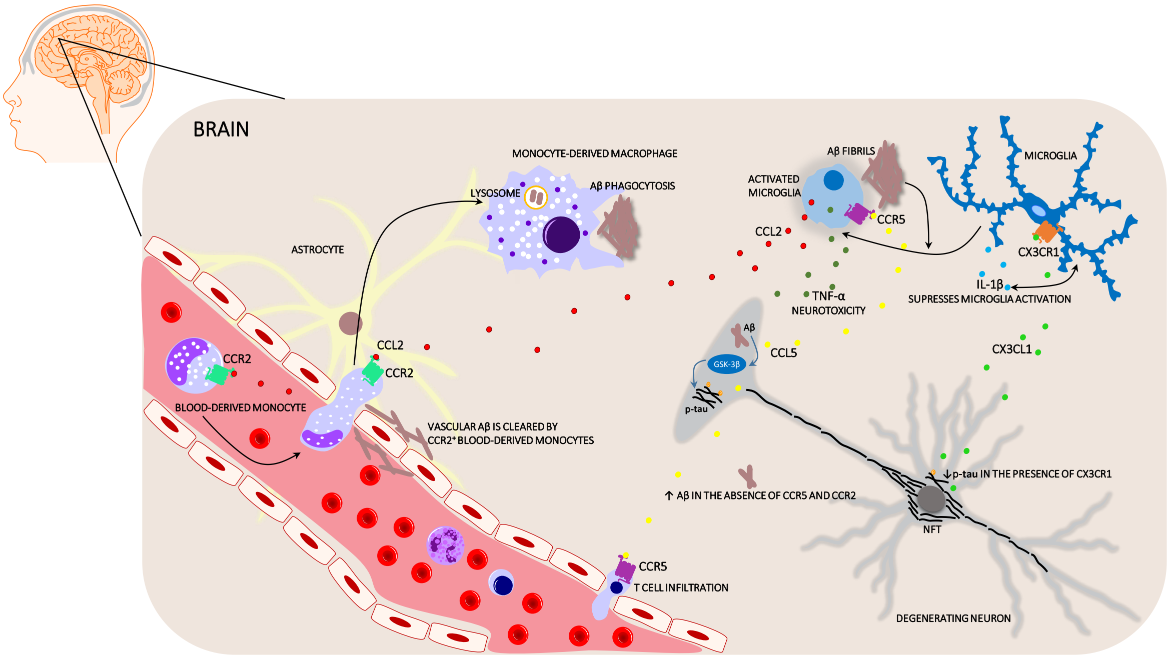
BRAIN
MONOCYTE-DERIVED MACROPHAGE
LYSOSOME
Aβ PHAGOCYTOSIS
ASTROCYTE
CCL2
CCR2
CCR2
BLOOD-DERIVED MONOCYTE
VASCULAR Aβ IS CLEARED BY
CCR2⁺ BLOOD-DERIVED MONOCYTES
CCR5
T CELL INFILTRATION
Aβ FIBRILS
ACTIVATED
MICROGLIA
CCL2
CCR5
MICROGLIA
CX3CR1
IL-1β
SUPRESSES MICROGLIA ACTIVATION
TNF-α
NEUROTOXICITY
Aβ
GSK-3β
p-tau
CCL5
CX3CL1
↓p-tau IN THE PRESENCE OF CX3CR1
↑ Aβ IN THE ABSENCE OF CCR5 AND CCR2
NFT
DEGENERATING NEURON

Figure 1.3 | Role of mononuclear phagocytes in Alzheimer's disease.
When in contact with Aβ aggregates, microglia and astrocytes produce inflammatory mediators, including cytokines and chemokines, such as CCL2, that are released into the blood stream, mediating CCR2-dependent recruitment and infiltration of monocytes into the brain. Once in the brain, these cells are able to phagocyte Aβ aggregates and contribute to the clearance of Aβ, both from the brain parenchyma and from vascular deposits. In addition to the role of CCR2 in blood-derived monocyte infiltration, other chemokine receptors, such as CCR5, are also essential for the transendothelial migration of T cells across the blood-brain barrier (BBB) (Man et al., 2007). In lipopolysaccharide-induced peripheral inflammation, CX3CR1 contributes to maintain microglia homeostasis, limiting its activation (Cardona et al., 2006) and, in AD, lack of CX3CR1 is associated with enhanced tau phosphorylation and microglia overactivation (Bhaskar et al., 2010).

Initially designated with specific protein names, chemokines are now classified on the basis of the number of amino acids between two cysteine residues: α-chemokines, with the first cysteine residues separated by one amino acid (CXC); β-chemokines, with adjacent cysteine residues (CC); lymphotactin, with only two cysteines, and fractalkine (CX3CL1) in which the first two cysteine residues are separated by three amino acids. These small chemoattractant proteins bind to chemokine receptors classified in the same manner. Over the years, specific chemokine receptors were associated with different immune cells and monocytes, in particular, CCR1, CCR2, CCR5, CCR8, CXCR4 and CX3CR1 (Luster, 1998).

Despite the possible beneficial role of monocytes in AD, almost all evidences suggesting that peripheral mononuclear cells can infiltrate the brain and differentiate into microglia-like cells, contributing to decrease Aβ deposition are, at this point, either indirect or have been associated with technical issues providing a strong bias to the experimental results. In 2006, Simard and coworkers transplanted GFP-expressing bone-marrow cells into the bloodstream of irradiated 2-months old APP_{Swe} mice to test whether cells associated with Aβ plaques were resident or blood-derived (Simard et al., 2006). The study concluded that a large percentage of the amyloid plaque-associated cells were GFP positive being able to help reduce amyloid deposits. In 2007, El Khoury and coworkers generated *Ccr2*-deficient *APP* mice and evaluated the Aβ content in the brain of these animals, as well as their mortality rate and microglia accumulation (El Khoury et al., 2007). The authors of this study concluded that *Ccr2*-deficient *APP* mice presented impaired microglia accumulation and a huge increase in vascular Aβ deposition (El Khoury et al., 2007), as expected by the lack of CCR2 in peripheral cells. Subsequent studies showed that depletion of perivascular macrophages in TgCRND8 AD mice significantly increased the number of thioflavin S-positive cortical vessels, while the stimulation of macrophage turnover reduced vascular $A\beta_{1\text{-}42}$ load (Hawkes and McLaurin, 2009). Moreover, it was shown that the administration of the granulocyte-colony stimulating factor (G-CSF) in APP/PS1 mice also improved cognitive performance, decreased Aβ deposition through the induction of microgliosis and, simultaneously, increased the mobilization of bone-marrow-derived cells to the brain (Sanchez-Ramos et al., 2009).

Although the above studies are very interesting, they present important technical issues that have to be taken into consideration when interpreting the results. First, at present, there is no specific marker that allows a clear distinction between monocytes and microglia in the CNS. While CD45 has been used for this purpose in some studies, questions remain regarding possible changes in the expression of this marker in infiltrating cells. Moreover, the low to intermediate levels of CD45 expression in resident microglia are generally difficult to interpret. On the ther hand, irradiation, chimerism or parabiosis have been used to eliminate bone-marrow cells from AD mice, before the injection of labeled cells from other sources. These techniques often confound the interpretation of results and impose practical limitations, since the use of irradiation can disrupt the BBB integrity, facilitating the entry of blood-derived cells into the brain and raising concerns on whether bone-marrow-derived cell migration into the CNS is a physiological process or an artifact introduced by irradiation (Soulet and Rivest, 2008; Prinz and Priller, 2010). Irradiated mice also present elevated levels of chemokines (Mildner et al., 2011), potentially contributing to an increase in blood cell recruitment to the brain, without direct correlation with AD pathology. To overcome this issue, Mildner and colleagues have used specific body (head protected) irradiation to obtain bone-marrow chimeras, providing evidence that peripheral macrophages, rather than parenchymal microglia, modulate Aβ deposition in a CCR2-dependent manner (Mildner et al., 2011) in APP_{Swe}/PS1 mice. The progressive cognitive decline observed in these mice was associated with a decrease in the numbers of $CX3CR1^{low}Ly6C^{high}CCR2^{+}Gr1^{+}$ circulating inflammatory monocytes (Naert and

Rivest, 2012a) and restoring CCR2 expression in bone-marrow cells was shown to reestablish memory capacities and decrease soluble Aβ accumulation (Naert and Rivest, 2012b).

Despite these compelling evidences, there are, up to date, few studies reporting the migration of peripheral phagocytes to the brain in conditions that do not compromise the integrity of the BBB. In 2010, Lebson and colleagues successfully injected CD11b^{+} bone-marrow monocytes into APP/PS1 mice, showing that these cells can enter the CNS without requiring the use of lethal irradiation (Lebson et al., 2010). More recently, Michaud and colleagues reported that blood patrolling monocytes are attracted to and crawl onto the luminal walls of Aβ positive-veins in APP/PS1/*Cx3cr1*$^{gfp/+}$ mice (Michaud et al., 2013). This study used intravital two-photon microscopy to study, *in vivo*, the ability of GFP^{+} cells to mediate the uptake of Aβ aggregates. The authors argue that these cells are able to efficiently degrade Aβ in the blood stream, in a manner enough to increase the efflux of Aβ from the brain parenchyma, creating an equilibrium-driven redistribution process. However, *Cx3cr1*$^{gfp/+}$ mice present both GFP^{+} microglia and monocytes, which, in this study, makes it practically impossible to distinguish both cell types. Moreover, in order to show that patrolling Ly6C^{low} monocytes are the subset of cells able to perform Aβ clearance in the blood vessels, the authors transplanted myeloablated APP/PS1 mice with *Nr4a1*$^{-/-}$*Gfp*$^{+/-}$ bone-marrow cells so that the animals could present low numbers of Ly6C^{low} monocytes. Once again, the study involved mice irradiation (Michaud et al., 2013).

As one can conclude from the findings gathered in these studies, there has been increasing evidence that monocytes infiltrate the AD brain and contribute to disease progression. However, to truly and definitively clarify the nature of this contribution, it is imperative to develop more powerful techniques capable of distinguishing the different subsets of mononuclear phagocytes in different tissue-specific environments, as well as to track the behavior of these cells, *in vivo* and in a pathological context, and to understand if different mononuclear phagocytes are differentially primed to certain brain microenvironments.

1.3. *MicroRNAs: powerful regulatory small RNAs*

Most genes involved in innate immune response pathways, particularly those originating transient transcripts, present multiple regulatory elements in their 3'UTR, which allow the recruitment of molecular effectors capable of performing rapid adjustments in transcript translation. In this regard, miRNAs have carved a particularly important niche as major regulators of gene expression, due to the ability of a single miRNA to regulate multiple mRNAs. This molecular property allows the cell to fine-tune entire molecular pathways and quickly adapt to changes in their surrounding environment. This has been shown to be of particular importance during immune cell development and differentiation, as well as during the initiation and termination of inflammatory responses (reviewed in (O'Neill et al., 2011; O'Connell et al., 2012; Li and Shi, 2013)).

MiRNAs are ≈22 nucleotide long oligonucleotides that, in animals, result from RNA polymerase II (Pol II) transcription activity (Fig. 1.4). They can be encoded in intragenic regions or intronic regions of coding genes (mirtrons), or, less frequently, in exonic regions, and their expression is regulated by dedicated promoters or promoters of their host genes (reviewed in (Ha and Kim, 2014)). The long Pol II RNA transcripts (pri-miRNAs) go through several stages of processing before originating mature miRNAs (Ha and Kim, 2014). For most conserved miRNAs, the first step of processing includes the cropping of the hairpin structures by a microprocessor complex, composed of the RNase III Drosha and its cofactor DGCR8, leading to the release of ≈65 nucleotide long stem loops (pre-miRNAs) (Fig. 1.4). These stem-loop structures are then translocated to the cytoplasm by exportin 5, where they are cleaved by the RNase III Dicer, near the terminal loop (Fig. 1.4). The resulting small RNA duplexes are loaded into an effector complex named RNA-inducing silencing complex (RISC), where they are unwound and one of the strands is exposed to facilitate binding to complementary mRNAs, resulting in translation repression by mRNA decay or, less frequently in mammals, in direct mRNA cleavage (Ha and Kim, 2014) (Fig.1.4).

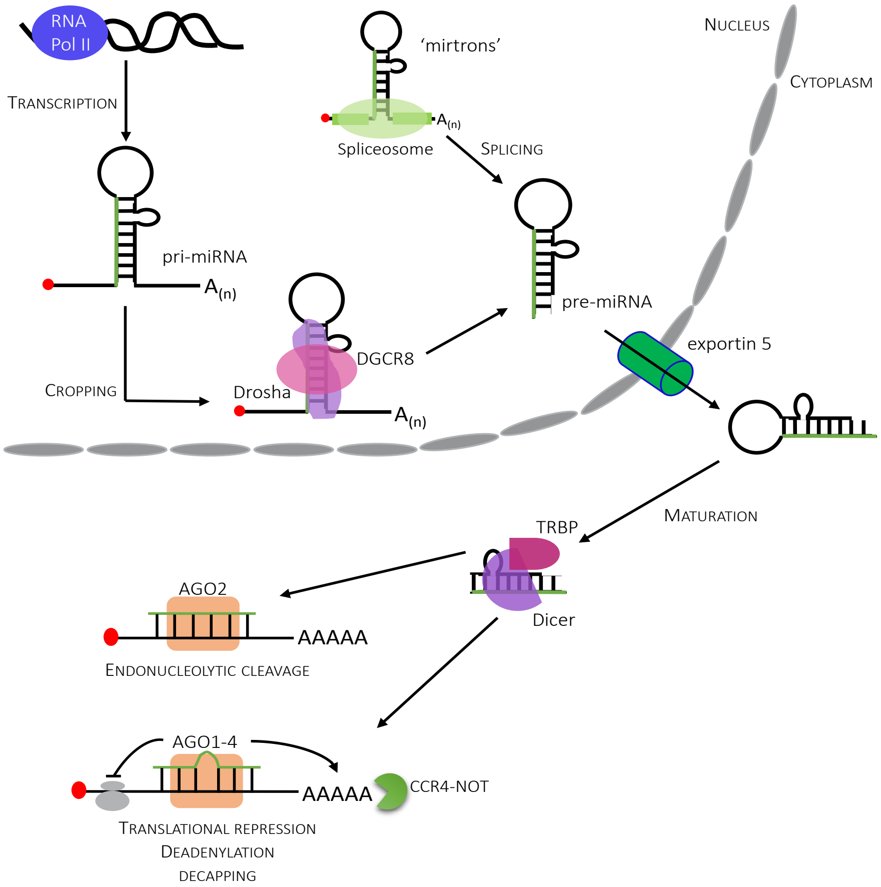
RNA
Pol II
Transcription
pri-miRNA
$A_{(n)}$
Cropping
Drosha
DGCR8
$A_{(n)}$
'mirtrons'
Spliceosome
$A_{(n)}$
Splicing
pre-miRNA
Nucleus
Cytoplasm
exportin 5
Maturation
TRBP
Dicer
AGO2
AAAAA
Endonucleolytic cleavage
AGO1-4
AAAAA
CCR4-NOT
Translational repression
Deadenylation
decapping

Figure 1.4 | Canonical and non-canonical pathways of miRNA biogenesis.
MiRNAs are encoded in intragenic regions, in their own genes or in introns and exons of protein-coding genes.

In the canonical biogenesis pathway, miRNAs are transcribed by the RNA Polymerase II (Pol II) to originate pri-miRNAs, which are processed by the RNase III Drosha and its cofactor DGCR8 to form pre-miRNAs. Since this process occurs in the nucleus, the pre-miRNA is then exported to the cytoplasm by exportin 5. In the non-canonical pathway, pre-miRNAs arise in a Drosha- and DGCR-8-independent manner deriving from intronic regions of protein-coding genes that are processed by splicing. Pre-miRNAs undergo maturation in the cytoplasm by the action of Dicer and TRBP, followed by loading onto argonaute (AGO) proteins to form an effector complex called RNA-induced silencing complex. Among the AGO family of proteins, AGO2 is the only protein able to mediate cleavage of perfectly matched target mRNAs. All AGO proteins are capable of inducing translational repression and decay of mRNA targets.

More than 60% of all human protein-coding genes present miRNA binding sites. Therefore, it is not surprising that miRNA biogenesis requires very strict regulation. Failure to achieve a perfect temporal and spatial control of miRNA expression has been shown to play a critical role in human disease, influencing not only the original diseased cells, but also the surrounding tissue. Of special note is the discovery of new forms of cell-to-cell communication, such as exosome-mediated miRNA transfer (Gupta and Pulliam, 2014), which revealed an important mechanism through which miRNAs can exert immunomodulatory effects across the CNS in both health and disease settings (Ponomarev et al., 2011).

1.3.1. *Immune-related miRNAs*

1.3.1.1. *Role of miRNAs in mononuclear phagocyte development*

Development processes require tightly spatio-temporal regulated gene expression programs which are achieved by a combinatorial action of transcription factors and miRNAs. As previously discussed, C/EBPα and PU.1 have been shown to be critical for monocyte/macrophage differentiation and microglia development. Several miRNAs are directly controlled by C/EBPα, including miR-223, which is also regulated by the transcription factor NFI-A (Fazi et al., 2005). However, while C/EBPα promotes miR-223 expression, NFI-A inhibits the expression of this miRNA (Fazi et al., 2005), which then represses NFI-A through a feedback loop. Therefore, when C/EBPα levels are high, miR-223 expression is enhanced and NFI-A levels decrease, promoting granulocyte differentiation. On the other hand, PU.1 is required to promote the skewing of granulocyte-macrophage progenitors to the monocyte lineage. PU.1 activates the transcription of miR-424 which stimulates monocyte differentiation through NFI-A translation repression (Rosa et al., 2007). Moreover, PU.1 confers stable inducibility of the miR-223 promoter activity, while C/EBP levels determine the magnitude of this promoter activation, thus contributing to another mechanism by which miR-223 is critical for myeloid function (Fukao et al., 2007). In addition to miR-223 and miR-424, miR-222, miR-155, and miR-503 play an important role in monocyte differentiation through combinatorial regulation (Forrest et al., 2010). Forrest and colleagues have shown that, when overexpressed, these miRNAs are able to cause cell-cycle arrest and partial differentiation in THP-1 cells (leukemia model). More recently, Lin and coworkers showed that downregulation of miR-199a-5p resulted from the up-regulation of PU.1 (demonstrated to negatively regulate the transcription of *miR-199a* gene), favoring monocyte/macrophage differentiation from CD34$^+$ hematopoietic progenitors and THP-1 cells (Lin et al., 2014). The oncogenic miR-17-92 cluster (which carries six miRNAs: −17, −18a, −19a, −20a, −19b-1, and −92a) has also been directly associated with the process of monocyte to macrophage differentiation (Pospisil et al., 2011). Upon differentiation into macrophages, the transcription factor PU.1 was found to induce the secondary determinant EGR2 which, in turn, directly represses miR-17-92 expression by promoting histone H3 demethylation within the CpG island of the miR-17-92 promoter. Conversely, EGR2 itself is targeted by miR-17-92, indicating the existence of a mutual regulatory relationship between miR-17-92 and EGR2 (Pospisil et al., 2011). All these studies show that, in addition to transcription factor networks, the combinatorial action of miRNAs regulated by these transcription factors and their action upon the transcription factors themselves is essential for the differentiation program of myeloid cells.

Given the similarities between macrophages and microglia, it is reasonable to assume that some of these regulatory loops involving miRNAs also play an important role in microglia differentiation in the brain. So far, the only study addressing miRNA contribution to microglia development was performed by Ponomarev and colleagues (Ponomarev et al., 2011; Ponomarev et al., 2013).These authors showed that miR-124, one of the most abundant miRNAs in the brain, is required to maintain the quiescent state of microglia. By targeting the transcription factor C/EBPα and the cyclins CDK4 and CDK6, miR-124 is able to reduce the expression of PU.1 and its downstream target, the M-CSF receptor, restricting cellular proliferation and potentiating the differentiation of primitive macrophages to adult microglia in the brain (Ponomarev et al., 2011). While during the first two weeks following birth, microglia isolated from the brain presented low levels of miR-124 and a CD45^{high}MHC class II^{high} phenotype, characteristic of active and proliferating cells, adult microglia presented the opposite phenotype, CD45^{low}MHC class II^{low}miR-124^{high} (Ponomarev et al., 2011; Ponomarev et al., 2013). The authors hypothesized that the high levels of miR-124 observed in adult microglia are a specific consequence of the CNS environment. This idea was based on their observation that sublethally irradiated mice, transplanted with bone-marrow GFP$^+$ progenitor cells exhibiting a CD45^{high}MHC class II^{high}miR-124^{low} phenotype, presented GFP$^+$CD11b$^+$ positive cells in the brain with a CD45^{low}MHC class II^{low}miR-124^{high} phenotype. To confirm this hypothesis, Ponomarev and colleagues co-cultured bone-marrow-derived macrophages with astroglial or neuronal cell lines, and they observed, in both cases, a downregulation of MHC class II and CD45 levels as well as an upregulation of miR-124 expression. Several suggestions were made concerning the mechanisms underlying miR-124 upregulation in microglia, including the direct transfer of miR-124 from neuronal cells to microglia through exosomal shuttle vesicles, direct cell-to-cell contact between these two cell types and the release of anti-inflammatory factors, such as CX3CL1 and TGF-β, by neuronal cells (Zhou et al., 2012; Ponomarev et al., 2013).

In addition to the role of miRNAs in mononuclear phagocyte development, these small regulatory RNAs have been proposed to function as markers for microglia *vs* macrophage differentiation. Eight miRNAs were found to be highly expressed in microglia, including miR-125b-5p, miR-342-3p and miR-99, while 24 miRNAs were identified as Ly6C monocyte-specific, including miR-223, miR-148a and miR-15b (Butovsky et al., 2014). These molecular signatures were compared with other tissue-specific macrophages, which allowed to establish a hierarchical clustering of the tested immune cell populations. From this analysis, it was possible to conclude that red pulp macrophages are the tissue resident macrophages that more closely resemble microglia (Butovsky et al., 2014).

1.3.1.2. *MiRNA regulation of inflammation*

The power of miRNAs to regulate inflammation hyperactivity has been known since early studies on miR-155 upregulation following LPS-stimulation in macrophages (O'Connell et al., 2007). As previously discussed, signaling through TLRs, following activation by PAMPs, involves the action of the adapter proteins MyD88 and TRIF. These cascades culminate in the activation of transcription factors such as NF-κB and c-Jun, responsible for the production of inflammatory cytokines and type I interferons. During this process, the expression of miRNAs is also upregulated and, among them, miR-155, miR-146a and miR-21 are the most thoroughly investigated. Depending on the nature of their molecular targets and their role in inflammation, miR-155 is considered a pro-inflammatory miRNA contributing to the propagation of inflammation, while miR-146a and miR-21 control the magnitude of this response.

Following TLR activation, miR-155 expression increases with the main goal of suppressing inhibitory proteins of inflammation, such as SOCS-1 and Src homology-2 domain-containing inositol 5-phosphatase 1 (SHIP1). These primary targets have been studied in the context of macrophage (O'Connell et al., 2009) and microglia (Cardoso et al., 2012) activation, and their downregulation was found to be critical for the development of inflammation. A less studied inflammatory pathway in microglia, in which miR-155 plays a primary role, involves p53. This protein is essential for miR-155 upregulation, which negatively regulates c-Maf expression promoting inflammation (Su et al., 2014).

Interestingly, although miR-146a is a negative modulator suppressing TLR signaling, similarly to miR-155, miR-146a is also upregulated during immune activation by the increase in the activity of NF-κB (Taganov et al., 2006). One of its main functions is to inhibit the expression of two components of the MyD88 signaling, IRAK1 and TRAF6 (Taganov et al., 2006), and also to inhibit NF-κB directly. In opposition to miR-155, miR-146a controls the propagation of inflammation by targeting these important adapters (Li et al., 2011) and has been shown to be involved in the "resolution" phase of inflammatory events. MiR-21 targets the programmed cell death protein 4 (PDCD4), leading to downregulation of NF-κB and induction of anti-inflammatory proteins, such as IL-10, which makes it a negative regulator of the immune response. Its expression is also induced during TLR activation in a MyD88-dependent manner. The opposite happens for other miRNAs, such as miR-125b and let-7 (Tili et al., 2007; Iliopoulos et al., 2009), which are downregulated during inflammation to avoid their binding to the 3'UTR of several pro-inflammatory cytokines, including TNF-α and IL-6.

In addition to the role of miRNAs in the regulation of inflammatory pathways, it has been proposed that they can function as markers of the spectrum of different macrophage activation phenotypes, which are expressed as a continuum along different patterns of gene expression. Currently, activation phenotypes are no longer classified only as M1 and M2, but can be subdivided in different substates, such as M2a, M2b and M2c, with M0 being considered a maintenance or restoration of the homeostatic balance state. Although differences between activation phenotypes are very difficult to prove *in vivo,* due to the lack of protein-based markers and powerful non-invasive techniques, similar polarizations have been proposed for microglia. While the disruption of the brain homeostatic balance (M1) is accompanied by an increase in miR-155-5p expression, as well as by a reduction in miR-124-3p, its reposition (M2a) and maintenance (M0) are accompanied by an increase in the expression of miR-145-5p and miR-124-3p, respectively (Freilich et al., 2013). These miRNAs may help to identify the activation phenotypes more prevalent in different disease settings and their modulation may allow to shift these phenotypes according to specific needs.

1.3.1.3. *MiRNAs in Alzheimer's disease-related neuroinflammation*

Several studies have reported the deregulation of different miRNAs in AD, including those required to control the expression of: apoptotic markers (miR-29), tau kinases (miR-15), cell cycle proteins and BACE1 (miR-107), cellular defenses against DNA damage (miR-181c), sirtuin (SIRT1), a de-acetylase involved in tau pathology (miR-9), APP and cyclooxygenase-2 (COX-2) (miR-101) and autophagy-mediated Aβ clearance (miR-106) (reviewed in (Hebert et al., 2008; Delay et al., 2012)). Almost all of these miRNAs were found to be deregulated in brain tissue collected from AD patients, in AD mouse models and in neurons exposed to Aβ. The networks of deregulated miRNAs in AD are surprisingly huge and a more comprehensive analysis is needed to disclose which of these miRNAs are deregulated in pre-clinical stages of AD (potentially contributing to the onset of dementia) or as a consequence of the deregulation of entire protein signaling pathways that underlie the disease. MiRNAs have also been pointed as potential biomarkers of AD in the CSF (Denk et al., 2015) and blood (Satoh et al., 2015), although standardized methods are needed to collect and analyze samples in order to correlate results from different laboratories, hospitals and patients cohorts.

In view of the essential role played by miRNAs in inflammation and maintenance of homeostasis in an injury situation, it is not surprising that miRNA deregulation has been thoroughly implicated in most neurological diseases harboring inflammatory responses. Examples of the connection of immune-related miRNAs with brain disease are described below and summarized in Table 1.1.

As one could expect, inflammation-related miRNAs have been found to be deregulated in AD. For example, miR-146a was shown to be upregulated, thus contributing to the chronicity of the inflammatory response in this disease (Fig. 1.5). This miRNA was one of the first miRNAs reported to be elevated in the brain regions of AD patients most affected by the disease and to be increased in response to pro-inflammatory mediators such as IL-1β, TNF-α and $A\beta_{1\text{-}42}$ (Lukiw, 2007; Jiang et al., 2013b). This upregulation was associated with decreased levels of the glycoprotein immune repressor complement factor (CFH), which is a major regulator of the complement response (Lukiw and Alexandrov, 2012), thus suggesting that miR-146a regulation in AD constitutes a nefarious event. However, this conclusion is now believed to be overly simplistic, since miR-146a seems to exert important immunomodulatory effects regarding microglia and macrophage activation.

Jayadev and colleagues demonstrated that presenilin 2 KO mice have low miR-146a levels in microglia, which results in increased NF-κB transcriptional activity, impacting microglial response (Jayadev et al., 2013). However, although miR-146a was found to be upregulated in prion disease mouse brain tissues and in microglia cell lines following TLR2 or TLR4 activation, such increase did not follow the kinetics of cytokine increase, since high levels of miR-146a have been observed even after cytokine expression returned to basal levels (Saba et al., 2012). A functional genomic analysis performed in the EOC microglia cell line revealed that miR-146a overexpression leads to downregulation of important phagocytosis and oxidative burst genes, such as the inducible nitric oxide synthase (iNOS) and IL-1β, and to alterations in downstream mediators of the NF-κB and JAK-STAT signaling pathways (Saba et al., 2012). Altogether, these findings suggest that miR-146a upregulation may not always have the purpose of increasing inflammation but, instead, may reflect an attempt of the immune system to keep it “in-check”.

Overexpression of TLRs and unchecked TLR signaling are associated with most neurodegenerative diseases (Frank et al., 2009; Paschon et al., 2015), including AD, in which different TLRs were shown to be overexpressed and thought to act as receptors for Aβ peptides in microglia, triggering activation of these cells. The let-7 family of miRNAs was recently suggested to play an unconventional role, acting as ligands for TLR7 (Lehmann et al., 2012).

Let-7 has been shown to be upregulated in AD patients, contributing to neurodegeneration and neuroinflammation (Lehmann et al., 2012).

Table 1.1 | Involvement of miRNAs in disease-related neuroinflammation.

Brain disease	miRNA	Functional role / molecular target	Ref
Japanese encephalitis virus	**miR-155**	Reduction of virus-induced gene expression	(Pareek et al., 2014)
	miR-146a	Evasion of inflammation / TRAF6, IRAK1, IRAK2, STAT1 Enhancement of viral replication / IFIT-1, IFIT-2	(Sharma et al., 2015)
Angiostrongyluscantonensis	**miR-146a**	Immunosuppression / TRAF6, IRAK1	(Yu et al., 2014a)
	miR-223	Inhibition of inflammation	(Yu et al., 2014b)
	miR-155	Activation of macrophages (protection)	(Yu et al., 2014b)
Ischemic stroke	**miR-122** **miR-148a** **let-7i** **miR-19a** **mir-320d** **miR-363** **miR-487b**	TLR and NF-κB signaling	(Jickling et al., 2014)
	miR-203	Inhibition of NF-κB signaling / MyD88	(Yang et al., 2015)
Multiple sclerosis/Experimental autoimmune encephalomyelitis	**miR-146a**	Disease biomarker Dysfunctional inflammation	(Fenoglio et al., 2011)
	miR-155 **miR-326** **miR-34a**	Dysfunctional inflammation, myelin phagocytosis / CD47	(Junker et al., 2009; Murugaiyan et al., 2011)
	miR-124	Regulation of microglia activation	(Ponomarev et al., 2011)
Alzheimer's disease	**let-7**	TLR7 activation	(Lehmann et al., 2012)
	miR-146a	Regulation of inflammation / CHF	(Lukiw and Alexandrov, 2012; Jayadev et al., 2013)
	miR-155	Dysfunctional inflammation / SOCS-1	(Guedes et al., 2014)
Parkinson's disease	**let-7**	Regulation of TLR expression / α-synuclein	(Junn et al., 2009; Beraud et al., 2011)
Prion disease	**miR-146a**	Regulation of inflammation	(Saba et al., 2012)
Amyotrophic lateral sclerosis	**miR-155** **miR-146b** **miR-29b** **let-7a/b** **mir-21** **miR-210**	Dysfunctional inflammation	(Butovsky et al., 2012; Parisi et al., 2013)

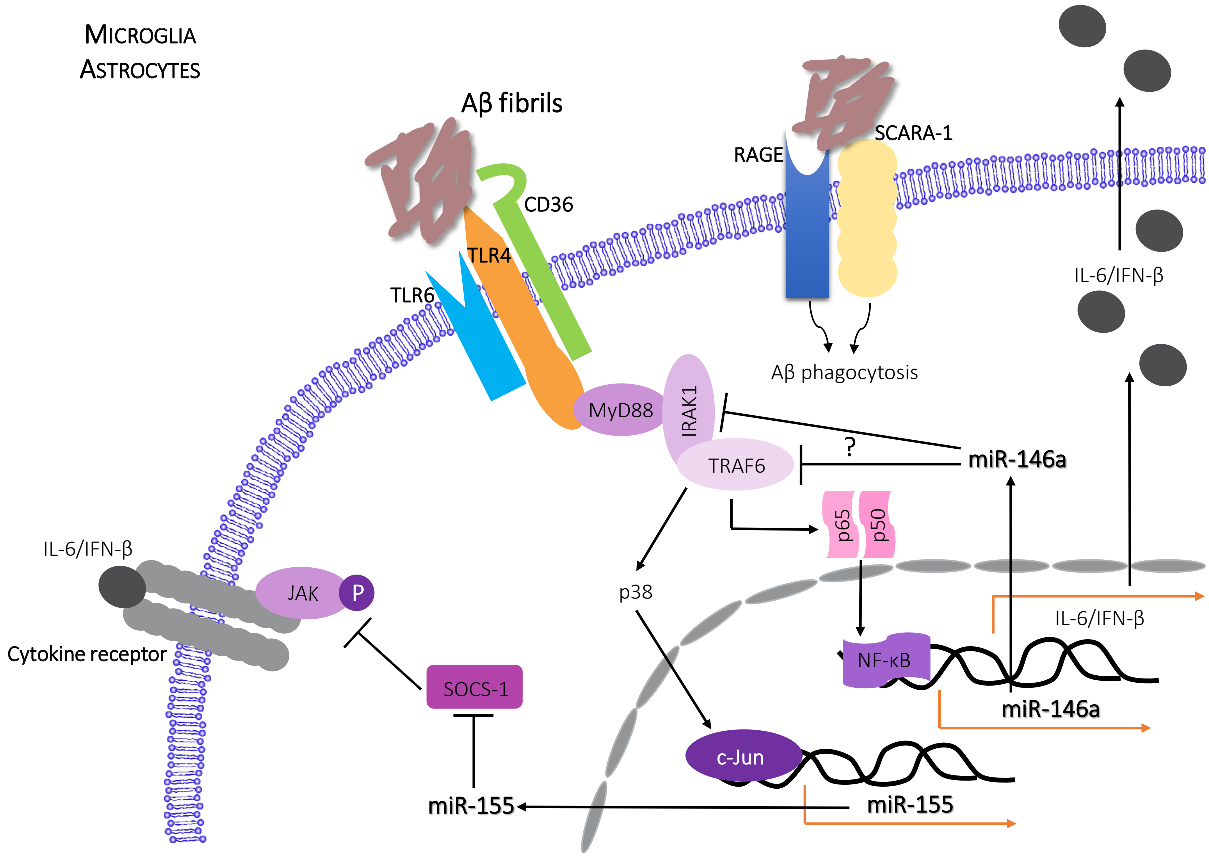

Figure 1.5 | MiR-155 and miR-146a neuroinflammatory mechanisms in AD.
The interaction of Aβ fibrils with different receptor complexes at the cell membrane of microglia and astrocytes leads to both cellular internalization and phagocytosis, as well as activation of standard MyD88-mediated inflammatory pathways, culminating in the activation of NF-κB and c-Jun. While c-Jun activity upregulates the expression of miR-155 contributing to suppressor of cytokine signaling (SOCS-1) inhibition and consequent propagation of inflammation, NF-κB-derived miR-146a upregulation can generate an immunomodulatory effect.

1.3.2. *MiRNA-based therapeutic applications in neuroimmune and neurodegenerative diseases*

Exploring gene therapy approaches to treat neurodegenerative disorders is an enormous challenge. The use of vectors that have the ability to transfect or infect the whole brain is a surreal approach and, in humans, would implicate brain surgery. Therefore, the use of peripheral cells, such as monocytes, as potential gene delivery systems constitutes an attractive perspective to treat brain injury. Although there is still a huge amount of work to do in this regard, researchers already started to investigate the hypothesis of genetically manipulating monocytes *ex vivo*. In 2010, Lebson and colleagues showed, for the first time, that CD11b^{+} monocytes isolated from the bone-marrow can be injected into APP/PS1 mice to successfully deliver a secreted diffusible form of neprilysin (NEP) to the brain, dramatically decreasing amyloid load (Lebson et al., 2010). Moreover, it is plausible to believe that in a near future, and based on the recently discovered molecular signatures of microglia and other myeloid cells, it will be possible to create new gene and drug delivery systems targeted to specific subsets of cells.

Given the pivotal role of miRNAs in the regulation of gene expression, miRNA-based therapies could reveal themselves highly promising to improve microglia activity, modulating signaling pathways linked with neuroinflammation. The fine-tuning activity of miRNAs allows them to target more than one protein involved in the same signaling pathway and their modulation can significantly change cell phenotypes that depend on the levels and activation of specific proteins. Such capacity reflects a molecular paradigm suitable for therapeutic intervention. Very recently, Butovsky and coworkers demonstrated that SOD1 mice present dysfunctional microglia due to downregulation of important transcription factors, upstream regulators and effector proteins (Butovsky et al., 2015). Disease severity in this model was related with miR-155 expression and early upregulation of inflammatory genes. Importantly, these authors showed that treatment with anti-miR-155 oligonucleotides, through intraventricular injection, derepressed microglia homeostatic genes and prolonged animal survival (Butovsky et al., 2015), providing us with one of the first examples of a successful miRNA-based therapeutic strategy designed to target unchecked inflammation in the brain. Due to the lack of minimally invasive diagnosis tools and effective therapeutic options for most CNS diseases, we believe that the use of miRNAs, both as disease biomarkers and therapeutic targets associated with cells of the immune lineage, although yet poorly explored, will tend to grow in the near future.

CHAPTER 2

Objectives

The impact of miRNAs in mononuclear phagocyte function in Alzheimer's disease (AD) is far from being understood. Although it is acknowledged that miRNAs are small regulatory RNAs that hold a huge potential as biomarkers and molecular targets in new therapeutic strategies, comprehensive studies are required in both animal and human models, in order to understand how the intricate networks of miRNA expression contribute to the function of neuroimmune cells, known to play a crucial role in the control of Aβ deposition in the AD brain. Importantly, understanding mononuclear phagocyte ontology is essential to decide when and how to modulate microglia activation, when to block or induce blood-derived monocyte recruitment to the brain and when to employ these cells as delivery systems for genes or drugs with a therapeutic impact on the CNS. Moreover, since the signaling pathways leading to Aβ phagocytosis and to the production of inflammatory mediators share common intervenients, it is essential to understand how epigenetic mechanisms, including miRNAs, regulate gene expression and cellular function during the different stages of dementia. In this context, and taking into consideration the state-of-the-art, the major goals of this Work were:

1. To study the contribution of different Aβ forms to the activation of mononuclear phagocytes, aiming at understanding the molecular mechanisms driving Aβ-mediated inflammation;
2. To characterize the activity of peripheral mononuclear phagocytes in the context of AD, particularly concerning cellular functions essential for Aβ clearance, such as chemotaxis and phagocytosis;
3. To understand the contribution of miRNAs to the establishment and maintenance of inflammatory phenotypes of mononuclear phagocytes in Alzheimer's disease, essential for their response to Aβ accumulation;
4. To explore the potential of inflammatory miRNAs, expressed in mononuclear phagocytes, as disease biomarkers to stage dementia and evaluate disease progression;
5. To understand the contribution of bone-marrow-derived monocytes to the clearance of Aβ from the brain in an AD mouse model;
6. To assess the potential of *ex vivo* therapeutic modulation of miRNA activity in bone-marrow-derived monocytes to decrease Aβ deposition in AD brain.

| CHAPTER 3

Early miR-155 upregulation contributes to neuroinflammation in Alzheimer's disease triple transgenic mouse model

Guedes, J.R., Custodia, C.M., Silva, R.J., et al. (2014). Early miR-155 upregulation contributes to neuroinflammation in Alzheimer's disease triple transgenic mouse model. Hum Mol Genet 23, 6286-6301.

Abstract

MicroRNAs (miRNAs) have emerged as a class of small, endogenous, regulatory RNAs that exhibit the ability to epigenetically modulate the translation of mRNAs into proteins. This feature enables them to control cell phenotypes and, consequently, modify cell function in a disease context. The role of inflammatory miRNAs in Alzheimer's disease (AD) and their ability to modulate glia responses are now beginning to be explored. In this study, we propose to disclose the functional role of miR-155-5p, one of the most well studied immune-related miRNAs, in AD-associated neuroinflammatory events, employing the 3xTg AD animal model. A strong upregulation of miR-155-5p levels was observed in the brain of 12-month-old 3xTg AD animals. This event occurred simultaneously with an increase of microglia and astrocyte activation, and before the appearance of extracellular Aβ aggregates, suggesting that less complex Aβ species, such as Aβ oligomers may contribute to early neuroinflammation. In addition, we investigated the contribution of miR-155-5p and the c-Jun transcription factor to the molecular mechanisms that underlie Aβ-mediated activation of glial cells. Our results suggest early miR-155-5p and c-Jun upregulation in the 3xTg AD mice, as well as in Aβ-activated microglia and astrocytes, thus contributing to the production of inflammatory mediators such as IL-6 and IFN-β. This effect is associated with a miR-155-5p-dependent decrease of suppressor of cytokine signaling 1 (SOCS-1). Furthermore, since c-Jun silencing decreases the levels of miR-155-5p in Aβ-activated microglia and astrocytes, we propose that miR-155-5p targeting can constitute an interesting and promising approach to control neuroinflammation in AD.

3.1. Introduction

Alzheimer's disease (AD), the most common form of elderly dementia, is characterized at the cellular and molecular level by pathological hallmarks that include the presence of extracellular senile plaques, intraneuronal phosphorylated tau (p-tau) aggregates, neuronal death and both local and systemic inflammation. The most important non-cellular component of senile plaques is β-amyloid (Aβ), a peptide resulting from the tandem cleavage of the amyloid precursor protein (APP) by β-secretase and γ-secretase. This peptide is able to self-aggregate originating Aβ dimers, Aβ oligomers and, at a more complex stage, Aβ fibrils. The cellular components of Aβ plaques include dystrophic neuritis, cell debris and activated microglia and astrocytes (El Khoury and Luster, 2008).

In the last decade, the neuroinflammatory component of AD has been subject of intense debate. The chronic deposition of Aβ in the brain stimulates the persistent activation of astrocytes and microglia cells, leading to cell proliferation and overproduction of inflammatory mediators, such as cytokines, chemokines and nitric oxide (NO), which are responsible for the attraction of more astrocytes and microglia cells to the sites of Aβ deposition (Dheen et al., 2005; Lucin and Wyss-Coray, 2009; Glass et al., 2010), as well as for the migration of peripheral mononuclear phagocytes to the brain (El Khoury et al., 2007). Despite the intense investigation in this field, the nature of astrocytes and microglia interaction with Aβ remains controversial with respect to the strength of cell response to different Aβ forms and their neurotoxic or neuroprotective role in AD. On one hand, the excessive production of proinflammatory mediators promotes chronic neuronal toxicity but, on the other hand, microglia and astrocytes have been shown to help clear Aβ deposits, delaying disease progression (Wyss-Coray et al., 2003; D'Andrea et al., 2004). Nevertheless, all studies performed so far strongly suggest an important involvement of inflammatory pathways in the pathophysiology of AD (Griffin et al., 1998; Parachikova et al., 2007) and reinforce the need to explore inflammation-related genes in therapeutics and diagnosis.

Although it is well documented that microglia constitutes the cellular type responsible for initiating the innate immune response against Aβ in the brain, it is becoming increasingly clear that astrocytes also play a critical role in the amplification of inflammatory and neurotoxic processes. The interaction between astrocytes and microglia cells has been studied in a physiological and pathological context, demonstrating that astrocytes are activated by microglia-released factors (Saijo et al., 2009; Agulhon et al., 2012) and also by Aβ (Heneka and O'Banion, 2007), these serving as immunomodulators of microglia-related immune responses. In glial cells, Aβ is recognized through Toll-like receptors (TLRs) 4 and 6 in the presence of CD36 (Walter et al., 2007; Letiembre et al., 2009; Stewart et al., 2010). The activation of TLR4 leads to: early nuclear factor-κB (NF-κB) activation and tumor necrosis factor (TNF-α) production; delayed

Janus tyrosine kinase 1/signal transducer and activator of transcription factors 1 (JAK1/STAT1) activation, which is regulated by Jun N-terminal kinase (JNK), resulting in the expression of the suppressor of cytokine signaling 1 (SOCS-1), which negatively regulates cytokines; and activation of the signaling pathway involving the mitogen-activated protein kinases (Gorina et al., 2011). These intracellular signaling pathways are also associated with activation of activator protein-1 (AP-1) transcription factor (which is composed of a dimer of c-Jun and c-Fos) by JNK that is related with apoptosis and inflammation. Neuronal apoptosis can be triggered by Aβ through activation of JNK (Tang et al., 2008) and, in glial cells, the inhibition of JNK activation leads to the production of interleukin-10 (IL-10), an anti-inflammatory cytokine (Bernardi et al., 2012). Interestingly, c-Jun was found to be activated in AD brains (Vukic et al., 2009) and our previous data have shown that silencing of c-Jun resulted not only in a blockade of neuronal death, but also in a decrease of brain inflammation in an excitotoxic lesion model *in vivo* (Cardoso et al., 2010). These results suggest a clear involvement of c-Jun in apoptosis and inflammatory responses in AD.

Small endogenous non-coding RNAs, also known as microRNAs (miRNAs) regulate gene expression primarily at the post-transcriptional level, exerting their function by targeting complementary mRNA molecules and inhibiting their translation. Their involvement in almost all biological functions and their capacity to promote the fine regulation of intracellular processes by targeting multiple mRNAs simultaneously make them a class of emerging molecules with potential to be used in therapy and diagnostics. Several miRNA networks, including miRNAs related with innate immunity and neuroinflammation have been found to be deregulated in AD (Cogswell et al., 2008; Lukiw et al., 2008; Li et al., 2011). MiR-155 is considered a proinflammatory miRNA and has been shown to play a central role in the regulation of the innate immune response, through modulation of cytokine and chemokine production (Thai et al., 2007; Cardoso et al., 2012; Guedes et al., 2013). In 2007, O'Connell and coworkers first described miR-155 as a key player in macrophage inflammatory response following TLR activation and suggested that its upregulation was dependent on the JNK pathway (O'Connell et al., 2007). Moreover in 2013, Onyeagucha suggested that miR-155 expression is regulated by the AP-1 transcription factor (Onyeagucha et al., 2013). In fact, these authors observed that attenuation of AP-1 activation through pharmacological inhibition of MEK activation or genetic inhibition of c-Jun activation, using dominant negative c-Jun (TAM67), suppressed miR-155 induction. Interestingly, our laboratory showed that miR-155-5p also increases in microglia, following lipopolysaccharide (LPS) stimulation (Cardoso et al., 2012), and regulates SOCS-1 levels, as well as cytokine and NO production, thus providing evidence that this miRNA can exert a proinflammatory role both in the peripheral immune system and the brain. Moreover, some observations suggest that miR-155 also plays a role in gene regulatory networks in astrocytes, due to its increased expression upon astrocyte activation (Mor et al., 2011), and is involved in proinflammatory cytokine upregulation in these cells by targeting SOCS-1 mRNA (Tarassishin et al., 2013).

Given the importance of miR-155-5p and c-Jun in inflammatory responses, in this work we proposed to investigate the role of these two cell modulators in Aβ-mediated neuroinflammation in the context of AD.

3.2. Materials and Methods

3.2.1. Materials

The anti-miR-155-5p locked nucleic acid (LNA) *in situ* hybridization probe as well as the quantitative reverse transcription (qRT) PCR primers for detection and determination of miR-155-5p were obtained from Exiqon (Denmark). The qRT-PCR primers for mRNA quantification were purchased from Qiagen (Germany). The anti-c-Jun siRNA (5′-AGTCATGAACCACGTTAAC-3′; siRNA c-Jun) and the non-silencing siRNA (siRNA Mut) used as control were purchased from Shangai GenePharma (P.R. China). The Lipofectamine$^{\text{TM}}$ RNAiMAX Transfection Reagent was purchased from Invitrogen (USA). The ionized calcium-binding adapter molecule 1 (IBA-1) antibody for immunohistochemistry was obtained from Wako Pure Chemical Industries, Ltd. (Japan) and the GFAP and Aβ antibodies were purchased from Chemicon International, Inc. (USA). The SOCS-1 and the c-Jun antibodies for western blot were purchased from Cell Signaling (USA) and the actin antibody was obtained from Sigma (USA). The $A\beta_{1\text{-}42}$ peptide was obtained from American Peptide (USA). All the other chemicals were obtained from Sigma, unless stated otherwise.

3.2.2. Animals

All efforts were made to minimize suffering and the number of animals used in this study, according to the guidelines of the Portuguese National Authority for Animal Health. The AD triple transgenic animals (3xTg AD mice) were obtained from Dr Frank LaFerla laboratory at the Department of Neurobiology and Behavior and Institute for Brain Aging and Dementia, University of California at Irvine. The animals were found to have the same phenotypic and behavioral characteristics, as previously described by Dr Frank LaFerla group (Oddo et al., 2003a; Oddo et al., 2003b). Briefly, human APP cDNA harboring the Swedish double mutation (KM670/ 671NL) and human four-repeat tau harboring the P301L mutation were co-microinjected into single-cell embryos of homozygous $PS1_{M146V}$ knock-in mice. The PS1 mice were originally generated on a hybrid 129/C57BL6 background (Guo et al., 1999). The animals ($n = 6$ for each experimental group) were maintained under controlled light and environmental conditions (12 h dark/light cycle, 23 ± 1°C, 55 ± 5% relative humidity), having free access to food and water. Age- and gender-matched non-transgenic animals were used as controls. The animals were killed at 3 or 12 months of age and the brains were removed following transcardial perfusion with 20 mL of an ice-cold 0.9% NaCl solution. One hemisphere of each brain was post-fixed (12 h) in a fixative solution of 4% paraformaldehyde (PFA) in 0.9% NaCl, and was kept for 2–3 days in a cryoprotective solution containing 25% sucrose. After this period, the brain hemisphere was dried and frozen at -80°C until further use. The other hemisphere was used for protein and mRNA extraction. For this purpose, the hemisphere was placed on an acrylic matrix and a 4 mm coronal section was cut with a stainless steel razor. The hippocampal and cortical regions from this section were dissected and kept at -80°C until protein or RNA extraction.

3.2.3. *Immunohistochemistry*

Immunohistochemistry of brain slices was performed as described previously (Simoes et al., 2012). Briefly, coronal sections of 30 μm were cut throughout the entire cortex and hippocampus at -20°C in a cryostat (LeicaCM 3050 S, Leica, Germany) and stored in 48-well multiwell plates in phosphate buffer saline (PBS) supplemented with 0.05 mM sodium azide at 4°C until immunohistochemical processing. Free-floating sections were permeabilized for 2 h with 0.1% Triton X-100 containing 10% normal goat serum (Gibco, Life Technologies, USA) at room temperature, followed by incubation with the primary antibodies against IBA-1 (1:1000), GFAP (1:1000) or Aβ (1:2000) in blocking solution, overnight at 4°C. Sections were then washed three times and incubated for 2 h at room temperature with the respective biotinylated antibodies (Vector Laboratories, USA). Bound antibodies were visualized using the VECTASTAIN® ABC kit, with 3,3′-diaminobenzidine tetrahydrochloride (DAB metal concentrate; Pierce) (Thermo Fisher Scientific, USA) as substrate. After washed three times, the sections were mounted in FluorSave™ Reagent (Calbiochem, Merk Millipore, USA) on microscope slides. All slices were observed by visible immunostaining, under a Zeiss Axiovert microscope (Carl Zeiss Microimaging, Germany), equipped with AxioCam HR color digital cameras (Carl Zeiss Microimaging) using ×5, ×20 and ×40 objectives.

3.2.4. *Microglia and astrocyte cell culture*

N9 microglia cells (immortalized mouse microglia cells) were cultured at 37°C in a humidified atmosphere containing 5% CO_2 and maintained in RPMI-1640 medium (Gibco, Life Technologies) supplemented with 5% heat-inactivated fetal bovine serum (FBS), 100 μg/mL streptomycin and 1 U/mL penicillin. N9 microglia cells were plated 24 h before the beginning of each experiment at a density of 100 000 cells/well in uncoated 12-well multiwell plates for RNA extraction.

Astrocyte primary cultures were prepared from 3-day-old C57/BL6 newborn mice. After digestion and dissociation of the dissected mouse cortices in HBSS solution (Hank's Buffered Salt Solution, 136.7 mM NaCl, 2.1 mM $NaHCO_3$, 0.22 mM KH_2PO_4, 5.3 mM KCl, 2.7 mM glucose, 10 mM HEPES, pH 7.3) supplemented with 0.25% trypsin, 0.001% DNase I and 10 μg/mL gentamicin, mixed glial cultures were prepared by resuspending the cell suspension in DMEM medium (10 mM $NaHCO_3$, 25 mM HEPES, 10 μg/mL gentamicin, pH 7.3) containing 10% FBS (Gibco, Life Technologies). Cells were seeded on 75 cm^2 flasks at a density of 3×10^6 cells per flask and maintained in the culture flasks for 10 days at 37°C in a humidified atmosphere containing 5% CO_2, with medium changes each 2–3 days. When the mixed glial cultures achieved 70% confluence, microglia and oligodendrocytes attached at the upper layer of the astrocyte culture were detached by shaking for 4 h in an orbital shaker at 220 rpm and 37°C. The purified astrocytes were trypsinized and plated in DMEM 10% FBS medium at a density 240 000 cells/well in uncoated 6-well multiwell plates for RNA extraction, at a density of 100 000 cells/well in 12-well multiwall plates for cell transfection and fluorescence microscopy experiments and at 20 000 cells/well in microslide eight-well ibiTreat chamber slides (ibidi, Germany) for *in situ* hybridization experiments. In all cases, after shaking, astrocytes were maintained in culture for 3 days before the beginning of the experiments. Regular characterization of primary astrocyte cultures by GFAP and CD11b immunostaining indicated the presence of over 97% astrocytes, confirming the purity of these cultures.

3.2.5. Preparation of amyloid-β (Aβ) oligomers and fibrils for microglia and astrocytes treatment

$A\beta_{1-42}$ oligomers and fibrils were prepared as previously described (Resende et al., 2008). Briefly, synthetic $A\beta_{1-42}$ peptide (American Peptides, USA) was dissolved in 1,1,1,3,3,3-hexafluoro-2-propanol (HFIP) to obtain a 1 mM solution. The HFIP was then evaporated in a Speed Vac (I´lshin Laboratory. Co., Ltd., Netherlands) and the dried peptide was resuspended in anhydrous dimethyl sulfoxide (DMSO) at a 5 mM solution. $A\beta_{1-42}$ oligomers were prepared by diluting the $A\beta_{1-42}$ solution in Phenol Red-free Ham's F-12 medium without glutamine to a 100 μM final concentration and incubated overnight at 4°C. The solution was then centrifuged at 15 000 g for 10 min at 4°C to remove insoluble aggregates, and the supernatant, containing soluble oligomers, was transferred to clean tubes and stored at 4°C. $A\beta_{1-42}$ fibrils were prepared by diluting the 5 mM $A\beta_{1-42}$ solution in DMSO to a concentration of 200 μM in 100 mM HEPES buffer (pH 7.5) and aged at 37°C for 7 days. The preparation was then centrifuged during 10 min at 15 000 g at room temperature and the supernatant, containing soluble oligomers, was discarded. The pellet containing Aβ fibrils (and possibly protofibrils) was resuspended in 100 mM HEPES buffer (pH 7.5). Protein concentrations of Aβ oligomers and fibrils were determined using the Bio-Rad Dc protein dye assay reagent.

The presence of different assembly forms (monomers, oligomers and fibrils) of Aβ_{1-42} in the different preparations and the purity of isolated oligomers and fibrils were evaluated by gel electrophoresis (Supplementary Material, Fig. S3.8). Aβ samples containing 10 µg of protein were diluted (1:2) with sample buffer (40% (w/v) glycerol, 2% (w/v) SDS, 0.2 M Tris–HCl, pH 6.8 and 0.005% (w/v) Coomassie G-250) and were separated by electrophoresis on a 4–16% Tris–Tricine SDS gel. Samples were not boiled to minimize disaggregation prior to electrophoresis. To facilitate the identification of proteins, a low-range rainbow protein standard was used. The gel was stained with Coomassie G-250 for 10 min, followed by overnight incubation with a destaining solution composed of 10% acetic acid and 30% methanol in H_2O. Analysis of band weight was performed using the Quantity One software (Bio-Rad, USA) and the percentage of the Aβ aggregation forms in each Aβ preparation is presented in the Supplementary Material, Table S3.1.

In order to accomplish Aβ-mediated cell activation, N9 microglia cells were treated with Aβ oligomers or fibrils at a 5, 10 and 20 µM concentration and astrocytes were treated with 10 and 30 µM Aβ oligomers or fibrils for 24 h. Alternatively, as a positive activation control, N9 microglia cells and astrocytes were incubated with LPS at 0.1 and 10 µg/mL concentrations, respectively.

3.2.6. Transfection experiments

The delivery of siRNAs (siRNA c-Jun or siRNA Mut) to N9 microglia cells and astrocytes was performed using the Lipofectamine™ RNAiMAX Transfection Reagent, according to the manufacturer's instructions (Invitrogen, USA). Briefly, Lipofectamine™ RNAiMAX Transfection Reagent in an Optimem (modification of Eagle''s Minimum Essential Media, 28.5 mM $NaHCO_3$) volume of 50 mL/well was mixed with the appropriate volume of siRNA stock solution to achieve a final siRNA concentration of 50 nM in each well. The mixture was further incubated for 30 min, at room temperature. For qRT-PCR experiments, immediately before transfection, cells were washed and the medium was replaced with Optimem for N9 microglia or DMEM supplemented with 5% FBS for astrocytes (950 mL/well). For fluorescence *in situ* hybridization experiments, astrocytes were plated in µ-slide eight-well ibiTreat chamber slides (ibidi) and transfected in a final volume of 200 mL/well in DMEM 5% FBS. For both qRT-PCR and *in situ* hybridization experiments, after a 4 h transfection period, the cell medium was replaced with fresh DMEM with 10% FBS, in the case of astrocyte cultures, or RPMI-1640 with 5% FBS in N9 microglia cells. Twenty-four hours after transfection, N9 microglia cells were exposed to 0.1 µg/mL LPS or 20 µM Aβ fibrils and primary astrocytes were exposed to 10 µg/mL LPS or 30 µM Aβ fibrils for 24 h. Following this incubation period, RNA extraction and *in situ* hybridization experiments were performed.

3.2.7. *Quantitative real-time PCR*

Total RNA, including small RNA species, was extracted from brain tissue of 3xTg AD and wild-type (WT) animals with 3 or 12 months, primary astrocyte cultures and N9 microglia cells using the miRCURY Isolation Kit Cells (Exiqon), according to the manufacturer's recommendations for cultured cells. Briefly, after cell lysis, the total RNA was adsorbed to a silica matrix, washed with the recommended buffers and eluted with 35 μL RNase-free water by centrifugation. After RNA quantification, cDNA conversion for miRNA quantification was performed using the Universal cDNA Synthesis Kit (Exiqon). For each sample, cDNA for miRNA detection was produced from 20 ng total RNA according to the following protocol: 60 min at 42°C followed by heat-inactivation of the reverse transcriptase for 5 min at 95°C. The cDNA was diluted 80× with RNase-free water before quantification by qRT-PCR. Synthesis of cDNA for mRNA quantification was performed using the iScript cDNA Synthesis Kit (Bio-Rad) and employing 1 μg total RNA for each reaction, by applying the following protocol: 5 min at 25°C, 30 min at 42°C and 5 min at 85°C. Finally, the cDNA was diluted 1:10 with RNase-free water.

Quantitative PCR was performed in a iQ5 thermocycler (Bio-Rad), using 96-well microtitre plates. The miRCURY LNA™ Universal RT microRNA PCR system (Exiqon) was used in combination with pre-designed LNA primers (Exiqon) for miR-155-5p and SNORD 110 (reference gene) quantification. A master mix was designed for each primer set and, for each reaction, 12 μL of the master mix were added to 8 μL of cDNA template. All reactions were performed in duplicate at a final volume of 20 μL per well, using the iQ5 Optical System Software (Bio-Rad). The reaction conditions consisted of polymerase activation/denaturation and well-factor determination at 95°C for 10 min, followed by 40 amplification cycles at 95°C for 10 s and 65°C for 1 min (ramp-rate 1.6°C/s).

mRNA quantification was performed using the iQ SYBR Green Supermix Kit (Bio-Rad). The primers for the target genes (SOCS-1, IL-6 and IFN-β) and for the reference gene HPRT were pre-designed by Qiagen (Qiagen, Germany). A master mix was prepared for each primer set, containing a fixed volume of SYBR® Green Supermix and the appropriate amount of each primer to yield a final concentration of 150 nM. For each reaction, 20 μL master mix was added to 5 μL template cDNA. All reactions were performed in duplicate (two cDNA reactions per RNA sample) at a final volume of 25 μL per well, using the iQ5 Optical System Software (Bio-Rad). The reaction conditions consisted of enzyme activation and well-factor determination at 95°C for 1 min and 30 s, followed by 40 cycles at 95°C for 10 s (denaturation), 30 s at 55°C (annealing), and 30 s at 72°C (elongation).

For both miRNA and mRNA quantification, a melting curve protocol was started immediately after amplification and consisted of 1 min heating at 55°C followed by 80 steps of

10 s, with a 0.5°C increase at each step. Threshold values for threshold cycle determination (Ct) were generated automatically by the iQ5 Optical System Software. The miRNA and mRNA fold increase or fold decrease, with respect to control samples, was determined by the Pfaffl method, taking into consideration the different amplification efficiencies of the different genes and miRNAs. The amplification efficiency of each target or reference RNA was determined according to the formula: $E = 10^{(-1/S)} - 1$, where S is the slope of the obtained standard curve.

3.2.8. In situ *hybridization*

Fluorescence *in situ* hybridization was performed in brain slices of 3xTg AD animals and WT littermates and in primary astrocytes, as described by Lu and Tsourkas (Lu and Tsourkas, 2009), with some modifications. Briefly, free-floating brain slices were mounted in microscope slides, washed with PBS, fixed with 4% PFA for 30 min at room temperature and permeabilized at 4°C in 70% ethanol for 4 h. Slices were then incubated with fresh acetylation solution [0.1 M triethanolamine and 0.5% (v/v) acetic anhydride] for 30 min at room temperature, rinsed twice in Tris-buffered saline (TBS) and pre-hybridized in the absence of the LNA probe in hybridization buffer [50% formamide, 5× SSC, 5× Denhardt's solution, 250 µg/mL yeast tRNA, 500 µg/mL salmon sperm DNA, 2% (w/v) blocking reagent, 0.1% CHAPs, 0.5% Tween] for 2 h at a temperature 22–25°C below the melting temperature of the probe. The hybridization step was carried out upon overnight incubation at the same temperature with DIG-labeled (digoxigenin-labeled) LNA probes for miR-155-5p. A scrambled probe (negative control) and U6 snRNA (positive control) were also used in this experiment (data not shown). Three stringency washes were performed at the same temperature used for probe hybridization to completely remove the non-hybridized probe. Endogenous peroxidase activity was inactivated by incubation in 3% hydrogen peroxide in TBS with 0.1% Tween-20 (TBS-T) for 30 min, followed by three washes with TBS-T. The slides were then placed in blocking solution (TBS-T, 10% heat-inactivated goat serum, 0.5% blocking agent) for 1 h at room temperature and incubated for the same period of time with an anti-DIG antibody (Roche, USA) conjugated with the hydrogen peroxidase. To amplify the antibody signal, slides were further incubated with a TSA plus Cy3 (PerkinElmer, USA) solution for 10 min in the dark, in accordance with the manufacturer's protocol. The slides were finally stained with the fluorescent DNA-binding dye Hoechst 33342 (Invitrogen Life Technologies, UK) (1 µg/mL) for 5 min in the dark, washed with cold PBS, and mounted in Mowiol (Sigma, USA).

For astrocyte *in situ* hybridization experiments, cells were seeded onto µslide eight-well ibiTreat chamber slides (ibidi) appropriate for confocal microscopy imaging. Following transfection with siRNAs and treatment with LPS, Aβ oligomers or Aβ fibrils, cells were treated as described above.

Confocal images were acquired in a point scanning confocal microscope Zeiss LSM

510 Meta (Zeiss, Germany), with a ×60 oil objective. Digital images were acquired using the LSM 510 META software. All instrumental parameters pertaining to fluorescence detection and image analyses were held constant to allow sample comparison.

3.2.9. Western blot

Total protein extracts were obtained from brain extracts collected from the cortex and hippocampus of 3xTg AD mice and their WT littermates. Briefly, tissue samples were homogenized at 4°C in lysis buffer (50 mM NaCl, 50 mM EDTA, 1% Triton X-100) supplemented with a protease inhibitor cocktail (Roche), 10 μg/mL dithiothreitol and 1 mM PMSF. Protein content was determined using the Bio-Rad Dc protein assay (Bio-Rad). Thirty micrograms of total protein were resuspended in loading buffer (20% glycerol, 10% SDS and 0.1% bromophenol blue), incubated for 5 min at 95°C and loaded into a 10% polyacrylamide gel. After electrophoresis, the proteins were blotted onto a PVDF membrane according to standard protocols and blocked in 5% non-fat milk, before being incubated with the appropriate primary antibody (anti-c-Jun 1:1000 or anti-SOCS-1 1:500) overnight at 4°C, and with the appropriate secondary antibody (1:20 000) (GE Healthcare, USA) for 2 h at room temperature. The membranes were then washed several times with saline buffer (TBS-T - 25 mM Tris–HCl, 150 mM NaCl, 0.1% Tween) and incubated with ECF (enhanced chemifluorescence substrate; 20 μL/cm^2 of membrane) for 5 min at room temperature. ECF detection was performed using a Molecular Imager Versa Doc MP 4000 System (Bio-Rad) and, for each membrane, the analysis of band intensity was performed using the Quantity One Software (Bio-Rad). Equal protein loading was shown by re-probing the membrane with anti-actin (1:20 000) antibody and with the appropriate secondary antibody.

3.2.10. Statistical analysis

All data are presented as mean ± standard deviation (SD) and are the result of at least three independent experiments performed in duplicate for *in vitro* studies or $n = 6$ for *in vivo* studies. One-way analysis of variance combined with Tukey's or Dunnett's multiple comparison tests were used for multiple comparisons in all experiments. Statistical differences are presented as probability levels of $P < 0.05$ (*), $P < 0.01$ (**) and $P < 0.001$ (***). Calculations were performed with a standard statistical software (GraphPad Prism 5).

3.3. Results

3.3.1. Inflammation precedes senile plaque deposition in the 3xTg AD model

Studies showing the co-localization of activated microglia and astrocytes with Aβ plaques in the post-mortem AD brain suggest the involvement of inflammatory pathways in disease progression (McGeer and McGeer, 2003). However, these evidences do not clarify the role of the immune system in the early stages of AD. The lack of human brain samples at early stages that could provide information on the inflammatory molecular mechanisms that precede the deposition of Aβ plaques led us to study the involvement of these signaling pathways in the 3xTg mouse model of AD. Although human studies have been essential to establish inflammation as an AD hallmark, experiments using transgenic AD mice allow associations between chronic inflammation and cognitive deficits, as well as the opportunity to test *in vivo* inflammation-based therapeutic strategies. The 3xTg mouse model of AD, developed in LaFerla's laboratory, progressively develops Aβ and tau pathology, with a temporal- and regional-specific profile that closely mimics its development in the human AD brain (Oddo et al., 2003a). According to Janelsins *et al.*, this mouse model also presents brain inflammation at early stages of the disease, as revealed by the increase in the number of F4/80$^+$ microglia/macrophages (Janelsins et al., 2005). At 6 months, 3xTg AD mice already displayed elevated levels of intraneuronal Aβ, hyperphosphorylated tau and microglia activation. However, only at 12 months it was possible to observe an increase of TFN-α receptor II-related mRNAs, which correlated with neuronal death (Janelsins et al., 2008).

Based on the above findings, our studies were performed in both 3- and 12-month-old (3 and 12 months) 3xTg AD mice. These time points allowed studying the involvement of microglia and astrocytes, two different cell types implicated in neuroinflammation, at different stages of disease progression. Moreover, since studies in humans and mice have established an early inflammatory component in AD, we aimed to disclose the contribution of miR-155-5p to this process. In order to correlate temporarily the appearance of Aβ plaques and neuroinflammation hallmarks, such as microglia activation, astrocyte proliferation and production of inflammatory cytokines, we performed immunohistochemistry studies in coronal brain sections of 3- and 12-months 3xTg AD animals, which were labeled both for microglia and astrocyte protein markers IBA-1 and GFAP (Fig. 3.1), respectively, and also for the Aβ peptide (Fig. 3.2). No significant changes were observed in 3xTg AD animals with respect to age-matched WT animals at 3 months (Supplementary Material, Fig. S3.1) in what concerns the number and phenotype of microglia and astrocytes. However, at 12 months, we observed extensive microglia and astrocyte proliferation in the hippocampus and cortex of 3xTg AD mice. These two brain regions are known to be strongly involved in AD and suffer the first loss of neuronal circuits in this disease (Pennanen et al., 2004). As shown in Figure 3.1, microglia from both the prefrontal cortex (Fig. 3.1B) and hippocampus (Fig. 3.1C) of 3xTg AD mice acquired an amoeboid phenotype, characteristic of the transition from a surveying to an activated state. This change was not observed in age-matched WT mice (Fig. 3.1D–F). Moreover, the number of microglia cells was highly increased in 3xTg AD animals with respect to WT mice. The same was true for astrocytes (Fig. 3.1G–I), especially in the hippocampus region.

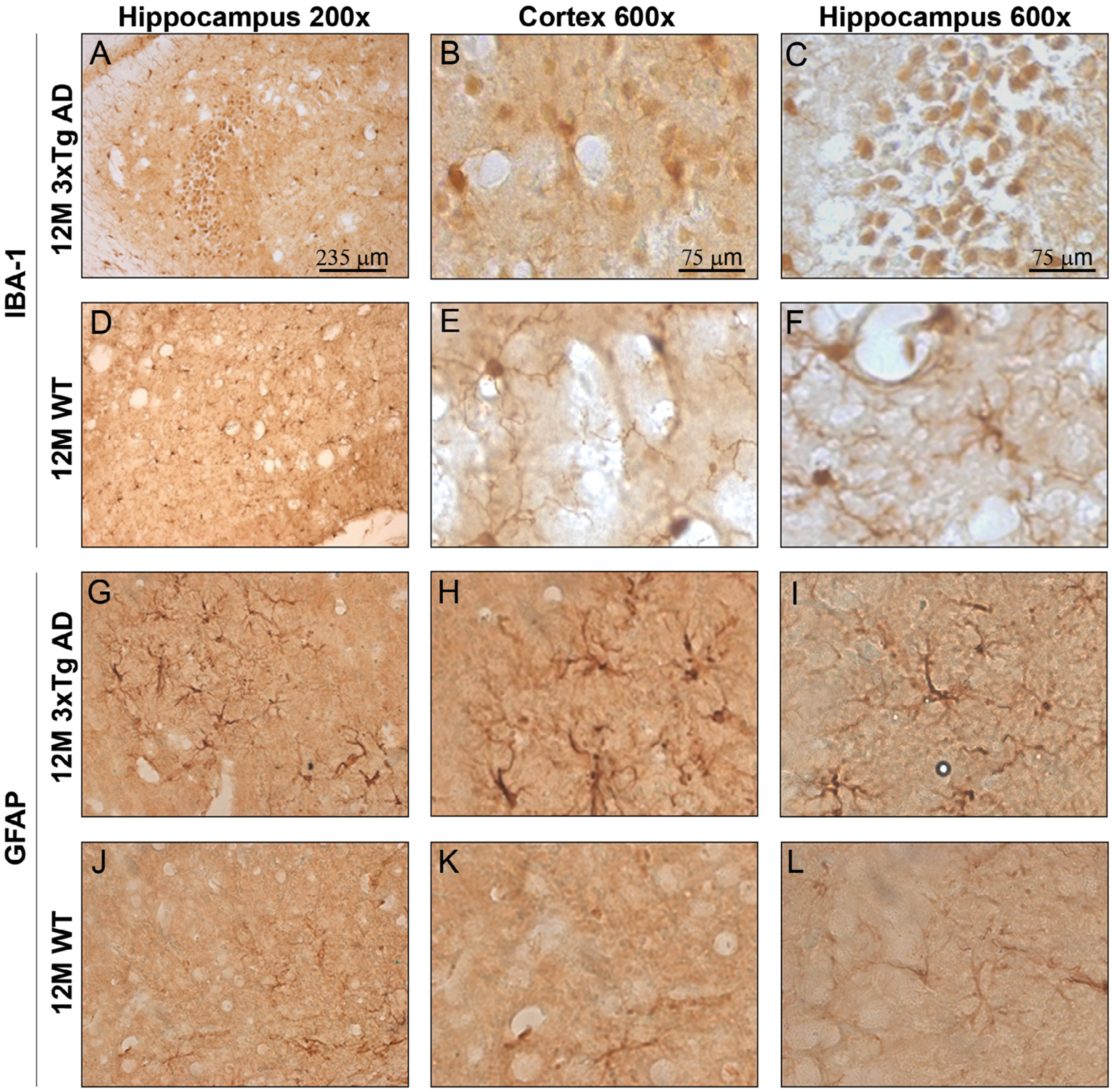

Figure 3.1 | Microgliosis and astrogliosis in 3xTg AD animals.
In order to identify astrocytes and microglia in the mouse brain, slices of 12-month 3xTg AD animals or their WT littermates were mounted in FluorSave™ Reagent on microscope slides and incubated with anti-IBA-1 or anti-GFAP antibodies to stain microglia and astrocytes, respectively. Following incubation with a biotinylated secondary antibody and visualization with 3,3′-diaminobenzidine tetrahydrochloride, pictures were taken under a Zeiss Axiovert microscope. Representative microscopy images of hippocampus (**A** and **D**) and cortex (**G** and **J**) are presented at ×200 magnification. A specific area of each image was zoomed 3× to obtain close up images showing the amoeboid (**B** and **C**) or ramified (**E** and **F**) morphology of microglia in each brain region. Astrocyte proliferation in the 3xTg AD animals (**H** and **I**) with respect to their WT littermates (**K** and **L**) can be observed at ×400 magnification for both brain regions. *n* = 6 animals for each experimental group

Since the presence of these neuroinflammatory features was only observed at 12 months, we further investigated if they were a consequence of the formation of intracellular or extracellular Aβ deposits. As expected, since intracellular human Aβ overproduction is one of the first neuropathological events in AD, intraneuronal Aβ immunostaining, using the WO-2 anti-human Aβ peptide, was found to be significantly enhanced in the hippocampus and prefrontal cortex of 3xTg animals with both 3 (Supplementary Material, Fig. S3.1) and 12 months (Fig. 3.2A–C), whereas human Aβ positive cells were not detected in age-matched WT littermates (Fig. 3.2D–F), confirming the selectivity of the Aβ antibody and the presence of this hallmark of the disease. In this study, 12-month 3xTg AD mice did not present large extracellular deposits of Aβ in the cortex and hippocampus, as was observed in the hippocampus of 18-month 3xTg AD (Fig. 3.2G–I), where such deposits exhibited the characteristic round and diffuse Aβ brown stains. However, at 12 months, small immunoreactive dots could already be observed in the extracellular space. Therefore, our study suggests the existence of an early inflammatory

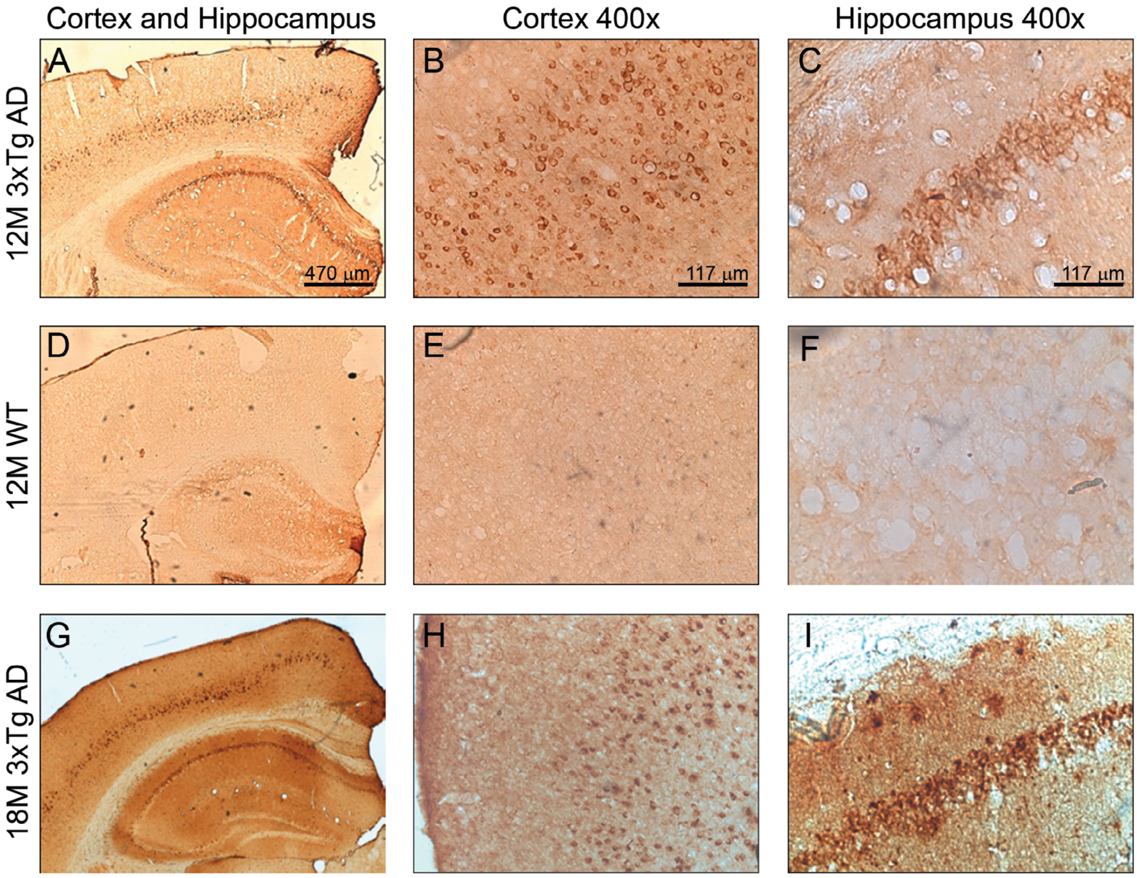

Figure 3.2 | Intraneuronal and extracellular Aβ accumulation in 3xTg AD mice.
In order to visualize Aβ deposition, brain slices of 3xTg AD animals and WT littermates were mounted in FluorSave^{TM} Reagent on microscope slides and incubated with an anti-human Aβ peptide antibody to stain Aβ plaques. Following incubation with a biotinylated secondary antibody and visualization with 3,3′-diaminobenzidine tetrahydrochloride, pictures were taken under a Zeiss Axiovert microscope. Microscopy images of the hippocampus and cortex of 12-month 3xTg AD and WT animals and 18-month 3xTg AD animals (**A, D** and **G**) are presented at ×50 magnification and are representative of *n* = 6 animals for each experimental group. A specific area of each

image was zoomed 4× to obtain close-up images of the cortex (**B, E** and **H**) and hippocampus (**C, F** and **I**). It is possible to observe the intracellular accumulation of Aβ in pyramidal CA1 and cortical neurons of 12-month 3xTg AD animals, but not in their WT aged-matched littermates. Extracellular senile plaques were only observed in 18-month 3xTg AD animals (**I**).

response of both microglia cells and astrocytes in 3xTg AD mice, which precedes the formation of extracellular Aβ plaques but not intraneuronal Aβ accumulation or the presence of proto-fibrillary Aβ.

Taking into consideration the increase in the number of microglia cells and astrocytes observed in 3xTg AD mice, we investigated if the levels of molecular mediators of the immune response were also upregulated in these animals (Fig. 3.3).A significant increase in the mRNA levels of both interleukin-6 (IL-6) (Fig. 3.3A) and interferon beta (IFN- β) (Fig. 3.3B) was detected by qRT-PCR in 3xTg AD animals at 12 months, whereas no significant differences were found for TNF-α and IL-1β, between 3xTg AD animals and their WT littermates (data not shown). Since no extracellular Aβ plaques were visible in the 3xTg AD animals at 12 months, the age-dependent increase observed in IL-6 and IFN-β mRNA levels may be a response to the accumulation of intraneuronal Aβ or to the production of less complex extracellular Aβ species, such as Aβ dimers, oligomers and proto-fibrils that are not so easily detected by immunohistochemistry. Furthermore, at 3 months, the levels of both IL-6 and IFN-β were found to be downregulated in the 3xTg AD animals with respect to their WT littermates. These levels can be explained, in part, by our observation of miR-125b-5p upregulation in 3-month 3xTg animals (Supplementary Material, Fig. S3.2). This miRNA is highly expressed in the brain and is considered an anti-inflammatory miRNA in macrophages (Tili et al., 2007), as well as a regulator of astrocyte proliferation (Pogue et al., 2010).

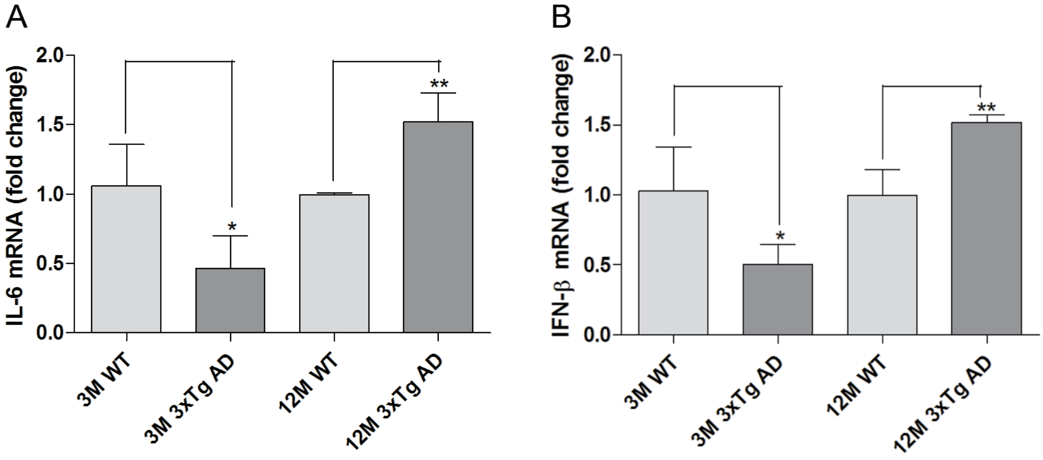

Figure 3.3 | Cytokine production in 3xTg AD animals.
Total RNA extracts containing hippocampal and cortical brain regions of 3xTg AD animals, at 3 and 12 months, or their WT littermates were used to quantify IL-6 (**A**) and IFN-β (**B**) mRNA levels by qRT-PCR. Results are expressed as mRNA fold change as compared with 3 or 12-month WT mice and are representative of $n = 6$ animals per experimental group. *$P < 0.05$ and **$P < 0.01$ with respect to age-matched WT littermates.

Interestingly, at 12 months, miR-125b-5p expression is decreased in 3xTg AD animals compared with WT mice (Supplementary Material, Fig. S3.2), which correlates with astrogliosis and with the strong inflammatory phenotype found at this age.

3.3.2. MiR-155 is upregulated in the brain of the 3xTg AD model

As discussed before, miRNAs regulate gene expression at a post-transcriptional level and have been shown to be directly involved in the regulation of inflammatory pathways. MiRNAs have also been directly related with neurodegeneration and global expression studies have revealed the deregulation of specific miRNAs in AD (Hebert and De Strooper, 2009; Delay and Hebert, 2011). These non-coding small RNA molecules are essential for neuronal survival and control of innate immune responses triggered by brain lesions or accumulation of aggregated proteins. MiR-155 is a proinflammatory miRNA, widely described in the peripheral immune system, which has been recently shown, by us and others, to be associated with neuroimmunity (Tarassishin et al., 2011; Cardoso et al., 2012; Ponomarev et al., 2013). Taking into consideration its important role in microglia (Cardoso et al., 2012) and astrocyte (Tarassishin et al., 2011) function and our observation that both these cell types are activated in the 3xTg AD mouse model, we investigated the contribution of this miRNA to the Aβ-dependent inflammatory response in AD.

In order to analyze miR-155-5p expression in 3- and 12-month animals, total RNA was extracted from brain homogenates (brain without the olfactory bulb and cerebellum) and miR-155-5p levels were quantified by qRT-PCR. MiR-155-5p was found to be significantly upregulated in 3xTg AD mice at 12 months, these animals presented a 3-fold increase in miR-155-5p levels with respect to their WT littermates (Fig. 3.4A). In addition, we observed that 3-month 3xTg AD animals already exhibited increased expression of miR-155-5p, albeit not statistically significant, and that the levels of this miRNA presented an age-dependent increase in 3xTg AD animals but not in WT animals. These results were consistent with *in situ* hybridization studies performed in coronal brain sections of 3- and 12-month 3xTg AD animals and WT littermates (Fig. 3.4B). In these experiments, a DIG-labeled (digoxigenin-labeled) LNA (Cogswell et al., 2008) probe specific for the 5′ terminal of miR-155-5p was used to label miR-155-5p. A specific U6 snRNA probe was used as positive control (data not shown). As expected, miR-155-5p labeling was strongly increased in brains slices of 12-month 3xTg AD mice when compared with 3-months transgenic animals and WT littermates. Nevertheless, 3-months 3xTg AD mice already presented a visible increase in miR-155-5p labeling in the hippocampus region, with respect to 3-month WT animals. Interestingly, the increase in miR-155-5p labeling was restricted almost exclusively to the cortex and hippocampus (Fig. 3.4B), the two regions where microglia and astrocyte activation had been previously observed.

In order to further investigate if astrocytes and microglia could be responsible for the

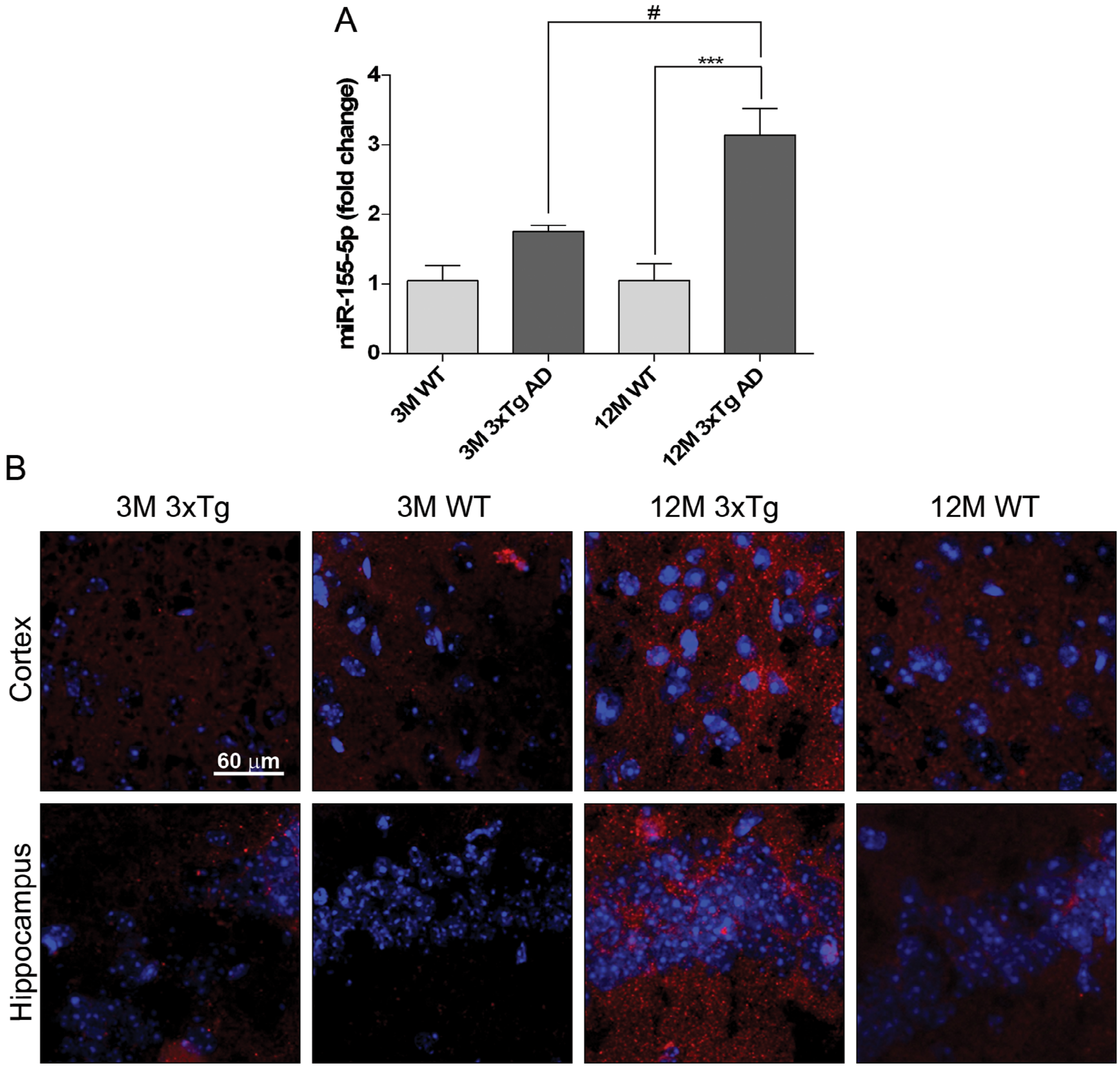

Figure 3.4 | MiR-155-5p levels in 3xTg AD mice.
Total RNA extracts containing hippocampal and cortical brain regions of 3xTg AD animals, at 3 and 12 months, or their age-matched WT littermates were used to quantify (**A**) miR-155-5p by qRT-PCR. Results are expressed as miRNA fold change with respect to 3-month WT mice. ***$P < 0.001$ with respect to age-matched WT littermates and $^{\#}P < 0.05$ with respect to 3-month 3xTg AD mice. (**B**) *In situ* hybridization was used to visualize miR-155-5p expression in brain slices of 3xTg AD animals and their WT littermates. The slices were labeled with a DIG-bound LNA probe specific for miR-155-5p detection (red), followed by nuclei labeling with Hoechst 33342 (blue) and mounted in microscope slides. Confocal images from the cortical and hippocampal regions of 3- and 12-months-old 3xTg AD animals and their WT littermates were acquired with a confocal Zeiss LSM 510 Meta microscope, using the ×60 oil objective. Both qRT-PCR and confocal results are representative of $n = 6$ animals per experimental group.

observed upregulation of miR-155-5p in 3xTg AD animals, we measured the levels of this miRNA in *in vitro* cultures of both cell types upon exposure to Aβ. Since the contribution of different Aβ forms to neuroinflammation remains poorly understood, both N9 microglia and astrocyte primary cultures were incubated with two different species of the Aβ peptide, Aβ fibrils and Aβ oligomers. These Aβ species were prepared as described in the Materials and Methods and the different aggregate sizes were confirmed using 4–16% Tris–Tricine SDS-PAGE gel electrophoresis. As can be observed in the Supplementary Material, Figure S3.8, the Aβ oligomers preparation did not present Aβ fibrils and only a small percentage of Aβ oligomers could be detected in the Aβ fibrils preparation (Supplementary Material, Table S3.1). The levels of miR-155-5p were quantified by qRT-PCR following a 24 h incubation period and LPS was used as a positive control in this experiment on the basis of our previous results showing that LPS is able to increase significantly miR-155-5p levels in both microglia (Cardoso et al., 2012) and astrocytes (unpublished data). We observed that miR-155-5p is upregulated upon incubation with Aβ fibrils in both microglia (Fig. 3.5A) and astrocytes (Fig. 3.5B). Regarding microglia, the exposure of N9 microglia cells to Aβ fibrils, at a concentration of 20 μM, triggered an overexpression of miR-155-5p similar to that obtained with LPS (8-fold). The same concentration of Aβ oligomers promoted a small increase in miR-155-5p levels, although this increase was not found to be statistically significant. In what concerns astrocytes, higher amounts of Aβ fibrils were necessary to promote a significant increase in miR-155-5p. Thirty micromolar of Aβ fibrils promoted a 4-fold increase in miR-155-5p levels, while LPS induced a 10-fold increase. Once again, Aβ oligomers showed a tendency to promote miR-155-5p upregulation, but the results were not statistically significant. Importantly, no upregulation

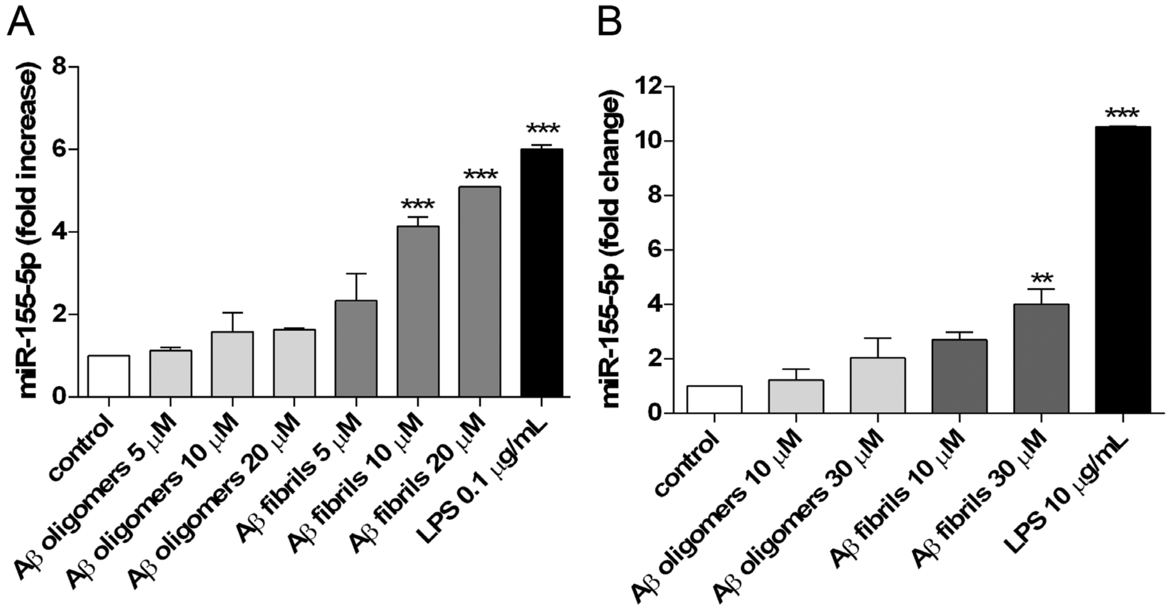

Figure 3.5 | MiR-155-5p expression in Aβ-activated microglia and astrocyte cultures.
N9 microglia cells or astrocyte primary cultures were plated and maintained in culture for 1 day before incubation with Aβ oligomers or Aβ fibrils. (**A**) N9 microglia cells were incubated with 5, 10 and 20 μM of Aβ for 24 h, while (**B**) astrocyte primary cultures were incubated with 10 and 30 μM of Aβ for the same period of time. Both cell types were incubated with LPS as a positive control (0.1 μg/mL in microglia and 10 μg/mL in astrocytes). Following the incubation period, total RNA was extracted from each condition and miR-155-5p levels were quantified by qRT-PCR. Results are expressed as miRNA fold change with respect to control (cells in the absence of stimulus) and are representative of three independent experiments performed in duplicate. **$P < 0.01$ and ***$P < 0.001$with respect to control.

of miR-155-5p was detected in primary hippocampal neurons incubated with Aβ fibrils at the same concentrations (data not shown), confirming that the upregulation of miR-155-5p observed in 3xTg AD animals must originate in the phenotypic changes observed in microglia and astrocytes. These results also suggest that Aβ fibrils are more efficient in promoting miR-155-5p expression *in vitro* than less complex Aβ species, such as oligomers.

Following our previous observation of an upregulation of IL-6 and IFN-β in 12-month 3xTg AD mice and, since it has been reported that miR-155-5p can influence cytokine production by interfering with the levels of several important immune modulators, such as SOCS-1 (Cardoso et al., 2012), we measured the mRNA levels of these cytokines in N9 microglia cells and astrocyte primary cultures, following cell incubation with Aβ fibrils or oligomers (Fig. 3.6). As shown, both IL-6 and IFN-β were upregulated in Aβ-stressed microglia and astrocytes with respect to non-activated cells. N9 microglia cells presented an upregulation of IL-6, following a 24 h incubation period with Aβ fibrils or with the highest concentration of Aβ oligomers (Fig. 3.6A). However, the IL-6 expression peak occurs 30 min following N9 microglia cells exposure to Aβ fibrils, suggesting a fast inflammatory response to this stimulus, which is maintained during at least a 24 h period (Supplementary Material, Fig. S3.3A). IL-6 mRNA expression is slower and less prominent following microglia activation with Aβ oligomers than with Aβ fibrils, showing only a 2-fold increase at 6 h and remaining constant until 24 h (Supplementary Material, Fig. S3.3A). Interestingly, and in contrast to IL-6, IFN-β was found to be more expressed in the presence of Aβ oligomers (Fig. 3.6C), presenting an expression peak at 18 h (Supplementary Material, Fig. S3.3C), although being also significantly increased in microglia cells stimulated with 20 μM of Aβ fibrils. The upregulation of IL-6 and IFN-β mRNAs in N9 microglia cells, in the presence of Aβ fibrils and Aβ oligomers, respectively, fully correlates with the secreted levels of both cytokines measured by ELISA (Supplementary Material, Fig. S3.4A and B). Furthermore, IL-4 and TNF-β release was also upregulated in N9 microglia incubated with Aβ fibrils, but not with Aβ oligomers (Supplementary Material, Fig. S3.4), suggesting that Aβ fibrils elicit a more robust inflammatory response. In what concerns astrocytes, only Aβ fibrils were able to upregulate IL-6 expression (Fig. 3.6B), with a 50-fold change with respect to non-activated cells, while IFN-β was only overexpressed upon cell incubation with 30 μM of Aβ oligomers (Fig. 3.6D). An interesting observation is that, although different Aβ forms lead to production of different levels of immune modulators in microglia and astrocytes, the pattern of the triggered immune responses is the same in both cell types. Indeed, while the proinflammatory cytokine IL-6 is upregulated in the presence of Aβ fibrils, the levels of the immunomodulatory cytokine IFN-β increase after exposure to Aβ oligomers.

Although we did not find differences in the levels of TNF-α and IL-1β in 3xTg AD mice, with respect to their WT littermates (data not shown), we were able to find a strong and early upregulation of both TNF-α and IL-1β in N9 microglia cells activated with Aβ fibrils or

Aβ oligomers, at 2 h and 30 min, respectively (Supplementary Material, Fig. S3.3B and D). However, 24 h after Aβ exposure, we could only detect an increase in TNF-α secretion following incubation with Aβ fibrils (Supplementary Material, Fig. S3.4C). The observed increase in the mRNA levels of IL-1β and TNF-α did not translate in increased cytokine secretion for N9 cells exposed to Aβ oligomers. Moreover, the mRNA expression of both these cytokines was also found to be increased in astrocytes incubated with Aβ fibrils, but not in astrocytes exposed to Aβ oligomers (Supplementary Material, Fig. S3.5).

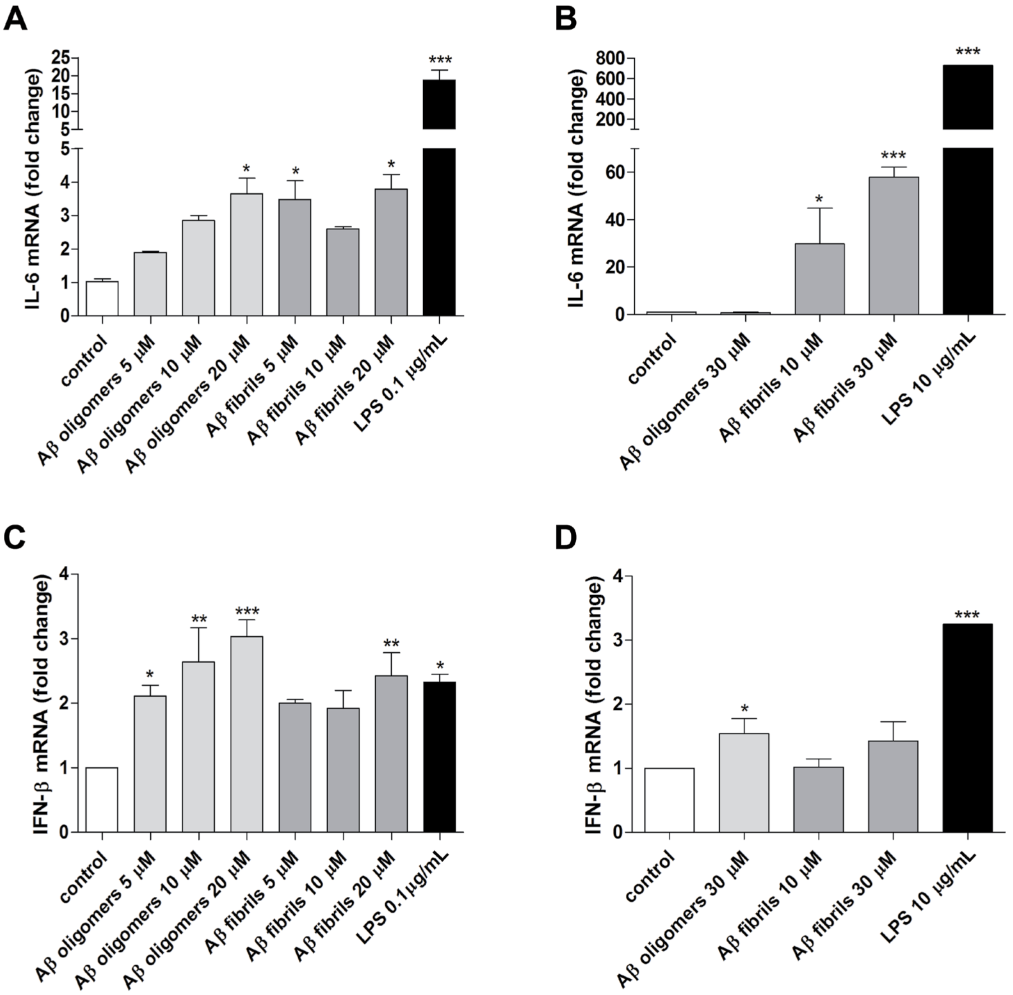

Figure 3.6 | IL-6 and IFN-β expression in Aβ-activated microglia and astrocyte cultures.
N9 microglia cells or astrocyte primary cultures were plated and maintained in culture for 1 day before incubation with Aβ oligomers or Aβ fibrils (**A** and **C**). N9 microglia cells were incubated with 5, 10 and 20 µM, of Aβ for 24 h, while (**B** and **D**) astrocyte primary cultures were incubated with 10 and 30 µM of Aβ for the same period of time. Both cell types were incubated with LPS as a positive control (0.1 µg/ mL in microglia and 10 µg/mL in astrocytes). Following the incubation period, total RNA was extracted from each condition and IL-6 and IFN-β levels were quantified by qRT-PCR. Results are expressed as mRNA fold change with respect to control (cells in the absence of stimulus) and are representative of three independent experiments performed in duplicate. *$P < 0.05$, **$P < 0.01$ and ***$P < 0.001$with respect to control.

3.3.3. SOCS-1 is downregulated in the brain of the 3xTg AD model

The strong overexpression of miR-155-5p in the 3xTg AD mice led us to search for molecular targets of this miRNA involved in inflammatory signaling, whose downregulation could help explain the upregulation of IL-6 and IFN-β observed in the brain of 3xTg AD animals. As we and others have previously reported, SOCS-1 is a molecular target of miR-155-5p and its expression is decreased upon miR-155-5p upregulation (Cardoso et al., 2012; Yao et al., 2012). This protein is also considered to be an important protagonist in the regulation of the innate immune response. The activation of TLRs or cytokine receptors induces SOCS-1 expression, which acts in a negative feedback loop to allow the return of immune cells to basal conditions and avoid the overstimulation of the immune response (Yoshimura et al., 2007). Moreover, SOCS-1 has already been proposed to play a role in CNS immunity and several studies have pointed its involvement in different neuropathological conditions (Baker et al., 2009).

Based on the above findings, we determined the levels of SOCS-1 in the 3xTg AD animals at 3 and 12 months and found that both mRNA and protein (Fig. 3.7) levels were dramatically decreased in 12-month 3xTg AD animals with respect to their WT littermates. As observed, the levels of SOCS-1 mRNA were already slightly decreased in 3-month 3xTg AD animals (Fig. 3.7A). Although this decrease was not statistically significant, it correlates with the small increase in miR-155-5p expression observed at this age (Fig. 3.4A). Furthermore, we observed a decrease in SOCS-1 mRNA levels when miR-155-5p was overexpressed in astrocyte primary cultures and an increase in SOCS-1 mRNA levels when astrocytes were transfected with a LNA-modified oligonucleotide complementary to miR-155-5p (anti-miR-155) (Supplementary Material, Fig. S3.6). Thus, we can conclude that in astrocytes, as well as previously shown in

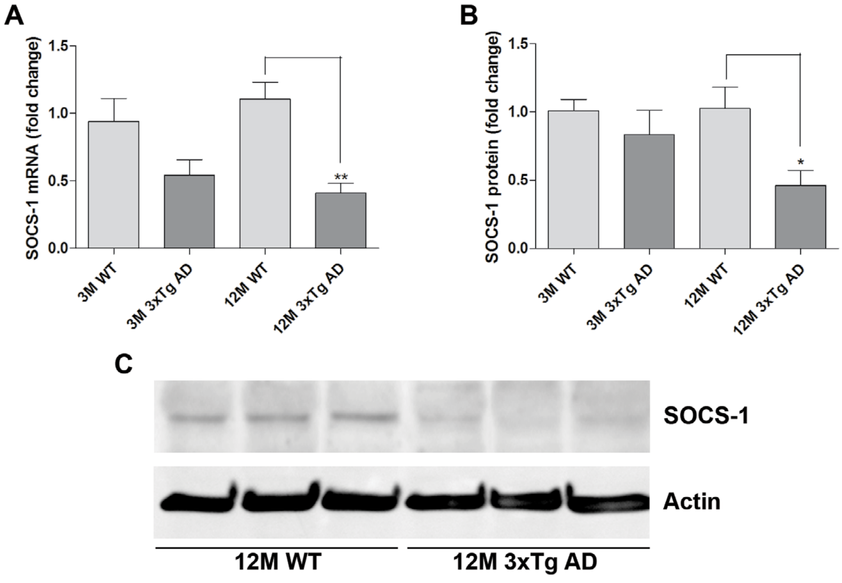

Figure 3.7 | SOCS-1 mRNA and protein levels in 12-month 3xTg AD mice.
Protein and RNA extracts of hippocampal and cortical brain regions were obtained from 3xTg AD animals at 3 and

12 months and their age-matched WT littermates. (**A**) SOCS-1 mRNA levels were quantified by qRT-PCR. Results are expressed as mRNA fold change with respect to 3-month WT mice. (**B**) SOCS-1 protein levels were quantified by western blot and are expressed as protein fold change with respect to 3-month WT mice. (**C**) Representative gel showing decreased levels of SOCS-1 in 3xTg AD mice at 12 months compared with age-matched WT littermates. All results are representative of $n = 6$ animals per experimental group. *$P < 0.05$ and **$P < 0.01$ with respect to 12-month WT mice.

microglia, SOCS-1 is a direct target of miR-155-5p and its expression can be regulated by the levels of this miRNA. Therefore, and taking into consideration the activation of both microglia and astrocytes in 3xTg AD animals, it stands to reason that the observed increase in miR-155-5p expression in this mouse model is at least partially responsible for the downregulation of SOCS-1.

3.3.4. C-Jun is responsible for miR-155 upregulation in the presence of the Aβ peptide

Although in the context of inflammation, miR-155 upregulation has been addressed multiple times in different pathological settings, the mechanisms regulating miR-155 expression have not been completely elucidated and different authors have proposed the involvement of the JNK or NF-κB signaling pathways in the control of the non-protein coding BIC gene (gene encoding miR-155) (O’Connell et al., 2007; Ma et al., 2011). In order to explore which transcription factor is responsible for the increase in the miR-155-5p levels observed in 3xTg AD mice, we evaluated the total protein levels of c-Jun, the transcription factor downstream of JNK, and NF-κB in 3xTg AD mice at 3 and 12 months and in their age-matched WT littermates. Western blot analysis revealed an early upregulation of c-Jun levels in 3-month 3xTg AD animals that was still present at 12 months (Fig. 3.8). As shown, a 2- and 2.5-fold increase in c-Jun expression was observed in 3xTg AD mice at 3 and 12 months, respectively, with respect to WT mice. However, no significant differences were observed in the expression of NF-κB between 3xTg AD and WT mice (Supplementary Material, Fig. S3.7).

Based on the results obtained *in vivo* concerning the levels of c-Jun in AD transgenic animals, we hypothesized that this transcription factor could contribute to miR-155-5p overexpression upon Aβ activation in microglia and astrocytes. In order to test this hypothesis, a siRNA sequence targeting c-Jun (siRNA c-Jun) was used to silence c-Jun translation in N9 microglia cells and astrocyte primary cultures. Twenty-four hours after transfection, both cell types were exposed to Aβ fibrils (20 μM in the case of microglia or 30 μM in astrocytes), since this Aβ species was previously shown to increase miR-155-5p expression. The levels of this miRNA were evaluated by qRT-PCR and *in situ* hybridization and a siRNA with a scrambled sequence (siRNA Mut) was used as control in this experiment, in order to detect the presence of unspecific effects related with the transfection process *per se*. We observed that in both N9 microglia cells (Fig. 3.9A) and astrocytes (Fig. 3.9B), the expression of miR-155-5p was

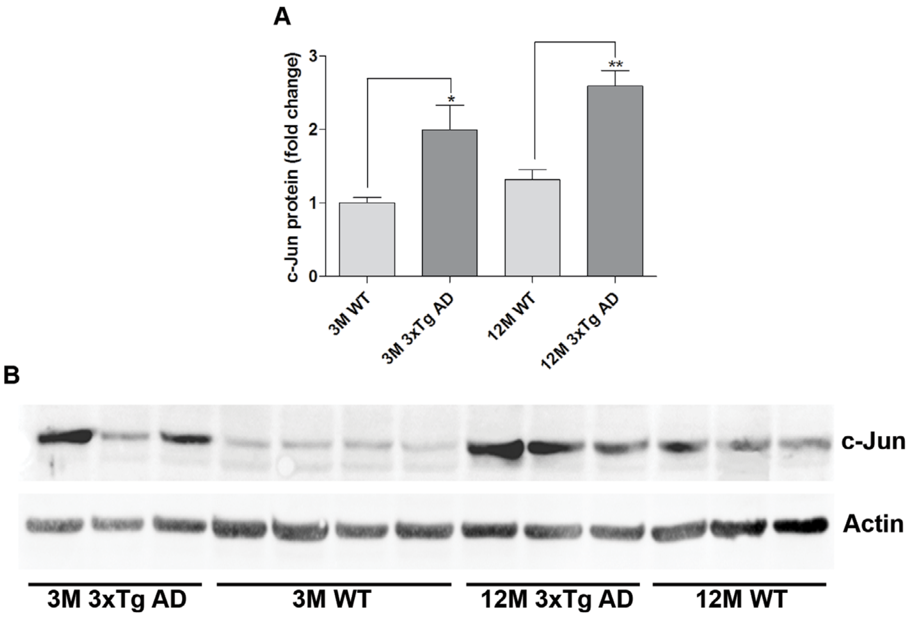

Figure 3.8 | C-Jun expression in 3xTg AD mice.
Protein extracts of hippocampal and cortical brain regions were obtained from 3xTg AD animals at 3 and 12 months and their age-matched WT littermates. (**A**) C-Jun protein levels were quantified by western blot and are expressed as protein fold change with respect to 3-month WT mice. (**B**) Representative gel showing increased c-Jun levels in 3xTg AD mice at 3 and 12 months with respect to WT littermates. All results are representative of *n* = 6 animals for each experimental group. *$P < 0.05$ and **$P < 0.01$ compared with age-matched WT littermates.

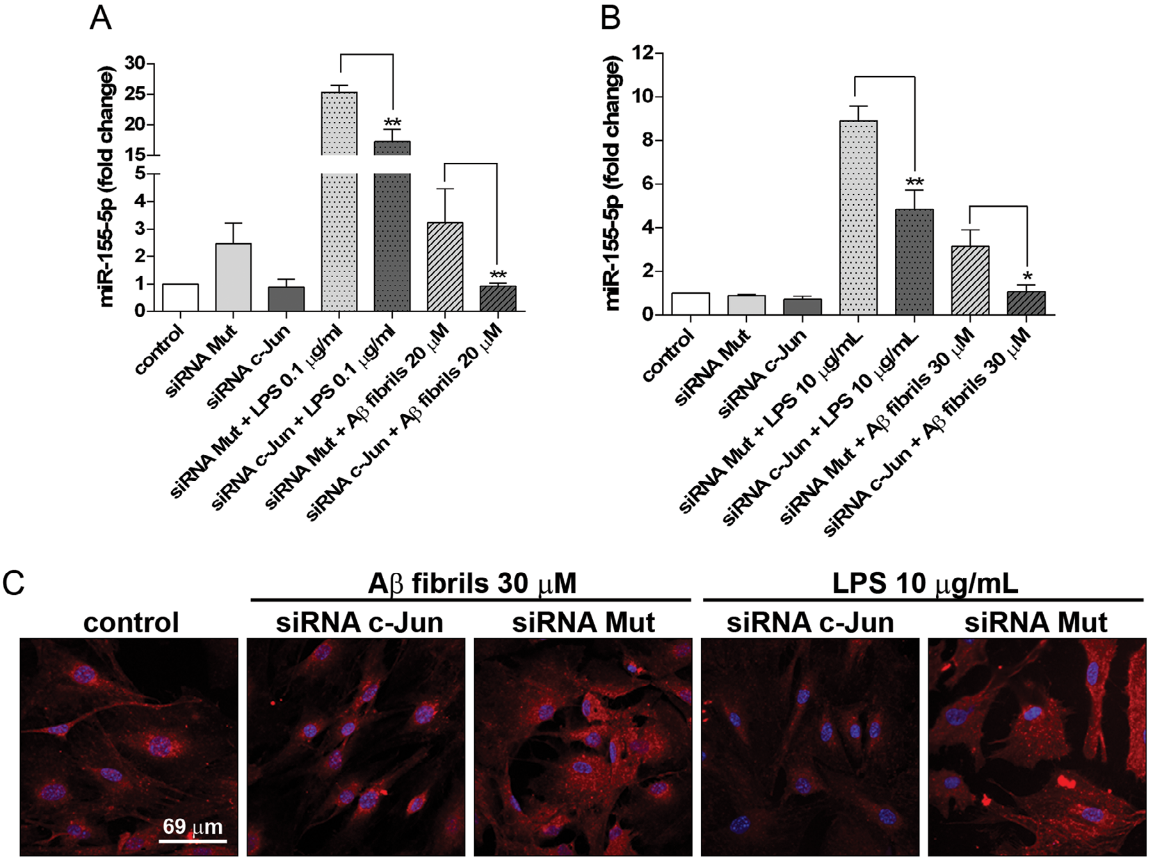

Figure 3.9 | MiR-155-5p expression in microglia and astrocytes following c-Jun silencing and Aβ exposure.
N9 microglia cells and astrocyte primary cultures were plated and maintained in culture for 1 day before cell

transfection with anti-c-Jun siRNA (siRNA c-Jun) or a non-targeting siRNA (siRNA Mut) at 50 nM. Four hours after transfection, the cell medium was replaced by fresh RPMI-1640 5% FBS (N9 microglia) or DMEM 10% FBS (astrocytes) and 24 h later, N9 microglia cells were exposed to 20 µM of Aβ fibrils or 0.1 µg/mL of LPS, while primary astrocytes were stimulated with 30 µM of Aβ fibrils or 10 µg/mL of LPS for 24 h. Following this period of time, total RNA was extracted from each condition and miR-155-5p levels were quantified by qRT-PCR in (**A**) N9 microglia cells or (**B**) astrocytes. Results are expressed as miRNA fold change with respect to control (untransfected cells). (**C**) *In situ* hybridization was used to visualize miR-155-5p expression in astrocyte cultures. Cells were labeled with a DIG-bound LNA probe specific for miR-155-5p detection (red), followed by nuclei labeling with Hoechst 33342 (blue). Confocal images from all experimental conditions were acquired with a confocal Zeiss LSM 510 Meta microscope, using the ×60 oil objective. All results are representative of three independent experiments performed in duplicate. $*P < 0.05$ and $**P < 0.01$ with respect to N9 microglia cells or astrocytes transfected with siRNA Mut and exposed to similar stimulus.

decreased in cells where c-Jun had been silenced prior to Aβ fibrils exposure, with respect to cells transfected with the siRNA Mut.

Similar results were observed in parallel experiments performed with cells activated with LPS (Fig. 3.9A and B). Moreover, upon c-Jun silencing, miR-155-5p expression was similar in Aβ -activated microglia and astrocytes, with respect to transfected or non-transfected non-activated cells. These results were corroborated by *in situ* hybridization studies, which also revealed a significant reduction in miR-155-5p labeling in astrocyte primary cultures. As can be observed in Figure 3.9C, the intensity and number of red dots inside astrocytes where c-Jun was silenced prior to cell activation with Aβ fibrils or LPS were much lower than those detected in astrocytes transfected with the siRNA Mut. Since c-Jun silencing *per se* did not reduce miR-155-5p levels, these findings allowed us to conclude that the observed reduction in miR-155-5p expression was strictly dependent on cell activation. Although altogether these results do not exclude the contribution of other transcription factors to miR-155-5p regulation, they strongly suggest that the JNK pathway and its terminal transcription factor c-Jun play an important role in miR-155-5p upregulation following microglia and astrocyte exposure to Aβ, and unveil the interesting possibility of using an inflammatory approach based on c-Jun silencing to decrease neuroinflammation in the context of AD.

3.4. *Discussion*

Neuroinflammation is a physiological response to brain injury as well as to the accumulation of protein aggregates, which characterizes several neurodegenerative disorders. In the last decade, a number of studies have reported genetic variations in immune-related genes associated with a high risk of Parkinson's disease and AD (Jones et al., 2010; Guerreiro et al., 2013; Holmans et al., 2013) and showed that the products of some of these genes, including inflammatory cytokines and chemokines, have the potential to be used as peripheral biomarkers of AD (Guerreiro et al., 2007; Albert et al., 2011). These studies also contributed to clarify, once and for all, the important contribution of the immune response in the context of AD.

Due to the ability of immune-derived brain cells to phagocyte not only foreign organisms but also endogenous particles, some authors have proposed an important role of these cells in regulating the levels of Aβ in the CNS. The expression of key receptors of the innate immune system, such as CD14, TLR2, TLR4 and TLR9, by immune-derived brain cells can be considered as a defense mechanism to prevent Aβ accumulation, since these receptors contribute to the modulation of Aβ fibrillar levels by increasing Aβ uptake by local microglia (Wyss-Coray, 2006; Rivest, 2009). However, these results must be considered carefully. In this regard, a recent study of *in vivo* two-photon microscopy revealed a strong impairment of microglial function (motility and phagocytic activity) in two different mouse models of AD, which correlated spatially and temporarily with the deposition of Aβ plaques (Krabbe et al., 2013). These findings, together with other studies showing a shift of chronic Aβ-exposed microglia to more pro-inflammatory phenotypes (M1) instead of pro-phagocytic phenotypes (M2) (Varnum and Ikezu, 2012), suggest that a shift in the type of immune response mediated by these cells in the AD brain may halt the translation into effective Aβ clearance at a certain stage of the disease, and even contribute to disease progression in the long run. Although the importance of immune cells within the CNS is now fully recognized, the question whether their function can be restored to promote a decrease in the amyloid burden remains. We believe that a complete disclosure of the molecular pathways underlying neuroinflammation prior to Aβ plaque deposition will be of utmost importance to resolve this issue.

Recently, the role of Aβ fibrils in neuronal toxicity was challenged and several reports have revealed that other levels of Aβ oligomerization, such as soluble oligomers, can be responsible for the early pathologic events in AD (Callizot et al., 2013), such as early LTP deficits (Oddo et al., 2003b). In our experimental model, the 3xTg AD mice, it was possible to identify a pro-inflammatory phenotype of microglia and astrocytes in 12-month-old animals, which preceded the appearance of Aβ deposits in the form of insoluble plaques (Fig. 3.1; Fig. 3.2). Although glial response to intraneuronal or pre-plaque Aβ is still poorly understood, in light of the new 'toxic beta-amyloid hypothesis', our results suggest that the activation of glial cells in the 3xTg AD mice is initiated by the accumulation of intraneuronal Aβ, as well as extracellular oligomeric and protofibrillar Aβ, and it may reflect the early stages of disease pathogenesis. These findings corroborate, at least in part, the results of Rebeck *et al.*, who suggested that intracellular Aβ triggers inflammation prior to extracellular Aβ accumulation (Rebeck et al., 2010).

In what concerns the molecular outcomes of microglia and astrocyte activation, such as cytokine expression, we observed an upregulation of both IL-6 and IFN-β mRNA levels in 12-month-transgenic animals (Fig. 3.3). Although these cytokines are described as having opposite effects regarding their immunomodulatory properties, since basal IFN-β expression is essential to trigger a proper inflammatory IL-6 cell response (Takaoka and Yanai, 2006), they can be secreted by glia cells simultaneously, and, IL-6 expression in particular, has been observed as a characteristic of Aβ-induced gliosis (Khandelwal et al., 2011). While recently Zaheer and coworkers observed IL-6 increased expression in 3xTg AD mice at 16 months (Zaheer et al., 2013), we demonstrated that this inflammatory mediator is already elevated at 12 months (Fig. 3.3). Moreover, our *in vitro* experiments revealed that, when in the presence of Aβ fibrils, glial cells overexpress IL-6 (Fig. 3.6A and B, Supplementary Material, Fig. S3.3A and Supplementary Material, Fig. S3.4A), one of the strongest inflammatory mediators, which is suggestive of an uncontrolled inflammatory response at late stages of Aβ-triggered neuroinflammation. These results are in agreement with the strong upregulation of miR-155-5p observed in 12-month 3xTg AD mice (Fig. 3.4A and B) and in microglia or astrocytes following exposure to Aβ fibrils (Fig. 3.5A and B), since to overexpress an inflammatory cytokine such as IL-6, these cells need to block the activity of SOCS-1, a protein usually responsible for suppressing cytokine expression and a direct target of miR-155-5p.

Our *in vitro* results show that IFN-β, considered to be an immunomodulatory cytokine due to its ability to enhance other cytokine signaling, is more expressed when glial cells are exposed to Aβ oligomers than to Aβ fibrils (Fig. 3.6C and D, Supplementary Material, Fig. S3.3C and Supplementary Material, Fig. S3.4B). This observation suggests that at early stages of Aβ aggregation, microglia and astrocytes try to control neuroinflammation caused by Aβ, which induces the release of cytokines that propagate inflammation throughout the brain. However, the significance of Aβ oligomer-induced IFN-β *in vivo* remains to be fully elucidated. In light of its immunosuppressive nature, IFN-β also induces the expression of SOCS-1 in human primary macrophages and in murine primary microglia, through STAT-1α transcription factor activation, leading to the inhibition of IFN-β signaling in a negative feedback loop (Qin et al., 2006). However, one of the most described membrane-bound Aβ receptor includes TLR4, and the activation of this receptor induces the expression of miR-155-5p, whose levels are significantly elevated in 3xTg AD mice at 12 months (Fig. 3.4A and B). Consequently, being a direct target of miR-155-5p, SOCS-1 protein is downregulated at this age (Fig. 3.7B and C). Based on these results, we suggest that IFN-β signaling is overactivated in AD, since the SOCS-1 negative feedback loop necessary to control IFN-β is abolished due to miR-155-5p upregulation.

Overall, our results point to an important contribution of miR-155-5p upregulation, and consequent SOCS-1 downregulation, to the immune response triggered by excessive production of the Aβ peptide in AD. Since miR-155-5p expression has been largely associated with the maintenance of a pro-inflammatory M1 phenotype in both macrophages and microglia (Guedes et al., 2013; Ponomarev et al., 2013) our findings also corroborate the hypothesis that prolonged exposure to Aβ peptide may promote chronic neuroinflammation, thus contributing to disease progression. In light of these results, we consider that miR-155-5p can constitute an interesting and promising molecular target in AD. Recently, our group has developed targeted stable nucleic acid lipid particles (SNALPs) that exhibit excellent features for systemic *in vivo* administration of LNAs in order to modulate miRNA expression in the brain (Costa et al., 2013). This strategy could be explored in the context of AD by targeting glia cells with the purpose of decreasing the levels of miR-155-5p.

It is known that miR-155-5p is encoded within the BIC gene and its expression can be induced in response to LPS and other TLR ligands, such as poly(I:C), IFN-β or TNF-α, and in negative feedback loops associated with miR-155-5p direct targets, such as transcription factors C/EBPβ (Worm et al., 2009) and PU.1 (Gatto et al., 2008). Nevertheless, miR-155-5p regulation processes are still relatively unknown, especially in a disease context. Some studies have suggested that miR-155-5p is induced after NF-κB activation (Ma et al., 2011), but other transcription factors have also been associated with the expression of the primary transcript BIC, including the transcription factor AP-1 (O'Connell et al., 2007), which is composed of homo- or heterodimers of c-Jun and c-Fos. The results obtained in our study indicate that, in the context of AD, miR-155-5p expression is regulated, at least in part, by the c-Jun transcription factor (Fig. 3.9). Moreover, this study revealed that this transcription factor, but not NF-κB, is upregulated at an early time point in this AD animal model (3-month 3xTg AD mice) (Fig. 3.8), long before Aβ extracellular deposition in the nervous tissue, suggesting a possible relation between c-Jun upregulation and intracellular Aβ production. Of note, c-Jun has also been previously shown to be an important regulator of Aβ-induced neuronal apoptosis (Tang et al., 2008). Importantly, in this work, we disclosed another function of c-Jun, which takes place prior to neuronal death and is related with the regulation of Aβ-associated inflammation in microglia and astrocytes. Taking into consideration these results and our previous work on c-Jun contribution to acute excitotoxic lesion, which showed that c-Jun silencing using siRNAs was able to reduce neuronal loss and microglia activation in the hippocampus (Cardoso et al., 2010), we propose that a similar silencing strategy can also be applied to control neuroinflammation at early stages of AD.

3.5. Supplementary Material

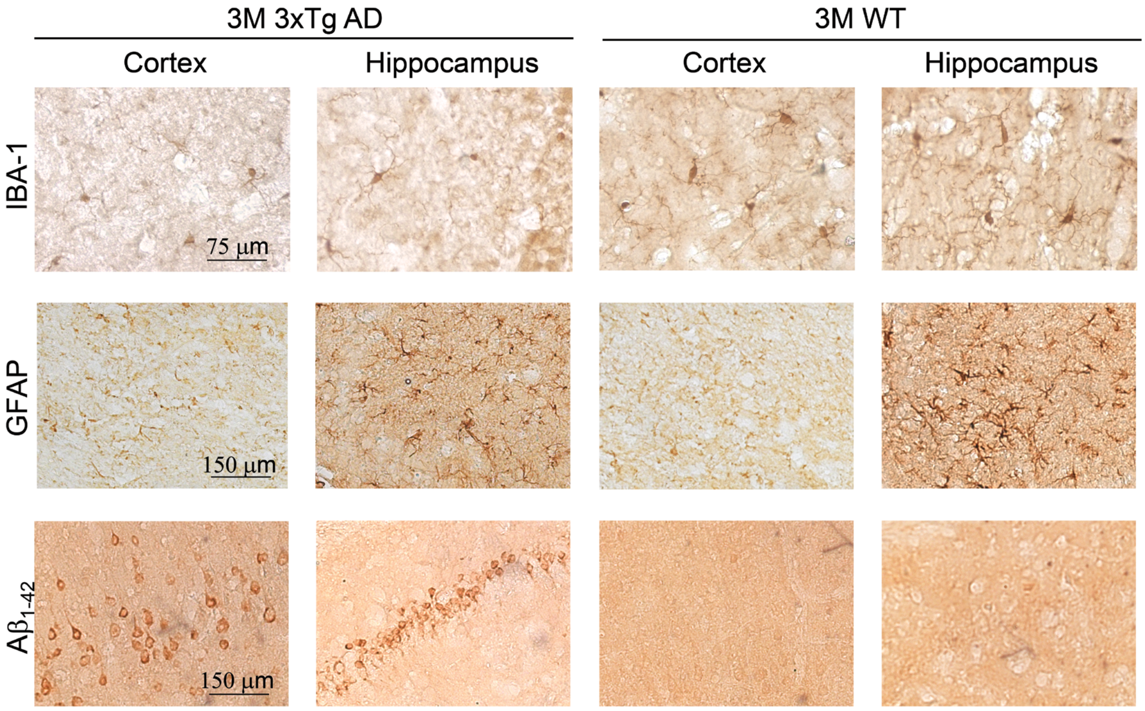

Figure S3.1 | IBA-1, GFAP and Aβ_{1-42} staining in 3 months old 3xTg AD animals.
Brain slices of 3-months 3xTg AD animals or their WT littermates were mounted in FluorSave^{TM} Reagent on microscope slides and incubated with IBA-1, GFAP or Aβ_{1-42} antibodies to stain microglia, astrocytes and the Aβ peptide, respectively. Following incubation with a biotinylated secondary antibody and visualization with 3,3'-diaminobenzidine tetrahydrochloride, pictures were taken under a Zeiss Axiovert microscope. Representative microscopy images of cortex and hippocampus were taken at a magnification of 200×. A specific area of each image was zoomed 3× or 1.5× to obtain close-up images showing the morphology of microglia or astrocytes in each brain region as well as intracellular Aβ accumulation. $n = 6$ animals for each experimental group.

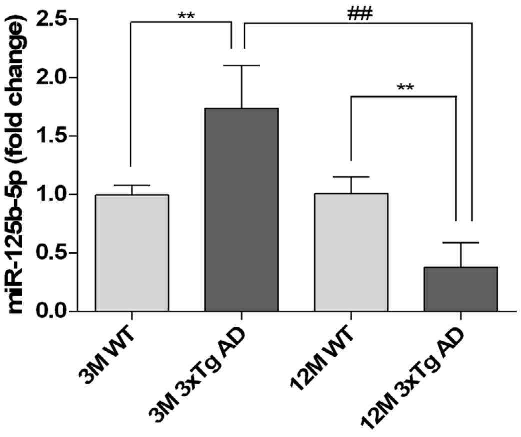

Figure S3.2 | MiR-125b-5p expression in 3xTg AD mice.
Total RNA extracts containing hippocampal and cortical brain regions of 3xTg AD animals, 3- and 12-months old, or their age-matched WT littermates were used to quantify miR-125b-5p by qRT-PCR. Results are expressed as miRNA fold change with respect to 3-months WT mice. **$P < 0.01$ with respect to age-matched WT littermates and $^{\#\#}P < 0.01$ with respect to 3 months 3xTg AD mice. Results are representative of $n = 6$ animals per experimental group.

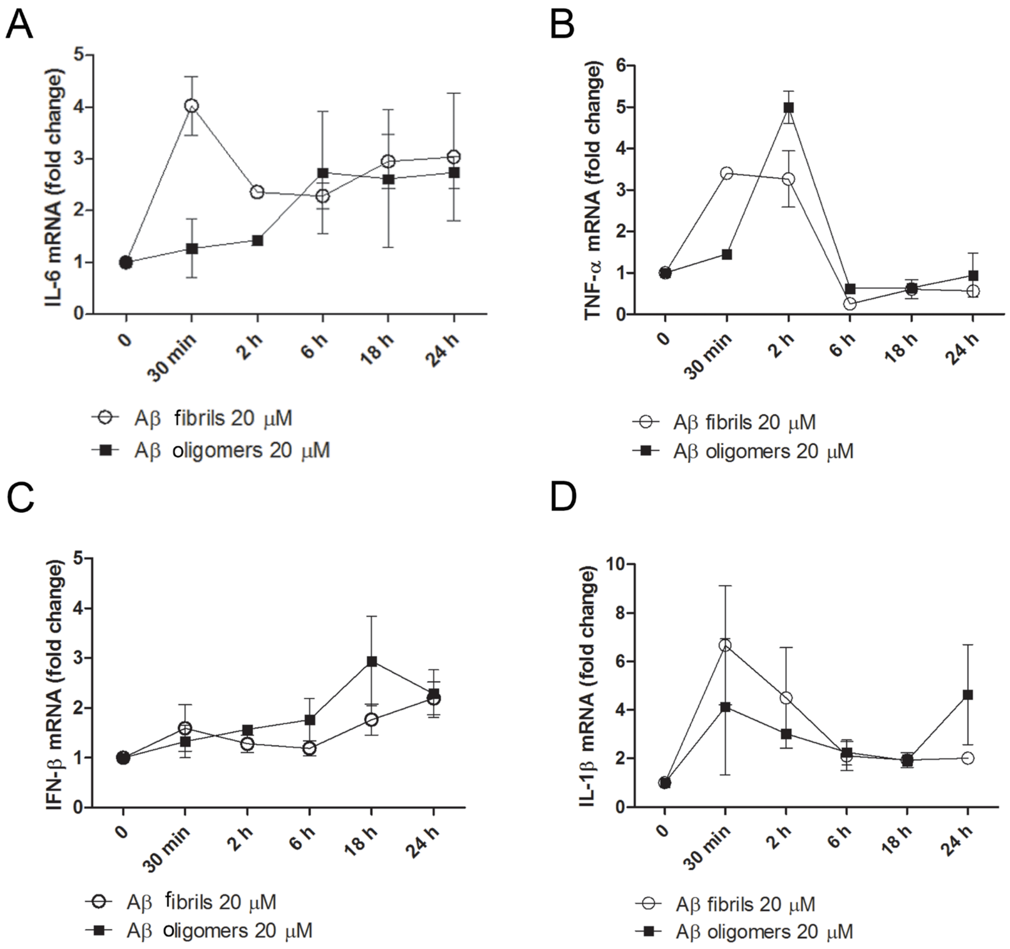

Figure S3.3 | Time-course study on cytokine expression in N9 microglia cells activated with Aβ oligomers or Aβ fibrils.

N9 microglia cells were plated and maintained in culture for 1 day before incubation with Aβ oligomers or Aβ fibrils. Cells were stimulated with 20 μM of Aβ fibrils or Aβ oligomers for 30 min, 2 h, 6 h, 18 h, and 24 h. Following this incubation period, total RNA was extracted from each condition and IL-6 (**A**), TNF-α (**B**), IFN-β (**C**) and IL-1β (**D**) mRNA levels were quantified by qRT-PCR. Results are expressed as mRNA fold change with respect to control (cells in the absence of stimulus) and are representative of two independent experiments performed in duplicate.

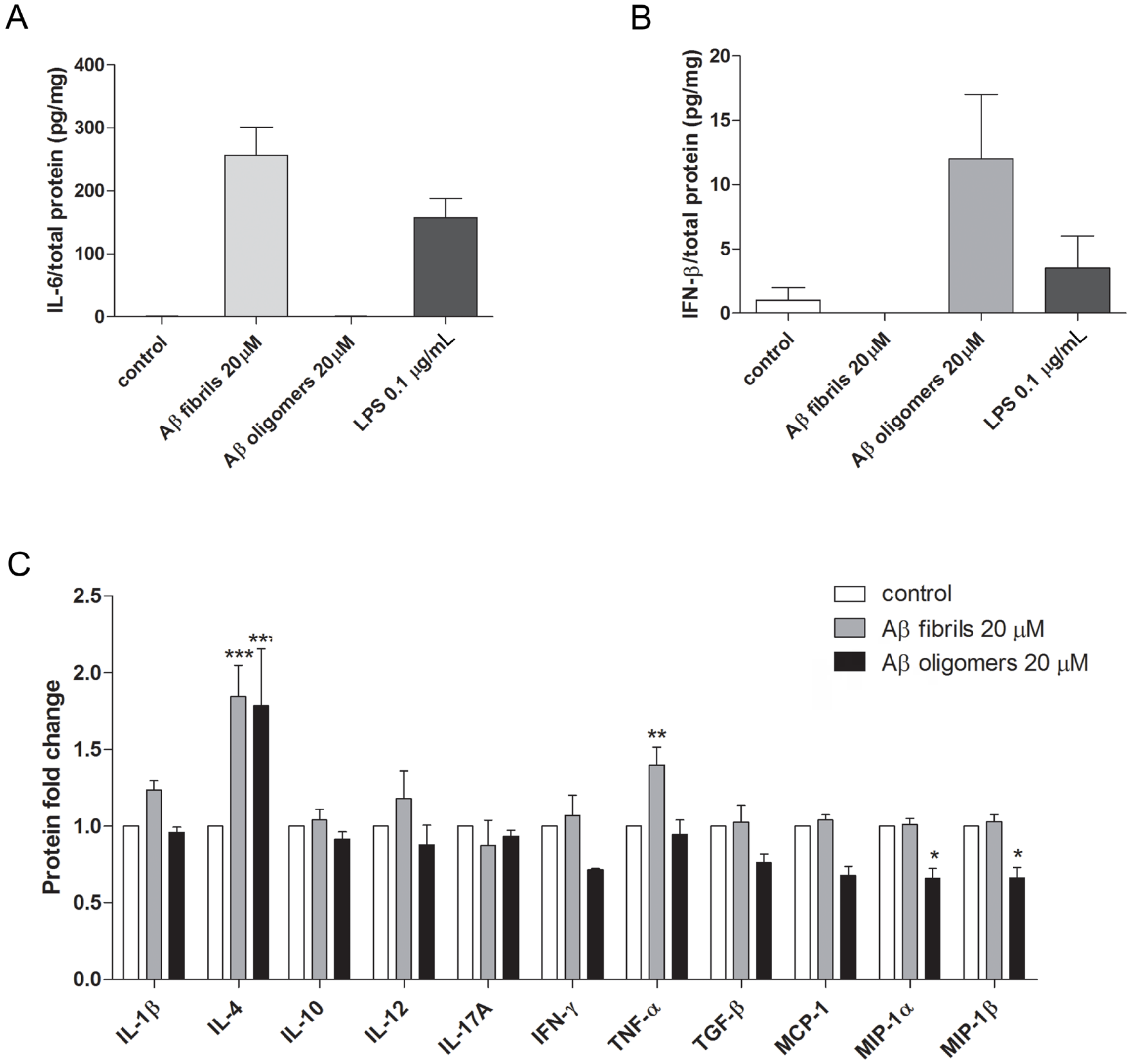

Figure S3.4 | Quantification of cytokine and chemokine secretion in Aβ-activated N9 microglia cells.
N9 microglia cells were plated and maintained in culture for 1 day before incubation with Aβ oligomers or Aβ fibrils. Cells were stimulated with 20 µM of Aβ fibrils or Aβ oligomers for 24 h. LPS 0.1 µg/mL was used as a positive control. Following the incubation period, the cell supernatant was collected from each experimental condition and cytokine and chemokine secretion was quantified by ELISA. The levels of secreted IL-6 (**A**) or IFN-β (**B**) are expressed as pg of IL-6 or IFN-β per mg of total protein. The screening of cytokine and chemokine release (**C**) is expressed as protein fold change with respect to control (non-activated cells). Results are representative of four (**A** and **B**) or two (**C**) independent experiments performed in duplicate. *$P < 0.05$, **$P < 0.01$ and ***$P < 0.001$with respect to control.

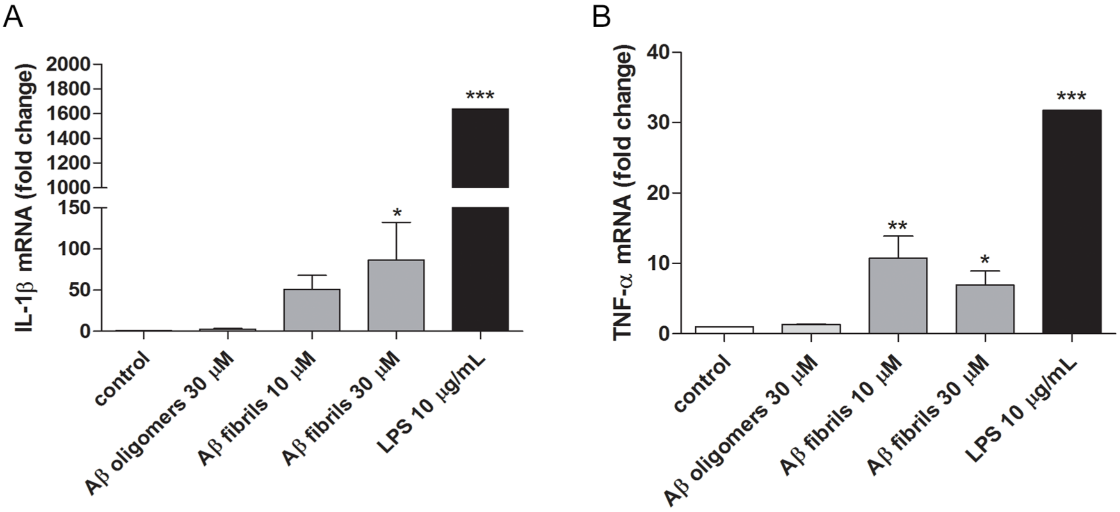

Figure S3.5 | IL-1β and TNF-α expression in astrocytes exposed to Aβ.
Astrocyte primary cultures were plated and maintained in culture for 1 day before incubation with Aβ oligomers or Aβ fibrils. Astrocytes were incubated with 10 and 30 µM of Aβ fibrils or Aβ oligomers, or 10 µg/mL of LPS (positive control) for 24h. Following this incubation period, total RNA was extracted from each condition and IL-1β (**A**) and TNF-α (**B**) mRNA levels were quantified by qRT-PCR. Results are expressed as mRNA fold change with respect to control (cells in the absence of stimulus) and are representative of three independent experiments performed in duplicate. *$P < 0.05$, **$P < 0.01$ and ***$P < 0.001$ with respect to control.

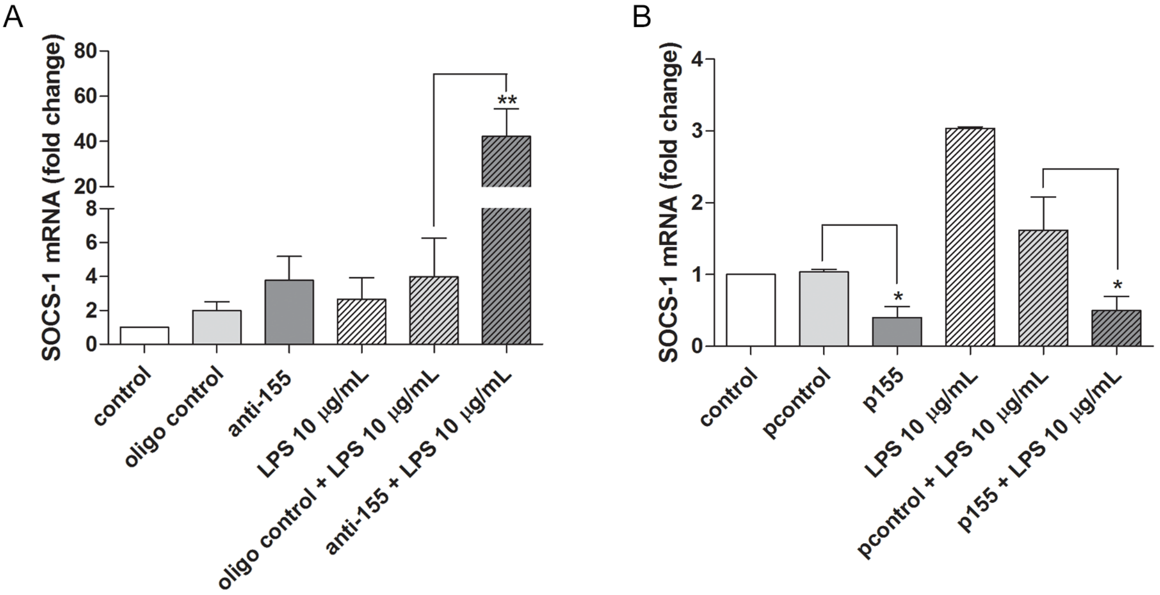

Figure S3.6 | SOCS-1 mRNA expression in astrocytes following miR-155-5p modulation.
Astrocyte primary cultures were plated and maintained in culture for 1 day before cell transfection with a (**A**) locked nucleic acid anti-miR-155-5p (anti-155) oligonucleotide (100 pmol/well) or a (**B**) plasmid DNA encoding miR-155-5p (1.6 µg p155/well). Astrocytes were transfected in DMEM 5% FBS and 4 h after transfection the cell medium was replaced by fresh DMEM 10% FBS. Twenty-four hours after transfection, astrocytes were stimulated with 10 µg/mL of LPS for 24h. Following this period of time, total RNA was extracted from each condition and SOCS-1 mRNA levels were quantified by qRT-PCR in cells where miR-155-5p expression was decreased (**A**) or increased (**B**). Results are expressed as mRNA fold change with respect to cells transfected with a control oligonucleotide (oligo control) or a plasmid DNA encoding GFP (pcontrol). All results are representative of three independent experiments performed in duplicate. *$P < 0.05$ and **$P < 0.01$ with respect to astrocytes transfected with a pcontrol or oligo control in the presence or absence of stimulus.

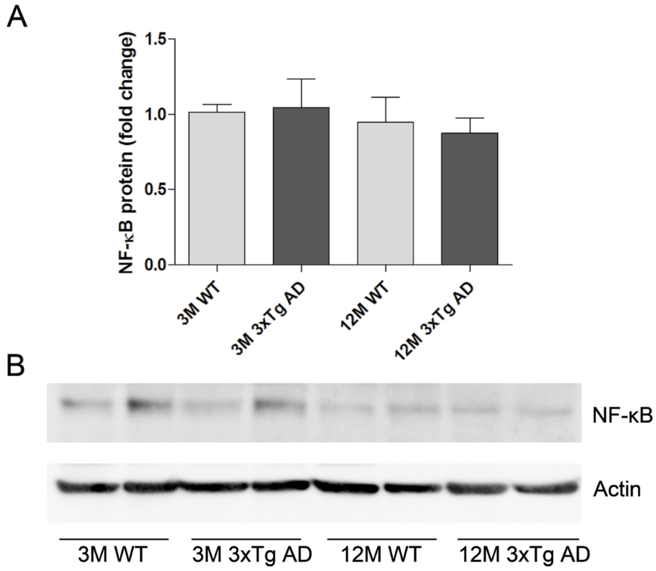

Figure S3.7 | NF-κB expression in 3xTg AD mice.
Protein extracts from hippocampal and cortical brain regions were obtained from 3xTg AD animals and their age-matched WT littermates at 3 and 12 months. (**A**) NF-κB protein levels were quantified by western blot and are expressed as protein fold change with respect to 3 months WT mice. (**B**) Representative western blot membrane showing unchanged NF-κB levels in 3xTg AD mice at 3 and 12 months with respect to WT littermates. All results are representative of *n* = 6 animals for each experimental group.

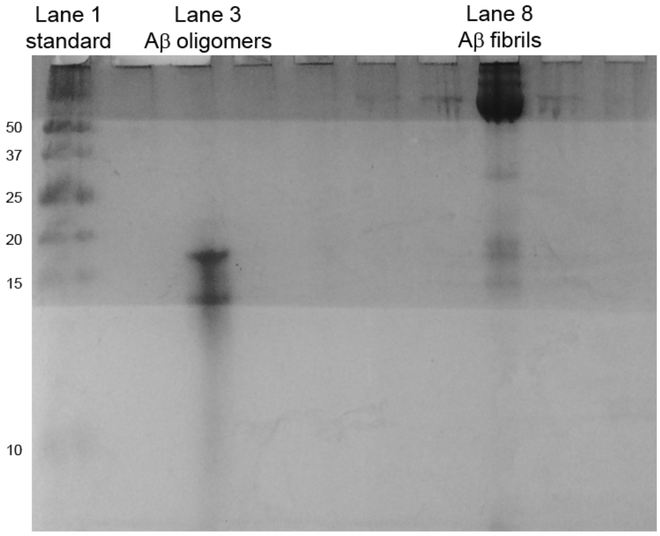

Figure S3.8 | Representative gel illustrating the different Aβ aggregated forms present in Aβ preparations.
Following the preparation of Aβ oligomers or Aβ fibrils, Aβ samples were subjected to a 4 –16% Tris–Tricine SDS-PAGE gel electrophoresis and dyed with Coomassie G-250. The different aggregated forms of the $A\beta_{1\text{-}42}$ peptide were detected based on molecular weight. Lane 1 represents the Low-Range Rainbow protein standard, Aβ oligomers preparation was loaded on Lane 3 and Aβ fibrils were loaded in Lane 8. The quantification of each band was performed using the Quantity One software (Bio-Rad).

Table S3.1 | Percentages of the Aβ assembly forms in the different Aβ preparations.

Aβ preparations	Aβ monomers %	Aβ oligomers %	Aβ fibrils %
Aβ oligomers	18.6	81.4	0
Aβ fibrils	5.8	33.8	60.4

| CHAPTER 4

MiRNA deregulation and chemotaxis and phagocytosis impairment in Alzheimer's disease

Guedes, J., Santana, I., Cunha, C., et al. MiRNA deregulation and chemotaxis and phagocytosis impairment in Alzheimer's disease. Alzheimer's & Dementia: Diagnosis, Assessment & Disease Monitoring (under revision)

Abstract

INTRODUCTION: Mononuclear phagocytes play a critical role during Alzheimer's disease (AD) pathogenesis due to their contribution to innate immune responses and Aβ clearance mechanisms.

METHODS: Blood-derived monocytes (BDMs) and monocyte-derived macrophages (MDMs) were isolated from blood of AD, mild cognitive impairment (MCI) patients and age-matched healthy controls for molecular and phenotypic comparisons.

RESULTS: The chemokine/chemokine receptor CCL2/CCR2 axis was impaired in BDMs from AD and MCI patients, causing a deficit in cell migration. Changes were also observed in MDM-mediated phagocytosis of Aβ fibrils, correlating with alterations in the expression and processing of the triggering receptor expressed on myeloid cells 2 (TREM2). Finally, immune-related miRNAs, including miR-155-5p, -154-5p, -200c-3p, -27b-3p and -128-3p were found to be differentially expressed in these cells.

DISCUSSION: This work provides evidence that chemotaxis and phagocytosis, two crucial innate immune functions, are impaired in AD and MCI patients. Correlations with miRNA levels suggest an epigenetic contribution to systemic immune dysfunction in AD.

4.1. Introduction

Blood-derived monocytes (BDMs) have been shown to have a beneficial role in Alzheimer's disease (AD) mouse models, associated with a higher ability to clear Aβ deposits in the brain (Lebson et al., 2010; Michaud et al., 2013; Koronyo et al., 2015) when compared to resident microglia. This contribution depends on the expression of chemokine receptors, such as CCR2, which mediate BDM migration and infiltration into the brain parenchyma (El Khoury et al., 2007; Naert and Rivest, 2012b), and phagocytosis-related proteins, such as the new AD risk protein, triggering receptor expressed on myeloid cells 2 (TREM2) (Guerreiro et al., 2013). However, in humans, the role of BDMs and monocyte-derived macrophages (MDMs), (which directly differentiate from BDMs within tissues) in AD is poorly explored. *In vitro*, macrophages of AD patients usually show minimal surface uptake and poor internalization of Aβ (Fiala et al., 2005), though the ability of their blood monocyte precursors to infiltrate the AD brain is yet poorly studied.

Both CCR2 and TREM2 have been directly implicated in AD pathology in different mouse models. Deficiency in CCR2 in the Tg2576 and APP_{Swe}/PS1 mice exacerbated amyloidosis (El Khoury et al., 2007; Naert and Rivest, 2011), while transplantation of CCR2 competent cells into APP_{Swe}/PS1/$CCR2^{-/-}$ restored cognitive functions (Naert and Rivest, 2012b). Two very recent studies implicated TREM2 in Aβ clearance *in vivo*, with contradictory results. While 5XFAD mice deficient in TREM2 showed increased accumulation of Aβ and a decrease in the number of microglia around plaques (Wang et al., 2015), in the APPPS1 mouse model the absence of TREM2 resulted in a reduction of Aβ load (Jay et al., 2015). In contrast with previous reports that restricted TREM2 expression to microglia cells (Hickman et al., 2013), the study in the APPPS1 model hypothesizes that the $TREM2^{+}$ cells found to surround Aβ plaques are blood-derived macrophages. Despite these evidences, it is unknown whether, in the context of human disease, these cells are able to migrate to the AD brain and phagocyte Aβ and how their function is regulated at the molecular level.

We have recently reported that overexpression of miR-155-5p occurs both in M1-activated microglia (Cardoso et al., 2012) and in the brain of 3xTg AD mice (Guedes et al., 2014) and is critical for the establishment of a chronic inflammatory phenotype. In this study we decided to further explore the ability of miRNAs to control immune-specific phenotypes, which hints at a potential use as early biomarkers of neuroinflammation (Butovsky et al., 2012). For this purpose, we compared the expression of immune-related miRNAs in AD and MCI patients, with that in healthy age-matched control subjects. Deregulation of miRNA expression and functional impairments in chemotaxis and phagocytosis observed in AD and MCI patients were correlated with the levels of emergent proteins in the realm of AD research. This work suggests that the deregulation of specific immune-related miRNAs in AD patients may contribute to the observed dysfunctions in chemotaxis and phagocytosis.

4.2. *Methods*

4.2.1. *Patient selection*

Subjects (*n* = 124) were recruited at the Neurology Department, Coimbra University Hospital: 36 age-matched healthy controls (Controls), 52 MCI patients (MCI) and 36 AD patients (AD) and were representative of the Portuguese Caucasian population. Patients' diagnostic investigation comprehended a standard clinical evaluation, routine laboratory tests and imaging studies (CT or MRI), SPECT and *ApoE* allele genotyping. *TREM2* genotyping for R47H mutation in exon 2 [associated with higher AD risk (Kleinberger et al., 2014)], was performed in all AD and MCI patients where TREM2 expression was assessed. PET, cerebrospinal fluid analysis and genetic studies were more restricted, although considered in younger patients.

A comprehensive cognitive-functional-psychological assessment battery was carried out by a team of neuropsychologists, following a standard protocol, and comprising several tests and scales: 1) Cognitive instruments as the MMSE (Folstein et al., 1975), the MoCA (Nasreddine et al., 2005), the ADAS-Cog (Mohs, 1983) and a comprehensive neuropsychological battery validated for the Portuguese population [Battery of Lisbon for the Assessment of Dementia; (Guerreiro, 1998)] were used to explore memory and other cognitive domains; 2) The Clinical Dementia Rating [CDR; (Morris, 1993)] was used for global staging and 3) The Geriatric Depression Scale [GDS-30; (Yesavage et al., 1983)] was used to exclude major depression. All MCI patients were classified at the global CDR staging of 0.5 (no functional impairment) and were selected according to Albert's (Albert et al., 2011) and Petersen's criteria (Petersen, 2004). The standard criteria for the diagnosis of AD patients were the Diagnostic and Statistical Manual of Mental Disorders – fourth edition (DSM-IV-TR) and the National Institute of Neurological and Communicative Disorders and Stroke-Alzheimer's Disease and Related Disorders [NINCDS-ADRDA; (McKhann et al., 2011)]. The AD group included patients with mild disease (CDR = 1) or moderate to severe (CDR = 2 and 3). The control group comprised 36 cognitively healthy adults belonging to the local community (recruited among the patients' spouses, hospital or university staff or their relatives), that were age, education, and gender matched to the patients. Controls had normal MMSE scores (> 24) and were fully autonomous in daily life activities (CDR) according to the information obtained through a general practitioner, and/or an informant. Moreover, to be eligible for this study, subjects (patients and controls) should be in a stable condition, without acute significant events or recent/undergoing changes in medication. Exclusion criteria were: 1) significant motor, visual or auditory deficits which could influence the neuropsychological performance; 2) neurological/psychiatric conditions other than MCI or AD; 3) CT or MRI demonstration of significant vascular burden (Roman et al., 1993); 4) diagnosis of diabetes, chronic inflammatory, neoplastic diseases or prescription of anti-inflammatory drugs; 5) major depression indicated by a GDS score of 20 or more points; 6) active smokers; 7) patients suffered from uncontrolled hypertension. Informed consent was obtained from all participants and the study was conducted in accordance with the tenets of the Declaration of Helsinki with the approval of the local ethics committee. Subjects' information/ classification was only disclosed in the end of the study.

4.2.2. *Isolation of BDMs*

For each study subject, a total of 20 mL of blood were collected in sterile 10 mL EDTA-coated tubes. Peripheral blood mononuclear cells (PBMCs) were isolated by density gradient centrifugation [800 g, 20 min at room temperature (RT)] using Histopaque® (Sigma, USA). BDM isolation was performed using magnetic separation, employing CD14 MicroBeads (Miltenyi Biotec, Germany). Briefly, PBMCs were incubated for 15 min at 4°C in the presence of magnetic microbeads associated with an anti-human CD14 antibody and then run through a single LS MACS Column (Miltenyi Biotec), placed under the magnetic field of a MidiMACS™ Separator (Miltenyi Biotec), and washed 3 times to remove unlabeled cells. The LS Column was removed from the MidiMACS and CD14+ monocytes were flushed out and used for all subsequent experiments. The purity of the CD14+ monocytes was determined by flow cytometry, using a monoclonal anti-CD14-FITC antibody (Sigma, USA), and was shown to be more than 96%.

4.2.3. *Flow cytometry analysis*

CCR2 and CXCR4 surface expression was analyzed by flow cytometry using phycoerythrin MAb anti-human CCR2 and CXCR4 antibodies (R&D Systems, USA) and the respective isotype controls. Immediately after isolation, BDMs were washed twice with PBS 10% FBS and incubated for 30 min at 4°C, in the dark and with rotation, in 100 μL of PBS 3% BSA. After this period, the cells were washed twice with PBS and analyzed immediately by flow cytometry in a FACScalibur flow cytometer (BD Biosciences, USA). For each sample, a total of 20 000 events were analyzed with Cell Quest Pro software (BD Biosciences, USA).

4.2.4. *Chemotaxis assay*

Cell migration experiments were performed using the ChemoTx® Disposable Chemotaxis System (Neuro Probe, Inc., USA), as previously described (Frevert et al., 1998). Immediately after isolation, BDMs were incubated with 10 μM calcein-AM (Sigma, USA), for 30 min at 37°C, and seeded in triplicate onto a 5 μm pore-membrane, in a total volume of 50 μL of RPMI-1640 without FBS/phenol red. Thirty μL of each chemoattractant, diluted in the same medium, were placed in each well (in triplicate) of a 96-well multiwell plate fitted under the membrane: 10 nM CCL2, 12.5 nM CXCL12 (PeproTech, USA) and 5 µM Aβ fibrils. After 4 h at 37°C in the dark, the membrane above the plate was removed and calcein fluorescence in each well, which was proportional to the number of cells that crossed the membrane, was determined at 517 nm in a Spectramax fluorimeter (λ_{ex} = 494 nm; λ_{em} = 517 nm; Molecular Devices, USA). The proper controls without chemoattractants were performed, as well as a standard curve with increasing numbers of seeded cells labeled with calcein-AM.

4.2.5. *Preparation of Aβ$_{1-42}$ fibrils and Aβ$_{1-42}$-FAM fibrils*

Aβ$_{1-42}$ fibrils were prepared as previously described (Resende et al., 2008) and aged at 37°C for 7 days. After centrifugation for 10 min at 15 000 g at RT, the supernatant, containing soluble oligomers, was discarded and the pellet containing Aβ fibrils (and possibly protofibrils) was resuspended in HAM's F12 buffer (pH 7.5) at a final concentration of 50 µM. The presence of different assembly forms (monomers, oligomers and fibrils) was evaluated by gel electrophoresis in non-denaturating conditions. For the preparation of Aβ$_{1-42}$-FAM fibrils, 0.1 mg of FAM-labeled Aβ$_{1-42}$ peptide (American Peptide Co., USA) was dissolved in the same buffer containing 4% DMSO, at a concentration of 50 µM and then aged for 24 h at 37°C in the dark.

4.2.6. *Primary cultures of MDMs and phagocytosis assay*

After BDM isolation, cells were plated in 8-well ibiTreat chamber slides (ibidi, Germany), in RPMI-1640 without FBS. After 12 h, 10% FBS and 50 ng/mL M-CSF (Sigma, USA) were added to the cultures and replaced every 3 days, during 7 days, to promote differentiation. MDMs were stimulated with 5 µM Aβ-FAM fibrils: Aβ fibrils 1:5 in RPMI-1640 10% FBS for 24 h. LysoTracker® Red DND-99 (Life Technologies, USA) was then added to stain lysosomes and incubated for 30 min at 37°C, at a 50 nM concentration. The nuclei were labeled with the DNA-binding dye Hoechst 33342 (Life Technologies, USA) upon incubation for 5 min in the dark. Confocal images were acquired in a point scanning confocal microscope Zeiss LSM 510 Meta (Zeiss, Germany), with a ×60 oil objective, using the LSM 510 META software. All instrumental parameters pertaining to fluorescence detection and image analyses were held constant to allow sample comparison.

4.2.7. *RNA extraction and qRT-PCR*

Total RNA was extracted using the miRCURY™ Isolation Kit – Cell & Plant (Exiqon, Denmark), according to the manufacturer's recommendations and quantified by NanoDrop. In order to screen the expression of immune-related miRNAs in monocytes, 5 ng of total RNA from each subject were transcribed using the Universal cDNA Synthesis Kit II (Exiqon). The cDNA was diluted 100× with ExiLENT SYBR Green master mix (Exiqon, Denmark) before the qRT-PCR reaction. For a selected number of subjects, a Pick-&-Mix microRNA PCR Panel (Exiqon), pre-designed to incorporate a set of 96 miRNA and control primers (Supplementary Material, Table S4.1), was employed and qRT-PCR results were analyzed using the GenEx qPCR analysis software (Exiqon). The expression of individual miRNAs, found to be differently expressed between groups, was confirmed by specific qRT-PCR assays using the same pre-designed LNA primers (Exiqon) employed in the Pick-&-Mix microRNA PCR Panel. SNORD44 was used as a reference gene.

The expression of specific genes was also assessed by qRT-PCR. In this case, 250 ng of total RNA were transcribed using the NZY First-Strand cDNA Synthesis Kit (Nzytech, Portugal). The relative expression of CCR2, CXCR4 and TREM2 was quantified using the SsoAdvanced™ Universal SYBR® Green Supermix (Bio-Rad, USA) and pre-designed primers from Qiagen (Germany). All reactions were performed in duplicate in a StepOne™ Plus device (Applied Biosystems, USA).

4.2.8. *ELISA for sTREM2*

Quantification of sTREM2 in plasma samples was performed by ELISA, as previously described (Kleinberger et al., 2014), using a rabbit anti-TREM2 monoclonal capture antibody and a mouse anti-TREM2 monoclonal antibody (detection antibody) conjugated with horseradish-peroxidase. Recombinant human TREM2 protein was used to generate a six-point standard curve (concentration range 62.5 pg/mL to 4000 pg/mL). The optical density in each well was determined at 450 nm, using a SpectraMax Gemini EM fluorimeter (Molecular Devices). Interplate and interday variability was determined and corrected using dedicated plasma samples.

4.2.9. *Statistical analysis*

All data are expressed as ± SEM and were analyzed for statistical significance using One-way ANOVA followed by Bonferroni's Multiple Comparison post hoc test, to compare normally distributed variables, except for CCR2 and CXCR4 surface expression which were analyzed with Two-way ANOVA followed by Bonferroni´s post hoc test. In order to analyze non-Gaussian data distributions (including sTREM2 quantification) and to control the effect of potential confounders, such as gender and age, we log-transformed variables (such as sTREM2 concentration) to achieve normal distributions. Differences were considered statistically significant for P values < 0.05, 0.01 and 0.001, as described in the figure legends. All tests were two-tailed and the data were analyzed using the GraphPad Prism 5 software.

4.3. Results

4.3.1. The presence of chemokine receptors is reduced at the cell surface of BDMs from AD and MCI patients

We analyzed the expression levels of CCR2 and CXCR4 in $CD14^+$ BDMs isolated from patients and control subjects. A total of 124 subjects divided in 3 groups were involved in this study: 36 healthy age-matched subjects (Controls), 36 AD patients and 52 MCI patients. Table 4.1 summarizes the clinical data available for each one of the patients groups. The 3 groups presented approximate age and gender distributions.

Table 4.1 | Characteristics of patient and control study populations.

Variable	Controls	AD	MCI
Number of patients (n)	36	36	52
Gender (F/M) (%)	58/42	64/36	46/54
Age (years)	70.3 ± 6.6	74.9 ± 8.8	73.6 ± 8.9
MMSE Score	> 24	15 ± 7.6	26.9 ± 2.9***
MoCA Score		9.8 ± 5.8	18.3 ± 4.7***
ADAS-cog Score	--	20.9 ± 7.6	9.6 ± 4.6***
Stage of Disease (CDR) (%)			
Mild	--	63,9	--
Moderate	--	27,8	--
Severe	--	8,3	--
ApoE *genotype ε4*	--	50 %	37 %

Mini-mental State Examination (MMSE); Montreal Cognitive Assessment (MoCA); Alzheimer´s Disease Assessment Scale-Cognitive (ADAS-Cog). Data are expressed as mean ± SD, except for gender [expressed in percentage of females – F (%) – and males – M (%)], Stage of Disease (CDR) (expressed in percentage of total subjects) and *ApoE* genotype *ε4* (expressed in percentage of *ε4* carries). For MMSE and MoCA, higher scores correspond to better performance and for the ADAS-cog, higher scores indicate greater impairment. MoCA and ADAS-cog were only performed in patients with CDR ≤ 1. One-way ANOVA was used to compare age between groups, followed by Tukey's post hoc test. Two-tailed T-test was used to compare MMSE, MoCA and AADS-cog Scores and Fisher's exact test was used for *ApoE* genotype. *** $P < 0.001$ vs. AD

We found that the mRNA levels of CCR2 (Fig. 4.1A) and CXCR4 (Fig. 4.1D) were increased by 2-fold in BDMs from AD patients, with respect to both Controls and MCI patients. However, such increase did not translate into an increase of the presence of CCR2 and CXCR4 receptors at the cell surface. Flow cytometry studies, performed in live cells, revealed that the percentage of $CCR2^-$ BDMs was increased in both AD and MCI patients, with respect to Controls, which was associated with a decrease in $CCR2^{high}$ populations (Fig. 4.1B). A reduction in the $CXCR4^{low}$ population was also observed in MCI patients, which presented a concomitant increase in CXCR4$^-$ cells (Fig. 4.1E). Figure 4.1C and F shows representative histograms illustrating the distribution of CCR2 and CXCR4 surface signals in the BDM cell population. These results lead us to hypothesize that AD patients present an impairment in CCR2 mRNA translation. Moreover, although bearing CCR2 and CXCR4 mRNA levels similar to Controls, MCI patients also presented a reduction in protein levels.

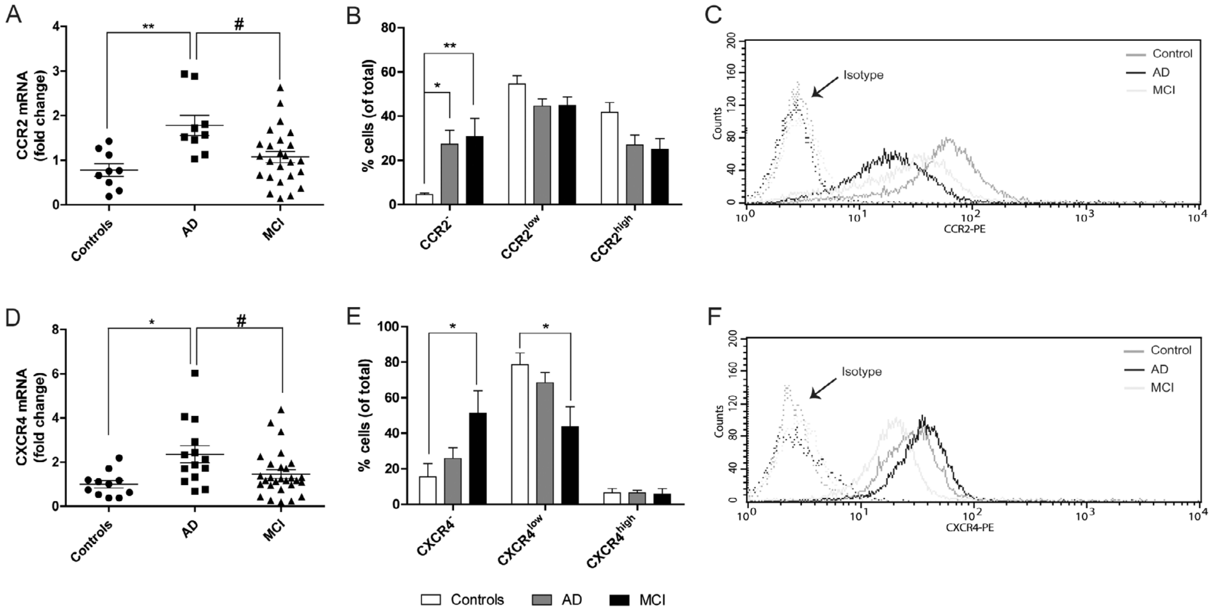

Figure 4.1 | Presence of surface chemokine receptors CCR2 and CXCR4 is reduced in BDM of AD and MCI patients.

The mRNA levels of chemokine receptors CCR2 (**A**) and CXCR4 (**D**) were quantified by qRT-PCR in CD14$^+$ BDMs from Controls, AD and MCI patients. Results are expressed as mRNA fold change with respect to the mean of Controls and are representative of at least $n = 9$ per group (One-way ANOVA $**P < 0.01$). $*P < 0.05$ and $**P < 0.01$ with respect to Controls and $^{\#}P < 0.05$ with respect to AD patients. CD14$^+$ BDM surface expression of CCR2 and CXCR4 proteins was analyzed by flow cytometry. Cell populations with negative, low and high expression of CCR2 (**B**) and CXCR4 (**E**) were quantified by histogram analysis. Results are expressed as the percentage of total cells and are representative of at least $n = 7$ per group. $*P < 0.05$ and $**P < 0.01$ with respect to control subjects (Two-way ANOVA followed by Bonferroni´s post hoc test). (**C, F**) Representative histograms of a control subject, an AD and a MCI patient for CCR2 and CXCR4 surface expression.

4.3.2. CCL2-driven chemotaxis is impaired in BDM of AD and MCI patients

To investigate if the lower availability of CCR2 and CXCR4 at the cell surface of AD and MCI BDMs presented functional consequences, influencing the ability of these cells to migrate in response to chemokine gradients, we performed a chemotaxis assay in the presence of CCL2 and CXCL12, the specific ligands for CCR2 and CXCR4. Immediately after isolation, BDMs were stimulated for 4 h with 10 nM CCL2 (Volpe et al., 2012) and 12.5 nM CXCL12 in NeuroProbe chemotaxis chambers (Fig. 4.2A). As expected, BDMs isolated from AD and MCI patients presented a significant reduction in cell migration in the presence of CCL2, with respect to BDMs from Controls (Fig. 4.2C). A similar tendency was observed in MCI following exposure to CXCL12 (Fig. 4.2D), albeit without statistical significance. These results directly correlated with the increased number of BDMs negative for CCR2 and CXCR4 observed in AD and MCI (Fig. 4.1B and E).

Although previous *in vitro* studies have suggested that Aβ soluble monomers do not act as a direct chemoattractant for immune cells (Baik et al., 2014), it is believed that monocytes can potentially bind to vascular Aβ deposits in brain vessels (Michaud et al., 2013). Therefore, we investigated if other forms of the Aβ peptide, such as Aβ fibrils, could act as chemoattractants, by performing a similar chemotaxis experiment using Aβ fibrils. A tendency for reduced cell migration for both MCI and AD patients was observed (Fig. 4.2B), suggesting that BDMs from these patients might be less sensitive to chemotaxis signals than Controls.

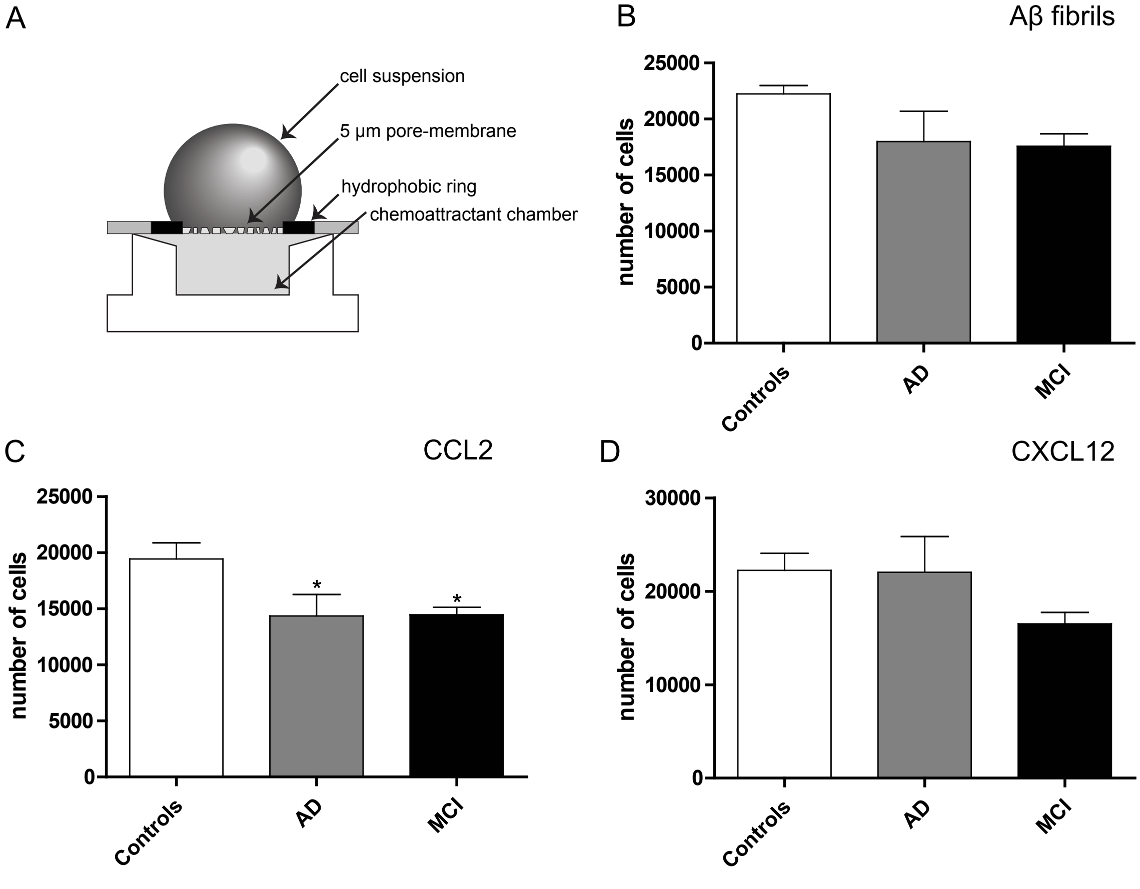

Figure 4.2 | CCL2-driven chemotaxis is impaired in AD and MCI BDMs.
BDM migration was evaluated using the (**A**) ChemoTx® Disposable Chemotaxis System (Neuro Probe). CD14$^+$ BDMs were labeled with 10 µM of calcein-AM and plated in a chemotaxis membrane. BDMs were stimulated with 5 µM Aβ fibrils (**B**), 10 nM CCL2 (**C**) or 12.5 nM CXCL12 (**D**), placed directly in the chemoattractant chamber. After 4 h, the calcein signal was measured by fluorimetry in the wells beneath the membrane. Results are expressed as the number of cells found in the chemoattractant chamber after a 4 h stimulation and are representative of at least $n = 9$ per group (One-way ANOVA $^*P < 0.05$, $P = 0.08$ and $P = 0.1$ for CCL2, Aβ and CCL12, respectively). $^*P < 0.05$ with respect to control subjects.

4.3.3. *Phagocytosis of Aβ fibrils by MDMs is compromised in both AD and MCI patients*

To evaluate phagocytosis efficiency of Aβ fibrils by MDMs, we isolated CD14$^+$ BDMs from AD, MCI patients and Controls, and promoted their differentiation into MDMs, which were incubated with Aβ-FAM fibrils for 24 h before assessing Aβ binding and internalization by confocal microscopy. LysoTracker® was used to label lysosomes and other acidic compartments and thus determine Aβ co-localization with these organelles. MDMs from Controls were able to bind, internalize and degrade Aβ fibrils very efficiently, since no big Aβ aggregates were visible inside the cells following the 24 h incubation period (Fig. 4.3A, left image). On the other hand, MDMs from AD patients showed poor Aβ fibril internalization and presented big Aβ aggregates associated with the cell membrane (Fig. 4.3A, middle image). Moreover, in these patients, intracellular Aβ aggregates failed to co-localize with acidic endocytic vesicles. In contrast to AD patients, MDMs from MCI showed a massive uptake of Aβ fibrils. Approximately 50% of MCI cells were able to degrade Aβ, while the other half presented accumulation of intracellular Aβ (Fig. 4.3A, right image). These observations translated into a significant increase in intracellular fluorescent signal in MCI, with respect to Controls and AD patients (Fig. 4.3B). Similar results were observed in a parallel experiment where internalized unlabeled Aβ was detected by immunocytochemistry (data not shown).

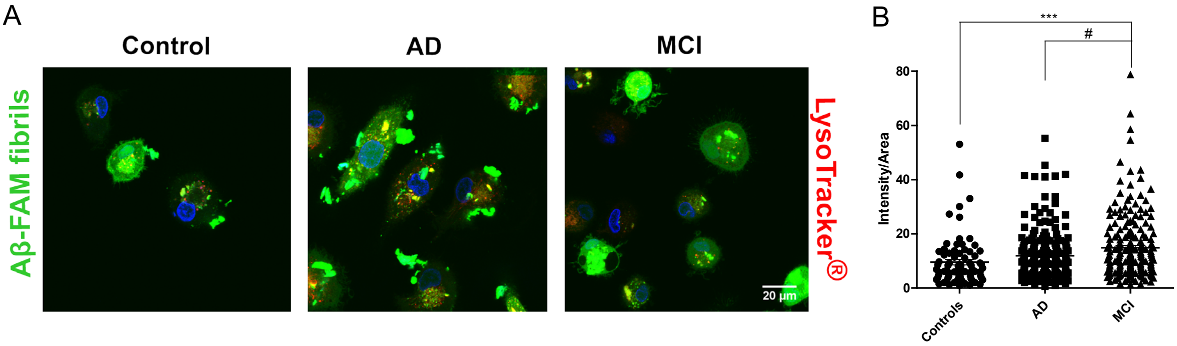

Figure 4.3 | Internalization of Aβ fibrils is compromised in AD MDMs, while MCI MDMs present increased Aβ fibril uptake.

CD14$^+$ BDMs were plated in 8-well ibidi plates and differentiated into MDMs. MDMs were incubated with 5 µM Aβ fibrils (1:5 Aβ-FAM fibrils: Aβ fibrils) for 24 h, followed by incubation with 100 nM LysoTracker® for 30 min at 37°C. Phagocytosis of Aβ-FAM fibrils was evaluated by confocal microscopy (**A**) using a Zeiss LSM 510 Meta with a 63x oil objective. The fluorescence intensity inside the cells (**B**) was quantified using the ImageJ software. For each subject (at least $n = 7$ per group), 6 images were taken and, in each image, the intensity of fluorescence/area of 4 cells was quantified (One-way ANOVA ***$P < 0.001$). ***$P < 0.001$ with respect to control subjects and $^{\#}P < 0.05$ with respect to AD patients.

4.3.4. *TREM2 expression is increased in MCI patients*

Rare variants of *TREM2* and other new immune-related genes have been recently associated with higher risk of developing AD (Harold et al., 2009; Lambert et al., 2009b;

Hollingworth et al., 2011a; Guerreiro et al., 2013). In the particular case of TREM2, reported mutations, including R47H, have been associated with an impairment in TREM2 processing by secretases and concomitant shedding of TREM2 ectodomain (sTREM2) (Wunderlich et al., 2013; Kleinberger et al., 2014). Although the R47H *TREM2* mutation was absent in our cohort, the fact that TREM2 has been implicated in the regulation of phagocytic activity (Kleinberger et al., 2014) led us to explore the expression profile of TREM2 in BDMs and MDMs from AD and MCI patients. We observed a high increase in TREM2 mRNA expression, in both BDMs and MDMs from MCI patients, with respect to AD patients (Fig. 4.4A and B) and TREM2 expression was only upregulated in MCI compared to Controls in MDMs (Fig. 4.4B). Interestingly, sTREM2 levels were elevated in the plasma of AD patients (Fig. 4.4C) with respect to both Controls and MCI, suggesting that TREM2 shedding is not directly proportional to TREM2 mRNA expression. Although a slight decrease in TREM2 mRNA levels was detected in BDMs from AD patients (Fig. 4.4A), which could potentially correlate with the observed decrease in Aβ phagocytosis, this effect was not present in AD MDMs (Fig. 4.4B). Nevertheless, the increase in TREM2 expression presented by MCI patients (Fig. 4.4B) can help explain the high Aβ uptake observed in these patients.

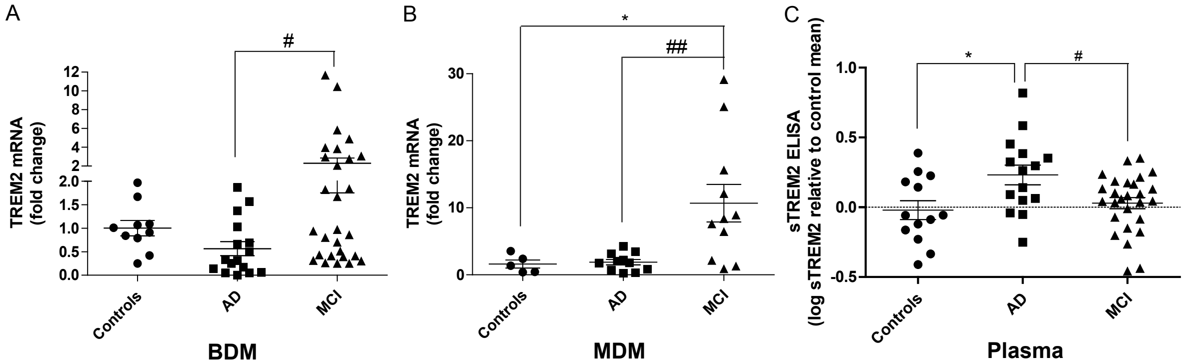

Figure 4.4 | Deregulation of TREM2 mRNA and sTREM2 levels in AD and MCI patients.
TREM2 mRNA expression was quantified by qRT-PCR in (**A**) CD14$^+$ BDMs and (**B**) MDMs of Controls, AD and MCI patients. Results are expressed as mRNA fold change with respect to the mean of Controls and are representative of at least *n* = 10 (**A**) and *n* = 5 (**B**) per group. $^*P < 0.05$ with respect to control subjects and $^{\#}P < 0.05$, $^{\#\#}P < 0.01$ with respect to AD patients. The soluble form of TREM2 (sTREM2) was quantified in plasma samples by ELISA (**C**). Results are expressed as log sTREM2 with respect to the mean of Controls and are representative of at least *n* = 13 per group (One-way ANOVA $^*P < 0.05$ for TREM2 expression in BDMs and $^{**}P < 0.01$ for TREM2 expression in MDMs and sTREM2). $^*P < 0.05$ with respect to control subjects and $^{\#}P < 0.05$ with respect to AD patients.

4.3.5. *Immune-related miRNAs are differentially expressed in AD and MCI patients*

Considering the important role of miRNAs in the control of immune responses, miRNA deregulation may help explain, from a mechanistic point of view, changes in cell-specific phenotypes. In this regard, we investigated the expression of immune-related miRNAs that, according to miRWalk (Dweep et al., 2011), are predicted to bind and regulate the transduction of proteins implicated in chemotaxis and phagocytosis. This database uses up to 8 different mathematical algorithms to search for miRNA putative binding sites in all known mRNAs, mitochondrial genes and 10 kb upstream gene flanking regions. Based on this information, we designed PCR arrays to quantify the levels of 90 miRNAs (Supplementary Material, Table S4.1) in BDMs from 12 AD, MCI patients and Controls. This study allowed to identify 5 miRNAs which were differentially expressed in the three experimental groups: miR-154-5p, -27b-3p, -200b-3p, -128-3p and -23a-3p. These findings were confirmed by single qRT-PCR assays in a larger cohort, using the same specific primer sets (Fig. 4.5A-E). Interestingly, all 5 miRNAs were overexpressed in BDMs from AD patients, with respect to either Controls, MCI patients or both, which clearly shows that AD patients present several deficiencies in miRNA networks associated with inflammation and innate immune response. Since miR-154-5p and miR-23a-3p (Fig 4.5H) share CCR2 as a predictive target, while miR-27b-3p has been shown to regulate the CXCL12/CXCR4 axis (Lu et al., 2012), the observed increase in these miRNAs may contribute

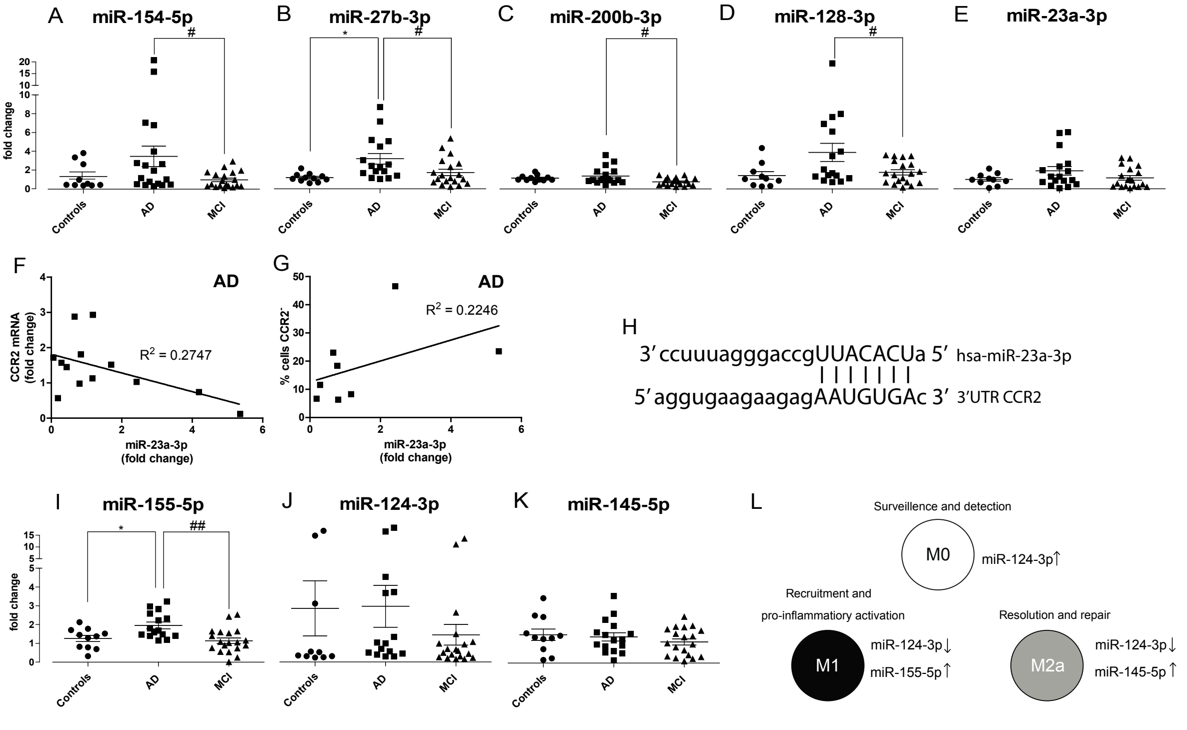

Figure 4.5 | Immune-related miRNAs are differentially expressed in AD and MCI patients.
Immune-related miRNAs (**A, B, C, D, E**) were quantified in CD14^{+} BDMs of Controls, AD and MCI patients by qRT-PCR, using individual qRT-PCR assays for each miRNA. Correlations between the levels of miR-23a-3p (fold change with respect to the mean of Controls) in AD patients and (**F**) mRNA CCR2 fold change or (**G**) the percentage of cells negative for CCR2 surface expression are shown. (**H**) Illustration of the miR-23a-3p binding site in the 3'UTR of CCR2 (source: miRNA.org). (**I, J, K**) M1, M0 and M2a-related miRNAs were quantified by qRT-PCR in BDMs. Results are expressed as miRNA fold change with respect to the mean of Controls and are representative of at least $n = 10$ *per* group (One-way ANOVA $*P < 0.05$ for miR-154-5p, -200b-3p and -128-3p expression and $**P < 0.01$ for miR-27b-3p and -155-p expression; $P = 0.166$ for miR-23a-3p expression and non-significant for miR-124-3p and -145-5p). $*P < 0.05$ with respect to Controls and $^{\#}P < 0.05$ and $^{\#\#}P < 0.01$ with respect to AD patients. (**L**) Illustration of M1, M0 and M2a signature miRNAs.

to the impairments observed in cell migration. MiR-23a-3p expression was found to inversely correlate with CCR2 mRNA levels (Fig. 4.5F) and to directly correlate with the percentage of cells negative for CCR2 (Fig. 4.5G). Since no differences in miRNA expression were found between Controls and MCI patients, we can anticipate that all 5 miRNAs have potential, as conversion biomarkers, to distinguish MCI from AD.

Evaluation of the expression of 3 miRNAs, miR-155-5p, miR-145-5p and miR-124-3p, which serve as signature markers for the M1, M2a and M0 activation phenotypes, respectively (Fig. 4.5L) (Freilich et al., 2013), did not reveal differences in miR-124-3p and miR-145-5p expression profiles (Fig. 4.5J and K), but showcased an increase in miR-155-5p levels in AD patients with respect to both Controls and MCI (Fig. 4.5I), suggesting a tendency towards the M1 phenotype.

4.4. *Discussion*

In this study we provide new evidence of the deregulation of specific immune-related miRNAs in BDMs from AD and MCI patients, which may have impact in disease pathogenesis. According to several miRNA prediction algorithms, at least two of the identified miRNAs, miR-23a-3p and miR-154-5p, are able to bind and potentially regulate the 3'UTR of the chemokine receptor CCR2. The elevated levels of both miR-154-5p and miR-23a-3p in AD patients (Fig. 4.5A and E) can help explain the observed reduction of CCR2 surface levels, since an overexpression of miRNAs able to bind to CCR2 mRNA might block its translation into protein. We hypothesized that the low CCR2 cell surface expression observed in BDMs from AD and MCI patients is directly responsible for the impairment in CCL2-driven chemotaxis detected in these patients (Fig. 4.2C). Although studies in mouse models indicate that the CCR2$^+$ BDM population is the only subset of cells able to efficiently restrict Aβ deposition (Naert and Rivest, 2013), our results show that, in the context of human disease, CCR2 protein levels are decreased in AD and MCI BDMs, which may reduce cell ability to migrate to the brain and clear Aβ deposits. Despite the heterogeneity of the MCI group, which reflects the status of AD pre-clinical stage, the decrease in CCR2 expression at the cell surface in MCI patients is prominent and can potentially reflect the progression to definitive dementia. Moreover, since chemokine receptors exert a scavenging role by binding and removing chemokines from circulation and tissues (Mahad et al., 2006), the reduction of CCR2$^+$ BDMs can contribute to the increased levels of CCL2 observed in the serum of AD patients (Galimberti et al., 2006). Therefore, although a global increase in CCR2 expression at the cell surface has been reported in AD PBMCs (Reale et al., 2008; Pellicano et al., 2010), we provide the missing link regarding CCR2 expression specifically in BDMs, which does not corroborate the beneficial role observed for monocytes in AD mouse models. Concerning the less studied CXCR4/CXCL12 axis, at least one study has reported, in parallel with increased cognitive deficits, downregulation of CXCL12 and CXCR4 in Tg2576 mice (Parachikova and Cotman, 2007), which is in line with our findings of a decrease in CXCR4 surface levels in MCI patients, as well as reduced migration towards CXCL12 (Fig. 4.1D and E; Fig. 4.2D).

Deficiencies in microglia-mediated Aβ phagocytosis have also been reported in AD (Krabbe et al., 2013), suggesting that microglia lose their ability to clear Aβ deposits with age and disease. The similar ontology between monocytes, macrophages and microglia (Ginhoux et al., 2010) and the above mentioned observations gave strength to the hypothesis that circulating monocytes could fulfill the role of microglia, providing an alternative pathway for Aβ clearance (Michaud et al., 2013). However, for this process to occur efficiently, both in vascular deposition sites and the brain parenchyma, blood monocytes would have to migrate, infiltrate the brain microenvironment and differentiate into efficient phagocytes. Our results illustrate an impairment in Aβ phagocytosis by AD MDMs, which was associated with a decrease in Aβ internalization (Fig. 4.3A) and corroborates previous published results (Fiala et al., 2005). Therefore, although in AD mouse models these cells have been shown to contribute to the decrease of Aβ load in the brain, in AD patients, their ability to clear Aβ is clearly compromised. Despite the higher Aβ internalization observed in MCI patients (Fig. 4.3A and B), their cells also fail to efficiently degrade the peptide, presenting intracellular accumulation of Aβ but no co-localization with lysosomes or other acidic vesicles (Fig. 4.3A). This suggests that the observed impairment in Aβ clearance may be multifactorial and is not restricted to full-blown AD.

Several of the recently identified AD risk genes have been directly related with innate immune responses, actin dynamics and clathrin-mediated endocytosis, suggesting that they may play a role in Aβ clearance. In this context, Kleinberger and coworkers have recently showed that primary microglia isolated from *Trem2* knockout mice present reduced phagocytic ability, while inhibition of TREM2 processing by ADAM10, which resulted in reduced sTREM2 shedding, was associated with an increase in phagocytosis in BV2 microglia cells (Kleinberger et al., 2014), probably through the increase of functional TREM2 at the cell surface.

In what concerns the human disease, only one study reported elevated TREM2 mRNA levels in peripheral blood of AD patients with respect to controls (Hu et al., 2014), though this study did not include the MCI stage. Moreover, in this study, TREM2 expression was quantified in RNA extracted from blood and, therefore, cannot be directly associated with the mononuclear phagocyte population and with the phagocytosis phenotype. Since the presence of functional TREM2 at the cell surface was previously associated with increased phagocytic activity (Kleinberger et al., 2014), our results led us to hypothesize that the upregulation of TREM2 mRNA expression observed in MDMs from MCI patients compared to both Controls and AD patients (Fig. 4.4B) may help explain the high Aβ uptake (Fig. 4.3B) by MDMs. In addition, the elevated levels of TREM2 mRNA in BDMs from MCI patients (Fig. 4.4A) can constitute evidence of an early dysfunction in the precursors of the effective phagocytes. Interestingly, given the variability in the MCI group, we detected a subgroup within MCI patients that presented similar TREM2 mRNA levels to those observed in AD BDMs (Fig. 4.4A). It would be interesting to perform a translational evaluation in these patients, to clarify if the shift in TREM2 expression reflects disease progression, since lower levels of TREM2 mRNA in BDMs from MCI patients (Fig. 4.4A) can suggest a more pronounced AD pre-clinical stage, and this idea could be explored in the clinic to help disease staging. We also observed that sTREM2 levels were upregulated in the plasma of AD patients, with respect to both MCI and Controls (Fig. 4.4C), which may indicate a reduction in the availability of functional TREM2 and help explaining the limited Aβ internalization by AD MDMs.

MiR-200b-3p and miR-128-3p, which were also found to be upregulated in BDMs from AD patients (Fig. 4.5C and D), can also be implicated in the observed impairment in Aβ phagocytosis. MiR-128 inhibition was shown to improve Aβ degradation in monocytes from AD patients, while its upregulation led to a decrease in the expression of lysosomal enzymes (Tiribuzi et al., 2014). Regarding miR-200b-3p, several databases predict its binding to the beta-1,4-mannosyl-glycoprotein 4-beta-N-acetylglucosaminyltransferase (MGAT3 mRNA). According to Fiala and coworkers, downregulation of MGAT3 may be related to defective Aβ phagocytosis (Fiala et al., 2007), suggesting a link between miR-200b-3p upregulation, MGAT3 downregulation and decreased Aβ clearance.

Interestingly, we also found that, eight of the new AD susceptibility genes (CR1, BIN1, PICALM, SORL1, MS4A4A, CD33, CD2AP and CLU) (Harold et al., 2009; Lambert et al., 2009b; Hollingworth et al., 2011a) are predicted targets of at least one miRNA shown to be differentially expressed (Supplementary Material, Table S4.2) and can potentially be regulated by miR-154-5p, -27b-3p, -200b-3p, -128-3p and -155-5p. This further strengthens the idea that miRNA deregulation can be a major player in sporadic AD. Moreover, the expression of the 5 miRNAs found to be upregulated in AD is significantly different from MCI patients (Fig. 4.5A-D and I), suggesting that measuring these miRNAs in the pre-clinical AD stage could benefit the clinicians, helping in the staging of dementia.

We have previously studied the role of miR-155-5p in different neuroinflammatory contexts and observed that overexpression of this miRNA in microglia exposed to LPS (Cardoso et al., 2012) or Aβ fibrils (Guedes et al., 2014) is associated with the classical M1 activation phenotype. In the present study only miR-155-5p was differentially expressed between the three experimental groups. Although no significant differences were found in the expression of IL-6 and TNF-α (Supplementary Material, Fig. S4.1A and B), miR-155-5p upregulation in AD patients (Fig. 4.5I) support the current belief that BDMs from AD patients tend towards a M1 phenotype. This finding further correlates with the observed decrease in Aβ phagocytosis, which has also been associated with the M1 activation state.

Overall, this work point towards a systemic dysfunction of the innate immune response mechanisms in AD, encompassing two essential immune cell functions, chemotaxis and phagocytosis. Nevertheless, the availability of BDMs renders these cells promising cellular targets for AD treatment and efforts should be made to fully disclosure the events responsible for the observed impairments. Considering the potential of miRNAs as biomarkers and molecular targets of disease, we believe that this study also contributes to shed light into the molecular mechanisms behind BDM and MDM dysfunction and opens new miRNA-based avenues for diagnosis and therapeutics in AD.

4.5. *Supplementary Material*

Table S4.1 | MiRNAs quantified by PCR arrays using Pick-&-Mix microRNA PCR Panels.

hsa-let-7a	hsa-miR-302b	hsa-miR-154-5p
hsa-let-7b	hsa-miR-519c-3p	hsa-miR-185
hsa-let-7c	hsa-miR-302c	hsa-miR-204
hsa-let-7d	hsa-miR-372	hsa-miR-212
hsa-let-7e	hsa-miR-373	hsa-miR-328
hsa-let-7f	hsa-miR-520d-3p	hsa-miR-335
hsa-let-7g	hsa-miR-520e	hsa-miR-421
hsa-let-7i	hsa-miR-410	hsa-miR-425
hsa-miR-17	hsa-miR-374a	hsa-miR-494
hsa-miR-20a	hsa-miR-374b	hsa-miR-495
hsa-miR-20b	hsa-miR-543	hsa-miR-506
hsa-miR-23a-3p	hsa-miR-9	hsa-miR-542-5p
hsa-miR-23b	hsa-miR-98	hsa-miR-599
hsa-miR-340	hsa-miR-106a	hsa-miR-873
hsa-miR-519d	hsa-miR-106b	hsa-miR-519c-3p
hsa-miR-93	hsa-miR-27a	hsa-miR-195
hsa-miR-125a-5p	hsa-miR-27b-3p	hsa-miR-26b
hsa-miR-125b	hsa-miR-7	hsa-miR-137
hsa-miR-128-3p	hsa-miR-18a	hsa-miR-155-5p
hsa-miR-98	hsa-miR-18b	hsa-miR-203
hsa-miR-144	hsa-miR-22	hsa-miR-132
hsa-miR-181a	hsa-miR-24	hsa-miR-126
hsa-miR-181b	hsa-miR-33a	hsa-miR-187
hsa-miR-181c	hsa-miR-33b	hsa-miR-200a
hsa-miR-181d	hsa-miR-124	hsa-miR-200b-3p
hsa-miR-19a	hsa-miR-140-5p	hsa-miR-200c
hsa-miR-19b	hsa-miR-146a	hsa-miR-320a
hsa-miR-21	hsa-miR-146b-5p	hsa-miR-320b
hsa-miR-211	hsa-miR-149	hsa-miR-29a
hsa-miR-302a	hsa-miR-150	hsa-miR-29b

Table S4.2 | AD risk genes predicted to be regulated by immune-related miRNAs differentially expressed in AD patients.

The 4 algorithms available in miRWalk used to perform this analysis were DIANA mT, miRanda, miRWalk and TargetScan.

miRNA	**154-5p**	**27b-3p**	**200b-3p**	**128-3p**	**155-5p**
CR1	🟥	🟩		🟨	
BIN1			🟥		
PICALM	🟩		🟥		🟩
SORL1		🟧	🟥	🟧	🟧
MS4A4A		🟩		🟨	🟧
CD33	🟥	🟩			🟩
CD2AP	🟩	🟩	🟩	🟨	
CLU			🟥	🟥	

🟩	4 databases
🟨	3 databases
🟧	2 databases
🟥	1 databases

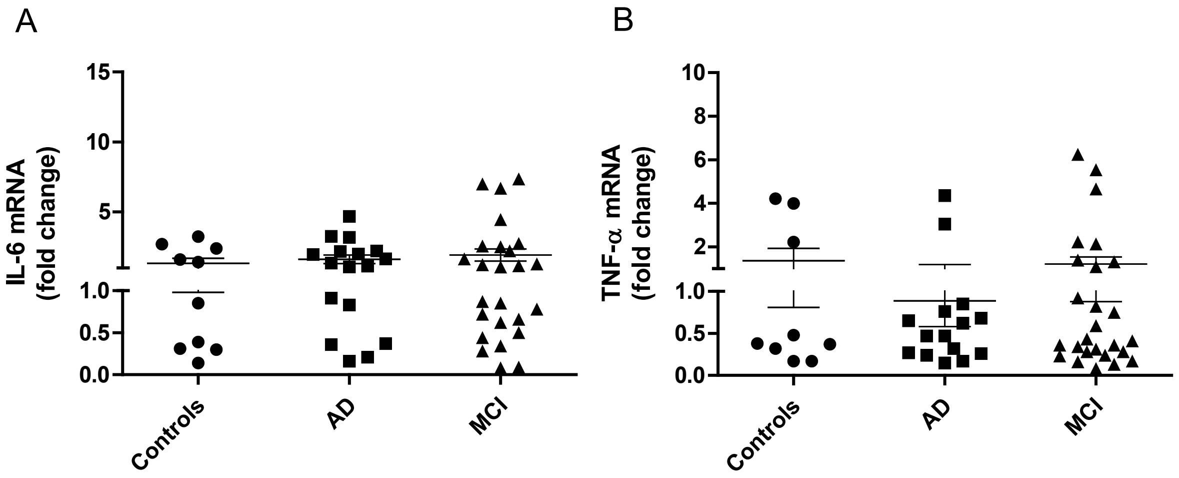

Figure S4.1 | IL-6 and TNF-α mRNA levels in BDMs of AD and MCI patients.

The levels of IL-6 (**A**) and TNF-α (**B**) mRNA were quantified by qRT-PCR in Controls, AD and MCI patients following CD14$^+$ BDM isolation. Results are expressed as mRNA fold change with respect to the mean of control subjects and are representative of at least $n = 10$ per group (One-way ANOVA $P = 0.65$ and $P = 0.73$ for IL-6 and TNF-α, respectively).

| CHAPTER 5

Ex vivo ***modulation of miR-23a in bone-marrow-derived monocytes injected in 5XFAD mice decreases vascular amyloid beta***

Guedes, J., Sorensen, E., Hickman, S., et al. *Ex vivo* modulation of miR-23a in bone-marrow-derived monocytes injected in 5XFAD mice decreases vascular amyloid beta (manuscript in preparation)

Abstract

MiRNAs are emerging as important and promising molecular targets for therapeutic interventions in central nervous system (CNS) disorders, including Alzheimer's disease (AD), due to their ability to modulate molecular pathways and shape fundamental cellular events. These features are particularly relevant regarding local and systemic immune responses triggered upon neurodegeneration, which have been recently suggested to play a major role in AD. Although the function of peripheral mononuclear monocytes infiltrating the CNS remains to be fully clarified in the context of this disease, it has been proposed that these cells contribute to improve cognitive deficits in AD mouse models by decreasing specific amyloid β (Aβ) deposits. Moreover, the chemokine receptor CCR2 has proven to be critical for the migration of these cells to the AD brain, also contributing to the clearance of vascular Aβ deposits.

In this work, we evaluated the effect of miR-23a-3p inhibition in bone marrow (BM)-derived monocytes on the expression of the chemokine receptor CCR2. We further investigated if the intravenous injection of these cells into 5XFAD mice, following *ex vivo* inhibition of miR-23a-3p expression, could reduce Aβ deposition in the mice brain. By employing Delivery Liposome System (DLS) cationic liposomes complexed with miR-23a-3p anti-sense oligonucleotides, increased levels of CCR2 mRNA were observed. Moreover, we demonstrated that intravenously injected BM-derived monocytes were able to infiltrate the brain of 5XFAD mice, as assessed by two-photon microscopy and flow cytometry. Importantly, stereology analysis, corroborated by ELISA, revealed that the *ex vivo* inhibition of miR-23a-3p in BM-derived monocytes, before their intravenous injection into 5XFAD mice, is sufficient to decrease the deposition of vascular Aβ, as well as the levels of soluble forms of this peptide. We have also observed that injection of BM-derived monocytes led to an efficient modulation of the immune milieu in 5XFAD brains, by decreasing the expression of activation markers typical of the M1 phenotype, such as interleukin 6 (IL-6). Overall, our findings provide and corroborate evidence on the importance of $CCR2^+$ monocytes for vascular Aβ clearance and suggest that miRNA modulation in peripheral mononuclear phagocytes holds a huge therapeutic potential and may, therefore, constitute a future gene therapy approach for AD.

5.1. Introduction

Alzheimer's disease (AD) is an irreversible and progressive neurodegenerative disorder with currently no effective therapeutic or preventive strategies. Memory loss and mental disabilities result from neuronal damage caused by the accumulation of neurotoxic factors, such as misfolded and aggregated proteins and inflammatory mediators. In the normal brain, amyloid β (Aβ) is produced and degraded at a homeostatic equilibrium, maintained by the action of microglia cells, which eliminate Aβ through phagocytosis and proteolytic degradation. However, in sporadic AD, these mechanisms are inefficient (Mawuenyega et al., 2010) and increasing amounts of soluble and insoluble Aβ peptides, especially $Aβ_{1-42}$, accumulate in extracellular deposits giving origin to the main AD hallmark, the Aβ plaques. Emerging evidence also suggests that neuroinflammation plays a crucial role in AD (Heneka et al., 2015). In this regard, recent epidemiological genome and epigenome-wide association studies (GWAS and EWAS) have implicated immune-related genes as genetic risk factors for the disease (Hollingworth et al., 2011a; Naj et al., 2011; Guerreiro et al., 2013; De Jager et al., 2014). This group of genes includes TREM2 and CD33, both membrane receptors important for Aβ uptake (Bradshaw et al., 2013; Kleinberger et al., 2014). In addition to an age-dependent decline in microglia function, accumulation of inflammatory cytokines resulting from Aβ-activated microglia has also been shown to impair their phagocytic ability (Hickman et al., 2008; Krabbe et al., 2013), contributing to Aβ accumulation.

The clearance of amyloidogenic species has also been attributed to other cells of the mononuclear phagocyte system, including bone-marrow (BM)-derived monocytes (Lebson et al., 2010; Koronyo et al., 2015). Although for many years studies with BM-irradiated mice shadowed the hypothesis of BM-derived monocytes being able to infiltrate the AD brain (Malm et al., 2005; Simard et al., 2006; Mildner et al., 2011), it is now accepted that these cells modulate Aβ deposition in a chemokine receptor 2 (CCR2)-dependent manner, at least in specific sites, such as walls of brain vessels. In 2007, our group showed that ablation of CCR2 in early Tg2576 mice increased Aβ levels in the brain and the deposit of perivascular Aβ (El Khoury et al., 2007). This result was later corroborated by Mildner and Naert and Rivest, who did not report differences in plaque pathology, although CCR2 ablation amplified vascular Aβ deposition (Mildner et al., 2011) and increased the levels of Aβ oligomers (Naert and Rivest, 2011). Importantly, transplantation of CCR2 competent cells into $APP_{Swe}/PS1/CCR2^{-/-}$ restored cognitive functions in Tg2576 mice (Naert and Rivest, 2012). Given the ability of peripheral myeloid cells to potentially migrate to the AD brain and the easier access to these cells when compared to microglia, they could serve as therapeutic targets or vehicles for central nervous system (CNS) diseases (Lebson et al., 2010). Importantly, in addition to presenting ontological similarities with microglia (Ginhoux et al., 2010), monocytes were found, among all immune cell subtypes, to be specifically implicated in AD, as evidenced from a very recent study revealing the presence of increased monocyte-specific eQTLs in AD variants (Raj et al., 2014).

Since the AD cases linked to genetic heritability account for only 1% of all AD cases, it is plausible to assume that at least part of AD sporadic cases are linked to other factors, such as epigenetic events. MiRNAs are small RNA molecules that, by regulating gene expression at a post-transcriptional level, can provide epigenetic switches to control linage-specific phenotypes. A specific miRNA signature was recently shown to be useful to distinguish microglia from other myeloid cells (Butovsky et al., 2014). In addition, inflammatory miRNAs, such as miR-155, have been found to be early deregulated in AD (Guedes et al., 2014). Finally, and summing to their potential as AD biomarkers (Satoh et al., 2015), miRNAs have recently emerged as therapeutic targets for CNS disorders (Ponomarev et al., 2011; Costa et al., 2015), including AD (Zhang et al., 2014). In this regard, a very recent study showed that the peripheral injection of miR-155 anti-sense oligonucleotides in SOD1 mice prolonged their survival by derepressing microglial miR-155-target genes (Butovsky et al., 2015). These gene therapy strategies, although in their infancy, have proved the potential of using nucleic acid anti-miRNAs as disease modulators.

In this work, we aimed to demonstrate that BM-derived monocytes are able to reach the brain parenchyma of 5XFAD mice in the absence of irradiation. We also investigated if *ex vivo* miR-23a-3p inhibition in these cells could lead to the increase in mRNA CCR2 expression and to the amelioration of AD pathological hallmarks, following their intravenous injection into 5XFAD mice. Finally, we evaluated the influence of injected BM-derived monocytes on the inflammatory brain environment of 5XFAD mice.

5.2. *Methods*

5.2.1. *Animals*

Transgenic mice with five familial AD (FAD) mutations (5XFAD) were purchased from The Jackson Laboratories (Bar Harbor, USA) and then bread and maintained in the animal care facilities at Massachusetts General Hospital. 5XFAD mice overexpress the mutant human APP (695) with the Swedish (K670N, M671L), Florida (I716V) and London (V717I) FAD mutations, along with the human PS1 harboring two mutations, M146L and L268V. 5XFAD mice were injected with BM-derived monocytes from *Cx3cr1*$^{\text{gfp/+}}$*Ccr2*$^{\text{rfp/+}}$ mice at 3 months of age and maintained in quarantine during the time of the experiments, being monitored for clinical conditions.

Cx3Cr1-GFP mice were a generous gift from Dan Littman (New York University, New York) and *Ccr2*-RFP mice were purchased from The Jackson Laboratories (strain B6.129(Cg)-*Ccr2*$^{tm2.1Ifc}$, stock #01758; Bar Harbor, USA). These mice were bred and maintained in the animal care facilities at Massachusetts General Hospital. In the generated heterozygous

Cx3cr1$^{gfp/+}$*Ccr2*$^{rfp/+}$ mice, one allele of the *Cx3cr1* gene was replaced by Green Fluorescent Protein (GFP) reporter gene (Jung et al., 2000a) and one allele of *Ccr2* was substituted by Red Fluorescent Protein (RFP) reporter gene (Saederup et al., 2010), preserving the function of the genes *Cx3cr1* and *Ccr2* in the second allele, which are located in the same chromosome. For our experiments, only the F1 het/het mice were used and identified by genotyping pups at the time of weaning. In *Cx3cr1*$^{gfp/+}$*Ccr2*$^{rfp/+}$ mice, monocyte populations are green and red and were identified by flow cytometry. *Cx3cr1*$^{gfp/+}$*Ccr2*$^{rfp/+}$ mice were used at ages ranging from 3-5 months and euthanized according to approved institutional procedures for the isolation of BM-derived monocytes.

All mice used in this study were maintained in a C57BL5 background and all the employed protocols were approved by the Massachusetts General Hospital Institutional Animal Care and Use Committee and met US National Institutes of Health guidelines for the humane care of animals.

5.2.2. Isolation and adoptive transfer of BM-derived monocytes

BM-derived monocytes were isolated from femurs and tibias of *Cx3cr1*$^{gfp/+}$*Ccr2*$^{rfp/+}$ mice using magnetic-activated cell sorting (MACS) and negative selection. Briefly, mice were euthanized and the lower limbs were removed, followed by detachment of the femurs and tibias. Cleaning of the bones was achieved by removing the muscle and tendons and BM total cells were flushed out with cold Hank's Balanced Salt Solution (HBSS; Mediatech, Inc., USA). BM total cell suspension was passed through a 70 µm cell strainer (Fisher Scientific, USA) and, after washing, red blood cells were lysed through incubation with 1 mL of RBC Lysis Buffer (Sigma, USA) per mouse for 2 min. A 1:10 dilution with RPMI-1640 (Gibco, Life Technologies, USA), supplemented with 10% heat inactivated fetal bovine serum (FBS; Gibco, Life Technologies, USA), was performed and cells were counted to determine the yield of BM total cells. Isolation of BM-derived monocytes was performed using the Monocyte Isolation Kit (BM) mouse (Miltenyi Biotec, Germany), according to the instructions of the manufacturer. For magnetic labeling, cell were ressuspended in beads buffer [Phosphate-buffered saline – PBS (Gibco, Life Technologies, USA) – 0.5% bovine serum albumin – BSA (Sigma, USA) – 2 mM ethylenediamine tetraacetic acid–EDTA (Sigma, USA)], blocked with FcR Blocking Reagent and labeled with Monocyte Biotin-Antibody Cocktail for 10 min at 4°C. After washing, cells were incubated with Anti-Biotin MicroBeads (10 min, 4°C) and applied onto LS columns. The flow-through containing unlabeled cells (enriched monocytes) was collected and GFP and RFP signals were immediately detected in a BD Accuri™ C6 (BD Biosciences, USA) to assess the purity of the isolated BM-derived monocytes, which was found to be 95%. For CD115 labeling, the Monoclonal Anti-mouse M-CSFR-APC (R&D Systems, USA) was used (1:1000) after blocking with TruStain fcX™ (anti-mouse CD16/32) Antibody.

Following isolation, BM-derived monocytes (1.5 × 10^6 *per* mouse) were injected into 3 months old (mo) 5XFAD mice via the tail vein (i.v.). Mice were sacrificed 48 h following injection, to evaluate monocyte infiltration into the brain, and 1 month following injection, to assess the effect of miR-23a-3p modulation in the injected BM-derived monocytes.

5.2.3. *Flow cytometry analysis of BM-derived monocyte-injected 5XFAD brain cells*

Flow cytometry was employed to evaluate infiltration of BM-derived monocytes in the brain of 5XFAD mice. Forty-eight hours following injection of BM-derived monocytes, 5XFAD mice were euthanized and perfused with PBS. Brains were removed and placed in a C tube (Miltenyi Biotec, Germany) with RPMI with 2 mM L-glutamine (no phenol red; Gibco, Life Technologies, USA), dispase (2 U/mL) and 0.2% collagenase type 3 (Worthington Biochemicals, USA), according to a previously established protocol (Hickman et al., 2008). Brains were processed using the gentle MACS Dissociator (Miltenyi Biotec, Germany), according to manufacturer's instructions. Briefly, three rounds of dissociation followed by incubation periods of 10 min at 37°C were performed and, after the second sequence, grade II DNase I (Roche Applied Science, USA) was added (40 U/L) and incubated for 10 additional minutes before the final dissociation round. The digestion enzymes were inactivated with PBS, 2 mM EDTA and 5% FBS, and the digested brain bits were triturated gently and passed over a 100 µm strainer (Fisher Scientific, USA). Cells were then ressuspended in a solution of 30% physiologic Percoll® (Sigma, USA) in RPMI/L-glutamine without phenol red and centrifuged at 850 g for 45 min room temperature (RT). The cell pellet was washed with PBS, ressuspended in PBS containing 0.5% BSA, and incubated with Alexa Fluor® 647 anti-mouse CD11b and Pacific Blue™ anti-mouse CD45 (Biolegend, USA) antibodies (1:100) for 30 min at 4°C. Cells were analyzed in a BD FACS Aria II (BD Biosciences, USA) and $CD11b^+CD45^+$ cells were gated in order to improve detection of GFP and RFP signals.

5.2.4. *Intravital microscopy*

To evaluate infiltration of BM-derived monocyte in the brain of 5XFAD, intravital microscopy (IVM) was performed. Twenty-four hours following cell injection, 5XFAD mice were injected intraperitonealy (i.p.) with 10 mg/kg Methoxy-X04 (MX04) Neuroptix, USA) (to label Aβ deposits) and a brain glass window surgery was performed 24 h later. To achieve surgical anesthesia, animals were injected i.p. with a saline solution of ketamine at 100 mg/kg and xylazine at 5 mg/kg body weight. Adequate depth of anesthesia was monitored routinely by observation of respiratory rate, as well as checking the pedal withdrawal/toe squeeze reflex withdrawal. Hair in the frontal and parietal regions of the skull was removed using #40 electrical hair clippers (Wahl, USA) and chemical depilatory cream (Nair, Churchill & Dwight Co., USA). The skin was then cleaned with ethanol solution and the subsequent surgery was performed under aseptic conditions. An injection of 2% lidocaine was given subcutaneously (s.c.) and allowed to take effect for 5 min. In order to immobilize the skull during surgery, mice were positioned on a Plexiglas stereotactic apparatus on a 37°C heating pad. A longitudinal incision was made between the occiput and the forehead. The skin was then cut in a circular manner on top of the skull, and the underlying periosteum was removed from the temporal crests using cotton-tipped wooden applicators (Medichoice, USA). Using a high speed drill with a burr tip size of 0.5 mm in diameter (FST), a 4 mm groove was etched over either the left or right parietal region of the skull. This groove was made thinner by cautious and continuous drilling of the groove until the bone flap became loose. Cold saline-soaked Surgifoam (Ethicon, USA) was used during the drilling process to avoid thermal injury of the cortical regions of the CNS and to clean away bone dust. Using canted needle-nosed forceps, the bone flap was separated from the dura mater underneath. After removal of the bone flap, the dura mater was continuously kept moist with physiological saline. The window was then sealed by adhering a 5 mm cover glass to the bone using a histocompatible cyanoacrylate tissue glue. In addition, a metal bar was glued anterior to the coverslip. The glue was allowed to dry for at least 30 min. In order to delineate patent vessels, QTracker655 (Life Technologies, USA) was injected retro-orbitally. The mice were then attached via the metal bar to a custom-built microscopy platform for imaging, while still under anesthesia. Z-stacks were imaged using a Ultima IV Multiphoton mycroscope (Bruker, USA) acquired using PrairieView Software and analyzed using Imaris (BitPlane).

5.2.5. Transfection of BM-derived monocytes

Delivery of anti-miR-23a-3p locked nucleic acids (LNA) oligonucleotides (anti-23a-3p; Exiqon, Denmark) or control LNA oligonucleotides (oligo control; Exiqon, Denmark) to BM-derived monocytes was achieved through complexation with Delivery Liposome System (DLS) cationic liposomes. DLS liposomes are composed of dioctadecylamidoglycylspermidine (DOGS) and 1,2-dioleoyl-sn-glycero-3-phosphoethanolamine (DOPE; Avanti Polar Lipids, USA), in a 1:1 mass ratio. DOGS was a kind gift from Prof. Bernard Lebleu (University of Montpellier, France). The stock solution of both lipids dissolved in 90% ethanol (Lavigne and Thierry, 1997) was kept at -20°C. To allow liposome formation, DLS liposomes were diluted 1:10 in H_2O and incubated for 30 min at RT. Right before cell transfection, anti-23a-3p oligonucleotides were gently mixed with DLS liposomes in a 1:19 (1 μg anti-23a-3p:19 μg DLS) mass ratio and incubated for 30 min at RT to allow lipoplex formation, through electrostactic interactions. The size of DLS liposomes and lipoplexes was measured in a Beckman Coulter N5 particle size analyzer (Beckman Coulter, USA).

Following isolation of BM-derived monocytes, cells were ressuspended in RPMI-1640 (Gibco, Life Technologies, USA) with 5% FBS in polypropylene tubes and incubated for 2 h at 37°C with the necessary amount of lipoplexes to achieve a concentration of 100 nM of anti-23a-3p. Cells were then washed and ressuspended in PBS before intravenous injection into 5XFAD mice. To determine transfection efficiency by flow cytometry, the same protocol was performed, employing anti-23a-3p oligonucleotides labeled with fluorescein isothiocyanate (FITC). In addition, the efficiency of miR-23a-3p knock-down was evaluated by quantifying miR-23a-3p expression through qRT-PCR.

5.2.6. *Immunohistochemistry*

5XFAD mice were sacrificed one month post-injection, at the age of 4 months. The animals were euthanized and perfused with PBS. The brains were removed and the right hemisphere was fixed in 4% paraformaldehyde (PFA) overnight and then transferred to a solution of 30% sucrose in PBS for cryoprotection. Coronal sections from the end of the olfactory bulb to the end of the hippocampus were cut at 50 μm on a cryostat and collected in PBS with azide. Free-floating immunohistochemistry protocols were employed to quantify plaque pathology using stereology and to perform microglia/monocyte labeling. To accomplish Aβ visible staining, brain slices were washed with PBS and endogenous peroxidase activity was quenched upon incubation with phenylhydrazine (Sigma, USA) for 30 min at 37°C. Following washing with PBS, sections were blocked and permeabilized with 10% normal goat serum (NGS; Gibco, Life Technologies, USA) 0.1% Triton X-100 (Sigma, USA) in PBS (blocking solution) for 1 h at RT and then incubated with the primary anti-Aβ antibody 6E10 (Convance, USA) 1:1000, in the same blocking solution, at 4°C overnight (o.n.) under constant agitation. On the next day, sections were washed with PBS and incubated with the secondary biotinylated antibody anti-mouse IgG 1:200 in blocking solution for 2 h at RT also under agitation. Following another washing step with PBS, bound antibodies were visualized using the VECTASTAIN® ABC kit, according to the instructions of the manufacturer and 3,3'-diaminobenzidine tetrahydrochloride (DAB metal concentrate; Pierce, Fisher Scientific, USA) was used as substrate. After washing with PBS, the brain sections were mounted onto microscope slides and dried o.n. at RT, followed by dehydration with an ethanol gradient and xylene. Slides were then covered with Eukitt® mounting medium (Sigma, USA) and a microscope coverslip. Brain sections were visualized in an Axio Imager 2 microscope (Carl Zeiss, Germany) equipped with ×5, ×20 and ×40 objectives and employing the ZEN Blue software (Carl Zeiss, Germany).

For IBA and CD45 fluorescence co-labeling, rabbit anti-Iba1 (Wako Pure Chemical Industries, Ltd., Japan) and rat anti-mouse CD45 (AbD Serotec, UK) antibodies were used. Briefly, sections were washed with PBS, permeabilized with PBS and 0.5% Triton X-100 for 30 min and blocked with PBS, 0.1% Triton X-100 and 10% NGS for 1 h at RT. Primary antibodies were incubated o.n. in PBS, 0.25% NSG (IBA-1 1:1000 and CD45 1:200) at 4°C under agitation and, on the next day, sections were washed and then incubated with the necessary secondary antibodies: anti-rabbit Alexa Fluor® 488 and anti-rat Alexa Fluor®567 (1:1000; Life Technologies, USA) for 2 h at RT, also under agitation. Aβ plaque labeling was accomplished using a solution of 1 μM MX04 (Tocris Bioscience, UK) diluted in PBS, which was prepared from a 100 μM stock solution of MX04 in 40% ethanol (dissolved at 60°C). Sections were incubated with MX04 for 10 min in the dark and at RT (under agitation). After washed several times with PBS, the brain sections were mounted onto microscope slides and visualized in a 710 LSM confocal microscope, equipped with ×20 and ×63 objectives, employing the Zen Black software.

5.2.7. *Stereology*

For each animal, 16 sections, distant in 300 μm, were analyzed using stereology, following a random choice of brain slices. A code letter was attributed to each animal to ensure blinding of the investigator performing the stereology analysis. Unbiased stereology estimation of Aβ load was performed as previously described (Heggland et al., 2015) with some modifications, using the commercial software Stereo Investigator (MBF Bioscience, USA). Briefly, following Aβ labeling, sections were visualized under an Axio Imager 2 (Carl Zeiss, Germany) and the regions of interest (ROIs) were identified in each section: cortex, hippocampus and subiculum. Dense and difuse Aβ plaques and vascular Aβ were counted in a sampling grid of 350 × 350 μm, using a counting frame of 200 × 200 μm and a grid point spacing of 250 μm (64 points per counting frame; Supplementary Material, Fig. S5.2). The same parameters were used for all ROIs in all animals and a 0.33 area sampling fraction was achieved.

5.2.8. *$A\beta_{1-42}$ ELISA*

Following brain harvesting, the two hemispheres from each injected 5XFAD mouse were separated and the left hemisphere was snapped-frozen for RNA and protein analysis. Cortex punches (4 mm^2) were used for $A\beta_{1-42}$ quantification in the soluble and insoluble protein fractions. Protein was extracted from each fraction by diluting the punches in RIPA buffer (50 mM NaCl, 50 mM EDTA, 1% Triton X-100) with 20% of a protease inhibitor cocktail (Roche Applied Science, USA), incubating the brain tissue for 20 min on ice and performing a 1:1 dilution with RIPA. Brain extracts were centrifuged at 1000 g, for 25 min at 4°C The supernatant was collected (soluble fraction) and the pellet was diluted in Tris HCl 25 mM 2% sodium dodecyl sulfate (SDS; Sigma, USA), followed by sonication (insoluble fraction). Protein content was determined using the Bio-Rad Dc protein assay (Bio-Rad, USA). Ten milligrams of protein were used to quantify $A\beta_{1-42}$ using the amyloid beta 42 ELISA Kit, Human

(Invitrogen, USA), according to the instructions of the manufacturer. Briefly, before pipetting the samples to the antibody-coated 96-well plate, protein extracts were appropriately diluted with the protein extraction buffer and Aβ_{1-42} standards were prepared by diluting recombinant Aβ_{1-42}. Samples and standards were incubated o.n. at 4°C with the Hu Aβ 42 Detection Antibody solution, followed by washing and incubation with the anti-rabbit IgG HRP Working Solution, for 30 min at RT. After addition of tetramethylbenzidine for 20 min in the dark, the development reaction was stopped and the optical density was determined at 450 nm, using a SpectraMax Gemini EM fluorimeter (Molecular Devices, USA). The appropriate chromogen blanks were performed and taken into consideration when calculating Aβ_{1-42} concentrations.

5.2.9. *RNA extraction and qRT-PCR*

Total RNA, including small RNA species, was extracted from the cortex of the left hemisphere of each injected 5XFAD and from transfected BM-derived monocytes isolated from *Cx3cr1*$^{gfp/+}$*Ccr2*$^{rfp/+}$ using the miRCURY Isolation Kit for Cells (Exiqon, Denmark), according to the recommendations of the manufacturer for tissue and cultured cells, respectively. Briefly, after tissue homogenization and cell lysis, the RNA was absorbed into a silica column and washed 3 times followed by elution with the recommended buffer. After quantification, cDNA transcription for miRNA detection was accomplished using 20 ng of total RNA and the Universal cDNA Synthesis Kit II (Exiqon, Denmark). cDNA was diluted 40× with RNase free-water before qRT-PCR quantification of miR-23a-3p, -124, -145 and -155, employing pre-designed LNA primers (Exiqon, Denmark). Quantitative PCR was performed in duplicates in a LightCycler® 480 II (for miR-23a-3p quantification; Roche Life Science, USA) and StepOne™ Plus device (for miR-124, -145 and -155; Applied Biosystems, USA) using the miRCURY LNA™ Universal RT microRNA PCR system (Exiqon, Denmark). SNORD44 was used as reference gene.

For quantification of mRNA expression, 1 µg of total RNA was transcribed using the iScript™ cDNA Synthesis Kit (for CCR2 quantification; Bio-Rad, USA) and the NZY First-Strand cDNA Synthesis Kit (for cytokine quantification; Nzytech, Portugal). cDNA was diluted 10× before preparation of the qRT-PCR reactions. The relative expression of cytokines was quantified using the SsoAdvanced™ Universal SYBR® Green Supermix (Bio-Rad, USA) and pre-designed primers from Qiagen (Germany) in a StepOne™ Plus device. For CCR2 mRNA quantification, the LightCycler®480 SYBR Green I Master was used, together with the following mouse CCR2 primers: ATCCACGGCATACTATCAACATC (forward) and CAAGGCTCACCATCATCGTAG (reverse). HPRT and GAPDH genes were used as reference genes [HPRT primer (Qiagen, Germany), GAPDH primer sequence GGCAAATTCAACGGCACAGT (forward) and AGATGGTGATGGGCTTCCC (reverse)]. In these case, all reactions were performed in duplicate in a LightCycler® 480.

5.2.10. *Statistical analysis*

All data are expressed as mean ± SEM and were analyzed for statistical significance using One-way ANOVA followed by Tukey's Multiple Comparison post hoc test, except in the case of stereology analysis of Aβ load, for which Two-way ANOVA was employed. Differences were considered statistically significant with a *P* value < 0.05, 0.01 and 0.001 indicated by * or $^{\#}$, as described in the figure legends. All tests were two-tailed and the data were analyzed using the GraphPad Prism 6 software.

5.3. *Results*

5.3.1. *BM-derived monocytes infiltrate into the brain of 5XFAD mice*

To investigate if peripheral mononuclear phagocytes could infiltrate into the brain of 5XFAD mice in the absence of irradiation, BM-derived monocytes, isolated from 3 mo *Cx3cr1*$^{\mathrm{gfp/+}}$*Ccr*2$^{\mathrm{rfp/+}}$ mice, were injected into the tail vein of age-matched 5XFAD mice. *Cx3cr1*$^{\mathrm{gfp/+}}$*Ccr*2$^{\mathrm{rfp/+}}$ mice present a GFP and a RFP knock-in in one allele of the *Cx3cr1* and *Ccr2* genes, respectively (Saederup et al., 2010). Although CX3CR1 and CCR2 expression is decreased in BM-derived monocytes isolated from *Cx3cr1*$^{\mathrm{gfp/+}}$*Ccr*2$^{\mathrm{rfp/+}}$ mice, with respect to homozygous mice expressing both alleles of the genes (data not shown), the exclusive use of heterozygous mice of this strain allowed to maintain the function of CX3CR1 and CCR2, two chemokine receptors expressed in monocytes and responsible for the regulation of chemotaxis processes. As blood monocyte subsets in mice comprise Ly6C$^{\mathrm{high}}$CCR2^{+}CX3CR1$^{\mathrm{mid}}$CD62L^{+}CD43$^{\mathrm{low}}$ and Ly6C$^{\mathrm{low}}$CCR2^{-}CX3CR1$^{\mathrm{high}}$CD62L^{-}CD43$^{\mathrm{high}}$ (Jakubzick et al., 2013), the use of the *Cx3cr1*$^{\mathrm{gfp/+}}$*Ccr*2$^{\mathrm{rfp/+}}$ mouse model allowed us to test all subsets of monocytes and follow their tissue infiltration.

We first determined which mouse tissue/organ would allow isolate monocytes with the highest yield and purity. For that purpose, *Cx3cr1*$^{\mathrm{gfp/+}}$*Ccr*2$^{\mathrm{rfp/+}}$ mice were euthanized and the BM, spleen and blood were collected and the respective cell suspensions analyzed for CD115 (universal monocyte marker), GFP and RFP markers. The total cell yields and CD115^{+}, GFP^{+} and RFP^{+} cell populations were comparable between BM and spleen samples (Supplementary Material, Fig. S5.1), suggesting that, although BM is considered an organ composed mainly of immune precursor cells, typical monocyte markers can be detected at a level similar to that found in organs with mature monocytes, such as the spleen (Swirski et al., 2009). Since the isolation of blood-circulating monocytes did not result in a good cell yield, we chose to use BM-isolated monocytes in all further experiments. As can be observed in Figure 5.1, before monocyte isolation using the MACS system, only 10% of total BM cells expressed GFP and RFP (Fig. 5.1A), while following this procedure 95% of the recovered cells were GFP and RFP positive (Fig. 5.1B) and, therefore, also expressed CX3CR1 and CCR2.

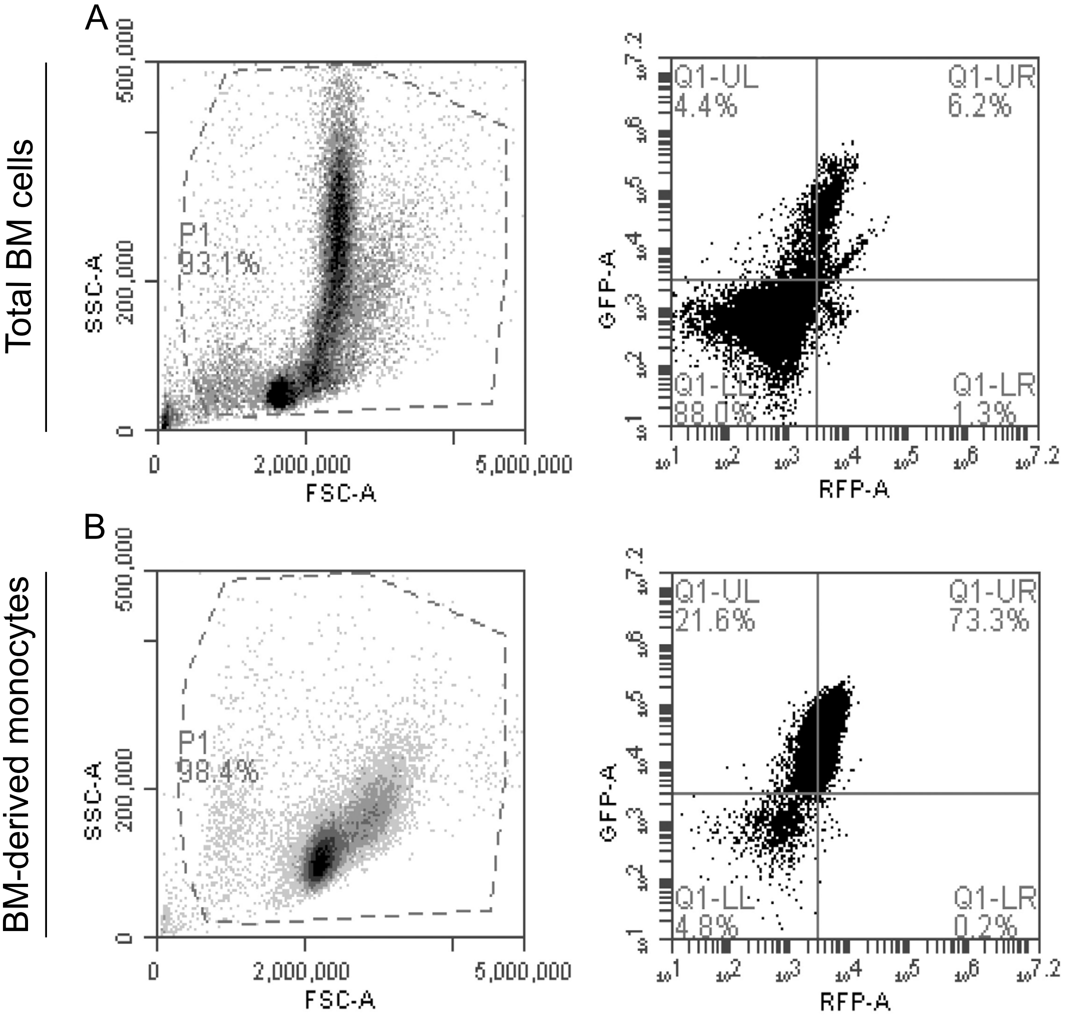

Figure 5.1 | Quantification of GFP and RFP expression in bone-marrow (BM) cells before and after magnetic-activated cell sorting (MACS).

Total BM cells were extracted from femurs and tibias of Cx3cr1$^{gfp/+}$Ccr2$^{rfp/+}$ mice by flushing the bones and BM-derived monocyte isolation was accomplished by MACS negative selection. GFP and RFP signals were assessed by flow cytometry before (**A**) and after (**B**) BM-derived monocyte isolation. Representative dot plots show that only 10% of total BM cells express GFP and/or RFP (**A**, right panel) while, after isolation, 95% of BM-derived monocytes are GFP and RFP positive (**B**, right panel), confirming the purity of the isolated cells. Results are representative of *n* = 3.

As reported by Oakley and coworkers, 5XFAD mice present Aβ plaques, the major hallmark of amyloid pathology, at the early age of 2 months (Oakley et al., 2006), thus constituting a robust and rapidly-induced mouse model of AD. In order to completely clarify the capacity of BM-derived monocytes to reach the brain in the context of AD, we intravenously injected the previously isolated GFP$^+$RFP$^+$ cells and investigated their presence in the brain of 5XFAD mice 48 h post-injection, either by flow cytometry or IVM. Flow cytometry analysis revealed that approximately 2% of brain CD11b$^+$CD45$^+$ cells, which include microglia, perivascular, choroid plexus and meningeal macrophages and corresponded to 8.7% of total brain cells (Fig. 5.2A), were GFP$^+$RFP$^+$ (Fig. 5.2B) and, therefore, migrated from the periphery. Microglia, which are characterized by a CD11b^{high}CD45^{int} profile, constituted a very distinct cell population in the upper left quadrant of the dot plot (green dots; Fig. 5.2A) and were GFP$^-$RFP$^-$ (green dots; Fig. 5.2B), while most of GFP$^+$RFP$^+$ cells were CD11b^{high}CD45^{high} (Fig. 5.2B). This result was further confirmed by IVM (Fig. 5.2C), 48 h after cell injection. Twenty-four hours before the cranial surgery, 5XFAD mice were injected with MX04 to label Aβ plaques and, although we were not able to identify blue plaques (which we observed in 5XFAD at 8 mo – data not shown), yellow cells (white arrows), corresponding to the co-localization of GFP and RFP signals, could be detected in the brain vessels and in the brain parenchyma (Fig. 5.2C), undoubtedly confirming the migration of the injected BM-derived monocytes to this organ in 5XFAD mice. This finding clearly suggests that monocytes from the periphery can play a very important role in AD pathogenesis.

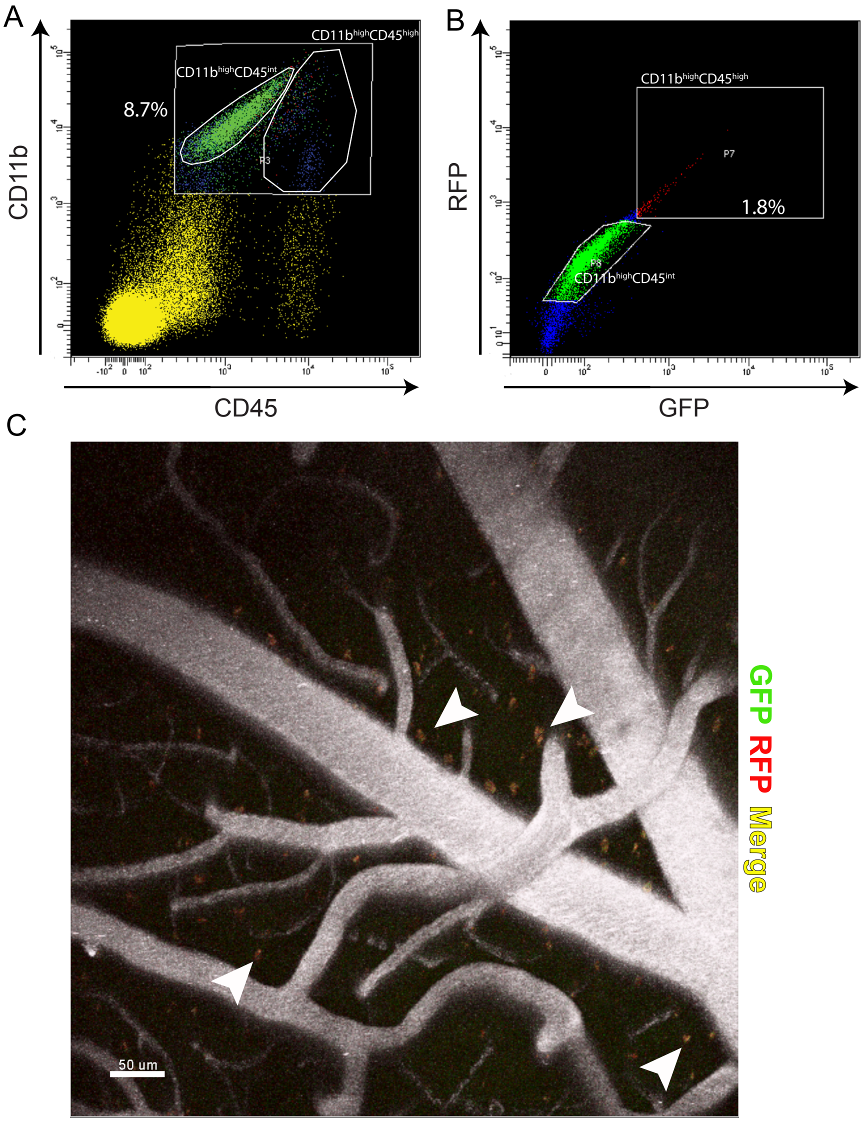
A
B
C
CD11b
CD45
RFP
GFP
CD11b^{high}CD45^{high}
CD11b^{high}CD45^{int}
8.7%
P3
CD11b^{high}CD45^{high}
P7
1.8%
P8
CD11b^{high}CD45^{int}
50 um
GFP
RFP
Merge

Figure 5.2 | Chemotaxis of monocytes into the brain of 3-months old 5XFAD mice.
BM-derived monocytes were isolated from Cx3cr1$^{gfp/+}$Ccr2$^{rfp/+}$ mice and immediately injected into the tail vein of 3 mo 5XFAD mice. Forty-eight hours following injection, brain infiltration of GFP$^+$RFP$^+$ BM-derived monocytes was assessed by flow cytometry (**A** and **B**) and intra-vital two-photon microscopy (**C**). In order to label brain vessels, QTracker655 was retro-orbitally injected during the brain glass window surgery (C). Quantification of GFP$^+$RFP$^+$ cells (**B**) in the CD11b$^+$CD45$^+$ brain population (**A**) showed that 1.8% of these cells were BM-

derived monocytes from the periphery. Orthogonal projections of two-photon microscopy Z-stacks show the co-localization of the GFP and RFP signals from BM-derived monocytes in the brain parenchyma (**C**; white arrows). Results are representative of *n* = 3 for each experiment.

5.3.2. Inhibition of miRNA-23a increases CCR2 expression in BM-derived monocytes

As previously reported, CCR2 mediates monocyte infiltration into the brain in AD mice and the lack of $CCR2^+$ monocytes has been shown to aggravate the AD phenotype (Naert and Rivest, 2013). Gene therapy approaches to restore CCR2 expression in $APP_{Swe}/PS1/CCR2^{-/-}$ BM cells were able to prevent cognitive decline in this AD mouse model (Naert and Rivest, 2012b). Importantly, we recently reported that AD patients present a decrease in $CCR2^+$ blood-derived monocytes when compared to age-matched control subjects, which was associated with impaired cell migration towards CCL2 (Guedes et al., under revision). These results suggested the hypothesis to improve CCR2 expression as a strategy to increase monocyte migration to the AD brain.

The use of miRNAs as therapeutic molecules to modify gene expression is starting to be explored in the context of CNS diseases, including those with a strong inflammatory component (Butovsky et al., 2015; Costa et al., 2015). Therefore, in this work, we decided to explore miRNA modulation as a possible strategy to increase CCR2 expression, aiming at potentiating the recruitment of monocytes to the brain. According to several miRNA prediction algorithms, miR-23a-3p is able to bind to CCR2 mRNA (Fig. 5.3C), potentially regulating its expression. Therefore, our approach to increase CCR2 levels in BM-derived monocytes isolated from $Cx3cr1^{gfp/+}Ccr2^{rfp/+}$ mice involved the inhibition of this miRNA through the *ex vivo* delivery of anti-sense LNA oligonucleotides. To achieve this purpose, we took advantage of DLS liposomes, a non-toxic cationic lipid-based delivery system which constitutes an efficient vector to deliver small oligonucleotides, to both adherent and suspension cell cultures (Trabulo et al., 2010). In order to test the capacity of DLS liposomes to deliver anti-23a-3p oligonucleotides to BM-derived monocytes, we transfected these cells, immediately following their isolation, with FITC-labeled anti-23a-3p LNA oligonucleotides, complexed with DLS liposomes at a 1:19 mass ratio. As can be observed in Figure 5.3A, flow cytometry analysis revealed that, 2 h after transfection, 99.6% of BM-derived monocytes were FITC positive, showing that anti-23a-3p oligonucleotides were efficiently internalized (Fig. 5.3A, right panel). Laser light scattering was employed to evaluate the size distribution of DLS liposomes and anti-23a-3p:DLS lipoplexes (Fig. 5.3B). As shown, both DLS liposomes and DLS lipoplexes presented two distinct populations of nanoparticles with different sizes: a less prevalent population with a mean size below 100 nm and a more prevalent population with a mean size of 270 nm for DLS liposomes and 340 nm for DLS lipoplexes (Fig. 5.3B). As expected, the size of DLS lipoplexes, which were generated through electrostatic interactions between the negatively charged anti-23a-3p oligonucleotides and the positively charged DOGS molecules, was slightly bigger than that of DLS liposomes Nevertheless, the size exhibited by the lipoplexes is suited for *ex vivo* transfection and no signs of cytotoxicity were observed following cell transfection (data not shown).

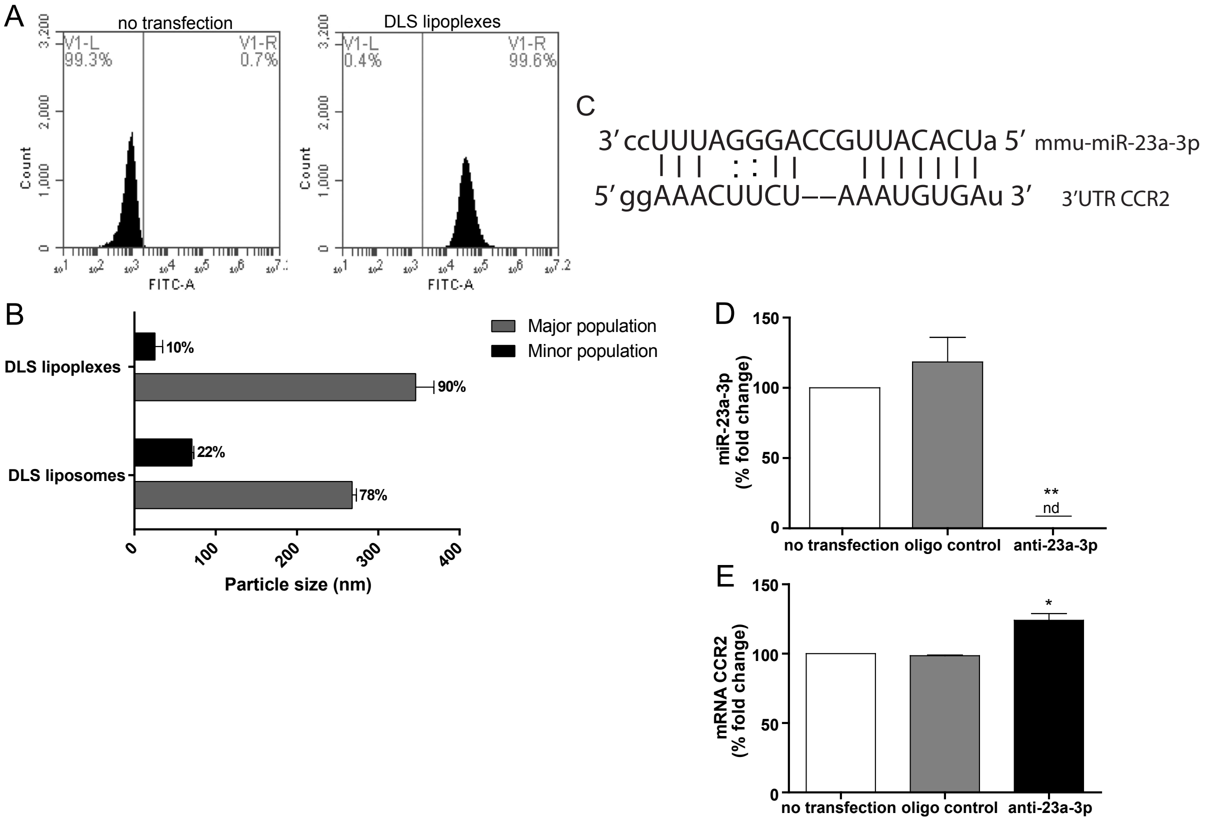

Figure 5.3 | Delivery of anti-miR-23a-3p (anti-23a-3p) mediated by the Delivery Liposome System (DLS) to BM-derived monocytes increases CCR2 mRNA levels.

Following BM-derived monocyte isolation, cells were transfected with DLS lipoplexes carrying locked nucleic acids (LNA) anti-23a-3p. Transfection efficiency was assessed by flow cytometry 2 h following the delivery of FITC-labeled anti-23a-3p oligonucleotides (**A**). Size characterization of the DLS liposomes and lipoplexes was performed by laser light scattering (**B**). Following BM-derived monocyte transfection, total RNA was extracted and miR-23a-3p and CCR2 mRNA levels were measured by qRT-PCR. DLS lipoplexes were able to decrease miR-23a-3p to undetected (*nd*) levels, with respect to cells transfected with a control oligonucleotide (oligo control) (**D**), and to increase CCR2 mRNA levels by 25% (**E**). Results are representative of $n = 2$ and are expressed as % fold change of control (non-transfected cells); * $P < 0.05$ and ** $P < 0.01$, One-way ANOVA, Tukey's post hoc test, with respect to BM-derived monocytes transfected with oligo control. (**C**) Illustration of the miR-23a-3p binding sites in the 3'UTR of CCR2 (source: miRNA.org).

In order to confirm that the intracellular delivery of anti-23a-3p oligonucleotides, observed by flow cytometry, translated into efficient release of these molecules within the cell cytoplasm and in the consequent inhibition of miR-23a-3p, its levels were measured by qRT-PCR, 2 h after transfection. It was possible to observe that, at this time point, miR-23a-3p expression was virtually undetectable in cells transfected with anti-23a-3p oligonucleotides, with respect to cells transfected with a control oligonucleotide (Fig. 5.3D), which does not bind to any known miRNA. However, since one miRNA can bind to several mRNA targets, it was also essential to assess if miR-23a-3p inhibition would result in an upregulation of CCR2 mRNA in these cells. For that purpose, CCR2 expression was evaluated in BM-derived monocytes 2 h after transfection by qRT-PCR. As shown in Figure 5.3E, an increase of 25% in CCR2 mRNA levels was observed in cells transfected with anti-23a-3p oligonucleotides when compared to cells transfected with a control oligonucleotide. Overall, these results clearly show that DLS lipoplexes are able to deliver LNA-based oligonucleotides to BM-derived monocytes leading to efficient inhibition and degradation of miR-23a-3p.

5.3.3. Injection of BM-derived monocytes into 5XFAD decreases cerebral vascular Aβ

Since miR-23a-3p inhibition was sufficient to increase CCR2 mRNA levels in BM-derived monocytes, thus suggesting that this strategy has the potential to result in a cell phenotypic change of these cells, we investigated if the injection of anti-23a-3p transfected cells into 5XFAD mice could have a positive impact on Aβ clearance in this animal model. To address this issue, we applied an experimental procedure outlined in Figure 5.4A. 5XFAD mice were injected at 3 months with BM-monocytes transfected with anti-23a-3p or a control oligonucleotide. In parallel, a third group of age-matched animals (n = 3) received a single injection of PBS. One month later, mice were sacrificed and brains collected to perform histological and biochemical analysis of Aβ deposition. An initial evaluation of Aβ staining in coronal brain slices of 5XFAD mice from the 3 experimental groups showed that, at 4 months, these animals presented heavy Aβ plaque burden in the cortex and subiculum (Fig 5.4B). The hippocampus also presented Aβ plaque deposits, more prominent in the dentate gyrus and in lower posterior region of this structure (Fig. 5.4B). Stereological analysis was performed on serial brain sections across these 3 brain regions, following immunolabeling with the anti-human monoclonal Aβ antibody (6E10). A more detailed analysis in the cortex showed that 3 different insoluble Aβ deposits could be differentiated: dense Aβ plaques (Fig. 5.4D, left panel, white arrow), diffuse Aβ plaques (Fig. 5.4D, right panel, grey arrow) and vascular Aβ deposits (Fig. 5.4C, left panel, black arrow). Therefore, these different Aβ deposits were stereologically quantified in the 3 experimental groups, as previously described (Heggland et al., 2015) with some modifications (Supplementary Material, Fig. S5.2). The injection of BM-derived monocytes into the tail vein of 5XFAD mice led to a decrease, albeit not statistically significant, in the number of dense and diffuse Aβ plaques, in both cortex and hippocampus ($P = 0.25$ and $P = 0.09$ between groups, respectively; Two-way ANOVA) (Fig. 5.4D and E, left and middle panels). This effect, which is independent of BM-monocyte transfection with the anti-23a-3p, was particularly notorious in the dentate gyrus and anterior hippocampus (Supplementary Material, Fig. S5.3A and B), while in the subiculum the number of Aβ plaques remained unchanged (Fig. 5.4E, right panel;

Supplementary Material, Fig. S5.3D). Interestingly, the specific modulation of miR-23a-3p in BM-derived monocytes caused a significant decrease in vascular Aβ ($P < 0.05$, Tukey's post hoc test), in both the cortex and hippocampus (Fig. 4E, left and middle panels), which was not observed upon injection of BM-derived monocytes transfected with the control oligonucleotides. Figure 5.4C shows representative images of these results, which further reinforce the important role of CCR2$^+$ monocytes in the cleaning of vascular Aβ deposits (El Khoury et al., 2007).

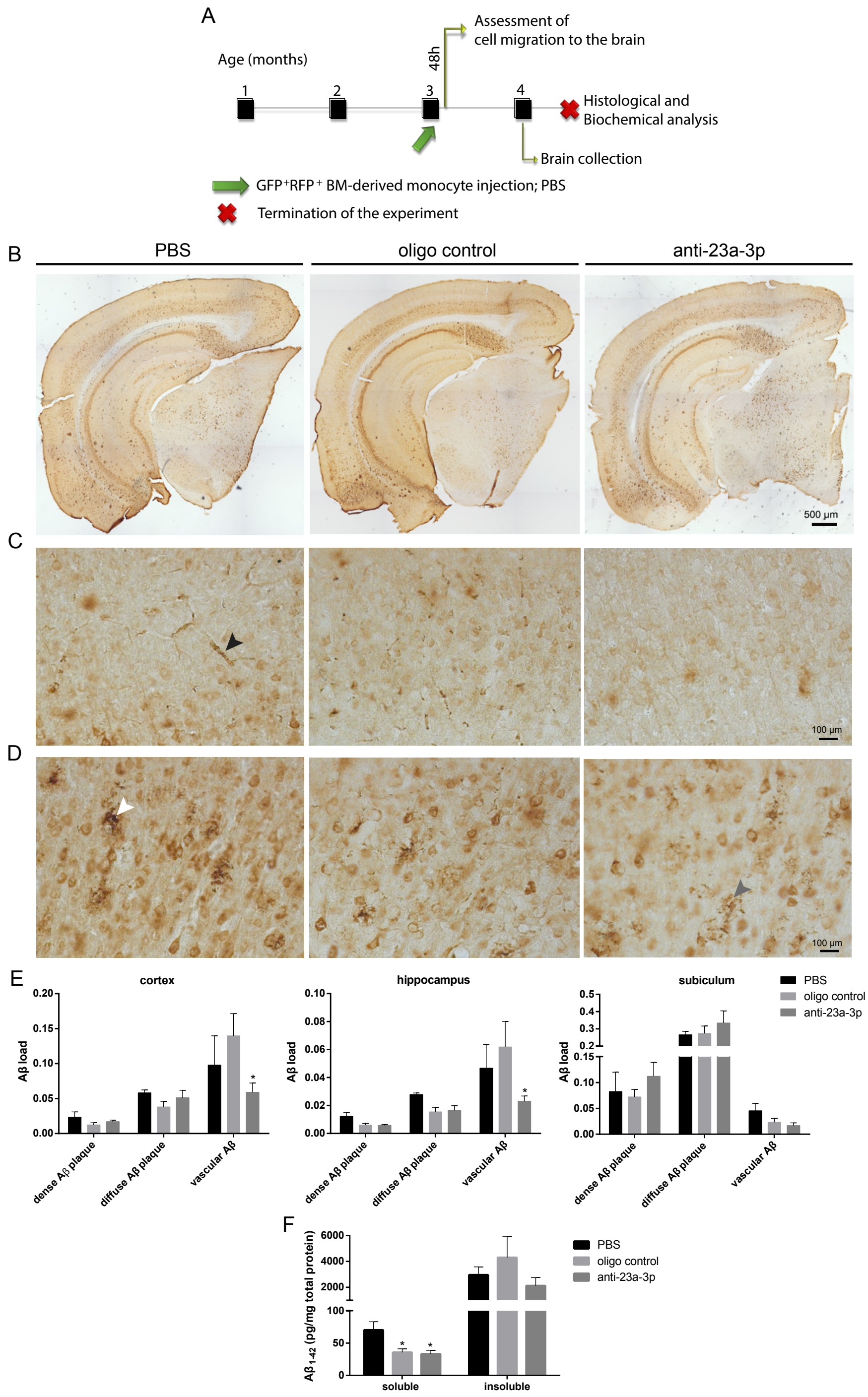

Figure 5.4 | 5XFAD mice injected with BM-derived monocytes, previously transfected with anti-23a-3p, present reduced vascular Aβ.

One month following injection of BM-derived monocytes, 5XFAD mice were sacrificed and brains were collected for immunohistochemistry and RNA and protein quantification. The right hemisphere was sliced and immunolabeled with the anti-human Aβ 6E10 antibody for stereological analysis of dense and diffuse Aβ plaques and vascular Aβ using the Stereo Investigator software. Images were taken under an Axio Imager Z2 microscope and are representative of $n = 3\text{-}5$ 5XFAD mice from each experimental group. (**A**) Schematic representation of the BM-monocyte injection experimental procedure. (**B**) Microscope images of entire slices are presented at a 5× magnification. (**C, D**) Close-up images from cortex show decreased vascular Aβ deposition (black arrow) in the brain of 5XFAD mice injected with BM-derived monocytes, previously transfected with anti-23a-3p, and a tendency towards a lower deposition of dense and diffuse Aβ plaques (white and grey arrows, respectively) (40× magnification). (**E**) Stereological quantification of the different Aβ deposits confirmed the observations inferred from the images. Results are representative of $n = 3\text{-}5$ for each animal group and are expressed as Aβ load in each region; $P = 0.25$, $P = 0.09$, $P = 0.54$ column factor for each brain region – cortex, hippocampus and subiculum, respectively and **** $P < 0.0001$ row factor for the 3 regions, Two-way ANOVA; * $P < 0.05$ Tukey's *post hoc* comparisons, with respect to 5XFAD injected with BM-derived monocytes, previously transfected with control oligonucleotides (oligo control). Soluble and insoluble cortical protein fractions were extracted from the left hemisphere and $A\beta_{1\text{-}42}$ was quantified by ELISA in each fraction. BM-derived monocyte injection decreased the amount of soluble $A\beta_{1\text{-}42}$ in the brain of 5XFAD mice, while the amount of insoluble $A\beta_{1\text{-}42}$ remained unchanged (**F**). Results are representative of $n = 3\text{-}5$ for each animal group and are expressed as pg $A\beta_{1\text{-}42}$ *per* mg of total protein; * $P < 0.05$ One-way ANOVA, Tukey's *post hoc* test, with respect to PBS-injected 5XFAD.

In addition to stereology-based quantification of Aβ plaques, the soluble and insoluble $A\beta_{1\text{-}42}$ levels in the cortical region were also determined by quantitative ELISA. Although the levels of insoluble $A\beta_{1\text{-}42}$ remained unchanged following injection of BM-derived monocytes, this approach significantly decreased soluble $A\beta_{1\text{-}42}$ by 50% (Fig. 5.4F). In this case, the specific inhibition of miR-23a-3p prior to the injection of BM-derived monocytes did not contribute to further reduce Aβ load.

5.3.4. *BM-derived monocytes cluster around Aβ plaques in injected 5XFAD mice*

Although it is described that $CCR2^+$ peripheral myeloid cells are recruited to the AD brain, where they bind to Aβ deposits (Mildner et al., 2011), once these cells are inside the CNS environment, it is difficult to effectively distinguish them from resident microglia. Until now, the only marker suggested to differentiate these two types of mononuclear phagocytes has been CD45, since resident microglia are believed to express low to intermediate levels of CD45, while peripheral monocyte-derived macrophages present a $CD45^{high}$phenotype (Prinz et al., 2011). Therefore, histological analysis of CD45 and IBA-1 markers by immunofluorescence, followed by labeling of Aβ plaques with MX04, allowed us to identify the presence of injected BM-derived monocytes around Aβ deposits in 5XFAD brains. In order to identify $CD45^+$ cells close to Aβ plaques in the cortex, we acquired confocal Z-stack images at high magnification (Fig. 5.5C, F and I, right panel). We found that 5XFAD mice injected with BM-derived monocytes, but not PBS-injected 5XFAD mice, presented $CD45^{high}$ cells around Aβ plaques (Fig. 5.5C, F and I, lower left panel). Moreover, as can also be observed in Figure 5.5, $IBA\text{-}1^+$ cells were found preferentially clustered nearby Aβ plaques and no differences in cell number or morphology were detected between the 3 experimental groups, in both cortex (Fig. 5.5A,

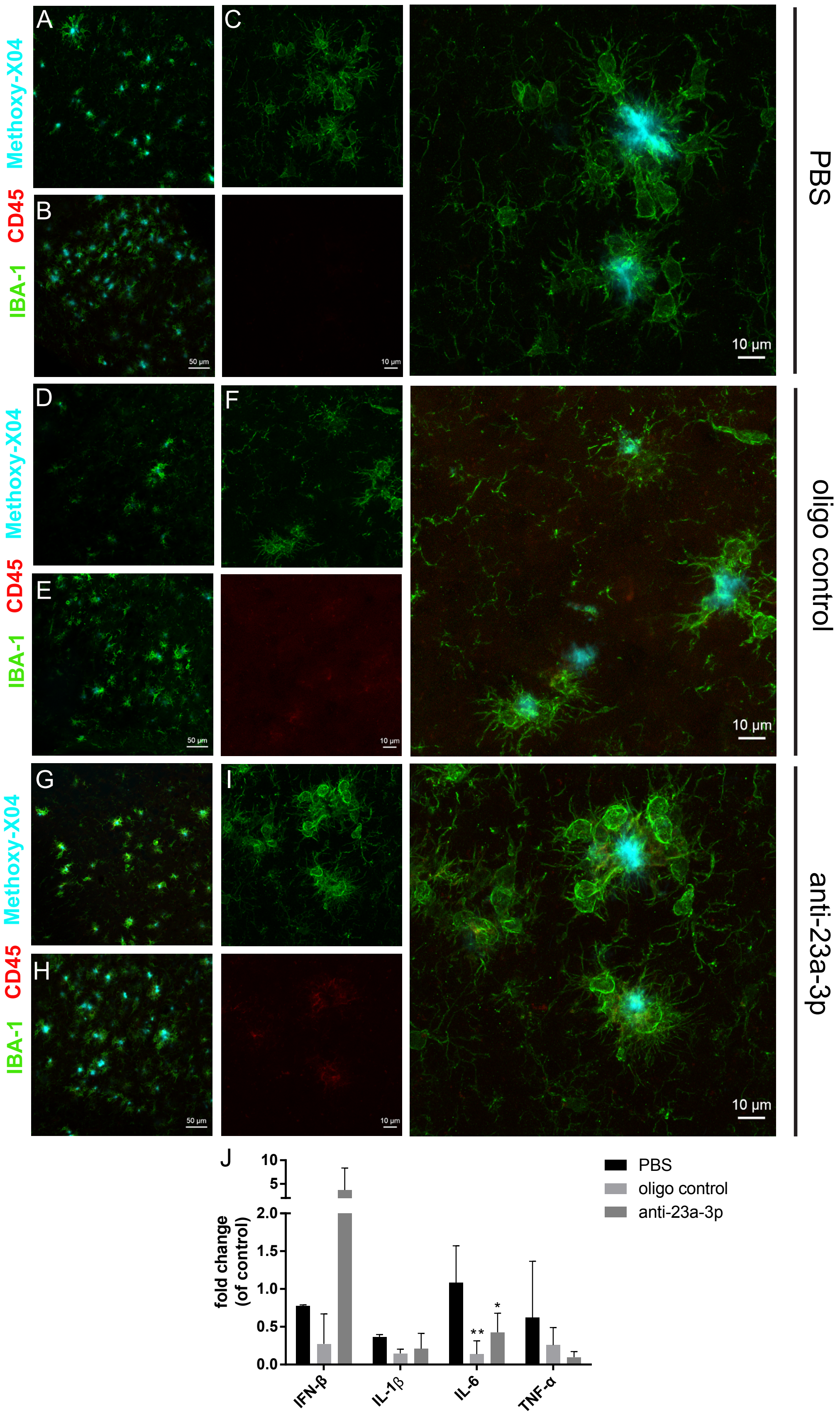
A
B
C
D
E
F
G
H
I
J
IBA-1 CD45 Methoxy-X04
IBA-1 CD45 Methoxy-X04
IBA-1 CD45 Methoxy-X04
50 µm
10 µm
10 µm
PBS
oligo control
anti-23a-3p
fold change (of control)
10
5
2.0
1.5
1.0
0.5
0.0
**
*
IFN-β
IL-1β
IL-6
TNF-α
PBS
oligo control
anti-23a-3p

Figure 5.5. | BM-derived monocytes cluster around Aβ plaques and suppress inflammation in 5XFAD mice. One month following injection of *ex vivo* modified BM-derived monocytes, 5XFAD mice were sacrificed and brains were collected for immunohistochemistry and RNA extraction. The right hemisphere was sliced and sequential slices were immunolabeled with IBA-1 and CD45 antibodies. Methoxy-X04 was used to label Aβ plaques. Images were taken under a 710 LSM confocal microscope and are representative of *n* = 3-5 5XFAD mice from each experimental group. Microscope images of cortex (**A, D, G**) and subiculum (**B, H, E**) show microglia and BM-derived monocytes clustering around Aβ plaques and are presented at a 20× magnification. (**C, F, I**) Maximum intensity projection of Z-stacks from cortex, presented at 63× magnification, show that IBA-1^{+}CD45^{high} cells are detected only in 5XFAD mice injected with BM-derived monocytes (upper left – IBA-1; lower left – CD45; right – merge). RNA was extracted of the left hemisphere (cortex) and the mRNA expression of several cytokines was quantified by qRT-PCR. BM-derived monocyte injection resulted in decreased expression of IL-6 in the brain of 5XFAD mice (**J**). Results are representative of *n* = 3-5 for each animal group and are expressed as fold change of the mean of PBS injected mice; $P = 0.3$, $P = 0.28$, $P = 0.008$ and $P = 0.28$ for IFN-β, IL-1β, IL-6 and TNF-α, respectively, One-way ANOVA; * $P < 0.05$ and ** $P < 0.01$, Tukey's *post hoc* test, with respect to PBS-injected 5XFAD.

D and G) and subiculum (Fig. 5.5B, E and H). These cells presented phenotypes ranging from fully ramified to amoeboid (Fig. 5.5C, F and I, top left panel).

Following the demonstration of the presence of injected BM-derived monocytes around Aβ deposits in 5XFAD brains, we investigated if these cells could modulate the inflammatory environment in the mice brain. Indeed, increasing evidence suggests that AD is characterized by strong immunological responses and that mononuclear phagocytes play a central role in the production of inflammatory mediators, such as IL-6, TNF-α and IL-1β, thus contributing to the proinflammatory environment observed in the brain of AD patients (Heneka et al., 2015). Therefore, experiments were performed to ascertain if the recruitment of BM-derived monocytes would influence the expression of these molecules. For this purpose, we measured the mRNA levels of several cytokines and found that the injection of BM-derived monocytes resulted in significantly decreased expression of IL-6 (Fig. 5.5J) in the cortex, independently of previous miR-23a-3p modulation. In addition, IL-1β and TNF-α were found to be slightly decreased in 5XFAD mice injected with BM-derived monocytes ($P = 0.28$; One-way ANOVA), while increased levels of IFN-β, although not statistically significant, were observed in 5XFAD injected with BM-derived monocytes modified with anti-23a-3p oligonucleotides (Fig. 5.5J; $P = 0.3$; One-way ANOVA).

Since miRNAs have been proposed as markers of the different activation phenotypes of innate immune cells, we measured the expression of miR-155, miR-124 and miR-145 (Freilich et al., 2013; Zhang et al., 2013), markers of the M1, M0 and M2a, respectively, aiming to assess the overall phenotype of mononuclear phagocytes in the brain of the injected 5XFAD mice. MiR-124 showed a tendency to be increased in 5XFAD mice injected with BM-derived monocytes, while miR-145 decreased (Supplementary Material, Fig. S5.4; $P = 0.36$ and $P = 0.1$, respectively; On-way ANOVA). Importantly, miR-155 expression was not detected in any of the experimental groups, suggesting that 5XFAD mice, at 4 months, do not present a strong pro-inflammatory environment, characteristic of the M1 phenotype.

5.4. Discussion

The results presented in this work provide new insights into the therapeutic potential of miRNA modulation in AD, particularly in what concerns the neuroimmune component of this disease. Owing to the inaccessibility to CNS local immune cells, the modulation of peripheral myeloid cells, which has the advantage of being easily performed *ex vivo*, is of special interest and could have a strong therapeutic impact. In this regard, monocytes and macrophages have been proposed to provide a unique therapeutic opportunity in the context of neuroinflammatory diseases. However, their repairing role in CNS degeneration has been considered unachievable due to their limited recruitment to the brain (Shechter and Schwartz, 2013). The use of these cells as therapeutic vehicles in AD is of particular relevance, since impairment of amyloid clearance mechanisms by microglia has been pointed as a possible cause for the accumulation of aggregated Aβ (Hickman and El Khoury, 2013). In fact, microglia ablation has been shown not to influence amyloid plaque formation (Grathwohl et al., 2009) and other cells of the myeloid linage, such as monocyte-derived macrophages, appear to be more efficient in promoting Aβ phagocytosis (Malm et al., 2005; Simard et al., 2006; Butovsky et al., 2007; Hawkes and McLaurin, 2009; Lebson et al., 2010; Michaud et al., 2013; Koronyo et al., 2015). Importantly, amyloid deposition inside and around blood vessels has been previously reported in AD (El Khoury et al., 2007; Duyckaerts et al., 2009; Mildner et al., 2011) and is the most important feature of cerebral amyloid angiopathy (CAA), in which exogenous Aβ expression is targeted to the blood vessels (Miao et al., 2005).

In this work, a single i.v. injection of BM-derived monocytes, previously transfected with anti-23a-3p oligonucleotides, was sufficient to decrease vascular Aβ accumulation in the cortex and hippocampus of 5XFAD mice (Fig. 5.4E). Since genetic ablation of CCR2 increases the levels of $A\beta_{1-42}$ in the brain of AD mouse models, a feature closely linked to amplified vascular Aβ accumulation (El Khoury et al., 2007; Mildner et al., 2011), we hypothesized that a strategy to increase CCR2 expression could lead to the opposite effect. Based on the ability of miR-23a-3p to strongly bind to CCR2 mRNA (Fig. 5.3C), we decided to modulate miR-23a-3p in BM-derived monocytes, through *ex vivo* delivery of anti-23a-3p oligonucleotides, with the purpose of increasing CCR2 expression, thus potentiating monocyte chemotaxis into the brain. In fact, miR-23a-3p inhibition was able to increase the mRNA levels of CCR2 (Fig. 5.3E) in BM-derived monocytes, which, when injected into 5XFAD mice, were able to decrease Aβ vascular deposits (Fig. 5.4E). Our results are in accordance with a recent report showing circulating monocytes adhering to brain blood vessels and clearing Aβ from their walls (Michaud et al., 2013) and further confirm the protective role of peripheral monocytes and the beneficial effect of their enhanced recruitment to AD brain.

In contrast with the results concerning vascular Aβ, no significant changes were observed in the deposition of dense and diffuse Aβ plaques in the brain parenchyma, following the specific modulation of miR-23a-3p in BM-derived monocytes. This result seems to be in accordance with previous studies showing that AD mice transplanted with either $CCR2^{-/-}$ or $CCR2^{+/+}$ BM cells do not show differences in parenchymal Aβ (Mildner et al., 2011). However, when measured by ELISA, the levels of soluble $A\beta_{1\text{-}42}$ were decreased in 5XFAD mice injected with BM-derived monocytes, when compared to PBS-injected 5XFAD mice (Fig. 5.4F). Although this effect was miR-23a-3p-independent and possibly CCR2-independent as well, it is still an interesting finding that deserves to be further investigated. It should be stressed that this result positively correlates with recent reports showing improved clearance of soluble Aβ following bexarotene treatment in APP/PS1ΔE9 mice (Fitz et al., 2013), which can be attributed to a potentiation of Aβ phagocytosis by mononuclear phagocytes (Mandrekar-Colucci et al., 2012). The infiltration of BM-derived monocytes into the 5XFAD brain (Fig. 5.2C) might, in part, explain the observed reduction in the levels of soluble $A\beta_{1\text{-}42}$, since less perivascular Aβ deposition could create a concentration gradient, leading to a possible efflux of the soluble Aβ from the CNS to the cerebrospinal fluid (CSF) (Mawuenyega et al., 2010) or to the plasma, as observed for bexarotene-treated animals (Bachmeier et al., 2013). However, as opposed to recent results reporting a decrease of insoluble $A\beta_{1\text{-}42}$ in AD mice injected with BM-derived monocytes (Koronyo et al., 2015), we did not find differences in this insoluble fraction (Fig. 5.4E). Since Aβ plaques are very sticky structures (Bolmont et al., 2008), it is possible that the insoluble Aβ peptides/fibrils in these deposits are not easily cleared by mononuclear phagocytes, limiting their mobilization as soluble Aβ species.

Research on peripheral myeloid cell infiltration into the AD brain has been, so far, quite controversial. This is mostly due to the fact that few studies addressing this phenomenon have skipped cranial or full-body irradiation, which permanently alters the cerebral vasculature (Soulet and Rivest, 2008; Prinz and Priller, 2010). Full-body irradiation has also been associated with a decrease in insoluble Aβ and an increase in CCL2 and TNF-α transcripts in $CD11b^{+}$ cells (Mildner et al., 2011). Therefore, the elimination of this confounding factor is essential to determine if the AD phenotype *per se* is capable of inducing the infiltration of mononuclear phagocytes into the brain. In this context, and in order to overcome this issue, instead of using an approach involving BM transplantation (which requires the use of irradiation), we injected BM-derived monocytes directly into the tail vein of 5XFAD mice. Importantly, these cells were isolated from $Cx3cr1^{gfp/+}Ccr2^{rfp/+}$ mice, thus allowing all monocytes to be labeled with both GFP and RFP under the control of the promoter of CX3CR1 and CCR2, two genes essential for monocyte function (El Khoury and Luster, 2008). The infiltration of BM-derived monocytes into the brain of 5XFAD mice was demonstrated 48 h following injection, as assessed by flow cytometry and IVM (Fig. 5.2). The GFP/RFP labeling allowed not only to confirm the purity of the isolated cells (Fig. 5.1), but also to reinforce the role of the chemokine receptors CX3CR1 and

CCR2 in brain infiltration of BM-derived monocytes. Moreover, by using a gating strategy based on these markers, it was possible to detect these cells in the brain parenchyma by flow cytometry (Fig. 5.2B), without having to gate cells according to the conventional CD11b^{+}CD45^{high}LyC6^{high} phenotype (Koronyo et al., 2015). Although Ly6C^{high} cells have been described as neutrophils and shown to be able to migrate into the brain of 5XFAD mice (Baik et al., 2014), monocytes also express Ly6C and, therefore, previous reports on the role of neutrophils in Aβ clearance may have missed an important contribution of monocytes in AD.

Even though CX3CR1 and CCR2 were previously described as markers to differentiate adult microglia from infiltrating monocyte-derived macrophages (microglia was believed to be CX3CR1^{high}CCR2^{-} and CNS-infiltrating monocytes appeared as CCR2^{high}CX3CR1^{low} or CCR2^{low}CX3CR1^{high} (Mizutani et al., 2012)), we were not able to detect GFP/RFP signal in 5XFAD brains one month after BM-derived monocyte injection. In this context, it is still a question of debate if these cells, once in the brain parenchyma, differentiate into microglia-like cells or maintain a macrophage phenotype (similar to cells derived from Ly6C^{high}CCR2^{+} inflammatory monocytes (Ginhoux and Jung, 2014)). Moreover, although *in vivo* imaging of circulating monocytes revealed their ability to clear vascular Aβ in APP$_{Swe}$/PS1*Cx3cr1*$^{gfp/+}$mice (Michaud et al., 2013) and, therefore, to detect Aβ clearance by CX3CR1^{+} cells *in vivo*, it is important to consider that resident microglia also express this marker.

In addition to the decrease of soluble Aβ, injection of BM-derived monocytes in 5XFAD mice induced changes in the molecular signature of the innate environment observed in 5XFAD brains. Plaque formation has been correlated with high levels of inflammatory mediators, such as IL-6, TNF-α and IL-1β (Lonskaya et al., 2015), and, interestingly, our results show that the injection of BM-derived monocytes into 5XFAD mice decreases IL-6 expression in the brain. This finding is in accordance with other studies where the levels of anti-inflammatory cytokine IL-10 were found to be increased following BM-derived monocyte injection (Koronyo et al., 2015) and suggests that these cells can contribute to draw the molecular inflammatory signature away from the M1 pro-inflammatory state (Freilich et al., 2013; Guedes et al., 2014). The observed tendency for an upregulation of miR-124, a downregulation of miR-145 and the absence of expression of miR-155 (Supplementary Material, Fig. S5.4) are in accordance with this hypothesis. In fact, although they clustered around Aβ plaques, as expected (Bolmont et al., 2008), we did not observe changes in microglia morphology in any of the animal groups (Fig. 5.5C, F and I, right panel). Importantly, CD45 signal was only observed in 5XFAD mice injected with BM-derived monocytes (Fig. 5.5F and I, bottom left panel). Although CD45 labeling is still controversial, the absence of this signal in PBS-injected 5XFAD constitutes evidence that some of the cells around Aβ plaques migrate from the periphery. It is also important to stress that most of IBA-1^{+} cells were not CD45^{+}, suggesting the presence of two independent cell types, microglia and BM-derived cells.

Finally, another important issue concerns monocyte/macrophage transfection, which has been considered a great challenge due to the lack of suitable nucleic acid delivery systems (Hohsfield et al., 2013) capable of mediating efficient transfection of immune cells. Nevertheless, the use of these cells as therapeutic vehicles towards CNS disease may overcome this issue in the near future. In this context, the delivery of miRNA mimics/anti-miRNAs oligonucleotides can be of great interest (Nakamachi et al., 2009; Naqvi et al., 2015), since these small nucleic acid molecules are easier to deliver to the intracellular compartment compared to plasmid constructs. Although gene therapy approaches for CNS diseases using miRNAs as molecular targets or therapeutic molecules have already been developed (Ponomarev et al., 2011; Zhang et al., 2014; Butovsky et al., 2015), to our best knowledge, no studies have been reported on the use of miRNAs to modulate the function of mononuclear phagocytes in AD. In fact, the only study presenting a gene therapy approach to AD and employing BM-derived monocytes was performed in 2010, by Lebson and collegues (Lebson et al., 2010). In this study, BM-derived monocytes were submitted to electroporation before injection with a neprilysin construction, leading to a transfection efficiency around 54%. Since DLS liposomes have been successfully applied in our previous studies to deliver splice correcting oligonucleotides (Trabulo et al., 2010) and anti-miRNA oligonucleotides (Cardoso et al., 2012; Costa et al., 2013b), in this work we employed this same strategy to deliver LNA anti-23a-3p oligonucleotides into BM-derived monocytes. This strategy proved to be highly promising, allowing to reach a transfection efficiency of almost 100% (Fig. 5.3A), which led to the complete inhibition of miR-23a-3p (Fig. 5.3D), without causing cytotoxicity. Since the injection of miR-23a-3p-transfected BM-derived monocytes into 5XFAD mice resulted in decreased Aβ vascular deposition, we can affirm that this is the first gene therapy approach involving miRNA-mediated modulation of BM-derived monocyte function in AD.

5.5. Supplementary Material

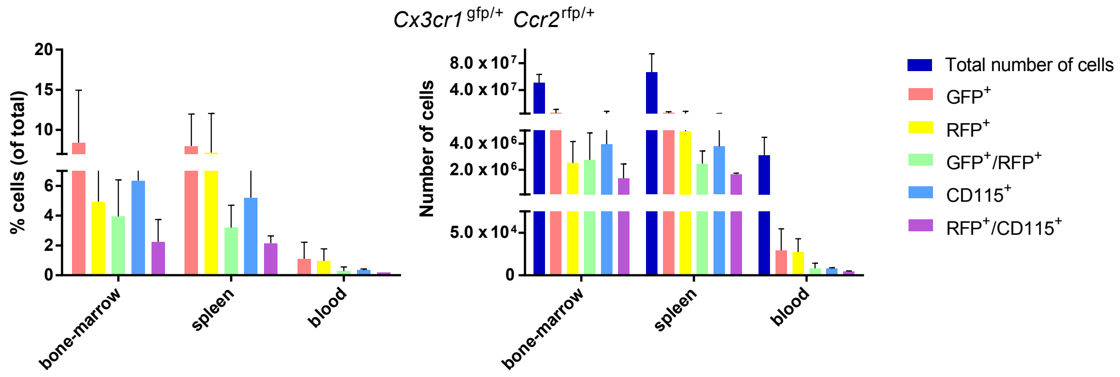

Figure S5.1 | Characterization of tissue-recovered monocytes following isolation.
Total cell suspensions were obtained from the bone-marrow, spleen and blood of Cx3cr1$^{gfp/+}$Ccr2$^{rfp/+}$ mice and analyzed by flow cytometry in order to determine the organ capable of providing the highest yield of monocytes. The number of recovered GFP^{+}RFP^{+} and CD115^{+} cells was very similar for both bone-marrow and spleen. Results are representative of *n* = 3.

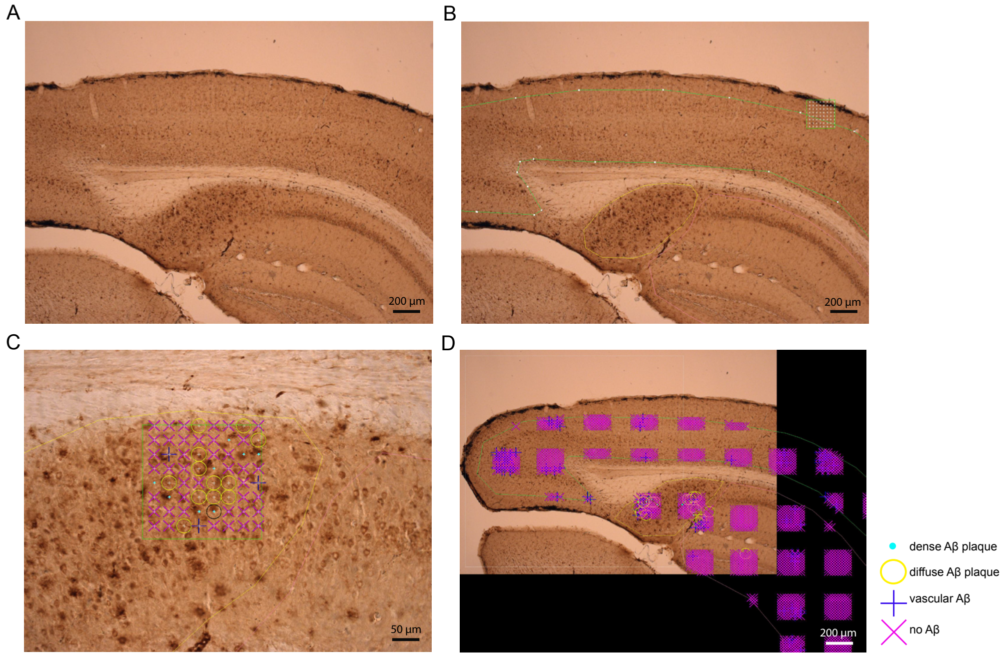

Figure S5.2 | Stereologic analysis to quantify dense, diffuse and vascular Aβ deposits.
Following brain collection, 50 µm coronal slices were cut from the entire right hemisphere. Sequential slices with a 300 µm spacing were systematically analyzed by stereology, using the Stereo Investigator software, following immunolabeling with the anti-human Aβ 6E10 antibody. (**A**) Representative image of part of the cortex, hippocampus and subiculum regions of interest (ROIs). ROIs were delineated and the same probe parameters were used for all areas: a counting frame of 200 × 200 µm and a sampling grid of 350 × 350 µm (**B**) and a grid point spacing of 250 µm (64 points *per* counting frame) (**C**). (**D**) Each of the different Aβ deposits was counted and the total number of points for each one was analyzed individually in each mouse.

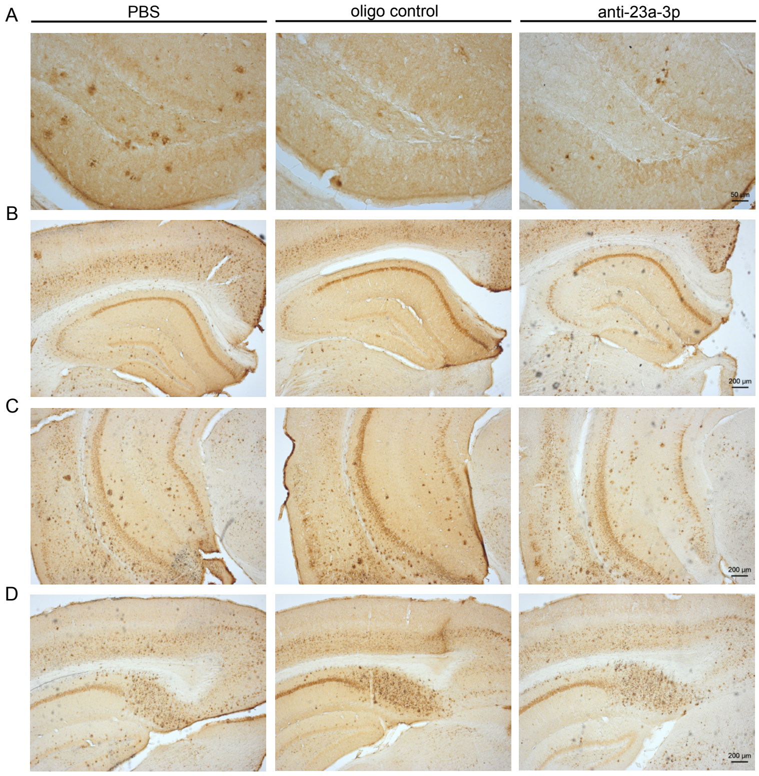

Figure S5.3 | Representative images of the hippocampus and subiculum of BM-monocyte-injected 5XFAD mice.

The right hemisphere was sliced and immunolabeled with the anti-human Aβ 6E10 antibody. Images were taken under an Axio Imager Z2 microscope and are representative of *n* = 3-5 5XFAD mice of each group. Microscope images of the dentate gyrus (**A**) are presented at a 20× magnification and images from the early (**B**) and late hippocampus (**C**) and subiculum (**D**) are presented at 5× magnification.

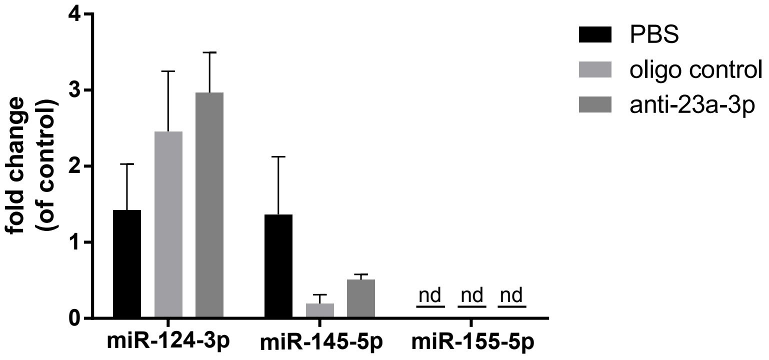

Figure S5.4 | BM-derived monocytes contribute to maintain an immunosuppressive environment in the brain of 5XFAD mice.

Total RNA was extracted from the left hemisphere of each 5XFAD mouse and the expression of miR-124, miR-145 and miR-155 was quantified by qRT-PCR. Results are representative of *n* = 3-5 for each animal group and are expressed as fold change with respect to PBS-injected mice; *P* = 0.36, *P* = 0.1 for miR-124 and miR-145, respectively, One-way ANOVA; *nd* – not detected.

| CHAPTER 6

General conclusions and future perspectives

Alzheimer's disease (AD) is one of the most important social and economic health challenges of the century and is now considered a public health priority by the World Health Organization. It is expected that, in 2050, 115.4 million individuals will suffer from dementia. In addition to the lack of effective treatments, it is still impossible to achieve a definitive clinical diagnosis before autopsy and it is extremely difficult to distinguish different types of dementia and to predict disease progression. Well-trained teams of physicians, nurses, phycologists and other health professionals have been doing an extraordinary work fighting this disease but, with the increase in life expectancy, the incidence of AD is growing disproportionally. The lack of clinical resources is related to the absence of answers for the questions: Why does AD start? Why do people develop dementia? What underlies the overaccumulation of Aβ aggregates in the brain of AD patients? Although we know that Aβ itself is neurotoxic, its deposition in the brain starts decades before the appearance of clinical symptoms and, therefore, it is indispensable to know which other Aβ-dependent mechanisms impact memory.

Since age is the strongest risk factor for AD, it is easy to understand that, in the AD brain, several pathological mechanisms can be triggered by time and by the effect the aging process has on cellular function. External risk factors, such as lifestyle, metabolic syndromes and infectious challenges are also considered important contributors to AD development. Moreover, in addition to the well-known risk factor *ApoE*, recent GWAS studies revealed that several of the recently identified risk genes for AD are related with innate immunity. In this context, we can conclude that both internal and external risk factors for AD culminate in one unique complex event: inflammation. The inflammatory profile observed in AD is the sum of local triggers, such as Aβ-derived activation of microglia, and systemic events, influenced by the above-mentioned genetic and environmental factors, both contributing to make inflammation an important hallmark of this disease.

Looking at this scenario and knowing that genetics can only account for, at most, 5% of all AD cases, it is reasonable to think that epigenetic mechanisms can easily play an important role in AD pathophysiology. In this context, miRNAs, especially those directly implicated in immune regulation, emerge as important players. Due to their intrinsic nature, miRNAs are able to bind to multiple targets in a specific cell type, while, simultaneously, different targets may display binding sites for the same miRNA. Moreover, when dealing with miRNA deregulation, it is expected to observe a cumulative effect of all targeted pathways, which, in the case of inflammatory miRNAs, is typically associated with the production of inflammatory mediators and the activation of cell death mechanisms.

Taking into account the above-mentioned considerations, this project was designed to study whether miRNA-dependent immune mechanisms could be explored in terms of diagnosis and therapeutics and if they could help explain early AD pathological mechanisms. Herein, we showed that an important inflammatory miRNA, miR-155-5p, is upregulated at an early age in the brain of an AD mouse model, following microglia and astrocyte activation with Aβ fibrils and, most importantly, in blood-derived monocytes (BDM) isolated from AD patients. MiR-155-5p along with five other immune-related miRNAs was found to be deregulated in AD patients when compared with mild cognitive impairment (MCI) patients, a pre-dementia stage which can rapidly progress to AD. We also showed that, in the AD brain, the increase of miR-155-5p can be due to an early upregulation of the transcription factor c-Jun and that, by targeting SOCS-1, miR-155-5p interrupts the negative feedback loop responsible for keeping neuroinflammation "in check". SOCS-1 downregulation results in overproduction of inflammatory mediators, thus inducing a chronic inflammatory environment associated with the M1 microglia activation phenotype, which has been considered one of the main causes for the lack of Aβ phagocytosis and clearance in late onset AD.

The peripheral immune system has also been implicated in AD. Since monocytes and microglia share similar progenitors during development, mononuclear phagocytes have been the most studied blood cells in AD. As we and others have shown, bone-marrow (BM)-derived monocytes are able to infiltrate the brain in AD mouse models and have the ability to impact Aβ deposition. This effect is dependent on the presence of a specific chemokine receptor, CCR2. In this work, we showed that miR-23a-3p, another miRNA deregulated in BDMs from AD patients, influences CCR2 expression. By inhibiting miR-23a-3p in BM-derived mouse monocytes, it was possible to upregulate CCR2 mRNA levels. Importantly, the systemic injection of these modified cells in a mouse model of AD was sufficient to lead to a drastic decrease of Aβ deposition in the brain blood vessels. Additionally, injection of the modified BM-derived monocytes also impacted the inflammatory environment in the brain, helping to restore homeostatic balance.

Although in mice peripheral mononuclear phagocytes seem to be beneficial in the context of AD, the question remains whether the knowledge derived from AD mouse models can be translated to humans, in particular to AD patients. If so, can we modulate the function of BDMs *ex vivo* with a therapeutic goal? To answer this question it was essential to study the function of BDMs from AD patients in terms of two different cellular outputs, which greatly influence Aβ deposition: chemotaxis and phagocytosis. BDMs have to reach the AD brain and, for that purpose, they have to respond efficiently to chemotactic stimuli such as CCL2 and Aβ itself. In addition, even if brain infiltration is successful, BDMs have to phagocyte and degrade Aβ deposits. In this work we demonstrated that AD BDMs lose the ability to migrate and phagocyte Aβ, when compared to age-matched healthy subjects. The characterization of these functions allowed us to understand that, from a cellular point of view, the stage of dementia associated with a clinical diagnosis of AD is probably already irreversible in terms of deregulation of monocyte function. Interestingly, the impairments observed in BDM chemotaxis and macrophage-mediated Aβ phagocytosis were related with a decrease in CCR2 expression at the cell surface and with an increase of sTREM2 in the plasma of AD patients. This last result suggested an upregulation of TREM2 shedding and, therefore, a limited capacity for Aβ internalization. In the case of MCI patients, several alterations were also observed, confirming that, in addition to the discovery of new tools to follow disease progression, it is urgent to discover novel biomarkers for very early dementia stages that precede mild cognitive impairment.

Given the ability of miR-23a-3p, miR-154-5p, miR-27b-3p, miR-200b-3p and miR-128-3p to bind to the mRNA of proteins associated with chemotaxis and phagocytosis, such as CCR2, CXCR4 and MGAT3, we believe that the deregulation of the expression of these miRNAs can be intrinsically related with the observed impaired phenotypes. Nonetheless, the role of inflammatory miRNAs in AD pathogenesis is far from being completely understood. To achieve this goal, it is necessary to evaluate miRNA expression in human microglia *vs* blood-monocytes, employing high-throughput techniques, long before the appearance of clinical symptoms. Furthermore, the identified miRNA networks should be correlated with the transcriptomes of microglia and monocytes since, from an epigenetic point of view, these cells can be deregulated at very early stages of disease. Finally, strategies should be envisioned to distinguish the confounding effects of age from those of the disease itself.

Regarding miR-155-5p, the definitive proof of a causative role of this miRNA in AD-associated neuroinflammation would be achieved by crossing a knockout of this miRNA with AD mouse models. This would allow to evaluate how the lack of miR-155-5p impacts microglia function and synapse architecture. In addition, it is important to validate CCR2 as a molecular target of miR-23a-3p and miR-154-5p and to further study how the modulation of these two miRNAs can impact chemotaxis of human cells. Importantly, the identification of miRNAs that potentiate phagocytosis is also essential, since these miRNAs could potentially increase Aβ phagocytosis by microglia or monocyte-derived macrophages, leading to a huge therapeutic impact in AD, both locally and systemically.

Altogether, the results presented in this Thesis confirm that miRNAs will undoubtedly play a vital role in the development of future strategies towards AD diagnosis and treatment, as biomarkers, molecular targets or even therapeutic tools. Given the demanding challenges of this disorder, it is imperative to focus our attention on these epigenetic modulators and their possible contribution to neuroinflammation, if we ever hope to win the battle against AD.

| REFERENCES

List of bibliographic references (ordered alphabetically)

2014 Alzheimer's disease facts and figures. (2014). Alzheimers Dement *10*, e47-92.

Afagh, A., Cummings, B.J., Cribbs, D.H., et al. (1996). Localization and cell association of C1q in Alzheimer's disease brain. Exp Neurol *138*, 22-32.

Agulhon, C., Sun, M.Y., Murphy, T., et al. (2012). Calcium Signaling and Gliotransmission in Normal vs. Reactive Astrocytes. Front Pharmacol *3*, 139.

Albert, M.S., DeKosky, S.T., Dickson, D., et al. (2011). The diagnosis of mild cognitive impairment due to Alzheimer's disease: recommendations from the National Institute on Aging-Alzheimer's Association workgroups on diagnostic guidelines for Alzheimer's disease. Alzheimers Dement *7*, 270-279.

Alliot, F., Godin, I., and Pessac, B. (1999). Microglia derive from progenitors, originating from the yolk sac, and which proliferate in the brain. Brain Res Dev Brain Res *117*, 145-152.

Alt, C., Runnels, J.M., Mortensen, L.J., et al. (2014). In vivo imaging of microglia turnover in the mouse retina after ionizing radiation and dexamethasone treatment. Invest Ophthalmol Vis Sci *55*, 5314-5319.

Bachmeier, C., Beaulieu-Abdelahad, D., Crawford, F., et al. (2013). Stimulation of the retinoid X receptor facilitates beta-amyloid clearance across the blood-brain barrier. J Mol Neurosci *49*, 270-276.

Baik, S.H., Cha, M.Y., Hyun, Y.M., et al. (2014). Migration of neutrophils targeting amyloid plaques in Alzheimer's disease mouse model. Neurobiol Aging *35*, 1286-1292.

Baker, B.J., Akhtar, L.N., and Benveniste, E.N. (2009). SOCS1 and SOCS3 in the control of CNS immunity. Trends Immunol *30*, 392-400.

Balin, B.J., and Hudson, A.P. (2014). Etiology and pathogenesis of late-onset Alzheimer's disease. Curr Allergy Asthma Rep *14*, 417.

Bard, F., Cannon, C., Barbour, R., et al. (2000). Peripherally administered antibodies against amyloid beta-peptide enter the central nervous system and reduce pathology in a mouse model of Alzheimer disease. Nat Med *6*, 916-919.

Beraud, D., Twomey, M., Bloom, B., et al. (2011). alpha-Synuclein Alters Toll-Like Receptor Expression. Front Neurosci *5*, 80.

Bernardi, A., Frozza, R.L., Meneghetti, A., et al. (2012). Indomethacin-loaded lipid-core nanocapsules reduce the damage triggered by Abeta1-42 in Alzheimer's disease models. Int J Nanomedicine *7*, 4927-4942.

Bhaskar, K., Konerth, M., Kokiko-Cochran, O.N., et al. (2010). Regulation of tau pathology by the microglial fractalkine receptor. Neuron *68*, 19-31.

Biber, K., Neumann, H., Inoue, K., et al. (2007). Neuronal 'On' and 'Off' signals control microglia. Trends Neurosci *30*, 596-602.

Bolmont, T., Haiss, F., Eicke, D., et al. (2008). Dynamics of the microglial/amyloid interaction indicate a role in plaque maintenance. J Neurosci *28*, 4283-4292.

Bonaiuto, C., McDonald, P.P., Rossi, F., et al. (1997). Activation of nuclear factor-kappa B by beta-amyloid peptides and interferon-gamma in murine microglia. J Neuroimmunol *77*, 51-56.

Bradshaw, E.M., Chibnik, L.B., Keenan, B.T., et al. (2013). CD33 Alzheimer's disease locus: altered monocyte function and amyloid biology. Nat Neurosci *16*, 848-850.

Bsibsi, M., Ravid, R., Gveric, D., et al. (2002). Broad expression of Toll-like receptors in the human central nervous system. J Neuropathol Exp Neurol *61*, 1013-1021.

Butovsky, O., Jedrychowski, M.P., Cialic, R., et al. (2015). Targeting miR-155 restores abnormal microglia and attenuates disease in SOD1 mice. Ann Neurol *77*, 75-99.

Butovsky, O., Jedrychowski, M.P., Moore, C.S., et al. (2014). Identification of a unique TGF-beta-dependent molecular and functional signature in microglia. Nat Neurosci *17*, 131-143.

Butovsky, O., Kunis, G., Koronyo-Hamaoui, M., et al. (2007). Selective ablation of bone marrow-derived dendritic cells increases amyloid plaques in a mouse Alzheimer's disease model. Eur J Neurosci *26*, 413-416.

Butovsky, O., Siddiqui, S., Gabriely, G., et al. (2012). Modulating inflammatory monocytes with a unique microRNA gene signature ameliorates murine ALS. J Clin Invest *122*, 3063-3087.

Callizot, N., Combes, M., Steinschneider, R., et al. (2013). Operational dissection of beta-amyloid cytopathic effects on cultured neurons. J Neurosci Res *91*, 706-716.

Cardona, A.E., Pioro, E.P., Sasse, M.E., et al. (2006). Control of microglial neurotoxicity by the fractalkine receptor. Nat Neurosci *9*, 917-924.

Cardoso, A.L., Costa, P., de Almeida, L.P., et al. (2010). Tf-lipoplex-mediated c-Jun silencing improves neuronal survival following excitotoxic damage in vivo. J Control Release *142*, 392-403.

Cardoso, A.L., Guedes, J.R., Pereira de Almeida, L., et al. (2012). miR-155 modulates microglia-mediated immune response by down-regulating SOCS-1 and promoting cytokine and nitric oxide production. Immunology *135*, 73-88.

Cecchini, M.G., Dominguez, M.G., Mocci, S., et al. (1994). Role of colony stimulating factor-1 in the establishment and regulation of tissue macrophages during postnatal development of the mouse. Development *120*, 1357-1372.

Cogswell, J.P., Ward, J., Taylor, I.A., et al. (2008). Identification of miRNA Changes in Alzheimer's Disease Brain and CSF Yields Putative Biomarkers and Insights into Disease Pathways. J Alzheimers Dis *14*, 27-41.

Condic, M., Oberstein, T.J., Herrmann, M., et al. (2014). N-truncation and pyroglutaminylation enhances the opsonizing capacity of Abeta-peptides and facilitates phagocytosis by macrophages and microglia. Brain Behav Immun *41*, 116-125.

Coraci, I.S., Husemann, J., Berman, J.W., et al. (2002). CD36, a class B scavenger receptor, is expressed on microglia in Alzheimer's disease brains and can mediate production of reactive oxygen species in response to beta-amyloid fibrils. Am J Pathol *160*, 101-112.

Costa, P.M., Cardoso, A.L., Custodia, C., et al. (2015). MiRNA-21 silencing mediated by tumor-targeted nanoparticles combined with sunitinib: A new multimodal gene therapy approach for glioblastoma. J Control Release *207*, 31-39.

Costa, P.M., Cardoso, A.L., Mendonca, L.S., et al. (2013a). Tumor-targeted Chlorotoxin-coupled Nanoparticles for Nucleic Acid Delivery to Glioblastoma Cells: A Promising System for Glioblastoma Treatment. Mol Ther Nucleic Acids *2*, e100.

Costa, P.M., Cardoso, A.L., Nobrega, C., et al. (2013b). MicroRNA-21 silencing enhances the cytotoxic effect of the antiangiogenic drug sunitinib in glioblastoma. Hum Mol Genet *22*, 904-918.

Cramer, P.E., Cirrito, J.R., Wesson, D.W., et al. (2012). ApoE-directed therapeutics rapidly clear beta-amyloid and reverse deficits in AD mouse models. Science *335*, 1503-1506.

Cuadros, M.A., Martin, C., Coltey, P., et al. (1993). First appearance, distribution, and origin of macrophages in the early development of the avian central nervous system. J Comp Neurol *330*, 113-129.

D'Andrea, M.R., Cole, G.M., and Ard, M.D. (2004). The microglial phagocytic role with specific plaque types in the Alzheimer disease brain. Neurobiol Aging *25*, 675-683.

Das, P., Howard, V., Loosbrock, N., et al. (2003). Amyloid-beta immunization effectively reduces amyloid deposition in FcRgamma-/- knock-out mice. J Neurosci *23*, 8532-8538.

Davalos, D., Grutzendler, J., Yang, G., et al. (2005). ATP mediates rapid microglial response to local brain injury in vivo. Nat Neurosci *8*, 752-758.

Davenport, C.M., Sevastou, I.G., Hooper, C., et al. (2010). Inhibiting p53 pathways in microglia attenuates microglial-evoked neurotoxicity following exposure to Alzheimer peptides. J Neurochem *112*, 552-563.

De Jager, P.L., Srivastava, G., Lunnon, K., et al. (2014). Alzheimer's disease: early alterations in brain DNA methylation at ANK1, BIN1, RHBDF2 and other loci. Nat Neurosci *17*, 1156-1163.

Delay, C., and Hebert, S.S. (2011). MicroRNAs and Alzheimer's Disease Mouse Models: Current Insights and Future Research Avenues. Int J Alzheimers Dis *2011*, 894938.

Delay, C., Mandemakers, W., and Hebert, S.S. (2012). MicroRNAs in Alzheimer's disease. Neurobiol Dis *46*, 285-290.

Denk, J., Boelmans, K., Siegismund, C., et al. (2015). MicroRNA Profiling of CSF Reveals Potential Biomarkers to Detect Alzheimer`s Disease. PLoS One *10*, e0126423.

Dheen, S.T., Jun, Y., Yan, Z., et al. (2005). Retinoic acid inhibits expression of TNF-alpha and iNOS in activated rat microglia. Glia *50*, 21-31.

Dickson, D.W., Farlo, J., Davies, P., et al. (1988). Alzheimer's disease. A double-labeling immunohistochemical study of senile plaques. Am J Pathol *132*, 86-101.

Doens, D., and Fernandez, P.L. (2014). Microglia receptors and their implications in the response to amyloid beta for Alzheimer's disease pathogenesis. J Neuroinflammation *11*, 48.

Doody, R.S., Raman, R., Farlow, M., et al. (2013). A phase 3 trial of semagacestat for treatment of Alzheimer's disease. N Engl J Med *369*, 341-350.

Duff, K., and Suleman, F. (2004). Transgenic mouse models of Alzheimer's disease: how useful have they been for therapeutic development? Brief Funct Genomic Proteomic *3*, 47-59.

Duyckaerts, C., Delatour, B., and Potier, M.C. (2009). Classification and basic pathology of Alzheimer disease. Acta Neuropathol *118*, 5-36.

Dweep, H., Sticht, C., Pandey, P., et al. (2011). miRWalk--database: prediction of possible miRNA binding sites by "walking" the genes of three genomes. J Biomed Inform *44*, 839-847.

El Khoury, J., and Luster, A.D. (2008). Mechanisms of microglia accumulation in Alzheimer's disease: therapeutic implications. Trends Pharmacol Sci *29*, 626-632.

El Khoury, J., Toft, M., Hickman, S.E., et al. (2007). Ccr2 deficiency impairs microglial accumulation and accelerates progression of Alzheimer-like disease. Nat Med *13*, 432-438.

Evans, T.A., Barkauskas, D.S., Myers, J.T., et al. (2014). High-resolution intravital imaging reveals that blood-derived macrophages but not resident microglia facilitate secondary axonal dieback in traumatic spinal cord injury. Exp Neurol *254*, 109-120.

Fagan, A.M., and Vos, S.J. (2013). Preclinical Alzheimer's disease criteria. Lancet Neurol *12*, 1134.

Fazi, F., Rosa, A., Fatica, A., et al. (2005). A minicircuitry comprised of microRNA-223 and transcription factors NFI-A and C/EBPalpha regulates human granulopoiesis. Cell *123*, 819-831.

Fenoglio, C., Cantoni, C., De Riz, M., et al. (2011). Expression and genetic analysis of miRNAs involved in CD4+ cell activation in patients with multiple sclerosis. Neurosci Lett *504*, 9-12.

Fiala, M., Lin, J., Ringman, J., et al. (2005). Ineffective phagocytosis of amyloid-ß by macrophages of Alzheimer's disease patients. J Alzheimers Dis *7*, 221-232.

Fiala, M., Liu, P.T., Espinosa-Jeffrey, A., et al. (2007). Innate immunity and transcription of MGAT-III and Toll-like receptors in Alzheimer's disease patients are improved by bisdemethoxycurcumin. Proc Natl Acad Sci U S A *104*, 12849-12854.

Fiala, M., Zhang, L., Gan, X., et al. (1998). Amyloid-beta induces chemokine secretion and monocyte migration across a human blood--brain barrier model. Mol Med *4*, 480-489.

Fitz, N.F., Cronican, A.A., Lefterov, I., et al. (2013). Comment on "ApoE-directed therapeutics rapidly clear beta-amyloid and reverse deficits in AD mouse models". Science *340*, 924-c.

Folstein, M., F., Folstein, S., E., and McHugh, P.R. (1975). "Mini-mental state". Journal of Psychiatric Research *12*, 189-198.

Fonseca, M.I., Ager, R.R., Chu, S.H., et al. (2009). Treatment with a C5aR antagonist decreases pathology and enhances behavioral performance in murine models of Alzheimer's disease. J Immunol *183*, 1375-1383.

Forrest, A.R., Kanamori-Katayama, M., Tomaru, Y., et al. (2010). Induction of microRNAs, mir-155, mir-222, mir-424 and mir-503, promotes monocytic differentiation through combinatorial regulation. Leukemia *24*, 460-466.

Frank, S., Burbach, G.J., Bonin, M., et al. (2008). TREM2 is upregulated in amyloid plaque-associated microglia in aged APP23 transgenic mice. Glia *56*, 1438-1447.

Frank, S., Copanaki, E., Burbach, G.J., et al. (2009). Differential regulation of toll-like receptor mRNAs in amyloid plaque-associated brain tissue of aged APP23 transgenic mice. Neurosci Lett *453*, 41-44.

Frankenberger, M., Sternsdorf, T., Pechumer, H., et al. (1996). Differential cytokine expression in human blood monocyte subpopulations: a polymerase chain reaction analysis. Blood *87*, 373-377.

Freilich, R.W., Woodbury, M.E., and Ikezu, T. (2013). Integrated expression profiles of mRNA and miRNA in polarized primary murine microglia. PLoS One *8*, e79416.

Frohman, E.M., van den Noort, S., and Gupta, S. (1989). Astrocytes and intracerebral immune responses. J Clin Immunol *9*, 1-9.

Fu, H., Liu, B., Frost, J.L., et al. (2012). Complement component C3 and complement receptor type 3 contribute to the phagocytosis and clearance of fibrillar Abeta by microglia. Glia *60*, 993-1003.

Fukao, T., Fukuda, Y., Kiga, K., et al. (2007). An evolutionarily conserved mechanism for microRNA-223 expression revealed by microRNA gene profiling. Cell *129*, 617-631.

Galea, I., Bechmann, I., and Perry, V.H. (2007). What is immune privilege (not)? Trends Immunol *28*, 12-18.

Galimberti, D., Fenoglio, C., Lovati, C., et al. (2006). Serum MCP-1 levels are increased in mild cognitive impairment and mild Alzheimer's disease. Neurobiol Aging *27*, 1763-1768.

Gatto, G., Rossi, A., Rossi, D., et al. (2008). Epstein-Barr virus latent membrane protein 1 trans-activates miR-155 transcription through the NF-kappaB pathway. Nucleic Acids Res *36*, 6608-6619.

Gautier, E.L., Shay, T., Miller, J., et al. (2012). Gene-expression profiles and transcriptional regulatory pathways that underlie the identity and diversity of mouse tissue macrophages. Nat Immunol *13*, 1118-1128.

Ginhoux, F., Greter, M., Leboeuf, M., et al. (2010). Fate mapping analysis reveals that adult microglia derive from primitive macrophages. Science *330*, 841-845.

Ginhoux, F., and Jung, S. (2014). Monocytes and macrophages: developmental pathways and tissue homeostasis. Nat Rev Immunol *14*, 392-404.

Glass, C.K., Saijo, K., Winner, B., et al. (2010). Mechanisms underlying inflammation in neurodegeneration. Cell *140*, 918-934.

Glenner, G.G., and Wong, C.W. (1984). Alzheimer's disease: initial report of the purification and characterization of a novel cerebrovascular amyloid protein. Biochem Biophys Res Commun *120*, 885-890.

Goldgaber, D., Harris, H.W., Hla, T., et al. (1989). Interleukin 1 regulates synthesis of amyloid beta-protein precursor mRNA in human endothelial cells. Proc Natl Acad Sci U S A *86*, 7606-7610.

Gorina, R., Font-Nieves, M., Marquez-Kisinousky, L., et al. (2011). Astrocyte TLR4 activation induces a proinflammatory environment through the interplay between MyD88-dependent NFkappaB signaling, MAPK, and Jak1/Stat1 pathways. Glia *59*, 242-255.

Gosselin, D., Link, V.M., Romanoski, C.E., et al. (2014). Environment drives selection and function of enhancers controlling tissue-specific macrophage identities. Cell *159*, 1327-1340.

Gotz, J., Chen, F., van Dorpe, J., et al. (2001). Formation of neurofibrillary tangles in P301l tau transgenic mice induced by Abeta 42 fibrils. Science *293*, 1491-1495.

Gotz, J., and Ittner, L.M. (2008). Animal models of Alzheimer's disease and frontotemporal dementia. Nat Rev Neurosci *9*, 532-544.

Grathwohl, S.A., Kalin, R.E., Bolmont, T., et al. (2009). Formation and maintenance of Alzheimer's disease beta-amyloid plaques in the absence of microglia. Nat Neurosci *12*, 1361-1363.

Griciuc, A., Serrano-Pozo, A., Parrado, A.R., et al. (2013). Alzheimer's disease risk gene CD33 inhibits microglial uptake of amyloid beta. Neuron *78*, 631-643.

Griffin, W.S., Sheng, J.G., Roberts, G.W., et al. (1995). Interleukin-1 expression in different plaque types in Alzheimer's disease: significance in plaque evolution. J Neuropathol Exp Neurol *54*, 276-281.

Griffin, W.S., Stanley, L.C., Ling, C., et al. (1989). Brain interleukin 1 and S-100 immunoreactivity are elevated in Down syndrome and Alzheimer disease. Proc Natl Acad Sci U S A *86*, 7611-7615.

Griffin, W.S.T., Sheng, J.G., Royston, M.C., et al. (1998). Glial-Neuronal Interactions in Alzheimer's Disease: The Potential Role of a 'Cytokine Cycle' in Disease Progression. Brain Pathology *8*, 65-72.

Guedes, J., Cardoso, A.L., and Pedroso de Lima, M.C. (2013). Involvement of microRNA in microglia-mediated immune response. Clin Dev Immunol *2013*, 186872.

Guedes, J.R., Custodia, C.M., Silva, R.J., et al. (2014). Early miR-155 upregulation contributes to neuroinflammation in Alzheimer's disease triple transgenic mouse model. Hum Mol Genet *23*, 6286-6301.

Guerreiro, M. (1998). Contributo da Neuropsicologia para o estudo das demências [Contribution of Neuropsychology to the study of dementia] (Unpublished doctoral dissertation). University of Lisbon, Lisbon.

Guerreiro, R., Wojtas, A., Bras, J., et al. (2013). TREM2 variants in Alzheimer's disease. N Engl J Med *368*, 117-127.

Guerreiro, R.J., Santana, I., Bras, J.M., et al. (2007). Peripheral inflammatory cytokines as biomarkers in Alzheimer's disease and mild cognitive impairment. Neurodegener Dis *4*, 406-412.

Guo, Q., Fu, W., Sopher, B.L., et al. (1999). Increased vulnerability of hippocampal neurons to excitotoxic necrosis in presenilin-1 mutant knock-in mice. Nat Med *5*, 101-106.

Gupta, A., and Pulliam, L. (2014). Exosomes as mediators of neuroinflammation. J Neuroinflammation *11*, 68.

Ha, M., and Kim, V.N. (2014). Regulation of microRNA biogenesis. Nat Rev Mol Cell Biol *15*, 509-524.

Hardy, J.A., and Higgins, G.A. (1992). Alzheimer's disease: the amyloid cascade hypothesis. Science *256*, 184-185.

Harold, D., Abraham, R., Hollingworth, P., et al. (2009). Genome-wide association study identifies variants at CLU and PICALM associated with Alzheimer's disease. Nat Genet *41*, 1088-1093.

Hashimoto, D., Chow, A., Noizat, C., et al. (2013). Tissue-resident macrophages self-maintain locally throughout adult life with minimal contribution from circulating monocytes. Immunity *38*, 792-804.

Hawkes, C.A., and McLaurin, J. (2009). Selective targeting of perivascular macrophages for clearance of beta-amyloid in cerebral amyloid angiopathy. Proc Natl Acad Sci U S A *106*, 1261-1266.

Hebert, S.S., and De Strooper, B. (2009). Alterations of the microRNA network cause neurodegenerative disease. Trends Neurosci *32*, 199-206.

Hebert, S.S., Horre, K., Nicolai, L., et al. (2008). Loss of microRNA cluster miR-29a/b-1 in sporadic Alzheimer's disease correlates with increased BACE1/beta-secretase expression. Proc Natl Acad Sci U S A *105*, 6415-6420.

Heggland, I., Storkaas, I.S., Soligard, H.T., et al. (2015). Stereological estimation of neuron number and plaque load in the hippocampal region of a transgenic rat model of Alzheimer's disease. Eur J Neurosci *41*, 1245-1262.

Heinz, S., Romanoski, C.E., Benner, C., et al. (2013). Effect of natural genetic variation on enhancer selection and function. Nature *503*, 487-492.

Heneka, M.T., Carson, M.J., Khoury, J.E., et al. (2015). Neuroinflammation in Alzheimer's disease. The Lancet Neurology *14*, 388-405.

Heneka, M.T., Kummer, M.P., and Latz, E. (2014). Innate immune activation in neurodegenerative disease. Nat Rev Immunol *14*, 463-477.

Heneka, M.T., and Landreth, G.E. (2007). PPARs in the brain. Biochim Biophys Acta *1771*, 1031-1045.

Heneka, M.T., and O'Banion, M.K. (2007). Inflammatory processes in Alzheimer's disease. J Neuroimmunol *184*, 69-91.

Hickman, S.E., Allison, E.K., and El Khoury, J. (2008). Microglial dysfunction and defective beta-amyloid clearance pathways in aging Alzheimer's disease mice. J Neurosci *28*, 8354-8360.

Hickman, S.E., and El Khoury, J. (2013). The neuroimmune system in Alzheimer's disease: the glass is half full. J Alzheimers Dis *33 Suppl 1*, S295-302.

Hickman, S.E., Kingery, N.D., Ohsumi, T.K., et al. (2013). The microglial sensome revealed by direct RNA sequencing. Nat Neurosci *16*, 1896-1905.

Hohsfield, L.A., Geley, S., Reindl, M., et al. (2013). The generation of NGF-secreting primary rat monocytes: a comparison of different transfer methods. J Immunol Methods *391*, 112-124.

Hohsfield, L.A., and Humpel, C. (2015). Migration of blood cells to beta-amyloid plaques in Alzheimer's disease. Exp Gerontol *65*, 8-15.

Hollingworth, P., Harold, D., Sims, R., et al. (2011a). Common variants at ABCA7, MS4A6A/MS4A4E, EPHA1, CD33 and CD2AP are associated with Alzheimer's disease. Nat Genet *43*, 429-435.

Hollingworth, P., Harold, D., Sims, R., et al. (2011b). Common variants at ABCA7, MS4A6A/MS4A4E, EPHA1, CD33 and CD2AP are associated with Alzheimer's disease. Nat Genet *43*, 429-435.

Holmans, P., Moskvina, V., Jones, L., et al. (2013). A pathway-based analysis provides additional support for an immune-related genetic susceptibility to Parkinson's disease. Hum Mol Genet *22*, 1039-1049.

Hu, N., Tan, M.S., Yu, J.T., et al. (2014). Increased expression of TREM2 in peripheral blood of Alzheimer's disease patients. J Alzheimers Dis *38*, 497-501.

Husemann, J., and Silverstein, S.C. (2001). Expression of scavenger receptor class B, type I, by astrocytes and vascular smooth muscle cells in normal adult mouse and human brain and in Alzheimer's disease brain. Am J Pathol *158*, 825-832.

Iliopoulos, D., Hirsch, H.A., and Struhl, K. (2009). An epigenetic switch involving NF-kappaB, Lin28, Let-7 MicroRNA, and IL6 links inflammation to cell transformation. Cell *139*, 693-706.

Iqbal, K., Gong, C.X., and Liu, F. (2014). Microtubule-associated protein tau as a therapeutic target in Alzheimer's disease. Expert Opin Ther Targets *18*, 307-318.

Jakubzick, C., Gautier, E.L., Gibbings, S.L., et al. (2013). Minimal differentiation of classical monocytes as they survey steady-state tissues and transport antigen to lymph nodes. Immunity *39*, 599-610.

Jana, M., Palencia, C.A., and Pahan, K. (2008). Fibrillar amyloid-beta peptides activate microglia via TLR2: implications for Alzheimer's disease. J Immunol *181*, 7254-7262.

Janelsins, M.C., Mastrangelo, M.A., Oddo, S., et al. (2005). Early correlation of microglial activation with enhanced tumor necrosis factor-alpha and monocyte chemoattractant protein-1 expression specifically within the entorhinal cortex of triple transgenic Alzheimer's disease mice. J Neuroinflammation *2*, 23.

Janelsins, M.C., Mastrangelo, M.A., Park, K.M., et al. (2008). Chronic neuron-specific tumor necrosis factor-alpha expression enhances the local inflammatory environment ultimately leading to neuronal death in 3xTg-AD mice. Am J Pathol *173*, 1768-1782.

Jay, T.R., Miller, C.M., Cheng, P.J., et al. (2015). TREM2 deficiency eliminates TREM2+ inflammatory macrophages and ameliorates pathology in Alzheimer's disease mouse models. J Exp Med *212*, 287-295.

Jayadev, S., Case, A., Alajajian, B., et al. (2013). Presenilin 2 influences miR146 level and activity in microglia. J Neurochem *127*, 592-599.

Jekabsone, A., Mander, P.K., Tickler, A., et al. (2006). Fibrillar beta-amyloid peptide Abeta1-40 activates microglial proliferation via stimulating TNF-alpha release and H2O2 derived from NADPH oxidase: a cell culture study. J Neuroinflammation *3*, 24.

Jiang, T., Yu, J.T., Zhu, X.C., et al. (2013a). TREM2 in Alzheimer's disease. Mol Neurobiol *48*, 180-185.

Jiang, W., Zhang, Y., Meng, F., et al. (2013b). Identification of active transcription factor and miRNA regulatory pathways in Alzheimer's disease. Bioinformatics *29*, 2596-2602.

Jickling, G.C., Ander, B.P., Zhan, X., et al. (2014). microRNA expression in peripheral blood cells following acute ischemic stroke and their predicted gene targets. PLoS One *9*, e99283.

Jones, L., Holmans, P.A., Hamshere, M.L., et al. (2010). Genetic evidence implicates the immune system and cholesterol metabolism in the aetiology of Alzheimer's disease. PLoS One *5*, e13950.

Jonsson, T., Stefansson, H., Steinberg, S., et al. (2013). Variant of TREM2 associated with the risk of Alzheimer's disease. N Engl J Med *368*, 107-116.

Jung, S., Aliberti, J., Graemmel, P., et al. (2000a). Analysis of Fractalkine Receptor CX3CR1 Function by Targeted Deletion and Green Fluorescent Protein Reporter Gene Insertion. Molecular and Cellular Biology *20*, 4106-4114.

Jung, S., Aliberti, J., Graemmel, P., et al. (2000b). Analysis of fractalkine receptor CX(3)CR1 function by targeted deletion and green fluorescent protein reporter gene insertion. Mol Cell Biol *20*, 4106-4114.

Junker, A., Krumbholz, M., Eisele, S., et al. (2009). MicroRNA profiling of multiple sclerosis lesions identifies modulators of the regulatory protein CD47. Brain *132*, 3342-3352.

Junn, E., Lee, K.W., Jeong, B.S., et al. (2009). Repression of alpha-synuclein expression and toxicity by microRNA-7. Proc Natl Acad Sci U S A *106*, 13052-13057.

Karch, C.M., Cruchaga, C., and Goate, A.M. (2014). Alzheimer's disease genetics: from the bench to the clinic. Neuron *83*, 11-26.

Karran, E., Mercken, M., and De Strooper, B. (2011). The amyloid cascade hypothesis for Alzheimer's disease: an appraisal for the development of therapeutics. Nat Rev Drug Discov *10*, 698-712.

Kettenmann, H., Hanisch, U.K., Noda, M., et al. (2011). Physiology of microglia. Physiol Rev *91*, 461-553.

Khandelwal, P.J., Herman, A.M., and Moussa, C.E. (2011). Inflammation in the early stages of neurodegenerative pathology. J Neuroimmunol *238*, 1-11.

Kierdorf, K., Erny, D., Goldmann, T., et al. (2013). Microglia emerge from erythromyeloid precursors via Pu.1- and Irf8-dependent pathways. Nat Neurosci *16*, 273-280.

Kim, K.W., Vallon-Eberhard, A., Zigmond, E., et al. (2011). In vivo structure/function and expression analysis of the CX3C chemokine fractalkine. Blood *118*, e156-167.

Kimura, A., Naka, T., Muta, T., et al. (2005). Suppressor of cytokine signaling-1 selectively inhibits LPS-induced IL-6 production by regulating JAK-STAT. Proc Natl Acad Sci U S A *102*, 17089-17094.

Kleinberger, G., Yamanishi, Y., Suarez-Calvet, M., et al. (2014). TREM2 mutations implicated in neurodegeneration impair cell surface transport and phagocytosis. Sci Transl Med *6*, 243ra286.

Koronyo, Y., Salumbides, B.C., Sheyn, J., et al. (2015). Therapeutic effects of glatiramer acetate and grafted CD115+ monocytes in a mouse model of Alzheimer's disease. Brain *138*, 2399-2422.

Korvatska, O., Leverenz, J.B., Jayadev, S., et al. (2015). R47H Variant of TREM2 Associated With Alzheimer Disease in a Large Late-Onset Family: Clinical, Genetic, and Neuropathological Study. JAMA Neurol.

Kozlowski, C., and Weimer, R.M. (2012). An automated method to quantify microglia morphology and application to monitor activation state longitudinally in vivo. PLoS One *7*, e31814.

Krabbe, G., Halle, A., Matyash, V., et al. (2013). Functional impairment of microglia coincides with Beta-amyloid deposition in mice with Alzheimer-like pathology. PLoS One *8*, e60921.

Kreutzberg, G.W. (1996). Microglia: a sensor for pathological events in the CNS. Trends Neurosci *19*, 312-318.

Kurotaki, D., Yamamoto, M., Nishiyama, A., et al. (2014). IRF8 inhibits C/EBPalpha activity to restrain mononuclear phagocyte progenitors from differentiating into neutrophils. Nat Commun *5*, 4978.

Lambert, J.C., Heath, S., Even, G., et al. (2009a). Genome-wide association study identifies variants at CLU and CR1 associated with Alzheimer's disease. Nat Genet *41*, 1094-1099.

Lambert, J.C., Heath, S., Even, G., et al. (2009b). Genome-wide association study identifies variants at CLU and CR1 associated with Alzheimer's disease. Nat Genet *41*, 1094-1099.

Lanzillotta, A., Sarnico, I., Benarese, M., et al. (2011). The gamma-secretase modulator CHF5074 reduces the accumulation of native hyperphosphorylated tau in a transgenic mouse model of Alzheimer's disease. J Mol Neurosci *45*, 22-31.

Laske, C., Schmohl, M., Leyhe, T., et al. (2013). Immune profiling in blood identifies sTNF-R1 performing comparably well as biomarker panels for classification of Alzheimer's disease patients. J Alzheimers Dis *34*, 367-375.

Lastres-Becker, I., Innamorato, N.G., Jaworski, T., et al. (2014). Fractalkine activates NRF2/NFE2L2 and heme oxygenase 1 to restrain tauopathy-induced microgliosis. Brain *137*, 78-91.

Lavigne, C., and Thierry, A.R. (1997). Enhanced antisense inhibition of human immunodeficiency virus type 1 in cell cultures by DLS delivery system. Biochem Biophys Res Commun *237*, 566-571.

Lebson, L., Nash, K., Kamath, S., et al. (2010). Trafficking CD11b-positive blood cells deliver therapeutic genes to the brain of amyloid-depositing transgenic mice. J Neurosci *30*, 9651-9658.

Lee, J., Breton, G., Oliveira, T.Y., et al. (2015). Restricted dendritic cell and monocyte progenitors in human cord blood and bone marrow. J Exp Med *212*, 385-399.

Lefterov, I., Schug, J., Mounier, A., et al. (2015). RNA-sequencing reveals transcriptional up-regulation of Trem2 in response to bexarotene treatment. Neurobiol Dis *82*, 132-140.

Lehmann, S.M., Kruger, C., Park, B., et al. (2012). An unconventional role for miRNA: let-7 activates Toll-like receptor 7 and causes neurodegeneration. Nat Neurosci *15*, 827-835.

Letiembre, M., Liu, Y., Walter, S., et al. (2009). Screening of innate immune receptors in neurodegenerative diseases: a similar pattern. Neurobiol Aging *30*, 759-768.

Leung, R., Proitsi, P., Simmons, A., et al. (2013). Inflammatory proteins in plasma are associated with severity of Alzheimer's disease. PLoS One *8*, e64971.

Li, T., Pang, S., Yu, Y., et al. (2013). Proliferation of parenchymal microglia is the main source of microgliosis after ischaemic stroke. Brain *136*, 3578-3588.

Li, Y., and Shi, X. (2013). MicroRNAs in the regulation of TLR and RIG-I pathways. Cell Mol Immunol *10*, 65-71.

Li, Y.Y., Cui, J.G., Dua, P., et al. (2011). Differential expression of miRNA-146a-regulated inflammatory genes in human primary neural, astroglial and microglial cells. Neurosci Lett *499*, 109-113.

Limatola, C., and Ransohoff, R.M. (2014). Modulating neurotoxicity through CX3CL1/CX-3CR1 signaling. Front Cell Neurosci *8*, 229.

Lin, H.S., Gong, J.N., Su, R., et al. (2014). miR-199a-5p inhibits monocyte/macrophage differentiation by targeting the activin A type 1B receptor gene and finally reducing C/EBPalpha expression. J Leukoc Biol *96*, 1023-1035.

Lonskaya, I., Hebron, M.L., Selby, S.T., et al. (2015). Nilotinib and bosutinib modulate preplaque alterations of blood immune markers and neuro-inflammation in Alzheimer's disease models. Neuroscience *304*, 316-327.

Lu, J., and Tsourkas, A. (2009). Imaging individual microRNAs in single mammalian cells in situ. Nucleic Acids Res *37*, e100.

Lu, M.H., Li, C.Z., Hu, C.J., et al. (2012). microRNA-27b suppresses mouse MSC migration to the liver by targeting SDF-1alphain vitro. Biochem Biophys Res Commun *421*, 389-395.

Lucin, K.M., and Wyss-Coray, T. (2009). Immune activation in brain aging and neurodegeneration: too much or too little? Neuron *64*, 110-122.

Lue, L.F., Rydel, R., Brigham, E.F., et al. (2001). Inflammatory repertoire of Alzheimer's disease and nondemented elderly microglia in vitro. Glia *35*, 72-79.

Lukiw, W.J. (2007). Micro-RNA speciation in fetal, adult and Alzheimer's disease hippocampus. Neuroreport *18*, 297-300.

Lukiw, W.J., and Alexandrov, P.N. (2012). Regulation of complement factor H (CFH) by multiple miRNAs in Alzheimer's disease (AD) brain. Mol Neurobiol *46*, 11-19.

Lukiw, W.J., Zhao, Y., and Cui, J.G. (2008). An NF-kappaB-sensitive micro RNA-146a-mediated inflammatory circuit in Alzheimer disease and in stressed human brain cells. J Biol Chem *283*, 31315-31322.

Lunnon, K., Ibrahim, Z., Proitsi, P., et al. (2012). Mitochondrial dysfunction and immune activation are detectable in early Alzheimer's disease blood. J Alzheimers Dis *30*, 685-710.

Luster, A.D. (1998). Chemokines--chemotactic cytokines that mediate inflammation. N Engl J Med *338*, 436-445.

Lynch, M.A. (2009). The multifaceted profile of activated microglia. Mol Neurobiol *40*, 139-156.

M., S.R., Torbett, B.E., Anderson, K.L., et al. (1996). Targeted disruption of the PU. 1 gene results in multiple hematopoietic abnormalities. The EMBO Journal *15*, 5647-5658.

Ma, X., Becker Buscaglia, L.E., Barker, J.R., et al. (2011). MicroRNAs in NF-kappaB signaling. J Mol Cell Biol *3*, 159-166.

Maes, O.C., Xu, S., Yu, B., et al. (2007). Transcriptional profiling of Alzheimer blood mononuclear cells by microarray. Neurobiol Aging *28*, 1795-1809.

Mahad, D., Callahan, M.K., Williams, K.A., et al. (2006). Modulating CCR2 and CCL2 at the blood-brain barrier: relevance for multiple sclerosis pathogenesis. Brain *129*, 212-223.

Malm, T.M., Koistinaho, M., Parepalo, M., et al. (2005). Bone-marrow-derived cells contribute to the recruitment of microglial cells in response to beta-amyloid deposition in APP/PS1 double transgenic Alzheimer mice. Neurobiol Dis *18*, 134-142.

Man, S.M., Ma, Y.R., Shang, D.S., et al. (2007). Peripheral T cells overexpress MIP-1alpha to enhance its transendothelial migration in Alzheimer's disease. Neurobiol Aging *28*, 485-496.

Mandrekar-Colucci, S., Karlo, J.C., and Landreth, G.E. (2012). Mechanisms underlying the rapid peroxisome proliferator-activated receptor-gamma-mediated amyloid clearance and reversal of cognitive deficits in a murine model of Alzheimer's disease. J Neurosci *32*, 10117-10128.

Mawuenyega, K.G., Sigurdson, W., Ovod, V., et al. (2010). Decreased clearance of CNS beta-amyloid in Alzheimer's disease. Science *330*, 1774.

McGeer, E.G., and McGeer, P.L. (2003). Inflammatory processes in Alzheimer's disease. Progress in Neuro-Psychopharmacology and Biological Psychiatry *27*, 741-749.

McKhann, G.M., Knopman, D.S., Chertkow, H., et al. (2011). The diagnosis of dementia due to Alzheimer's disease: recommendations from the National Institute on Aging-Alzheimer's Association workgroups on diagnostic guidelines for Alzheimer's disease. Alzheimers Dement *7*, 263-269.

Miao, J., Xu, F., Davis, J., et al. (2005). Cerebral Microvascular Amyloid β Protein Deposition Induces Vascular Degeneration and Neuroinflammation in Transgenic Mice Expressing Human Vasculotropic Mutant Amyloid β Precursor Protein. The American Journal of Pathology *167*, 505-515.

Michaud, J.P., Bellavance, M.A., Prefontaine, P., et al. (2013). Real-time in vivo imaging reveals the ability of monocytes to clear vascular amyloid beta. Cell Rep *5*, 646-653.

Michelucci, A., Heurtaux, T., Grandbarbe, L., et al. (2009). Characterization of the microglial phenotype under specific pro-inflammatory and anti-inflammatory conditions: Effects of oligomeric and fibrillar amyloid-beta. J Neuroimmunol *210*, 3-12.

Mildner, A., Schlevogt, B., Kierdorf, K., et al. (2011). Distinct and non-redundant roles of microglia and myeloid subsets in mouse models of Alzheimer's disease. J Neurosci *31*, 11159-11171.

Mizuno, T., Kawanokuchi, J., Numata, K., et al. (2003). Production and neuroprotective functions of fractalkine in the central nervous system. Brain Res *979*, 65-70.

Mizutani, M., Pino, P.A., Saederup, N., et al. (2012). The fractalkine receptor but not CCR2 is present on microglia from embryonic development throughout adulthood. J Immunol *188*, 29-36.

Mohs, R., C., Rosen, W., G., Davis, K., L. (1983). The Alzheimer's disease assessment scale: an instrument for assessing treatment efficacy. Psychopharmacol Bull *19*, 448-450.

Mor, E., Cabilly, Y., Goldshmit, Y., et al. (2011). Species-specific microRNA roles elucidated following astrocyte activation. Nucleic Acids Res *39*, 3710-3723.

Morris, J.C. (1993). The Clinical Dementia Rating (CDR): current version and scoring rules. Neurology *43*, 2412-2414.

Murphy, G.M., Jr., Yang, L., and Cordell, B. (1998). Macrophage colony-stimulating factor augments beta-amyloid-induced interleukin-1, interleukin-6, and nitric oxide production by microglial cells. J Biol Chem *273*, 20967-20971.

Murugaiyan, G., Beynon, V., Mittal, A., et al. (2011). Silencing microRNA-155 ameliorates experimental autoimmune encephalomyelitis. J Immunol *187*, 2213-2221.

Naert, G., and Rivest, S. (2011). CC chemokine receptor 2 deficiency aggravates cognitive impairments and amyloid pathology in a transgenic mouse model of Alzheimer's disease. J Neurosci *31*, 6208-6220.

Naert, G., and Rivest, S. (2012a). Age-related changes in synaptic markers and monocyte subsets link the cognitive decline of APP(Swe)/PS1 mice. Front Cell Neurosci *6*, 51.

Naert, G., and Rivest, S. (2012b). Hematopoietic CC-chemokine receptor 2 (CCR2) competent cells are protective for the cognitive impairments and amyloid pathology in a transgenic mouse model of Alzheimer's disease. Mol Med *18*, 297-313.

Naert, G., and Rivest, S. (2013). A deficiency in CCR2+ monocytes: the hidden side of Alzheimer's disease. J Mol Cell Biol *5*, 284-293.

Nagele, R.G., Wegiel, J., Venkataraman, V., et al. (2004). Contribution of glial cells to the development of amyloid plaques in Alzheimer's disease. Neurobiol Aging *25*, 663-674.

Naj, A.C., Jun, G., Beecham, G.W., et al. (2011). Common variants at MS4A4/MS4A6E, CD2AP, CD33 and EPHA1 are associated with late-onset Alzheimer's disease. Nat Genet *43*, 436-441.

Nakamachi, Y., Kawano, S., Takenokuchi, M., et al. (2009). MicroRNA-124a is a key regulator of proliferation and monocyte chemoattractant protein 1 secretion in fibroblast-like synoviocytes from patients with rheumatoid arthritis. Arthritis Rheum *60*, 1294-1304.

Nalivaeva, N.N., and Turner, A.J. (2013). The amyloid precursor protein: a biochemical enigma in brain development, function and disease. FEBS Lett *587*, 2046-2054.

Naqvi, A.R., Fordham, J.B., and Nares, S. (2015). miR-24, miR-30b, and miR-142-3p regulate phagocytosis in myeloid inflammatory cells. J Immunol *194*, 1916-1927.

Nasreddine, Z.S., Phillips, N.A., Bedirian, V., et al. (2005). The Montreal Cognitive Assessment, MoCA: a brief screening tool for mild cognitive impairment. J Am Geriatr Soc *53*, 695-699.

Nicolas, M., and Hassan, B.A. (2014). Amyloid precursor protein and neural development. Development *141*, 2543-2548.

Nimmerjahn, A., Kirchhoff, F., and Helmchen, F. (2005). Resting microglial cells are highly dynamic surveillants of brain parenchyma in vivo. Science *308*, 1314-1318.

O'Connell, R.M., Chaudhuri, A.A., Rao, D.S., et al. (2009). Inositol phosphatase SHIP1 is a primary target of miR-155. Proc Natl Acad Sci U S A *106*, 7113-7118.

O'Connell, R.M., Rao, D.S., and Baltimore, D. (2012). microRNA regulation of inflammatory responses. Annu Rev Immunol *30*, 295-312.

O'Connell, R.M., Taganov, K.D., Boldin, M.P., et al. (2007). MicroRNA-155 is induced during the macrophage inflammatory response. Proc Natl Acad Sci U S A *104*, 1604-1609.

O'Neill, L.A., Sheedy, F.J., and McCoy, C.E. (2011). MicroRNAs: the fine-tuners of Toll-like receptor signalling. Nat Rev Immunol *11*, 163-175.

Oakley, H., Cole, S.L., Logan, S., et al. (2006). Intraneuronal beta-amyloid aggregates, neurodegeneration, and neuron loss in transgenic mice with five familial Alzheimer's disease mutations: potential factors in amyloid plaque formation. J Neurosci *26*, 10129-10140.

Oddo, S., Caccamo, A., Kitazawa, M., et al. (2003a). Amyloid deposition precedes tangle formation in a triple transgenic model of Alzheimer's disease. Neurobiology of Aging *24*, 1063-1070.

Oddo, S., Caccamo, A., Shepherd, J., et al. (2003b). Triple-Transgenic Model of Alzheimer's Disease with Plaques and Tangles: Intracellular Abeta and Synaptic Dysfunction. Neuron *39*, 409-421.

Okello, A., Edison, P., Archer, H.A., et al. (2009). Microglial activation and amyloid deposition in mild cognitive impairment: a PET study. Neurology *72*, 56-62.

Onyeagucha, B.C., Mercado-Pimentel, M.E., Hutchison, J., et al. (2013). S100P/RAGE signaling regulates microRNA-155 expression via AP-1 activation in colon cancer. Exp Cell Res *319*, 2081-2090.

Parachikova, A., Agadjanyan, M.G., Cribbs, D.H., et al. (2007). Inflammatory changes parallel the early stages of Alzheimer disease. Neurobiol Aging *28*, 1821-1833.

Parachikova, A., and Cotman, C.W. (2007). Reduced CXCL12/CXCR4 results in impaired learning and is downregulated in a mouse model of Alzheimer disease. Neurobiol Dis *28*, 143-153.

Pareek, S., Roy, S., Kumari, B., et al. (2014). MiR-155 induction in microglial cells suppresses Japanese encephalitis virus replication and negatively modulates innate immune responses. J Neuroinflammation *11*, 97.

Parisi, C., Arisi, I., D'Ambrosi, N., et al. (2013). Dysregulated microRNAs in amyotrophic lateral sclerosis microglia modulate genes linked to neuroinflammation. Cell Death Dis *4*, e959.

Paschon, V., Takada, S.H., Ikebara, J.M., et al. (2015). Interplay Between Exosomes, microRNAs and Toll-Like Receptors in Brain Disorders. Mol Neurobiol.

Pellicano, M., Bulati, M., Buffa, S., et al. (2010). Systemic immune responses in Alzheimer's disease: in vitro mononuclear cell activation and cytokine production. J Alzheimers Dis *21*, 181-192.

Pellicano, M., Larbi, A., Goldeck, D., et al. (2012). Immune profiling of Alzheimer patients. J Neuroimmunol *242*, 52-59.

Pennanen, C., Kivipelto, M., Tuomainen, S., et al. (2004). Hippocampus and entorhinal cortex in mild cognitive impairment and early AD. Neurobiology of Aging *25*, 303-310.

Perry, V.H., Nicoll, J.A., and Holmes, C. (2010). Microglia in neurodegenerative disease. Nat Rev Neurol *6*, 193-201.

Petersen, R., C., Smith, G., E., Waring, S., C., et al. (1999). Mild Cognitive Impairment. Archives of Neurology *56*, 303.

Petersen, R.C. (2004). Mild cognitive impairment as a diagnostic entity. J Intern Med *256*, 183-194.

Petersen, R.C. (2011). Clinical practice. Mild cognitive impairment. N Engl J Med *364*, 2227-2234.

Pogue, A.I., Cui, J.G., Li, Y.Y., et al. (2010). Micro RNA-125b (miRNA-125b) function in astrogliosis and glial cell proliferation. Neurosci Lett *476*, 18-22.

Ponomarev, E.D., Veremeyko, T., Barteneva, N., et al. (2011). MicroRNA-124 promotes microglia quiescence and suppresses EAE by deactivating macrophages via the C/EBP-alpha-PU.1 pathway. Nat Med *17*, 64-70.

Ponomarev, E.D., Veremeyko, T., and Weiner, H.L. (2013). MicroRNAs are universal regulators of differentiation, activation, and polarization of microglia and macrophages in normal and diseased CNS. Glia *61*, 91-103.

Pospisil, V., Vargova, K., Kokavec, J., et al. (2011). Epigenetic silencing of the oncogenic miR-17-92 cluster during PU.1-directed macrophage differentiation. EMBO J *30*, 4450-4464.

Prinz, M., and Priller, J. (2010). Tickets to the brain: role of CCR2 and CX3CR1 in myeloid cell entry in the CNS. J Neuroimmunol *224*, 80-84.

Prinz, M., Priller, J., Sisodia, S.S., et al. (2011). Heterogeneity of CNS myeloid cells and their roles in neurodegeneration. Nat Neurosci *14*, 1227-1235.

Puzzo, D., Gulisano, W., Palmeri, A., et al. (2015). Rodent models for Alzheimer's disease drug discovery. Expert Opin Drug Discov *10*, 703-711.

Qin, H., Wilson, C.A., Lee, S.J., et al. (2006). IFN-beta-induced SOCS-1 negatively regulates CD40 gene expression in macrophages and microglia. FASEB J *20*, 985-987.

Raj, T., Rothamel, K., Mostafavi, S., et al. (2014). Polarization of the effects of autoimmune and neurodegenerative risk alleles in leukocytes. Science *344*, 519-523.

Ransohoff, R.M., and Cardona, A.E. (2010). The myeloid cells of the central nervous system parenchyma. Nature *468*, 253-262.

Reale, M., Iarlori, C., Feliciani, C., et al. (2008). Peripheral chemokine receptors, their ligands, Cytokines and Alzheimer's disease. J Alzheimers Dis *14*, 147-159.

Rebeck, G.W., Hoe, H.S., and Moussa, C.E. (2010). Beta-amyloid1-42 gene transfer model exhibits intraneuronal amyloid, gliosis, tau phosphorylation, and neuronal loss. J Biol Chem *285*, 7440-7446.

Resende, R., Ferreiro, E., Pereira, C., et al. (2008). Neurotoxic effect of oligomeric and fibrillar species of amyloid-beta peptide 1-42: involvement of endoplasmic reticulum calcium release in oligomer-induced cell death. Neuroscience *155*, 725-737.

Rivest, S. (2009). Regulation of innate immune responses in the brain. Nat Rev Immunol *9*, 429-439.

Rogers, J., Li, R., Mastroeni, D., et al. (2006). Peripheral clearance of amyloid beta peptide by complement C3-dependent adherence to erythrocytes. Neurobiol Aging *27*, 1733-1739.

Roman, G.C., Tatemichi, T.K., Erkinjuntti, T., et al. (1993). Vascular dementia: diagnostic criteria for research studies. Report of the NINDS-AIREN International Workshop. Neurology *43*, 250-260.

Rosa, A., Ballarino, M., Sorrentino, A., et al. (2007). The interplay between the master transcription factor PU.1 and miR-424 regulates human monocyte/macrophage differentiation. Proc Natl Acad Sci U S A *104*, 19849-19854.

Rozemuller, J.M., Eikelenboom, P., and Stam, F.C. (1986). Role of microglia in plaque formation in senile dementia of the Alzheimer type. An immunohistochemical study. Virchows Arch B Cell Pathol Incl Mol Pathol *51*, 247-254.

Saba, R., Gushue, S., Huzarewich, R.L., et al. (2012). MicroRNA 146a (miR-146a) is over-expressed during prion disease and modulates the innate immune response and the microglial activation state. PLoS One *7*, e30832.

Saederup, N., Cardona, A.E., Croft, K., et al. (2010). Selective chemokine receptor usage by central nervous system myeloid cells in CCR2-red fluorescent protein knock-in mice. PLoS One *5*, e13693.

Saijo, K., Crotti, A., and Glass, C.K. (2013). Regulation of microglia activation and deactivation by nuclear receptors. Glia *61*, 104-111.

Saijo, K., and Glass, C.K. (2011). Microglial cell origin and phenotypes in health and disease. Nat Rev Immunol *11*, 775-787.

Saijo, K., Winner, B., Carson, C.T., et al. (2009). A Nurr1/CoREST pathway in microglia and astrocytes protects dopaminergic neurons from inflammation-induced death. Cell *137*, 47-59.

Salter, M.W., and Beggs, S. (2014). Sublime microglia: expanding roles for the guardians of the CNS. Cell *158*, 15-24.

Sanchez-Ramos, J., Song, S., Sava, V., et al. (2009). Granulocyte colony stimulating factor decreases brain amyloid burden and reverses cognitive impairment in Alzheimer's mice. Neuroscience *163*, 55-72.

Saresella, M., Marventano, I., Calabrese, E., et al. (2014). A complex proinflammatory role for peripheral monocytes in Alzheimer's disease. J Alzheimers Dis *38*, 403-413.

Satoh, J., Kino, Y., and Niida, S. (2015). MicroRNA-Seq Data Analysis Pipeline to Identify Blood Biomarkers for Alzheimer's Disease from Public Data. Biomark Insights *10*, 21-31.

Sharma, N., Verma, R., Kumawat, K.L., et al. (2015). miR-146a suppresses cellular immune response during Japanese encephalitis virus JaOArS982 strain infection in human microglial cells. J Neuroinflammation *12*, 30.

Shechter, R., and Schwartz, M. (2013). Harnessing monocyte-derived macrophages to control central nervous system pathologies: no longer 'if' but 'how'. J Pathol *229*, 332-346.

Sheng, J.G., Griffin, W.S., Royston, M.C., et al. (1998). Distribution of interleukin-1-immunoreactive microglia in cerebral cortical layers: implications for neuritic plaque formation in Alzheimer's disease. Neuropathol Appl Neurobiol *24*, 278-283.

Simard, A.R., Soulet, D., Gowing, G., et al. (2006). Bone marrow-derived microglia play a critical role in restricting senile plaque formation in Alzheimer's disease. Neuron *49*, 489-502.

Simoes, A.T., Goncalves, N., Koeppen, A., et al. (2012). Calpastatin-mediated inhibition of calpains in the mouse brain prevents mutant ataxin 3 proteolysis, nuclear localization and aggregation, relieving Machado-Joseph disease. Brain *135*, 2428-2439.

Soulet, D., and Rivest, S. (2008). Bone-marrow-derived microglia: myth or reality? Curr Opin Pharmacol *8*, 508-518.

Stancu, I.C., Ris, L., Vasconcelos, B., et al. (2014). Tauopathy contributes to synaptic and cognitive deficits in a murine model for Alzheimer's disease. FASEB J *28*, 2620-2631.

Stewart, C.R., Stuart, L.M., Wilkinson, K., et al. (2010). CD36 ligands promote sterile inflammation through assembly of a Toll-like receptor 4 and 6 heterodimer. Nat Immunol *11*, 155-161.

Su, W., Hopkins, S., Nesser, N.K., et al. (2014). The p53 transcription factor modulates microglia behavior through microRNA-dependent regulation of c-Maf. J Immunol *192*, 358-366.

Swirski, F.K., Nahrendorf, M., Etzrodt, M., et al. (2009). Identification of splenic reservoir monocytes and their deployment to inflammatory sites. Science *325*, 612-616.

Taganov, K.D., Boldin, M.P., Chang, K.J., et al. (2006). NF-kappaB-dependent induction of microRNA miR-146, an inhibitor targeted to signaling proteins of innate immune responses. Proc Natl Acad Sci U S A *103*, 12481-12486.

Takahashi, R.H., Capetillo-Zarate, E., Lin, M.T., et al. (2010). Co-occurrence of Alzheimer's disease ss-amyloid and tau pathologies at synapses. Neurobiol Aging *31*, 1145-1152.

Takaoka, A., and Yanai, H. (2006). Interferon signalling network in innate defence. Cell Microbiol *8*, 907-922.

Tang, S.C., Lathia, J.D., Selvaraj, P.K., et al. (2008). Toll-like receptor-4 mediates neuronal apoptosis induced by amyloid beta-peptide and the membrane lipid peroxidation product 4-hydroxynonenal. Exp Neurol *213*, 114-121.

Tarassishin, L., Bauman, A., Suh, H.S., et al. (2013). Anti-viral and anti-inflammatory mechanisms of the innate immune transcription factor interferon regulatory factor 3: relevance to human CNS diseases. J Neuroimmune Pharmacol *8*, 132-144.

Tarassishin, L., Loudig, O., Bauman, A., et al. (2011). Interferon regulatory factor 3 inhibits astrocyte inflammatory gene expression through suppression of the proinflammatory miR-155 and miR-155*. Glia *59*, 1911-1922.

Thai, T.H., Calado, D.P., Casola, S., et al. (2007). Regulation of the germinal center response by microRNA-155. Science *316*, 604-608.

Tili, E., Michaille, J., Cimino, A., et al. (2007). Modulation of miR-155 and miR-125b Levels following Lipopolysaccharide/TNF-α Stimulation and Their Possible Roles in Regulating the Response to Endotoxin Shock. J. Immunol. *179*, 5082-5089.

Tiribuzi, R., Crispoltoni, L., Porcellati, S., et al. (2014). miR128 up-regulation correlates with impaired amyloid beta(1-42) degradation in monocytes from patients with sporadic Alzheimer's disease. Neurobiol Aging *35*, 345-356.

Tokutake, T., Kasuga, K., Yajima, R., et al. (2012). Hyperphosphorylation of Tau induced by naturally secreted amyloid-beta at nanomolar concentrations is modulated by insulin-dependent Akt-GSK3beta signaling pathway. J Biol Chem *287*, 35222-35233.

Trabulo, S., Resina, S., Simoes, S., et al. (2010). A non-covalent strategy combining cationic lipids and CPPs to enhance the delivery of splice correcting oligonucleotides. J Control Release *145*, 149-158.

Tremblay, M.E., Lowery, R.L., and Majewska, A.K. (2010). Microglial interactions with synapses are modulated by visual experience. PLoS Biol *8*, e1000527.

Tremblay, M.E., Stevens, B., Sierra, A., et al. (2011). The role of microglia in the healthy brain. J Neurosci *31*, 16064-16069.

Twine, N.A., Janitz, K., Wilkins, M.R., et al. (2011). Whole transcriptome sequencing reveals gene expression and splicing differences in brain regions affected by Alzheimer's disease. PLoS One *6*, e16266.

van Furth, R., and Cohn, Z.A. (1968). The origin and kinetics of mononuclear phagocytes J Exp Med *128* 415-435.

Varnum, M.M., and Ikezu, T. (2012). The classification of microglial activation phenotypes on neurodegeneration and regeneration in Alzheimer's disease brain. Arch Immunol Ther Exp (Warsz) *60*, 251-266.

Vodopivec, I., Galichet, A., Knobloch, M., et al. (2009). RAGE does not affect amyloid pathology in transgenic ArcAbeta mice. Neurodegener Dis *6*, 270-280.

Volpe, S., Cameroni, E., Moepps, B., et al. (2012). CCR2 acts as scavenger for CCL2 during monocyte chemotaxis. PLoS One *7*, e37208.

Vukic, V., Callaghan, D., Walker, D., et al. (2009). Expression of inflammatory genes induced by beta-amyloid peptides in human brain endothelial cells and in Alzheimer's brain is mediated by the JNK-AP1 signaling pathway. Neurobiol Dis *34*, 95-106.

Walker, D.G., Link, J., Lue, L.F., et al. (2006). Gene expression changes by amyloid beta peptide-stimulated human postmortem brain microglia identify activation of multiple inflammatory processes. J Leukoc Biol *79*, 596-610.

Walter, S., Letiembre, M., Liu, Y., et al. (2007). Role of the toll-like receptor 4 in neuroinflammation in Alzheimer's disease. Cell Physiol Biochem *20*, 947-956.

Wang, Y., Cella, M., Mallinson, K., et al. (2015). TREM2 Lipid Sensing Sustains the Microglial Response in an Alzheimer's Disease Model. Cell *160*, 1061-1071.

Wegiel, J., Imaki, H., Wang, K.C., et al. (2004). Cells of monocyte/microglial lineage are involved in both microvessel amyloidosis and fibrillar plaque formation in APPsw tg mice. Brain Res *1022*, 19-29.

Weiner, H.L., and Frenkel, D. (2006). Immunology and immunotherapy of Alzheimer's disease. Nat Rev Immunol *6*, 404-416.

Wilkinson, K., and El Khoury, J. (2012). Microglial scavenger receptors and their roles in the pathogenesis of Alzheimer's disease. Int J Alzheimers Dis *2012*, 489456.

Worm, J., Stenvang, J., Petri, A., et al. (2009). Silencing of microRNA-155 in mice during acute inflammatory response leads to derepression of c/ebp Beta and down-regulation of G-CSF. Nucleic Acids Res *37*, 5784-5792.

Wunderlich, P., Glebov, K., Kemmerling, N., et al. (2013). Sequential proteolytic processing of the triggering receptor expressed on myeloid cells-2 (TREM2) protein by ectodomain shedding and gamma-secretase-dependent intramembranous cleavage. J Biol Chem *288*, 33027-33036.

Wynn, T.A., Chawla, A., and Pollard, J.W. (2013). Macrophage biology in development, homeostasis and disease. Nature *496*, 445-455.

Wyss-Coray, T. (2006). Inflammation in Alzheimer disease: driving force, bystander or beneficial response? Nat Med *12*, 1005-1015.

Wyss-Coray, T., Loike, J.D., Brionne, T.C., et al. (2003). Adult mouse astrocytes degrade amyloid-beta in vitro and in situ. Nat Med *9*, 453-457.

Yamasaki, R., Lu, H., Butovsky, O., et al. (2014). Differential roles of microglia and monocytes in the inflamed central nervous system. J Exp Med *211*, 1533-1549.

Yan, S.D., Chen, X., Fu, J., et al. (1996). RAGE and amyloid-beta peptide neurotoxicity in Alzheimer's disease. Nature *382*, 685-691.

Yang, Z., Zhong, L., Zhong, S., et al. (2015). miR-203 protects microglia mediated brain injury by regulating inflammatory responses via feedback to MyD88 in ischemia. Mol Immunol *65*, 293-301.

Yao, R., Ma, Y.L., Liang, W., et al. (2012). MicroRNA-155 modulates Treg and Th17 cells differentiation and Th17 cell function by targeting SOCS1. PLoS One *7*, e46082.

Yates, S.L., Burgess, L.H., Kocsis-Angle, J., et al. (2000). Amyloid beta and amylin fibrils induce increases in proinflammatory cytokine and chemokine production by THP-1 cells and murine microglia. J Neurochem *74*, 1017-1025.

Ydens, E., Cauwels, A., Asselbergh, B., et al. (2012). Acute injury in the peripheral nervous system triggers an alternative macrophage response. J Neuroinflammation *9*, 176.

Yeamans, C., Wang, D., Paz-Priel, I., et al. (2007). C/EBPalpha binds and activates the PU.1 distal enhancer to induce monocyte lineage commitment. Blood *110*, 3136-3142.

Yesavage, J.A., Brink, T., L., Rose, T., L., et al. (1983). Development and validation of a geriatric depression screening scale: a preliminary report. J Psychiatr Res. *17*, 37-49.

Yokokura, M., Mori, N., Yagi, S., et al. (2011). In vivo changes in microglial activation and amyloid deposits in brain regions with hypometabolism in Alzheimer's disease. Eur J Nucl Med Mol Imaging *38*, 343-351.

Yona, S., Kim, K.W., Wolf, Y., et al. (2013). Fate mapping reveals origins and dynamics of monocytes and tissue macrophages under homeostasis. Immunity *38*, 79-91.

Yoshimura, A., Naka, T., and Kubo, M. (2007). SOCS proteins, cytokine signalling and immune regulation. Nat Rev Immunol *7*, 454-465.

Yoshiyama, Y., Higuchi, M., Zhang, B., et al. (2007). Synapse loss and microglial activation precede tangles in a P301S tauopathy mouse model. Neuron *53*, 337-351.

Yu, L., Liao, Q., Chen, X., et al. (2014a). Dynamic expression of miR-132, miR-212, and miR-146 in the brain of different hosts infected with Angiostrongylus cantonensis. Parasitol Res *113*, 91-99.

Yu, L., Liao, Q., Zeng, X., et al. (2014b). MicroRNA expressions associated with eosinophilic meningitis caused by Angiostrongylus cantonensis infection in a mouse model. Eur J Clin Microbiol Infect Dis *33*, 1457-1465.

Zaheer, S., Thangavel, R., Wu, Y., et al. (2013). Enhanced expression of glia maturation factor correlates with glial activation in the brain of triple transgenic Alzheimer's disease mice. Neurochem Res *38*, 218-225.

Zhang, J., Hu, M., Teng, Z., et al. (2014). Synaptic and cognitive improvements by inhibition of 2-AG metabolism are through upregulation of microRNA-188-3p in a mouse model of Alzheimer's disease. J Neurosci *34*, 14919-14933.

Zhang, Y., Zhang, M., Zhong, M., et al. (2013). Expression profiles of miRNAs in polarized macrophages. Int J Mol Med *31*, 797-802.

Zhong, L., Chen, X.F., Zhang, Z.L., et al. (2015). DAP12 Stabilizes the C-terminal Fragment of the Triggering Receptor Expressed on Myeloid Cells-2 (TREM2) and Protects against LPS-induced Pro-inflammatory Response. J Biol Chem *290*, 15866-15877.

Zhou, X., Spittau, B., and Krieglstein, K. (2012). TGFbeta signalling plays an important role in IL4-induced alternative activation of microglia. J Neuroinflammation *9*, 210.

Zujovic, V., Benavides, J., Vige, X., et al. (2000). Fractalkine modulates TNF-alpha secretion and neurotoxicity induced by microglial activation. Glia *29*, 305-315.